THE HALF-WIDTH AND SEPARATION OF THE COMPONENTS OF A CLOSE HIGH-Q DOUBLET AND THE NORMAL MODES OF VIBRATION OF CIRCULAR RINGS WITH RECTANGULAR CROSS-SECTIONS

by

VELLUR MOHANAN M.Sc.

A Doctoral Thesis

Submitted in partial fulfilment of the requirements for the award of the Degree of Doctor of Philosophy of the Loughborough University of Technology.

September 1980

Supervisors:- DR. T. CHARNLEY
and
DR. R. PERRIN
Department of Physics

ACKNOWLEDGEMENTS

I would like to express my sincere gratitude to my supervisors, Drs. T. CHARNLEY and R. PERRIN of the Department of Physics for their guidance, encouragement and co-operation during the period of the present course. I am also thankful to Prof. J.F. RAFFLE for offering me a place in the department in the first place and for his overall supervision. My thanks are also due to the technical staff of the Physics workshop, especially to MR. F.T. HATELY and MR. J.F. OAKLEY, and to other members of the Department, especially to MRS. M.A. STANIEC and MISS J.M. SHARPE of the General Office.

I express my thanks to MRS. D.K. NANDRA for typing of the thesis.

Also I wish to express my indebtedness to the Commonwealth Scholarship Commission in the United Kingdom for their financial assistance.

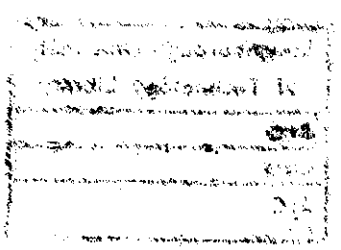

TO

SARASA

AND

SEEMA

CONTENTS

Chapter III/cont'd ... Page

SUMMARY

With axially symmetrical vibrating systems like rings, cones and bells most of the normal modes occur as degenerate doublets with the two components having equal Q values. If a slight asymmetry is introduced into the system - either structural or metallurgical - these doublets split slightly and often interest centres on the amount of this splitting. The easiest method to measure this is both to drive and detect at one point midway between the two nodal/antinodal meridians of the two components. By driving the system at this "symmetry" radian frequency of the doublet response a beating decay is observed if the drive is switched off after attaining the steady state. The beat frequency of the decaying oscillations is equal to the splitting of the two components. Obviously, this method fails when the splitting is so small that the beat period exceeds the decay time. The response curve still shows a double peak and the method described below enables one to estimate the separation and half-width of the components from its shape.

Also a simple method, using least-squares technique, is given for obtaining the half-width and resonance frequency of a high-Q singlet in the presence of a constant background signal.

The normal modes of vibration of a free circular ring fall mainly into four types viz. radial (inextensional), axial, torsional and extensional (radial). The classical theory of LOVE deals with thin rings of circular cross-sections in which the effects of transverse shear and rotatory inertia are neglected. Different authors have improved this classical theory by taking into account the effects of cross-sectional shape, centre-line extension, rotatory inertia, shear deflection, warping etc. to deal with thick ring vibration. However, there existed no substantial experimental data to verify the various theories, especially for the torsional and extensional modes. Hence it was necessary to undertake a systematic experimental investigation of the various modes of ring vibration. This has helped to establish a criterion for the conditions under which the thin ring formulae may be used without serious error and to formulate an empirical correction to apply in the case of a thick ring.

CHAPTER 1

INTRODUCTION

1.1 STATEMENT OF THE PROBLEM

With axially symmetrical vibrating systems like bells, cones and rings it can be proved by group theoretical arguments that most of the normal modes occur as degenerate doublets [1] where the two components have equal Q values. For example the nodal pattern for the radial motion of the bell consists of n circles with $n \geq 0$ and 2m meridians with $m \geq 0$. The modes with $m = 0$ are all singlets while for $m > 0$ most of the modes occur in nearly degenerate pairs or doublets, the nodal meridians of one component of the doublet coinciding with the antinodal meridians of the other.

In practice this axial symmetry is often slightly broken due to geometrical or metallurgical imperfections of the real structure and these doublets usually split slightly and interest then centres on the amount of this splitting. The easiest method to measure this is both to drive and detect at one point midway between the nodal/antinodal meridians of the two components called the "equal-amplitude point" [2]. As the driving frequency is swept through resonance a double peak is obtained as shown in Figure 3.1. By driving the system at ω_m, the "symmetry" radian frequency of the doublet response curve, a beating-decay is observed if the drive is switched off after attaining the steady state. Obviously this method cannot be used when the splitting is so small that the beat period exceeds the decay time. Under these conditions the response curve still shows a double peak and the method described below enables one to estimate the splitting and half-width of the components from its shape.

1.2 MODAL DEGENERACY

The phenomenon of "modal degeneracy" is a common occurrence in plate and shell type structures. Unless precautions are taken difficulties may arise in determining the natural frequencies and damping levels of the various modes during vibration measurements using standard

procedures. The observed data may correspond to the recording of an apparent mode due to the superposition of certain nearby modes.

The degenerate superposition modes occur when two distinct modes are associated with the same natural frequency. For example, in the classical theory of thin ring vibration the pairs of degenerate eigen-functions have forms $\Psi_1 \sim \sin(n\theta)$ and $\Psi_2 \sim \cos(n\theta)$ where θ is the polar angle in the plane of the ring and n is an integer [3]. A familiar example for the existence of split doublets is seen in bell warble which is due to beats between the two split components.

1.3 CLOSE NATURAL FREQUENCIES

The existence of close natural frequencies in a complex engineering structure like an aircraft or building can be the source of serious vibration problems as they may render the structure susceptible to self-excited oscillation [4]. Hence, it is very important to be able to detect their presence, especially in the design stage, during a resonance test. As a result considerable research has been carried out in the past to propose or formulate new techniques in dealing with closely spaced natural frequencies [5,6,7,8,9]. In the majority of these works multi-degree freedom systems of high levels of damping are involved and complex data reduction techniques are used in the interpretation of the experimental results. Hence, it is necessary to have a simple practical method to deal with the particular problem of high-Q degenerate doublets, especially when the component separation is too small for the beating-decay method to be used.

1.4 MATERIAL DAMPING

The phenomenon of damping or internal friction is an important material property in the performance of machines and structures. It arises from the removal of vibration energy by radiation or dissipation and is generally measured under conditions of resonant or near-resonant motion. It plays an important role in the dynamical stability of a vibrating structure. High damping is desirable in engineering structures like a turbine or crankshaft to minimise the operating stresses, but low level of damping

is preferred in bells, tuning forks and musical instruments. Hence an optimum degree of damping is essential for the proper functioning of any mechanical system.

The ability of materials to contain vibrational energy via damping is due to various physical mechanisms. In the case of metals the prominent ones are thermo-elasticity (on both micro and macro scales), grain boundary viscosity, point defect relaxation, eddy-current effects, stress-induced ordering, electronic effects, and snoek effect [10]. According to ZENER the damping mechanism in metals in the audio-frequency range is largely due to transverse thermal currents associated with the grain boundaries [11].

1.5 MATHEMATICAL MODELLING

As the damping forces in real systems are of a complicated nature, mathematical modelling is necessary in order to obtain realistic results out of analytical studies. The simplest among the various models are the idealised spring and the classical dashpot. The former shows a restoring force proportional to displacement and the latter produces a damping force proportional to velocity. As these models are inadequate to describe the behaviour of real materials they have been combined together to obtain the two parameter models, viz. the Maxwell model and the Kelvin-Voigt model, as shown in Figure 1.1. The Maxwell model is a fair approximation to the behaviour of a visco-elastic liquid and the Kelvin-Voigt model nearly represents the behaviour of a visco-elastic solid. Although the Kelvin-Voigt model has some drawbacks this is the simplest model which allows representation as a complex quantity under harmonic excitation. There is also a finite steady-state response under steady-state harmonic excitation and the vibration of the system is a damped simple harmonic motion. It can be shown that for high-Q systems the response amplitude is independent of damping except in the vicinity of resonance where it depends critically on the Q values.

In order to overcome the drawbacks of Maxwell and Kelvin-Voigt models they have been combined in various ways to obtain various three-parameter models called "the standard linear solid" [12]. Continuing this process one obtains the two famous models viz. the generalised Maxwell model

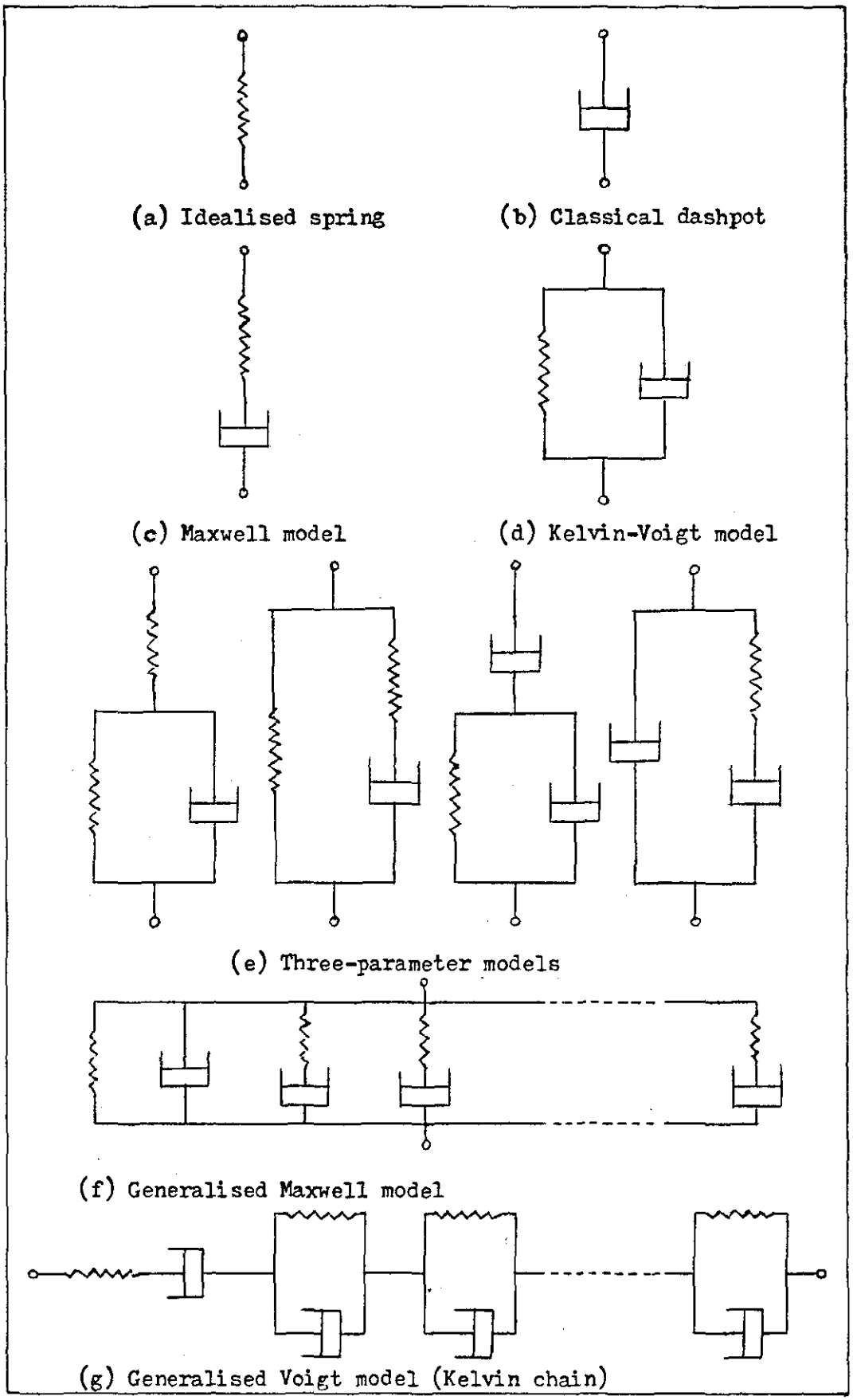

Figure 1.1 Mathematical models.

and the generalised Voigt model (Kelvin Chain). Details of these models and the continuing search for further simple models can be seen elsewhere [10,13,14].

1.6 LINEAR MODELS

Linear models are preferred due to their analytical feasibility, computational efficiency and sufficient accuracy in dealing with high-Q systems. The obvious choice is the Kelvin-Voigt model (viscous damping), and the equation of motion of a particle of mass m having a single degree of freedom attached to that model under harmonic excitation can be written as:

$$m\ddot{x} + c\dot{x} + kx = F_0 e^{j\omega t} \tag{1.1}$$

By trying a solution of the form

$$x = Ae^{j\omega t} \tag{1.2}$$

it can be proved that the energy dissipated per cycle at the dash-pot is given by

$$E = \pi A^2 \omega c \tag{1.3}$$

Experimental results of KIMBALL and LOVELL [15], WEGEL and WALTHER [16], LAZAN [10] etc. have shown that for many engineering materials E is proportional to A^2, but practically independent of the driving frequency. To this end consideration was given to a damper in which the damping coefficient is inversely proportional to ω and the damping force is given by $-\frac{h}{\omega}\dot{x}$, instead of $-c\dot{x}$. The energy dissipation then becomes independent of ω. This is called a hysteretic damper in which the damping force is proportional to displacement and is in phase with velocity.

Also, the total restoring force in a viscous damper given by $f_t = kx + c\dot{x}$ can be rewritten as $f_t = k(1 + j\eta)x$, where $\eta = \omega c/k = \frac{h}{k}$ is a dimensionless measure of damping known as loss factor. The quantity $k(1 + j\eta)$

can be referred to as the "complex stiffness" [13], where both k and η are assumed to be independent of frequency. This notion of complex stiffness is very convenient in the analysis of built-up multi-degree freedom systems and has been used extensively in the study of aircraft vibration and flutter analysis [17].

A harmonic oscillator under steady-state excitation experiences damping forces which are truly neither "viscous" nor "hysteretic" in character. However, for high-Q systems with single degree of freedom they approximate very closely to each other [18]. Again, hysteretic damping can only be used for complex exponential forms of solution and applies only to harmonic motion. To deal with free vibration the basic definition of the hysteretic damper has to be modified and the mathematical complexity of these modifications makes it unattractive [19].

It may be recalled that the idea of structural or hysteretic damping was introduced to account for frequency independent damping based on certain previous experimental evidence. Our experience with high-Q systems like a cone or bell has shown a certain frequency dependence for the damping observed in different modes. Also, the idea of a damping force proportional to velocity i.e. $f_d = -c\dot{x}$, is reasonable only when the motion x contains a single predominant frequency and hence the solution of equation (1.1) is appropriate only if it centres around a response of this frequency. This is exactly the present situation where the resonant response is mainly due to contribution in one particular mode - hereafter referred to as "singlet" for convenience. Hence there is full justification in using viscous damping theory to deal with high-Q systems, and equation (1.1) can be used without any difficulty.

1.7 DEFINITIONS OF DAMPING

Basically damping implies a deviation from perfect elasticity. Hence there are various ways of defining damping depending upon the particular phenomenon observed. In particular damping has been defined in terms of the energy dissipation, resonant magnification factor, band-width of half-power points, loss tangent (all considered under sinusoidal steady-state excitation), derivative of phase angle with respect to

resonance frequency, cyclic decay of free vibration, temporal decay of free vibration, spatial attenuation of plane waves in a slender rod [13], and the transmitted and reflected strain pulses [20]. Among these, the specific damping energy viz. the damping energy per cycle per unit volume, is considered to be more a basic property of the material and the resonant magnification factor is supposed to be a system characteristic. It can be shown that for high-Q systems all these different definitions are mathematically related to one another and the values of half-width obtained by different methods agree well.

1.8 METHODS OF MEASUREMENT

There are four main general methods of measuring internal friction or material damping: 1) the torsional pendulum method, 2) the resonant method, 3) the ultrasonic attenuation or pulse method [21], and 4) the Hopkinson pressure bar method [20]. The torsional pendulum method is generally employed in the low frequency region where the specimen in the shape of a wire forms the elastic member of the pendulum. The resonant method is mainly used in the audio-frequency region where the measuring frequency is determined by the geometry of the system. The ultrasonic pulse method is used for very high frequencies of the order of megacycles. Hopkinson pressure bar method, which is an impact method, is mainly used for determining the stress-strain characteristics of visco-elastic materials at high rates of strain [20].

A resonance test is carried out to determine 1) the principal modes, 2) the associated natural frequencies, and 3) the level of damping in each mode [22]. The system is excited either acoustically or magnetically and the vibration response is measured by using a capacitive or piezo-electric pick-up. In the simple case of resonance testing the structure is excited at one point and the responses are measured at a number of points. For complicated structures another approach is to use multiple exciters located at various points having controlled force amplitudes and phase relationships [13]. There are various data reduction techniques associated with the first method.

1.9 DATA REDUCTION TECHNIQUES

1.9.1 Reverberation Method

In this simple and straight forward method the external source is tuned to the resonance frequency of the structure under investigation. The voltage output of the pick-up is fed to a logarithmic recorder via a measuring amplifier. After attaining the steady state, if the oscillator is switched off, a straight-line decay curve is obtained on a logarithmic scale the slope of which gives a measure of the decay time. The response in each isolated normal mode decays exponentially at the natural frequency of that mode. For a 60 dB decay the half-width is given by the relation $B = 2.2/\tau$ where τ is the reverberation time in sec. The decay method serves to check the purity of the modes and provides an independent means of measuring the damping level.

1.9.2 Frequency Response Method

In this classical method, sometimes called the peak-amplitude method, the system is excited harmonically and the vibration response is measured over a range of frequency. Resonance is said to occur when the response amplitude reaches a local maximum. Though simple the method suffers from serious drawbacks which were first exposed by KENNEDY and PANCU [5].

The method is suitable only for high-Q systems without closely spaced resonant frequencies. The major disadvantage of this method is that it takes no account of the phase change near resonance while measuring the half-width. As the driving frequency is swept through resonance the phase undergoes a remarkable change of 180^{o} which can be very informative in the damping measurements.

The identification of the natural frequency as the point of maximum amplitude response suffers from a minor analytical snag. If can be shown that the peaks do not occur exactly at the natural frequency of the system i.e. $\omega_o = \sqrt{k/m}$, but at frequencies slightly displaced one way or the other from ω_o. This discrepancy can be avoided if velocity resonance is considered instead of displacement resonance. The method further assumes that the peak around a singlet arises solely from one

mode and there is no off-resonant contribution in the measured response. The damping is then calculated from the sharpness of the resonance peak by using the relation $Q = \omega_o/B$ where B is the half-width.

1.9.3 The Kennedy-Pancu Method [5]

In this method both the amplitude and phase of vibration are measured and plotted on the Argand plane. Its basis is the geometry of the theoretical Argand diagram, and for a high-Q system with a single degree of freedom it is a circle. The treatment is based on the following assumptions: 1) The contribution from off-resonant vibration is either negligible or constant in the vicinity of a singlet and 2) there is no coupling between the normal modes.

The data reduction technique consists of fitting an equivalent circle through a set of measured data points. The resonance frequency is identified by the maximum frequency spacing technique when the rate of change of arc length attains a local maximum. The half-power points correspond to the ends of the diameter of the circle on either side of the resonance frequency and the damping level is obtained by using the relation $Q = \frac{\omega_o}{B}$ as before.

The main attraction of this method is its ability to separate or identify closely spaced natural frequencies. The response loops in these cases will be more or less distorted and the method provides an easy way of getting "the best fit circle" to measure ω_o and B. The accuracy of determination of these parameters is less affected by the presence of other modes than in the peak-amplitude method. Also, the effect of extraneous vibration is manifested in shifting the response loop to one side or the other so that the displaced origin of the equivalent circle gives a measure of the off-resonant vibration.

1.9.4 Phase Response Method

The idea of using the phase angle plots to measure damping was introduced by PENDERED and BISHOP [23]. There are two ways of doing this. In the first approach the half-width is measured corresponding to points on the

phase response satisfying the relation $\tan\phi = \pm 1$. This is similar to the peak amplitude method and is subjected to the same approximation. The second approach uses the linearity of the phase response curve over the region in the immediate vicinity of resonance in using the relation

$$B = 2/\text{slope } \frac{d\phi}{dp} \quad \text{at resonance}$$

to obtain the half-width (see next chapter for derivation). For a pure mode the natural frequency corresponds to the point where the phase is zero (velocity resonance) or 90° (displacement resonance) on the phase response curve and the slope is measured at this point. To use this relation it is only necessary to measure the phase over a small region around ω_o and the half-width determination does not depend critically on the location of the resonance peak as in the peak-amplitude method. This is a major analytical advantage over the previous methods. The accuracy of these two techniques will depend upon the off-resonant contribution as before.

1.9.5 Phase-Separation Technique

This method was originated by STAHLE and FORLIFER [24]. Here the real part i.e. the inphase component, of the acceleration response of a single-degree-of-freedom system with structural damping troughs just below (ω_b) and peaks just above (ω_a) resonance and is zero at the resonant frequency as shown in Figure 1.2. The loss factor is determined by using the relation

$$\eta = \frac{(\omega_a/\omega_b)^2 - 1}{(\omega_a/\omega_b)^2 + 1}$$

Also resonance is said to occur when the quadrature component of the acceleration response attains its maximum value in either a positive or negative direction. The quadrature response peaks more sharply than the total response and at resonance is equal to the total response.

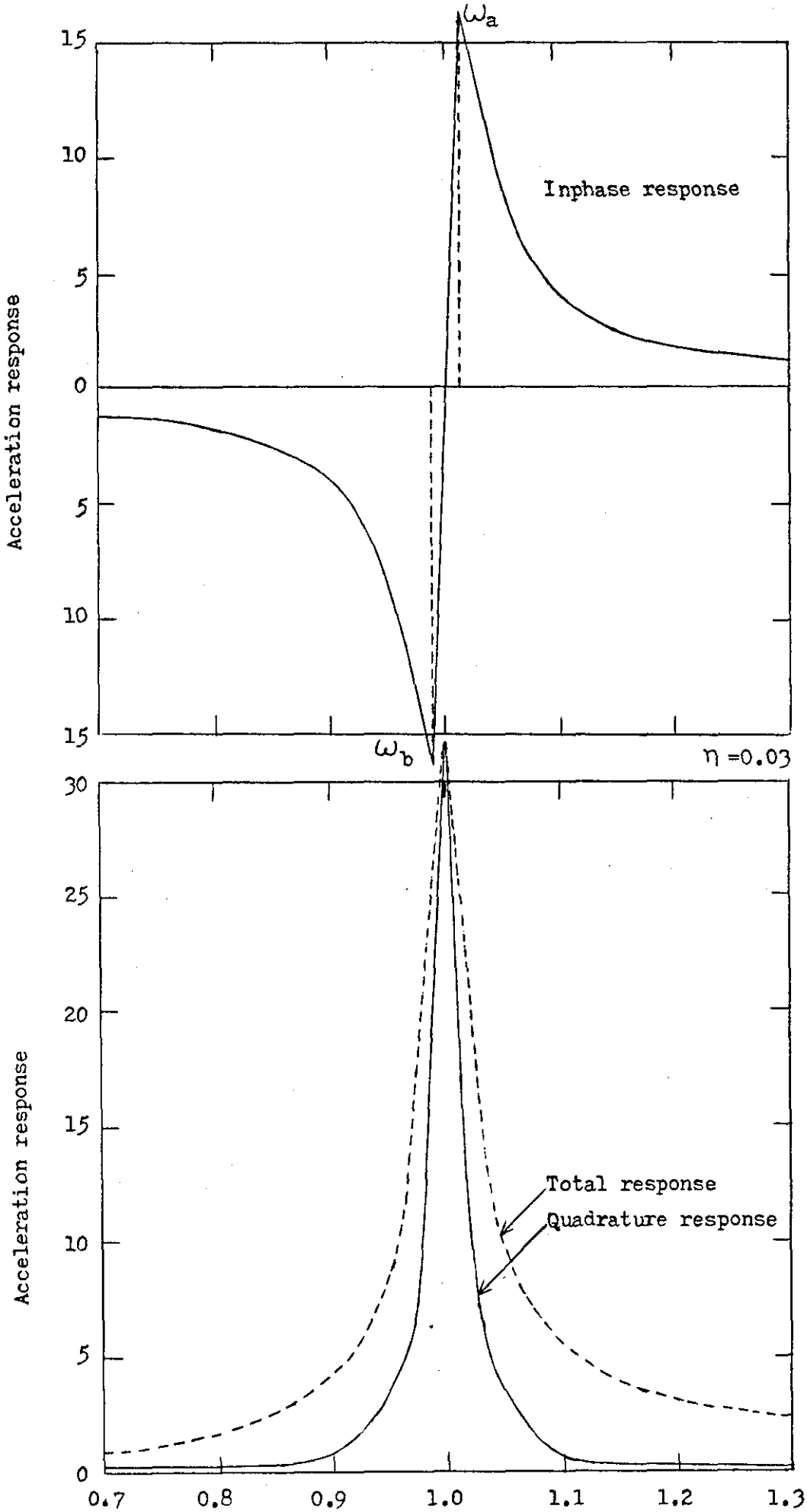

Figure 1.2 Theoretical response of a single-degree-of-freedom system with structural damping.(Reproduced from C.V.STAHLE 1962 Aerospace Engineering 21, 56-57,91-96.Phase separation technique for ground vibration testing.)

1.10 PRESENT INVESTIGATION

The results of the present investigations on symmetrical high-Q systems are given in the next three chapters.

In Chapter II the theory of singlet resonance based on viscous damping is reviewed with the governing equation recast in terms of the resonance frequency ω_0 and half-width B. The effect of extraneous vibration in distorting the response curves is also discussed in a tentative analytical study aimed at finding a practical solution.

In Chapter III a new method for obtaining the separation 2ℓ and half-width B of the components of a close high-Q doublet is described in detail. The theory is tested against the experimental data collected for a typical symmetrical vibrating system.

In Chapter IV an optimisation technique is given to obtain ω_0 and B of a high-Q singlet in the presence of a constant back-ground signal.

In the next four chapters are presented the details of an experimental investigation of the normal modes of vibration of circular rings of rectangular cross-sections.

CHAPTER II

SINGLET RESONANCE

2.1 INTRODUCTION

The study of the behaviour of a forced damped harmonic oscillator is of considerable importance in understanding the vibration response of complicated real structures. The theory of viscous damping is well suited for high-Q systems where it is assumed that the harmonic motion of the equivalent mass introduces a damping force which is proportional to and in phase with the velocity. It transpires that the calculations for a close high-Q doublet are simplified if the controlling differential equation viz. equation (1.1), is recast in a more general form in terms of the natural frequency ω_o and half-width B of the real system and corresponding substitutions are made in the solution. This is advantageous because both ω_o and B are directly measurable quantities whereas the equivalent mass and spring constant k may be difficult to determine. The response peak of such a system, which is due to the contribution of a particular mode, is referred to as a "singlet" for convenience and the purpose of this chapter is to review the theory of the singlet response curves.

2.2 SINGLET RESPONSE CURVE

The modified equation of motion of a forced damped harmonic oscillator can be written as [25]

$$\ddot{x} + B\dot{x} + \omega_o^2 x = A_o \ell^{j\omega t} \qquad (2.1)$$

where ω_o and B, as will be seen, are the resonant radian frequency and the half-width in the velocity response curve for the system.

By using the trial solution of equation (1.2) it can be shown that the velocity response of the system controlled by equation (2.1) is

$$v = \frac{A_o e^{j(\omega t - \phi)}}{\sqrt{B^2 + (\omega - \frac{\omega_o^2}{\omega})^2}} \qquad (2.2)$$

where

$$\tan\phi = \frac{\omega^2 - \omega_o^2}{\omega B} \quad . \qquad (2.3)$$

ω_o is clearly the radian frequency corresponding to the maximum velocity v (max).

In practice it is very difficult to measure the absolute value of v_{rms} but is easy to compare it with $v(max)_{rms}$. Hence it is convenient to define a normalised rms velocity $\alpha = v_{rms}/v(max)_{rms}$. It is also useful to define $P = \omega - \omega_o$, the "detuning" of the radian frequency from resonance. Making these substitutions into equations (2.2) and (2.3) one gets

$$\alpha = \frac{B}{\sqrt{B^2 + P^2(\frac{P + 2\omega_o}{P + \omega_o})^2}} \qquad (2.4)$$

and

$$\tan\phi = \frac{P(P + 2\omega_o)}{B(P + \omega_o)} \quad . \qquad (2.5)$$

Differentiating equation (2.5) with respect to P gives

$$\frac{d}{dP}(\tan\phi) = \frac{1}{B}\left[1 + (\frac{\omega_o}{P + \omega_o})^2\right]$$

which at resonance reduces to

$$\frac{d}{dP}(\tan\phi)\Big|_{P = 0} = \frac{2}{B} \quad ,$$

enabling one to obtain B directly from phase measurements if required.

Now consider the half-power points where $\alpha^2 = \frac{1}{2}$ for which P takes a positive value P_1 and a negative value P_2 respectively. From equation (2.4) we get

$$B = P_1 \left(\frac{P_1 + 2\omega_o}{P_1 + \omega_o}\right) = - P_2 \left(\frac{P_2 + 2\omega_o}{P_2 + \omega_o}\right) \quad , \qquad (2.6)$$

which on rearrangement gives

$$P_{1,2} = - (\omega_o \pm B/2) + \sqrt{\omega_o^2 + (B/2)^2} \quad , \qquad (2.7)$$

so that $P_1 - P_2 = B$, enabling one to identify B with the half-width of the rms velocity vs. radian frequency response curve. Substituting equation (2.6) into equation (2.5) confirms that $\tan\phi = \pm 1$ at the half-power points which gives yet another way of obtaining B from phase response if desired.

2.3 HIGH-Q SINGLET

Restricting consideration to very high values of Q forces the non-negligible values of α to fall within a small range of P values such that $P << \omega_o$. Under these conditions equations (2.4) and (2.5) reduce to

$$\alpha \frac{B}{\sqrt{B^2 + 4P^2}} \qquad (2.8)$$

$$\tan\phi = \frac{2P}{B} \quad . \qquad (2.9)$$

In our work on bells, cones and rings the Q-values generally met are typically of the order of 1000 and above. In such cases the above approximate equations have been found to hold up well provided background signals were insignificant. The latter equation then means that a plot of $\tan\phi$ vs. P should be linear with slope 2/B. Any non-linearity

observed indicates that either 1) equation (2.1) is inappropriate or 2) $P<<\omega_o$ is violated or 3) background vibrations are significant. In any event this gives a sensitive test of whether or not the necessary conditions for equation (2.8) to hold are satisfied. It can be shown further that under high-Q approximation $d(\tan\phi)/dP = 2/B$ for all values of P, and that $P_1 = -P_2$ so that the velocity resonance curve becomes symmetrical with $B = 2P_1$.

If now we define the quality factor

$$Q = \frac{\text{Resonant radian frequency (Vel.)}}{\text{Half-width}}, \quad \text{then } Q = \frac{\omega_o}{B} \text{ is}$$

true for all cases not just for low levels of damping.

By definition $P = 0$ at resonance. This means that the maximum value of $\alpha = 1.0$ and the value of phase is zero at resonance. This is of considerable practical advantage in dealing with relative velocity measurements and in removing the arbitrary nature of the measured phase values by adding or subtracting the value at resonance.

From equation (2.9) we get $\frac{d\phi}{dP} = 2/B(1 + \frac{4P^2}{B^2})$, which at resonance reduces to $\frac{d\phi}{dP}\Big|_{P=0} = 2/B$ as before so that half-width can be obtained in terms of the slope of the phase response at resonance. This relation was first obtained by PENDERED and BISHOP [23] for displacement resonance using the receptance concept.

Thus there are two different ways of obtaining the half-width out of phase response measurements. In the first method the half-width is obtained from the frequency interval between points on the phase response at which $\tan\phi = \pm 1$. This is analogous to the peak amplitude method and is subject to the same approximations. In the second method the half-width is obtained in terms of the slope of the phase response curve at resonance.

In their comparison of the relative accuracy of the above two ways of obtaining the half-width, PENDERED and BISHOP [23] have shown that the second method gave half-width values higher than that for the first

method by a factor $\frac{\pi}{4}$ because of the assumption of linearity of the phase response over the range of the half-width and of the inherent approximation involved in the first method. This discrepancy can be avoided if we take the slope of the $\tan\phi$ vs. P plot which is linear through-out the region of interest.

An analytical study of the effect of linearity on the accuracy of the relation $B = 2/\left(\frac{d\phi}{dP}\right|_{P=0}$ has shown that the accuracy of this method can be improved if the slope determination is really confined to the straight line portion of the characteristic. Over this region the accuracy can be further improved if small dP values of the order of 0.2 rad s^{-1} or so are considered in the immediate vicinity of ω_0.

2.4 INPHASE AND QUADRATURE COMPONENTS

From equation (2.9) it follows that

$$\sin\phi = \frac{2P}{\sqrt{B^2 + 4P^2}} \quad \text{and} \quad \cos\phi = \frac{B}{\sqrt{B^2 + 4P^2}}$$

so that the inphase component of the normalised velocity is

$$\alpha_I = \alpha\cos\phi = \frac{B^2}{B^2 + 4P^2} \tag{2.10}$$

and the quadrature component is

$$\alpha_Q = \alpha\sin\phi = \frac{2BP}{B^2 + 4P^2} \tag{2.11}$$

The response curves for the inphase and quadrature components are shown in Figure 2.1 along with that for α. It is obvious that the inphase component becomes maximum when P = 0 with maximum value of 1.0 as that for α. It can be shown that the quadrature component becomes maximum when $P = \pm B/2$ with maximum value of 0.5. Its value becomes zero at resonance. Moreover the response curve for the inphase component is sharper than that for the total response thereby giving added advantage

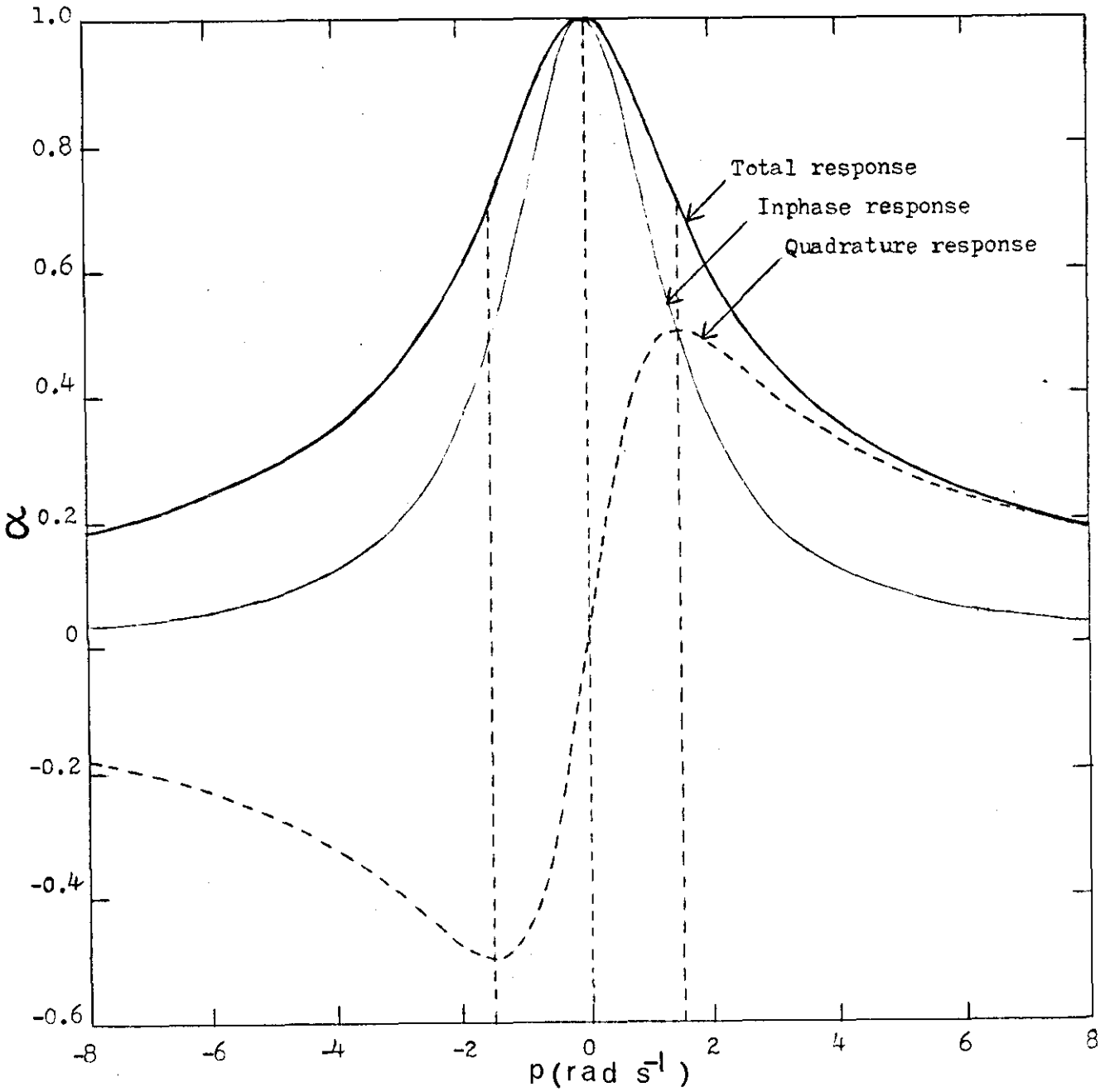

Figure 2.1 Inphase and quadrature components of singlet resonance.

during vibration analysis. The phase separation technique of data reduction is based on separating the inphase and quadrature components during resonance testing [24].

The half-width now is equal to the frequency interval corresponding to points on the inphase response curve where the value of α_I is half its maximum value at resonance. For the quadrature response the half-width now is equal to the frequency interval corresponding to points on the response curve where α_Q reaches its maximum value of 0.5 in either direction.

2.5 EFFECT OF OFF-RESONANT CONTRIBUTION

In the foregoing analysis of singlet resonance it is assumed that each response curve is due to the contribution in one particular mode and that there is no extraneous vibration present in that mode. This ideal condition is seldom realised in practice and the response curves of practical vibrating systems are found to be distorted to some extent due to a variety of reasons which include the closeness of other natural frequencies, modal superposition, over-lapping resonant characteristics due to damping, modal degeneracy etc.

The idea of constant off-resonant contribution was used by KENNEDY and PANCU [5] in formulating their vector technique of modal analysis. They assumed that the off-resonant vibration is constant in amplitude and phase as the system passes through resonance. However, as there is a phase change of nearly π radians as resonance is swept through, the effect of off-resonant vibration on the velocity response above the resonant frequency will be different from the effect below, resulting in the asymmetry of the response curves.

GLADWELL [26] has proposed a method to estimate the loss factor out of a symmetrical peak by taking into account a constant off-resonant contribution in the vicinity of the peak which is assumed to be due to a single mode only. The analysis consists of solving a cubic equation formed from the amplitude response at three points on the response curve viz. the highest point and another two points on one side of the peak, against a constant background.

Of late various authors have dealt with the problem of background contribution and distortion of response curves and mode shapes by using different techniques. EWINS [27] has given a method to estimate the true peak amplitude of a damped structure from an analysis of the undamped response at two frequencies on either side of the resonant frequency in question. SOEDEL and DHAR [28] have formulated an orthogonalisation procedure to determine the number of basic modes contributing to the observed superposition modes.

2.6 A TENTATIVE ANALYTICAL STUDY

In a tentative analytical study of the effect and nature of background contribution in producing asymmetrical response curves the equations (2.10) and (2.11) were used to obtain the following 4 special cases:

(1) $\alpha_I = \alpha\cos\phi + C_1$ $\quad C_1 = 0.1, 0.2, \ldots\ldots$

$\alpha_Q = \alpha\sin\phi$

(Inphase component + constant)

(2) $\alpha_I = \alpha\cos\phi - C_1$

$\alpha_Q = \alpha\sin\phi$

(Inphase component - constant)

(3) $\alpha_I = \alpha\cos\phi$

$\alpha_Q = \alpha\sin\phi + C_2$ $\quad C_2 = 0.1, 0.2, \ldots\ldots$

(Quadrature component + constant)

(4) $\alpha_I = \alpha\cos\phi$

$\alpha_Q = \alpha\sin\phi - C_2$

(Quadrature component - constant)

The total normalised velocity was calculated in each case by adding the inphase and quadrature components vectorially and the resultant phase response was obtained by dividing the quadrature component by

the inphase component. The results are shown graphically in Figures 2.2, 2.3 and 2.4 along with the original undistorted response curves (thick lines).

An examination of these response curves reveals many interesting aspects of off-resonant vibration. The background signals really distort the response curves and shift the peak response frequency to one side or the other of the true resonant frequency - curves (3) and (4) of Figure 2.2. In the absence of any apparent distortion the values of the half-width obtained can be erroneous - curves (1) and (2) of Figure 2.2.

The effect of background signals on phase response curves can be as disastrous as with the velocity response curves. Instead of having zero phase at resonance the response curves get shifted to one side or the other of the undistorted response curve. This introduces serious distortion in the response curves and limits the linear portion of the characteristics - curves (3) and (4) of Figure 2.3. As before, the apparent absence of distortion never ensures the accuracy of the calculated half-width values - curves (1) and (2) of Figure 2.3. Under these conditions the $\tan\phi$ vs. P plots are far from being linear as shown in Figure 2.4.

On plotting the total normalised velocity and the resultant phase of the above special cases in the Argand plane one gets the response circles as shown in Figure 2.5. The fact that the original circle (thick line) is only shifted to one side or the other, depending upon the nature of background signals, instead of becoming distorted, shows the superiority of the vector plots over the conventional methods in dealing with extraneous vibration.

From the above details and the accompanying response curves it is quite obvious that the normal data reduction techniques can never be employed with confidence in dealing with asymmetrical response curves. Although the results of the above special cases can not be interpreted to obtain any useful conclusion, they give an overall picture of what is going on when a resonant mode is affected by background signals.

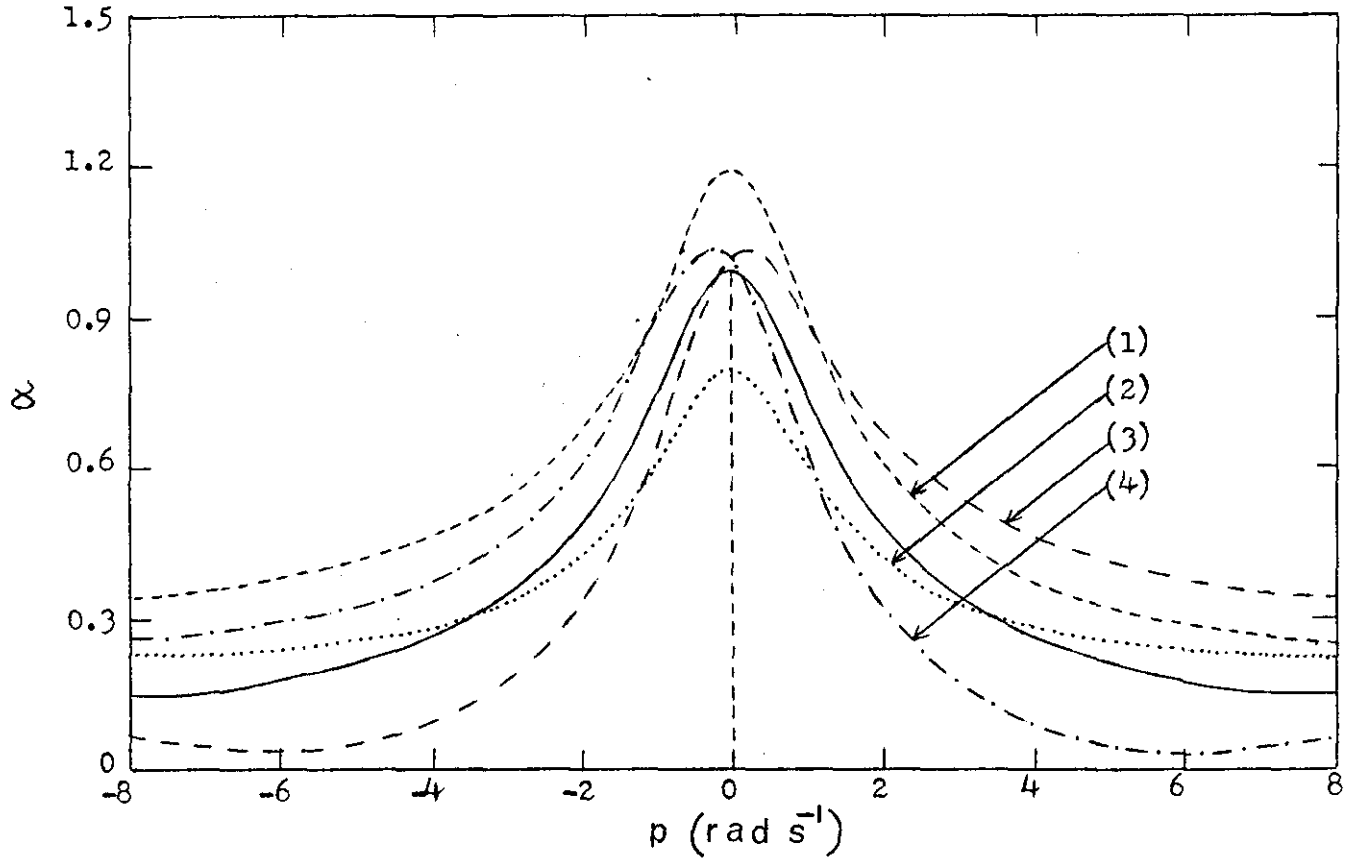

Figure 2.2 Effect of background contribution on normalised velocity response of singlet resonance (solid line: original response curve).

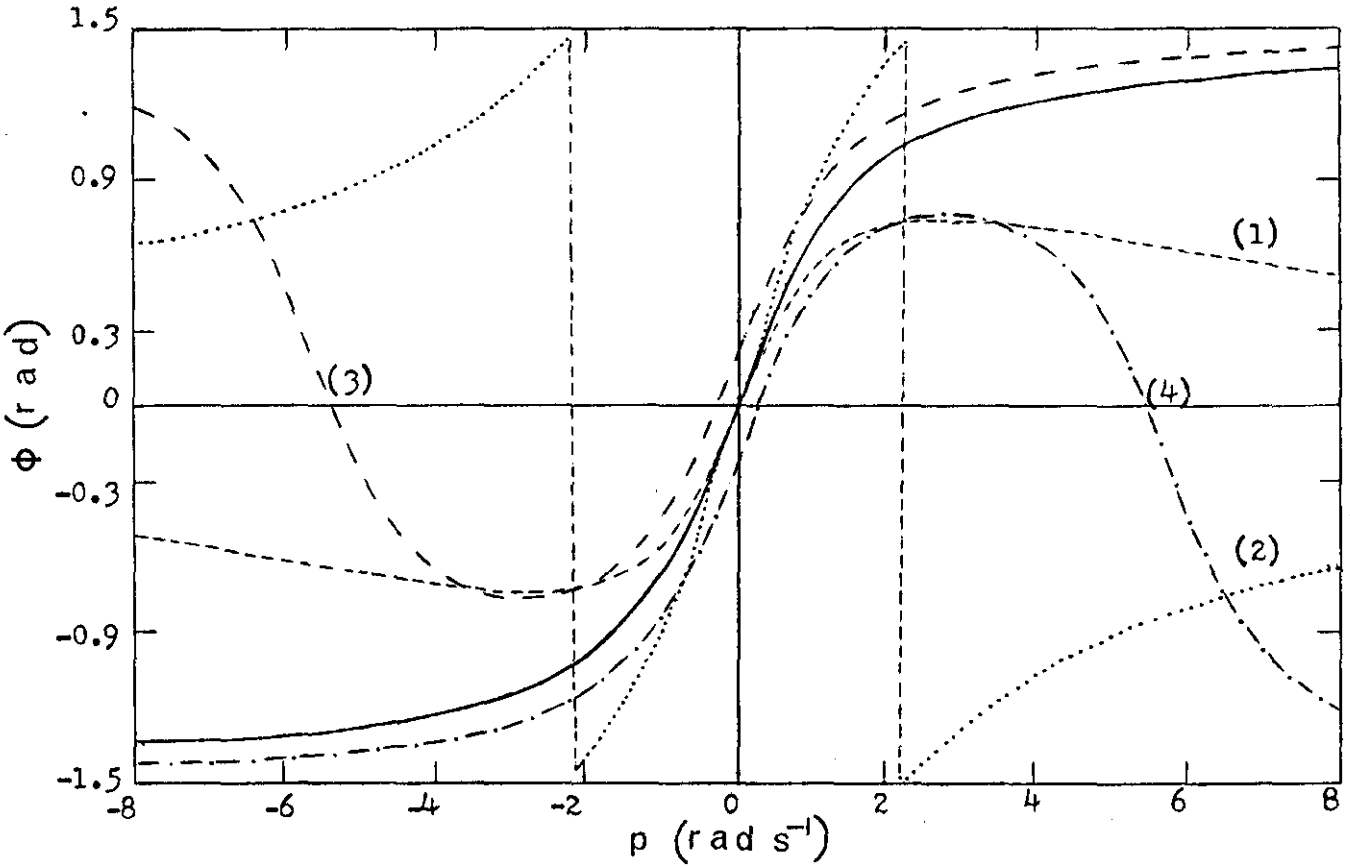

Figure 2.3 Effect of background contribution on phase response of singlet resonance(solid line: original response curve).

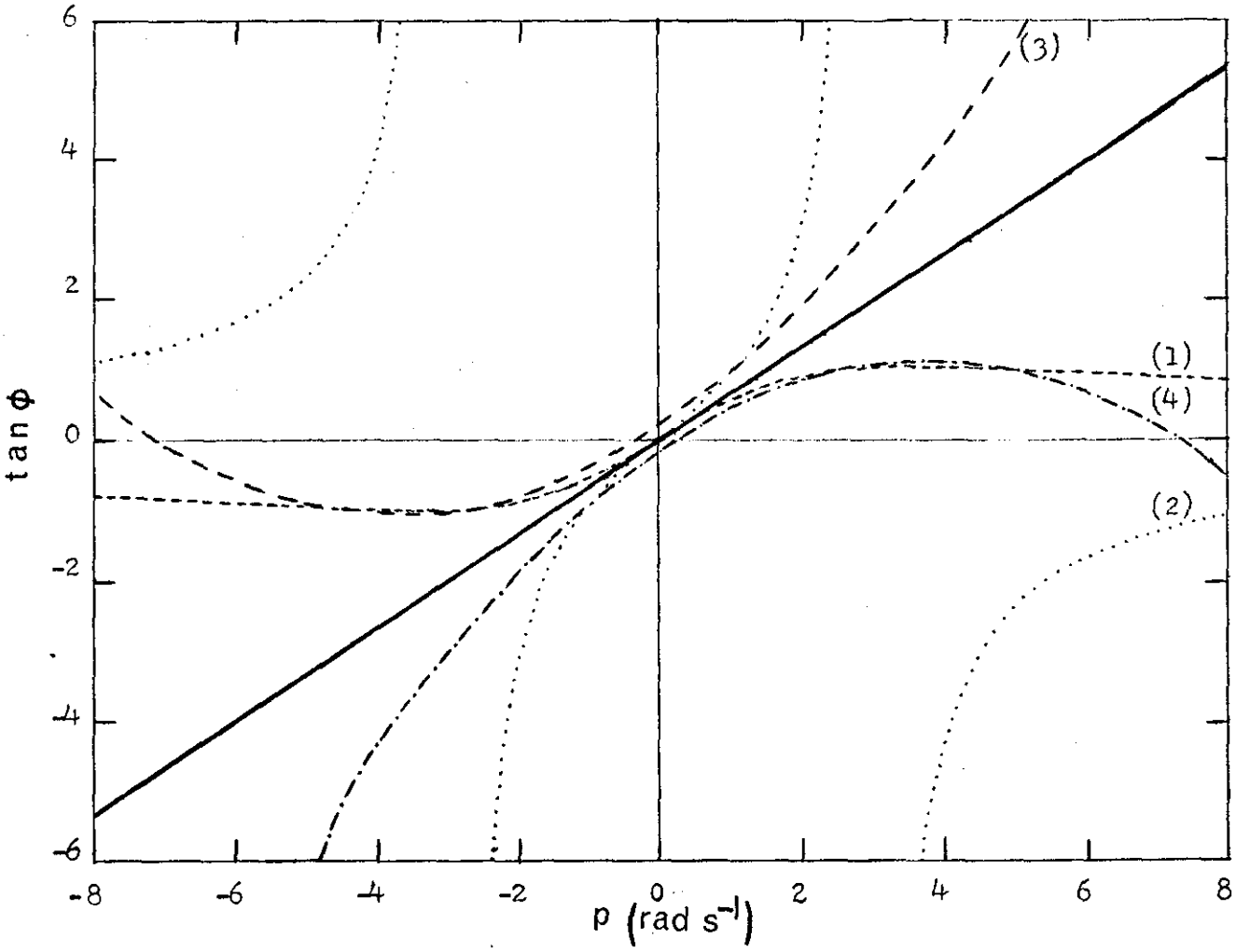

Figure 2.4 Effect of background contribution on tan ϕ vs. p plots of singlet resonance(solid line : original response curve).

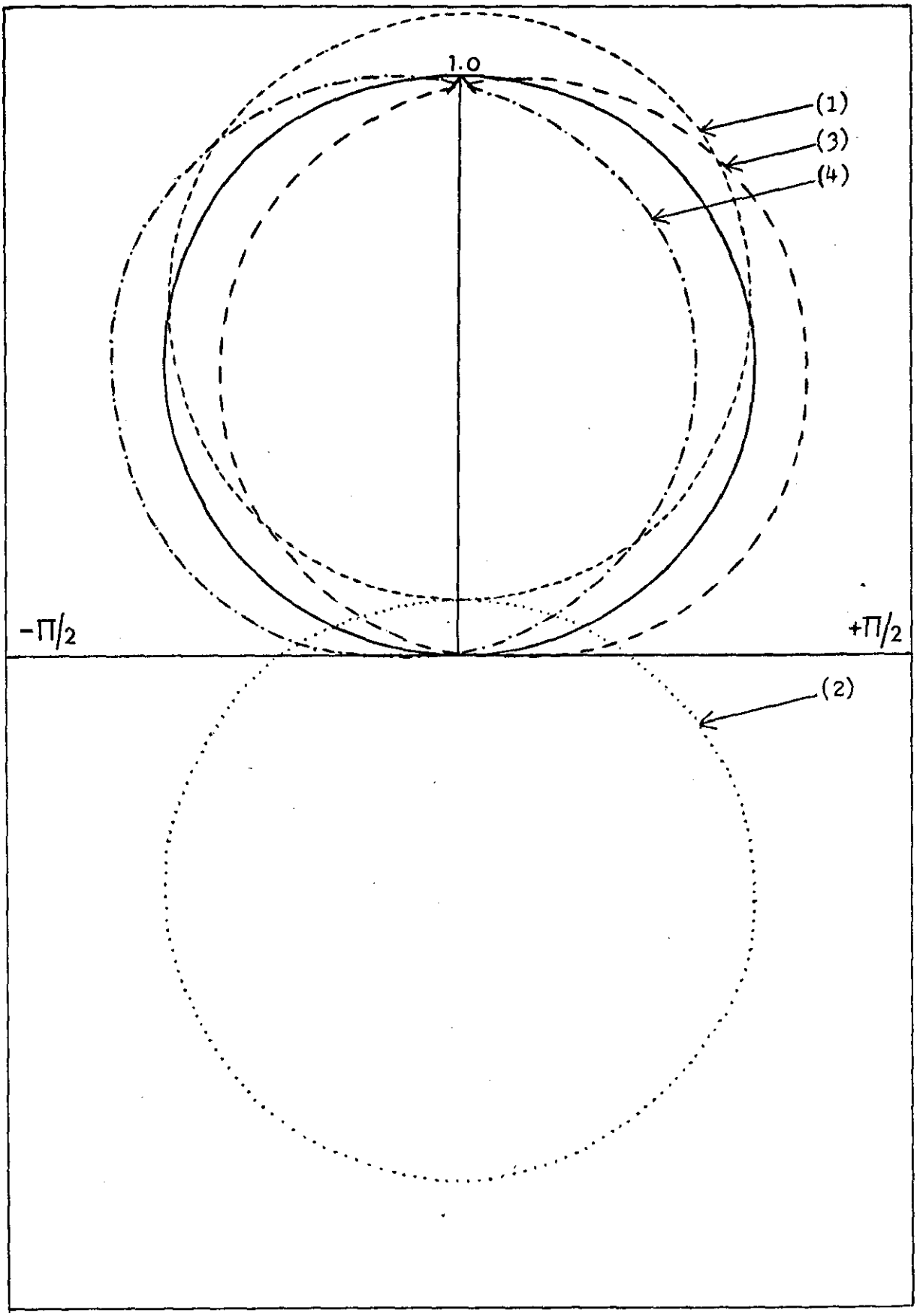

Figure 2.5 Effect of background contribution on vector plots of singlet resonance.

2.7 EXPERIMENTAL EVIDENCE

The above interpretation of the effect of background signals on singlet response curves has helped in the explanation of the velocity and phase responses,obtained in the case of the symmetrical vibrating system of a circular plate suspended freely at three points, as shown in Figure 2.6 (see next chapter for details of the measuring instruments). The plate was excited acoustically with the help of a loudspeker and the vibration response was measured by a capacity transducer.

The observed response curves are similar to those shown in Figures 2.2 and 2.3 for the case of inphase component minus background contribution. Obviously there is no distortion present in the velocity response curve and the phase response shows the peculiar nature of going beyond $\pm\pi/2$ radians towards the tails of resonance. This experimental evidence strongly supports the correctness of the overall approach in dealing with off-resonant vibration.

2.8 A PRACTICAL SOLUTION

In dealing with practical vibration problems one is not certain about the level and nature of the background signals present in the system. Hence one has to rely entirely on the experimental observations in calculating the half-width and resonant frequency. Although vector plots are able to differentiate extraneous contributions effectively, their usefulness is limited in practice due to a variety of reasons. First of all, one has to observe the velocity and phase values at constant frequency intervals. As the system passes through resonance, the rapid changes in velocity and phase offer considerable difficulty in taking observations. Then, there is the process of fitting an equivalent circle through the plotted data points, and finally one has to determine the resonant frequency by maximum frequency spacing technique. All these operations can introduce varying degrees of inaccuracy in the calculated values of ω_0 and B their overall magnitude can be of the same order as in the peak-amplitude or phase method. All these difficulties can be avoided if one can account for the main factors which distort the theoretical response curves using the least-squares curve-fitting technique. The details and formulation of this method are given in Chapter IV.

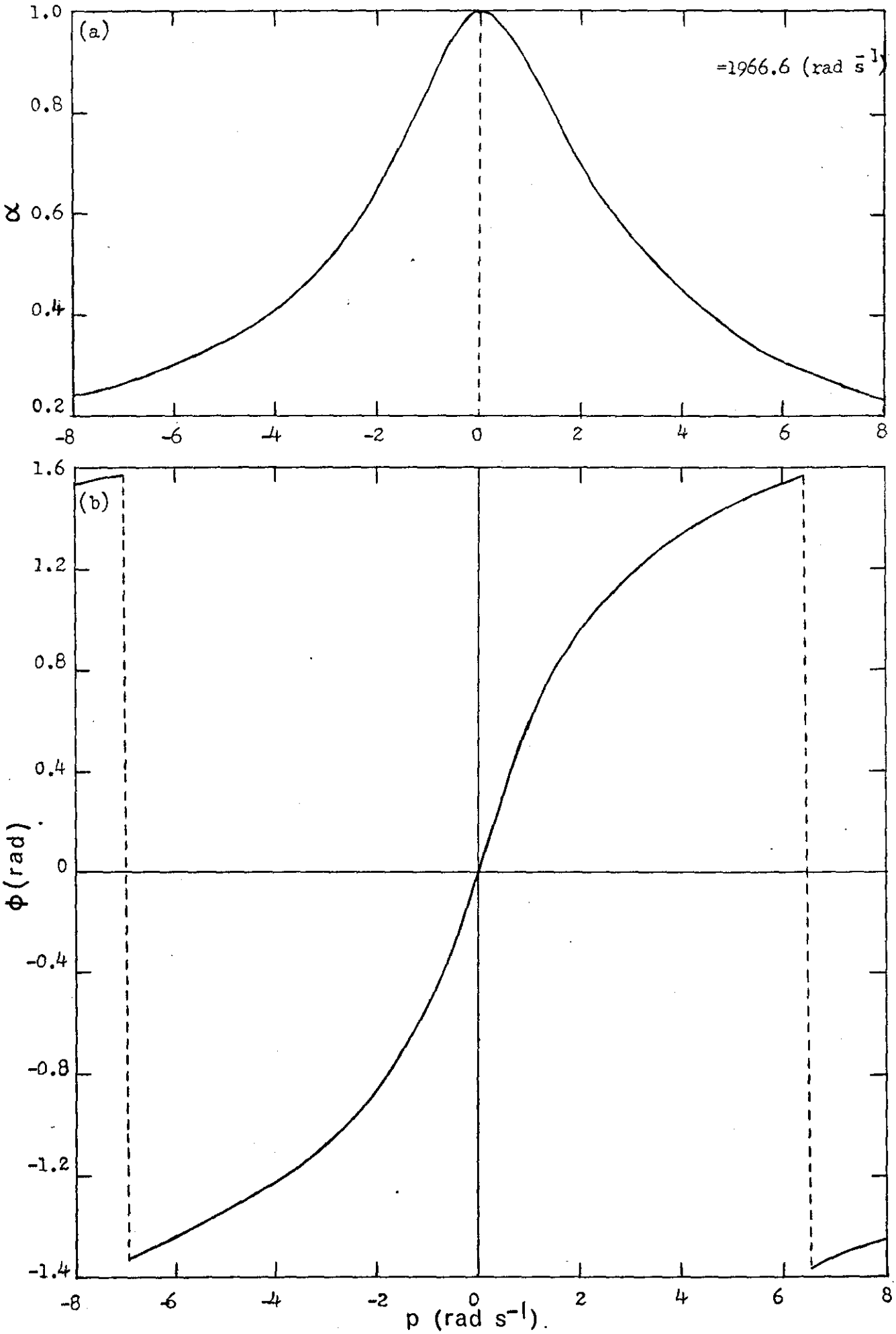

Figure 2.6 Experimental response curves of a high-Q singlet
(a) velocity response (b) phase response.

CHAPTER III

DOUBLET RESONANCE

3.1 INTRODUCTION

The phenomenon of doublet resonance is a peculiarity of axi-symmetric vibrating systems in which the characteristic eigen-frequencies split slightly under conditions of geometrical or metallurgical imperfections. As these are often mistakenly identified as closely spaced natural frequencies, they are unique in many respects: both components have equal Q-values; negligible coupling exists between them and there is also a well defined separation between the components satisfying certain selection rules [3]. Under normal excitation procedures, often one component predominates over the other, as both are not excited equally. Hence in order to find the separation and half-width of the components of a close high-Q doublet, the easiest way is to excite and measure at an "equal-amplitude point" [2] midway between the nodal/antinodal meridians of the two components. As the driving frequency is swept through a double peak, as shown in Figure 3.1(a), is obtained. By exciting the system at the "symmetry" radian frequency ω_m of the double peak response curve until a steady state is reached and then switching off the drive a beating decay is obtained with the beating frequency being equal to the component separation of the doublet. This method becomes useless as the splitting becomes so small that the beat period exceeds the decay time. The response curve still shows a double peak and the method described below enables one to obtain the separation and half-width of the components from the shape of the response curve [25].

3.2 CLOSE DOUBLET RESPONSE CURVE

The response curve of a close doublet measured at an equal amplitude point, as shown in Figure 3.1(a), is the result of adding vectorially two similar singlet responses whose resonant frequencies differ by an amount of the order of their common half-width, as shown in Figure 3.1(b). Let the two components of the doublet be designated by A and B and let ω_A and ω_B be their resonant radian frequencies. It is now

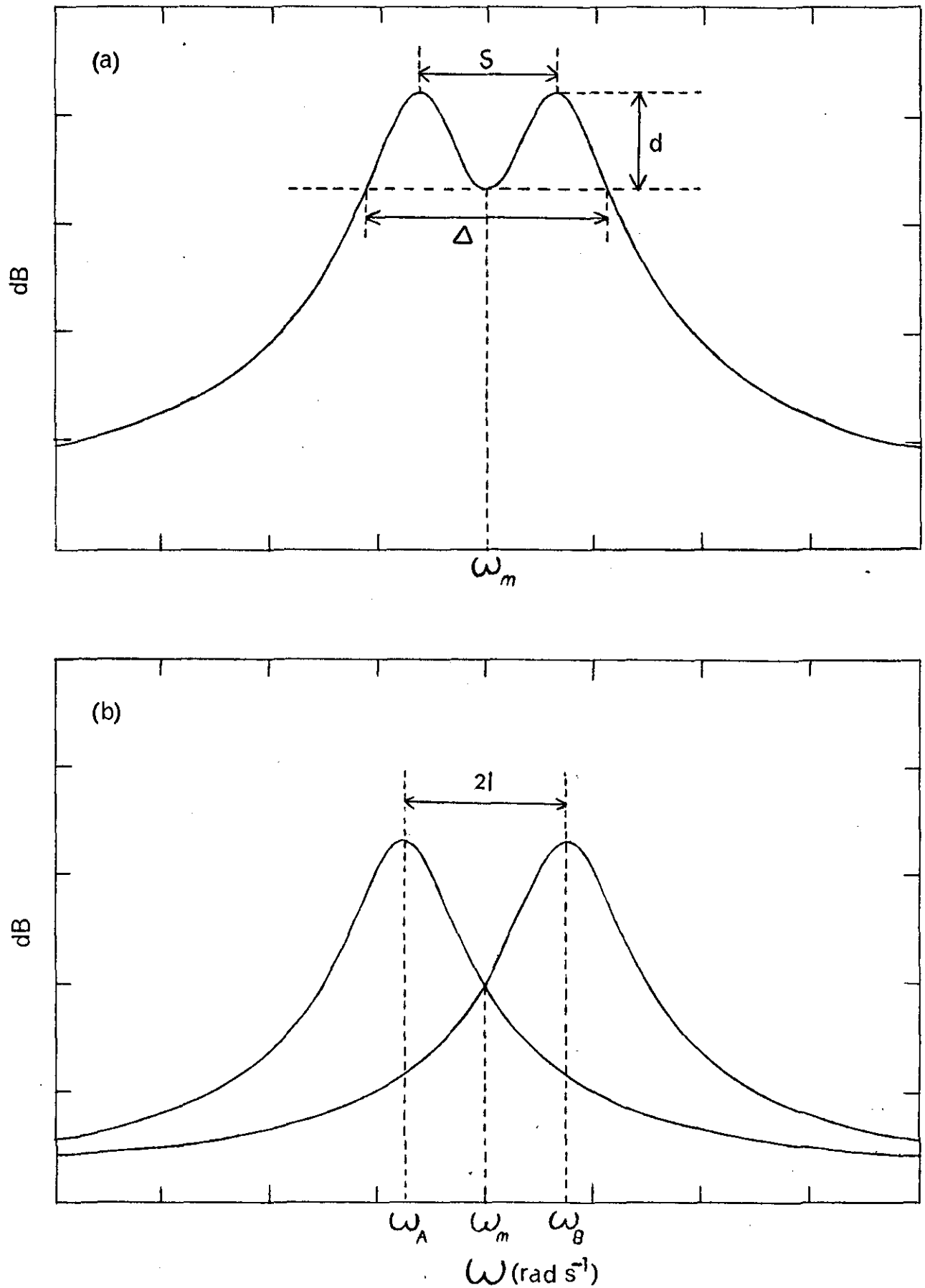

Figure 3.1 (a) Response curve of a close doublet measured at an equal amplitude point; (b) the components which add to give the response curve in (a).

convenient to measure the de-tuning q from the symmetry radian frequency ω_m by defining $q = \omega - \omega_m$. Thus in applying the singlet formulae to component A one must put $P = q + \ell$ while for component B the substitution must be $P = q - \ell$, where $\ell = \omega_B - \omega_m = \omega_m - \omega_A$.

Using equations (2.10) and (2.11) of the previous chapter one can now write the sum of the inphase components as

$$\beta_I = \frac{B^2}{B^2 + 4(q + \ell)^2} + \frac{B^2}{B^2 + 4(q - \ell)^2}$$

and that for the quadrature components as

$$\beta_Q = \frac{2B(q + \ell)}{B^2 + 4(q + \ell)^2} + \frac{2B(q - \ell)}{B^2 + 4(q - \ell)^2}$$

so that

$$\tan\Phi = \frac{\beta_Q}{\beta_I} = \frac{2q}{B} \times \frac{B^2 + 4(q^2 - \ell^2)}{B^2 + 4(q^2 + \ell^2)} \qquad (3.1)$$

It follows from this that $\Phi = 0$ for $q = 0$ and for $B^2 + 4(q^2 - \ell^2) = 0$, the second of the conditions giving $q = \pm\sqrt{\ell^2 - B^2/4}$.

Figure 3.2 illustrates the shapes of the Φ vs. q curves when $2\ell > B$, $= B$, $< B$ respectively. The spacing δ becomes zero at $2\ell = B$: i.e., when the separation of the components is equal to their common half-width. Provided B is known, e.g. from decay measurements at a node/anti-node point, and $2\ell > B$ it is possible to obtain a value for 2ℓ from the observed value of δ by using $\delta = 2\sqrt{\ell^2 - B^2/4}$.

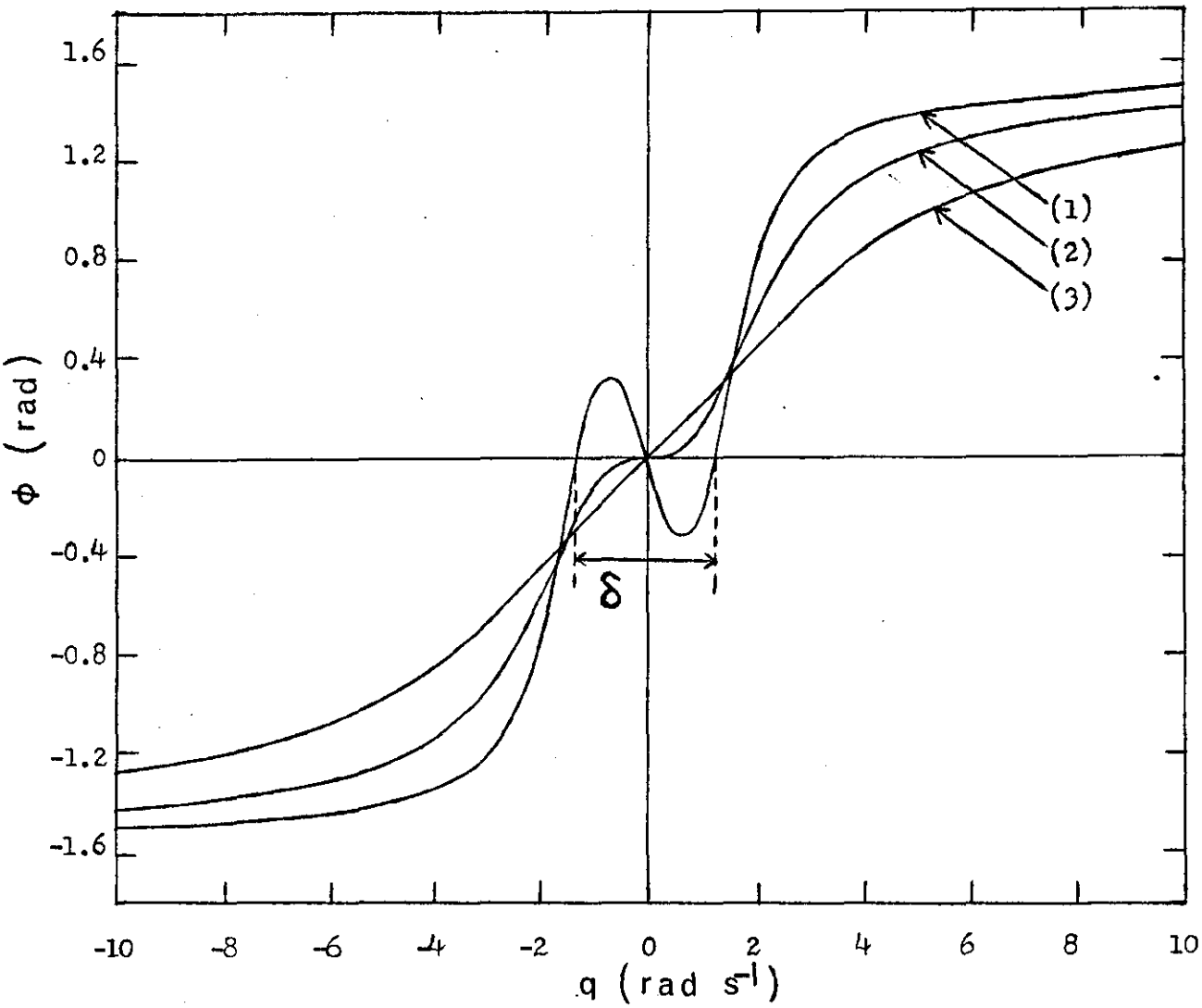

Figure 3.2 Phase as a function of detuning.
(1) $2\lambda = 3$ rad s^{-1} and $B = 1.5$ rad s^{-1}.
(2) $2\lambda = 3$ rad s^{-1} and $B = 3.0$ rad s^{-1}.
(3) $2\lambda = 3$ rad s^{-1} and $B = 6.0$ rad s^{-1}.

Differentiating equation (3.1) with respect to q yields

$$\sec^2\phi \frac{d\phi}{dq} = \frac{2}{B} \frac{B^2 + 4(q^2 - \ell^2)}{B^2 + 4(q^2 + \ell^2)} + \frac{2q}{B} \frac{d}{dq}\left[\frac{B^2 + 4(q^2 - \ell^2)}{B^2 + 4(q^2 + \ell^2)}\right],$$

which at q = 0 reduces to

$$\frac{d\phi}{dq} = \frac{2}{B} \frac{B^2 - 4\ell^2}{B^2 + 4\ell^2} = m \quad . \tag{3.1.1}$$

But $\delta = 2\sqrt{\ell^2 - B^2/4}$ so that $4\ell^2 = \delta^2 + B^2$. Substituting for $4\ell^2$ in equation (3.1.1) one gets

$$B^3 + \frac{\delta^2}{2} B + \frac{\delta^2}{m} = 0, \tag{3.2}$$

which is a reduced cubic equation in B which can be solved either by using Cardan's solution or by successive approximation. Thus B is obtained in terms of the slope at ω_m and the observed value of δ.

The combined rms velocity, β, normalised on the maximum rms velocity of one component, is given by

$$\beta^2 = \beta_I^2 + \beta_Q^2 = \frac{4B^2(B^2 + 4q^2)}{B^4 + 8B^2(q^2 + \ell^2) + 16(q^2 - \ell^2)^2} \cdot \tag{3.3}$$

β^2 will be maximum when $\frac{d(\beta^2)}{dq} = 0$: i.e. the maxima in Figure 3.1(a) lie at

$$q_{max} = \pm \tfrac{1}{2}\sqrt{4\ell(B^2 + \ell^2)^{\frac{1}{2}} - B^2} \quad . \tag{3.4}$$

The radian frequency separation between the observed peaks is therefore

$$S = \sqrt{4\ell(B^2 + \ell^2)^{\frac{1}{2}} - B^2} \qquad (3.5)$$

The two peaks merge to a single flattened peak when $B^4 = 16\ell^2(B^2 + \ell^2)$, which corresponds to $\ell = 0.243B$: i.e. when the separation of the components, 2ℓ, is a little less than half their half-width. Hence for a doublet to occur ℓ should be greater than $0.243B$.

3.3 A NUMERICAL ANALYSIS

Rearrangement of equation (3.5) yields

$$\frac{S}{B} = \sqrt{K(K^2 + 4)^{\frac{1}{2}} - 1} \qquad (3.5.1)$$

where $K = 2\ell/B$. Now one can evaluate S/B numerically as a function of K. Then by dividing each value of K by the corresponding value of S/B one gets $2\ell/S$ as a function of S/B as shown in Figure 3.3. From this figure one can see that (a) for $S/B>7$ the observed separation S agrees with the true separation 2ℓ of the components to better than 1%, (b) for $S/B>0.7$ the observed peaks are always separated more than the components but the discrepancy is never more than about 10%, and (c) for $S/B<0.7$ the observed peaks are closer than the components and $2\ell/S$ increases very rapidly as S/B decreases.

As has been mentioned earlier the main objective of this investigation was to find a method for obtaining the separation and half-width of the doublet components when the beating-decay method can not be used. A reasonable estimate for the limit of usefulness of the beating-decay method is obtained by requiring that at least one beat should occur during the time for a 30dB decay, which may be expressed as $2\ell/B>0.91$. Thus one is seeking a method which is useful in the region $2\ell/B\lesssim 1$. The other methods so far considered - involving measurement of δ, m, and S - are useless in this region.

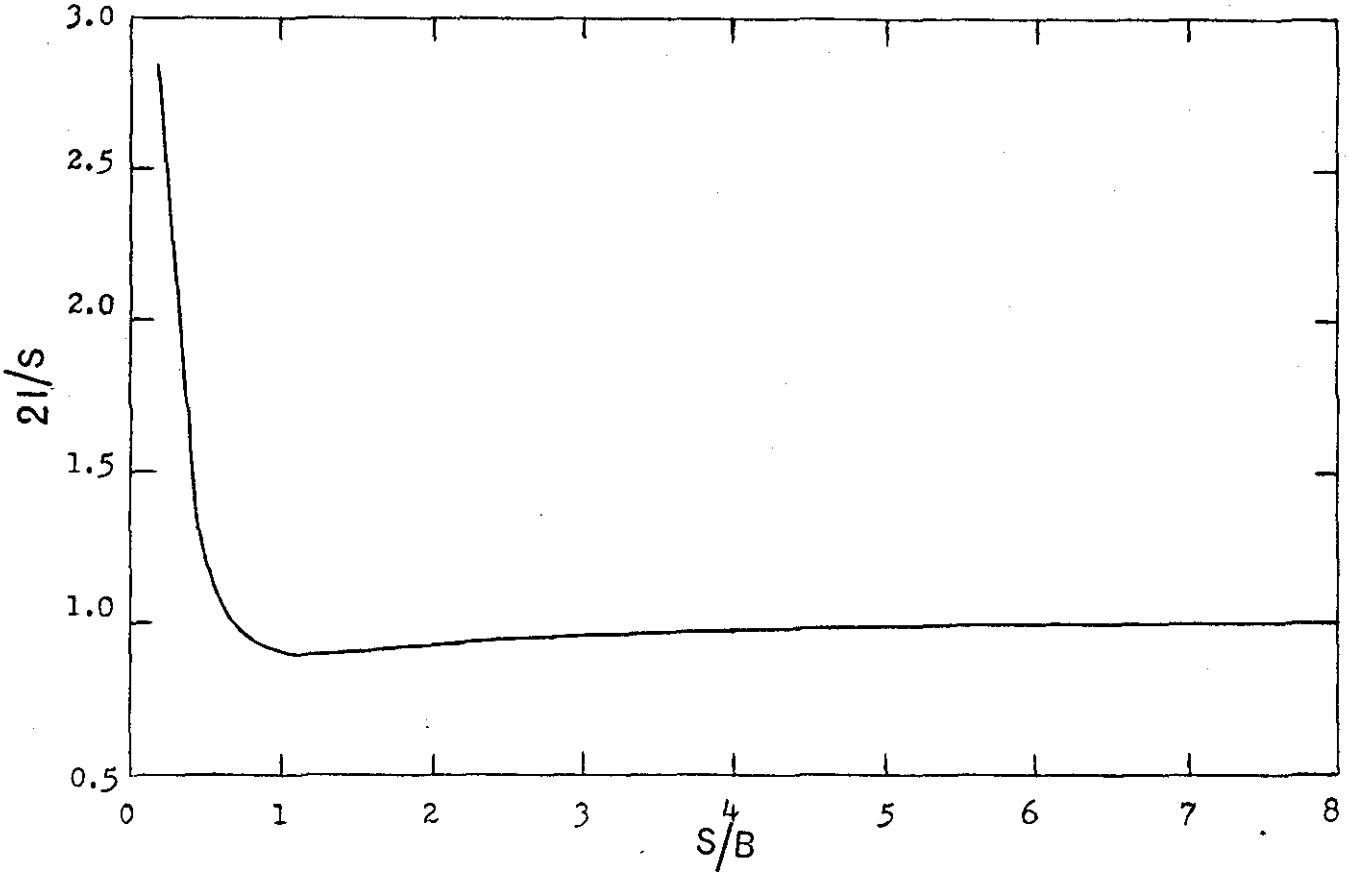

Figure 3.3 2l/S as a function of S/B.

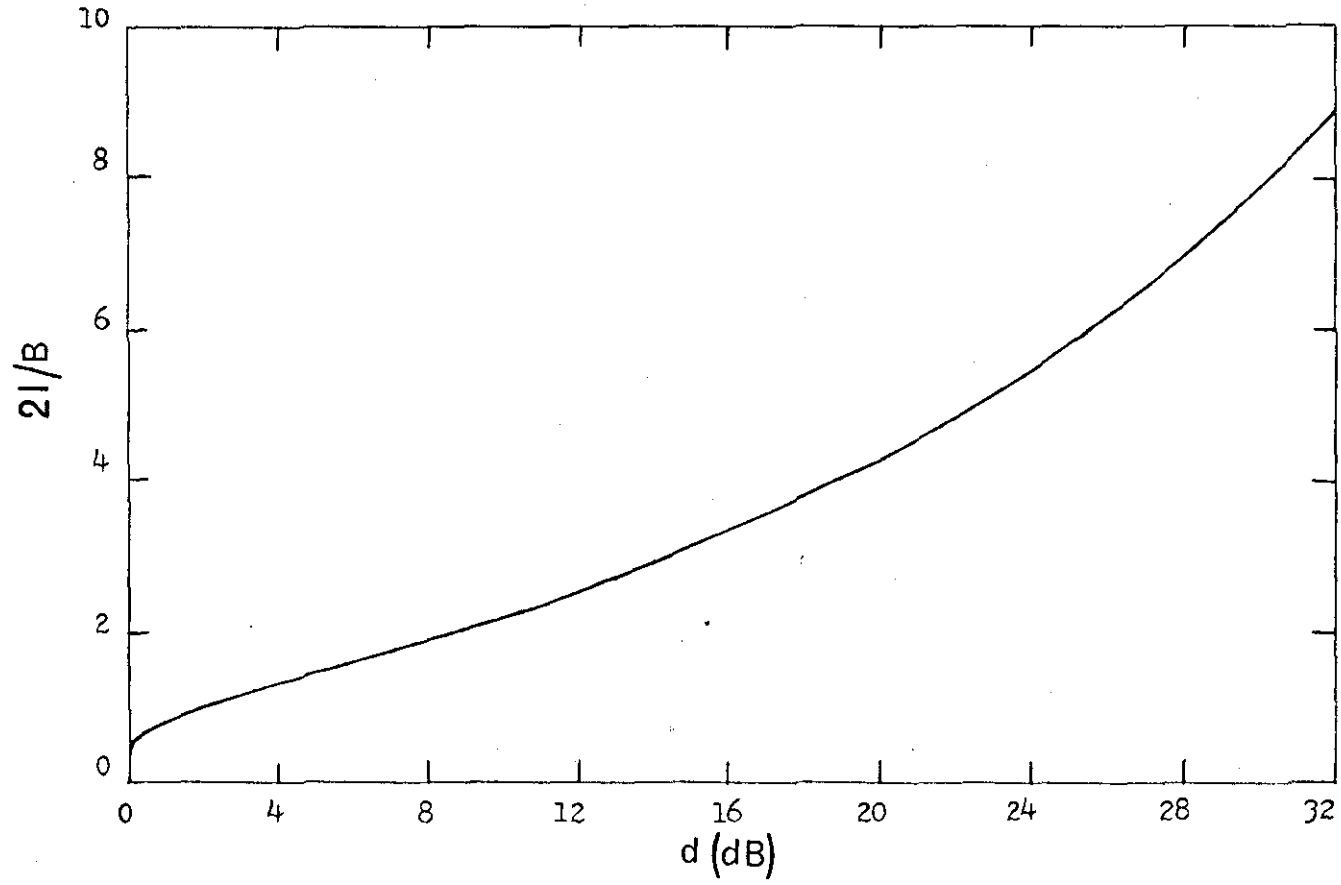

Figure 3.4 2l/B as a function of d.

Another practical disadvantage of the S measurement is that in the region of interest the observed peaks become so flat that the radian frequencies of the two maxima can not be measured accurately. However, this flatness means that considerable precision can be achieved in measuring the "dip", d, of the curve in Figure 3.1(a). This quantity is conveniently expressed in decibels as $d = 10 \log(\beta^2_{max}/\beta^2_{min})$. Substituting for q in equation (3.3) from equation (3.4) yields

$$\beta^2_{max} = \frac{B^2}{2\ell(\sqrt{B^2 + \ell^2} - \ell)} \qquad (3.6)$$

while putting $q = 0$ in equation (3.3) gives

$$\beta^2_{min} = \frac{4B^4}{(B^2 + 4\ell^2)^2} \qquad (3.7)$$

so that

$$d = 10 \log \left[\frac{(B^2 + 4\ell^2)^2}{8B^2\ell(\sqrt{B^2 + \ell^2} - \ell)}\right] = 10 \log \left[\frac{(1 + K^2)^2}{4K(\sqrt{1 + K^2/4} - K/2}\right], \qquad (3.8)$$

where $K = 2\ell/B$ as before. Equation (3.8) can be used to calculate d numerically as a function of Kso as to produce Figure 3.4.

As the end slopes of the curve in Figure 3.1(a) are very steep the quantity Δ, the radian frequency difference between the two points on the curve having the same value of β as the central minimum, can be measured with some precision. Therefore by putting $q = 0$ and $q = \Delta/2$ in equation (3.3) and equating one can get

$$B^2\Delta^2 + B^4 - 16B^2\ell^2 - 16\ell^4 = 0$$

which on rearrangement becomes

$$(\Delta/B)^2 = K^4 + 4K^2 - 1 \ . \qquad (3.9)$$

Given experimental values for d and Δ one can obtain 2ℓ and B as follows:

Using Figure 3.4 one can read off the value for K corresponding to the measured value of d (A more accurate value for K can be obtained by using this initial value to solve equation (3.8) by successive approximation). Substituting the value of K so obtained in equation (3.9) one gets Δ/B, whence B since Δ is known, and then 2ℓ can be found from $K = 2\ell/B$.

Using the same numerical values for K in the construction of Figures 3.3 and 3.4 enables the information to be recast into a plot of $2\ell/S$ vs. d as shown in Figure 3.5. The curve is very useful in getting an estimate of the error introduced by taking the observed peak separation S as the true separation 2ℓ. If, for example, the dip d observed on the response curve is 18dB then one can see from Figure 3.5 that the true separation of the two components is 97% of the separation of the observed peaks.

3.4 EXPERIMENTAL SET-UP

In order to measure the separation and half-width of the components of a close doublet of a symmetrical vibrating system the experimental set-up shown in Figure 3.6 was used.

A steel disc of 250 mm in diameter and of thickness 1.0 mm supported rigidly at its centre in a horizontal plane constituted the vibrating system. The driving system consisted of an oscillator and a magnetic tranducer. The oscillator frequency could be adjusted manually to within 0.1Hz, or swept mechanically at any of several speeds from a logarithmic recorder. The detector system consisted of a capacity pick-up feeding into a measuring amplifier and a slave filter following the

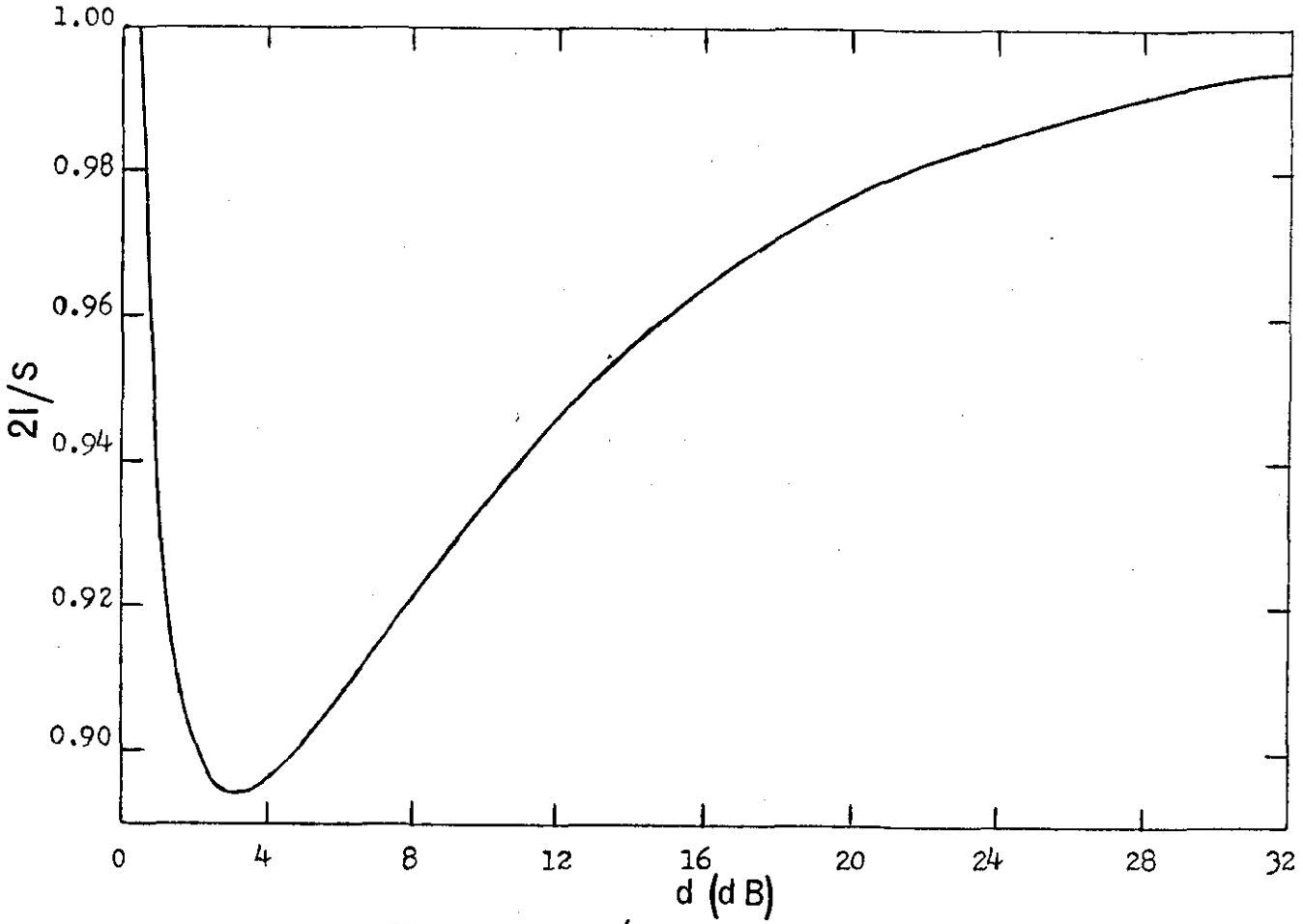

Figure 3.5 2I/S as a function of d.

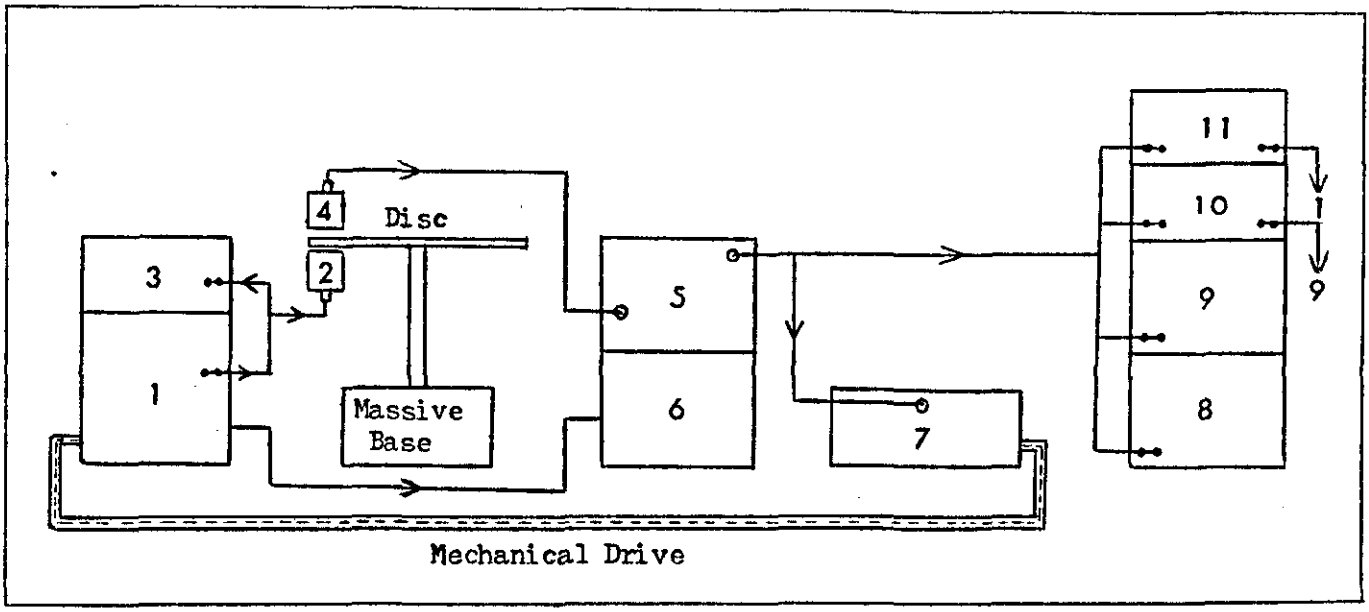

1. B & K Beat frequency oscillator Type 1022.
2. B & K Magnetic Transducer Type MM0002.
3,9. Advance Instruments Timer-counter Type TC9B/S.
4. B & K Capacity Transducer Type MM0004.
5. B & K Measuring amplifier Type 2606.
6. B & K Heterodyne slave filter Type 2020.
7. B & K Level recorder Type 2305.
8. Solartron oscilloscope.
10. Leveller of reference [29].
11. B & K Phase meter Type 2971.

Figure 3.6 Experimental set-up.

frequency of the oscillator. The output of the measuring amplifier was then fed into an oscilloscope, a level recorder and a counter.

The disc was excited at a point near the rim from below with the magnetic transducer. The capacity pick-up was held directly above this. The positioning of the magnetic transducer was critical in driving the system in the linear region where each singlet showed a straight line decay on a logarithmic scale on cutting off the input power. If the magnetic transducer was kept very close to the disc surface eddy current damping might cause non-linearity in the decay curves. A number of trial measurements involving different separations between the magnetic transducer and the disc surface had helped to find an optimum distance of 0.6-0.7 mm necessary for obtaining linear decay curves. Moreover, the input power fed to the transducer was found to affect the linearity at this optimum separation. An input voltage of about 10-15V @ 6000 Ω of the oscillator output impedance was found to give linear decay curves in majority of the cases.

To ensure that the two components of the doublet get excited with equal ease it was necessary to keep the capacity transducer at the same azimuth and as close as possible to the driver while making measurements around equal amplitude points [2]. This positioning is also critical during measurements at node/antinode point around a singlet. Attaching a narrow probe to the capacity pick-up had helped to locate the positions of the equal amplitude points and the singlets without much difficulty.

3.5 TEST OF THE NEW METHOD

There are three different ways of collecting information from the above experimental set-up.

The first set of measurements was made at an equal amplitude point where the response curve on a logarithmic plot had the shape shown in Figure 3.7. The positioning of the disc for equal amplitude measurements was very critical and the peaks were usually taken as being of equal height when they differed by less than 0.2dB. THe frequency and the voltage output - which was proportional to velocity - were measured at five

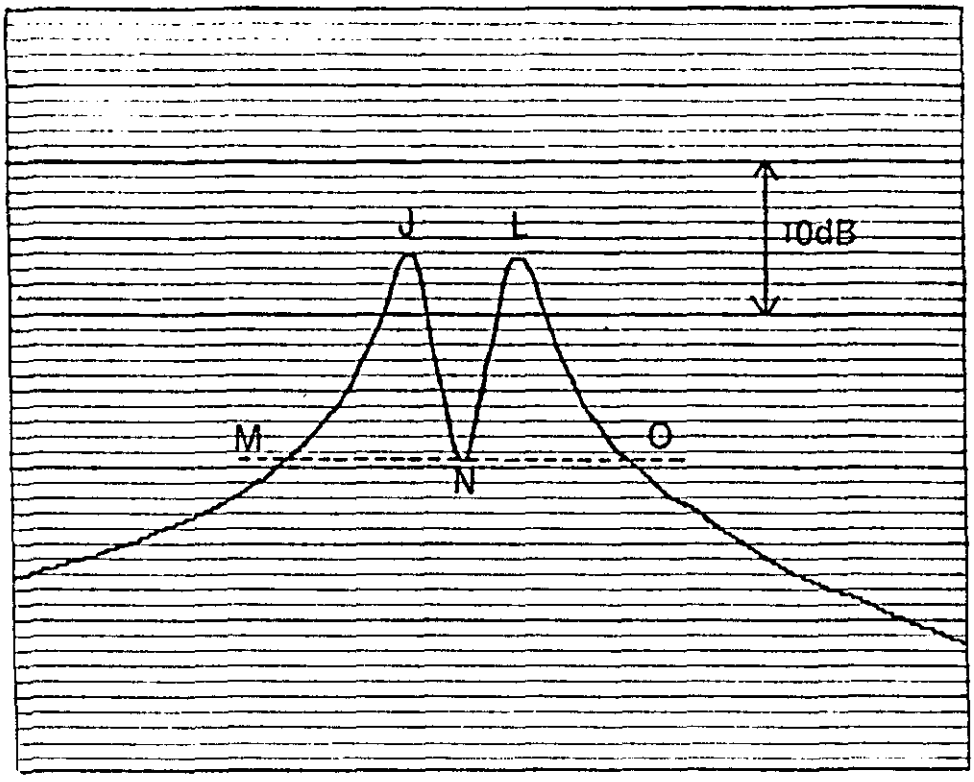

Figure 3.7 An example of a close doublet seen at an equal amplitude point.

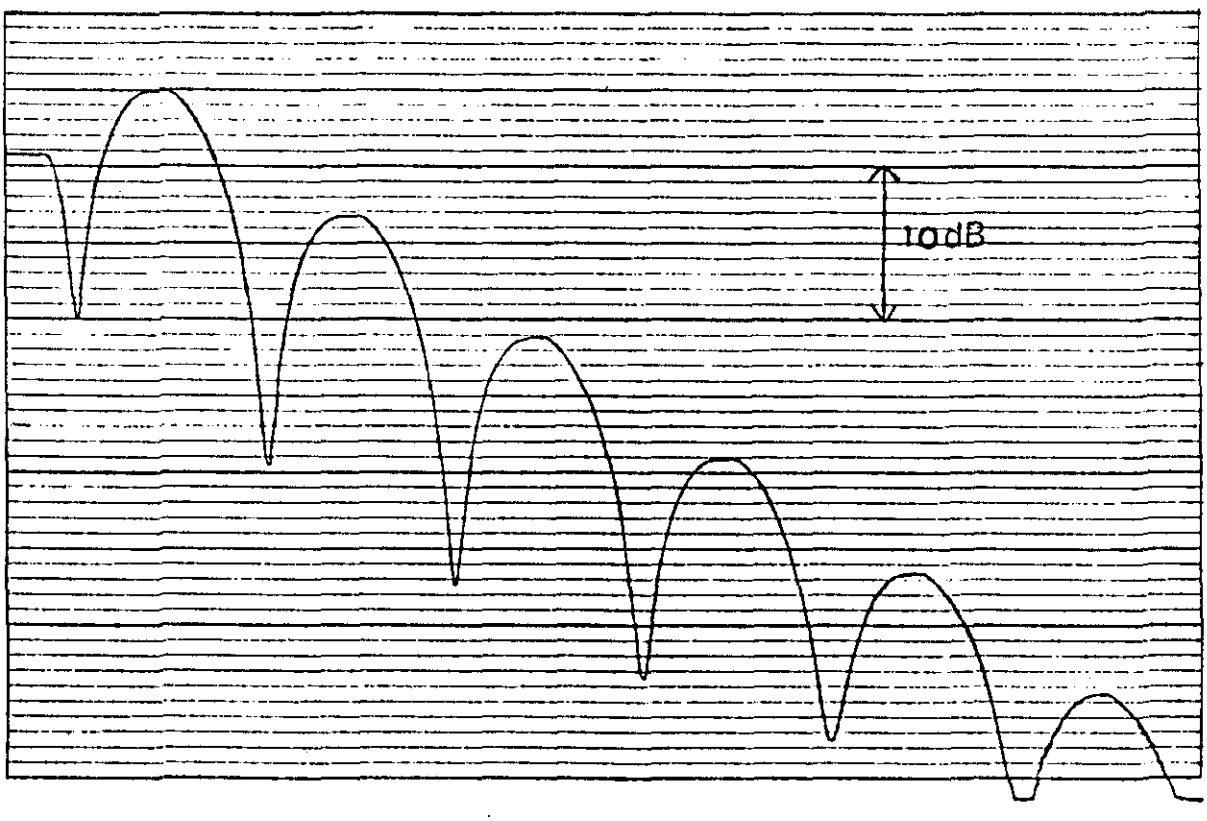

Figure 3.8 A typical beating-decay curve of a close doublet.

key points and are given in Table 3.1. The mean value of the voltages at J and L was used in the calculation for d. The values of 2ℓ and B obtained from these measurements are listed under "New Method" in Table 3.3.

Next, the frequency was adjusted to that of N at the same equal amplitude point. On switching off the input power from the oscillator a beating-decay was obtained on a logarithmic scale as shown in Figure 3.8. The common tangent to the tops of the beats gave the reverberation time τ, whence B was obtained by using $B = 2.2/\tau$. The results are presented in Table 3.3 under the heading "Beating-decay".

It has to be noted that there must be a common tangent to *all* the beats, as otherwise the system is behaving in a non-linear manner which invalidates both the above methods. To ensure that the system was in a linear regime the frequency was adjusted to that of N and then the velocity was increased to that previously measured at the peak J before cutting off the input power. A genuine common tangent to the beats then guaranteed that the system was behaving linearly throughout the investigation of that particular doublet.

The third method used was the "direct" one of driving and measuring first at an antinode of one component and then at an antinode of the other. The positioning of the disc is not so critical in the measurement of B as one can obtain a straight line decay on a logarithmic scale at a point midway between two adjacent equal amplitude points. The values of B obtained from these measurements are shown in Table 3.2.

The main disadvantage of the direct method lies in the determination of 2ℓ as a small difference between two large numbers. Starting at an antinode for the lower frequency component if one gradually moves towards the antinode of the other component, an apparent singlet will be observed throughout except for a very small region near the equal amplitude point. The frequency of this apparent singlet will vary gradually from that of the lower frequency component to that of the higher. Only at the antinode position the peak will show the exact value of the frequency, the frequencies being slightly different on

TABLE 3.1

Measurements at an equal amplitude point

Mode	Frequencies (Hz)					Velocity signals (volts)			d(dB)	Δ(Hz)	Beat Frequency (Hz)	Reverberation time τ (sec)
	J	L	M	N	O	J	L	N				
1	2342.85 ±0.05	2344.28 ±0.05	2341.21 ±0.05	2343.57 ±0.05	2345.82 ±0.05	4.64 ±0.01	4.35 ±0.01	0.89 ±0.01	14.1 ±0.1	4.61 ±0.07	1.29 ±0.01	5.20 ±0.02
2	2765.18 ±0.08	2766.02 ±0.08	2764.61 ±0.08	2765.64 ±0.08	2766.56 ±0.08	3.45 ±0.01	3.45 ±0.01	1.76 ±0.01	5.85 ±0.03	1.95 ±0.05	0.78 ±0.01	4.56 ±0.03
3	3219.57 ±0.10	3220.92 ±0.10	3218.54 ±0.10	3220.20 ±0.10	3221.81 ±0.10	5.63 ±0.01	5.47 ±0.01	1.91 ±0.01	9.25 ±0.03	3.27 ±0.07	1.18 ±0.02	4.01 ±0.01
4	3706.38 ±0.13	3707.89 ±0.13	3705.08 ±0.13	3707.20 ±0.13	3709.20 ±0.13	4.25 ±0.01	4.22 ±0.01	1.33 ±0.01	10.06 ±0.04	4.12 ±0.09	1.40 ±0.02	3.56 ±0.01
5	4777.60 ±0.20	4778.97 ±0.20	4776.69 ±0.20	4778.17 ±0.20	4779.77 ±0.20	3.70 ±0.01	3.63 ±0.01	1.94 ±0.01	5.54 ±0.04	3.08 ±0.15	1.22 ±0.01	2.78 ±0.01

TABLE 3.2

Measurements at node/antinode points

Mode	1st Point			2nd Point		
	Frequency (Hz)	τ (sec)	B (Hz)	Frequency (Hz)	τ (sec)	B (Hz)
1	2344.26 ±0.01	5.10 ±0.02	0.431 ±0.001	2343.00 ±0.02	5.13 ±0.02	0.429 ±0.002
2	2765.69 ±0.01	4.55 ±0.05	0.483 ±0.005	2766.42 ±0.01	4.54 ±0.05	0.484 ±0.004
3	3219.70 ±0.01	3.95 ±0.06	0.557 ±0.008	3220.78 ±0.03	3.92 ±0.05	0.561 ±0.005
4	3706.49 ±0.01	3.50 ±0.05	0.628 ±0.008	3707.86 ±0.01	3.51 ±0.05	0.627 ±0.010
5	4779.58 ±0.02	2.73 ±0.05	0.806 ±0.015	4778.77 ±0.02	2.73 ±0.05	0.805 ±0.015

TABLE 3.3

Comparison of the three methods

Mode	2ℓ (Hz)			B (Hz)		
	New	Beating-decay	Direct	New	Beating-decay	Direct (mean)
1	1.30 ±0.02	1.29 ±0.01	1.26 ±0.02	0.44 ±0.01	0.423 ±0.002	0.430 ±0.002
2	0.80 ±0.01	0.790 ±0.005	0.74 ±0.01	0.51 ±0.01	0.482 ±0.003	0.484 ±0.003
3	1.15 ±0.02	1.18 ±0.02	1.08 ±0.02	0.55 ±0.01	0.548 ±0.003	0.559 ±0.007
4	1.40 ±0.02	1.39 ±0.02	1.37 ±0.01	0.63 ±0.01	0.619 ±0.003	0.628 ±0.009
5	1.27 ±0.05	1.22 ±0.01	1.19 ±0.03	0.84 ±0.03	0.791 ±0.005	0.806 ±0.015

either side of this position. This means that on both sides of the antinode of the higher frequency component the apparent singlet will have slightly lower frequencies and for the lower frequency component the corresponding values may be a little high. Although the resonant frequency at any point can be measured with considerable precision by using a leveller circuit [29] to measure the frequency of the decaying free oscillations, there is still an unquantifiable error involved due to the probe being slightly misplaced from the true positions of the antinode by a small but unknown distance, and this will always reduce the value of 2ℓ obtained from direct method below its true value. This is evident from the results given in Table 3.3 where none of the "direct" values for 2ℓ exceeds the corresponding "beating-decay" value. Moreover, the direct method is tedious and offers no practical advantage over either of the other methods.

3.6 THE EFFECT OF UNEQUAL VALUES OF B

The present theory of doublet analysis is based on the assumption that the two components have the same value of B. However, from a theoretical stand point it can be argued that the breaking of symmetry which causes the separation between the two otherwise degenerate resonant frequencies may also have caused a separation between the corresponding half-widths. It is likely that the fractional separation in the half-widths, if really occurred, would have been of a similar order of magnitude to the fractional separation between the two resonant frequencies. Its absolute magnitude would therefore be so small as to be well within the experimental error of the measurements described above. This view is consistent with the results presented in Table 3.2.

It is important when making measurements on close high-Q doublets, by any method, to ensure that if any external damping has to be introduced, it is applied equally to both components. In the ease of a disc supported at its centre or a cone held at its apex there is no difficulty to achieve the above condition. However, with a ring the point of support must be an equal amplitude point. Hence, in order to add support damping and mass loading equally to both components it is necessary to move the point of support for each doublet investigated. Since unequal

external damping can lead to equal peaks being observed in positions which are not true equal amplitude points, it is essential to ensure that the reverberation times measured at a pair of node/antinode points are equal.

3.7 HALF-WIDTH FROM PHASE RESPONSE

It has been mentioned earlier that equation (3.2) could be used to measure B from the shape of the phase response, when $2\ell/B>1$, from a knowledge of δ and slope at ω_m. Also 2ℓ could be obtained from $\delta = 2\sqrt{\ell^2 - B^2/4}$ provided B is known. In order to measure the phase the output of the measuring amplifier was fed to the phase meter. The reference voltage was fed from the oscillator itself. The D.C. output of the phase meter was fed to the level recorder when the phase response, as shown in Figure 3.9, was obtained on a linear scale. The measurement was made at an equal amplitude point as before. From the response curve the value of δ and slope m were determined whence B was obtained by solving equation (3.2). The results are shown in Table 3.4 along with the values of B and 2ℓ obtained from beating-decay measurements. In general, the phase method gave higher values for B than the reverberation method.

3.8 OFF-DOUBLET REGIONS

It is interesting to study the shapes of the response curves viz. β vs. q and Φ vs. q when $2\ell/B$ differs appreciably from 1.0. That is, for the same value of 2ℓ one is interested to study the response curves when Q changes from 100 upwards ($2\ell/B$ changes from 0.05 upwards). A computer programme was used to make the calculations (See Appendix I for the computer programme). The results are shown graphically in Figures 3.10 and 3.11 for the normalised velocity and phase responses respectively.

As is implied in equation (3.4)

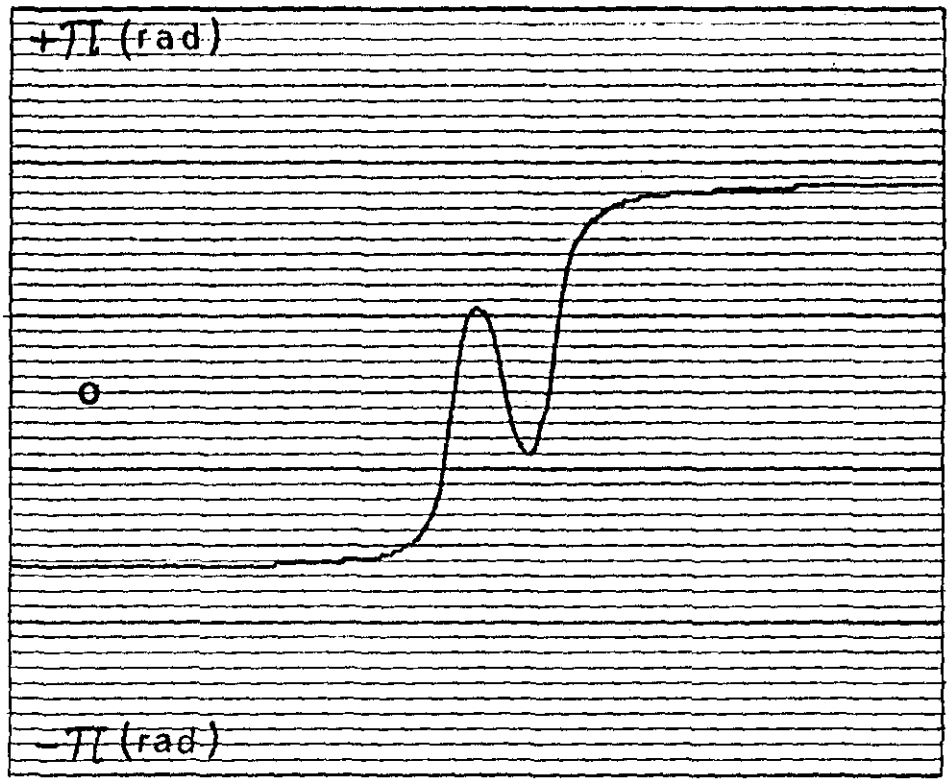

Figure 3.9 Phase response of a close doublet plotted on a linear scale.

TABLE 3.4

Half-width from phase measurements

Mode	ω_o (Hz)	2l (Hz)	δ (Hz)	m (s)	B (Hz)	
					Beating-decay	Phase
1	1278.22	1.310	1.21	0.71	0.320	0.38
		±0.01	±0.09	±0.1	±0.003	±0.03
2	1601.74	1.290	1.15	0.70	0.320	0.38
		±0.005	±0.02	±0.01	±0.003	±0.03
3	1958.79	2.306	2.30	0.75	0.356	0.40
		±0.018	±0.25	±0.06	±0.007	±0.03
4	2261.22	1.726	1.78	0.56	0.425	0.49
		±0.006	±0.06	±0.01	±0.005	±0.06
5	2342.30	1.302	1.20	0.38	0.480	0.58
		±0.004	±0.02	±0.02	±0.003	±0.02

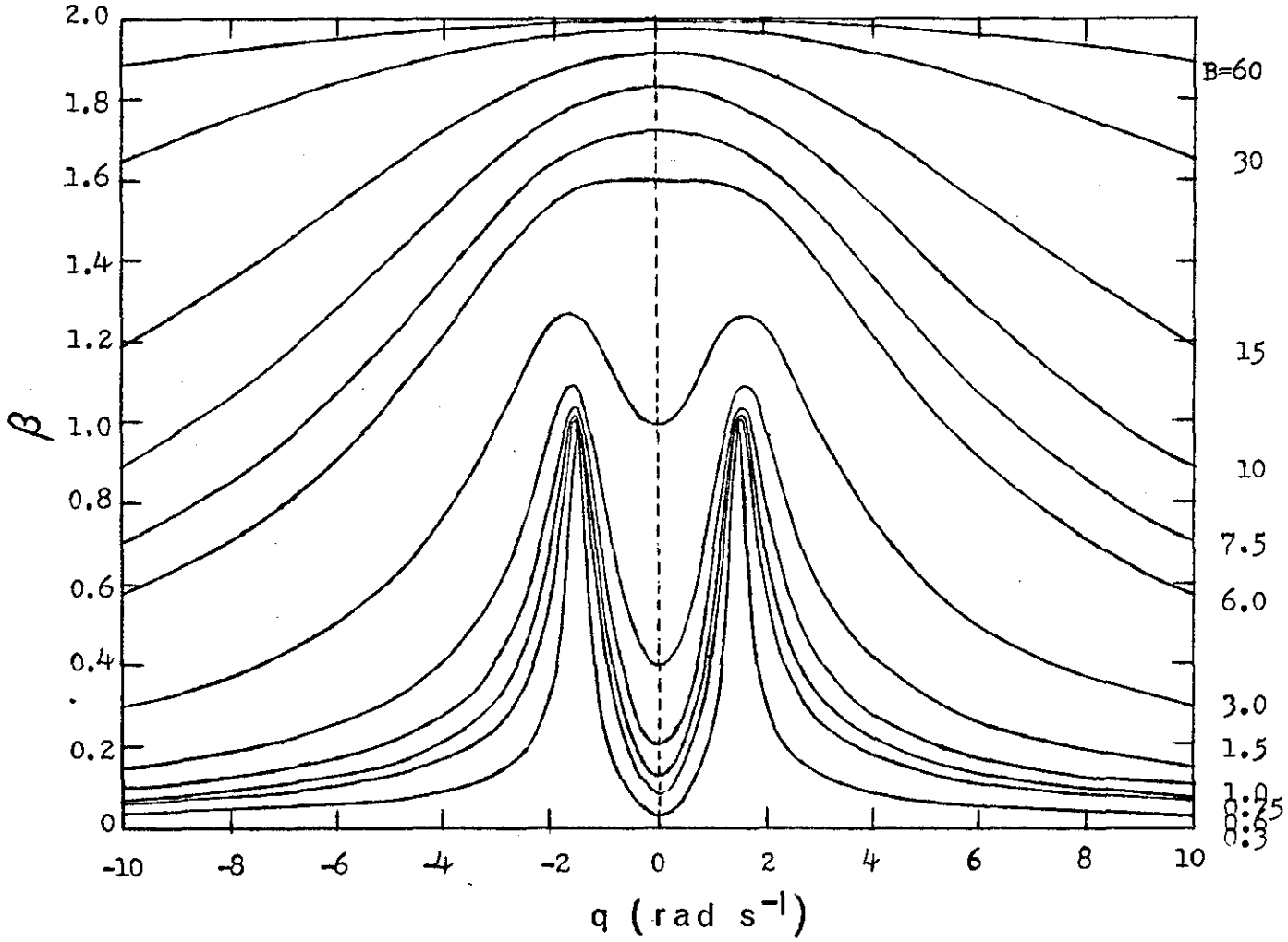

Figure 3.10 β as a function of detuning for different values of B and $2\Omega = 3.0$ rad s^{-1}.

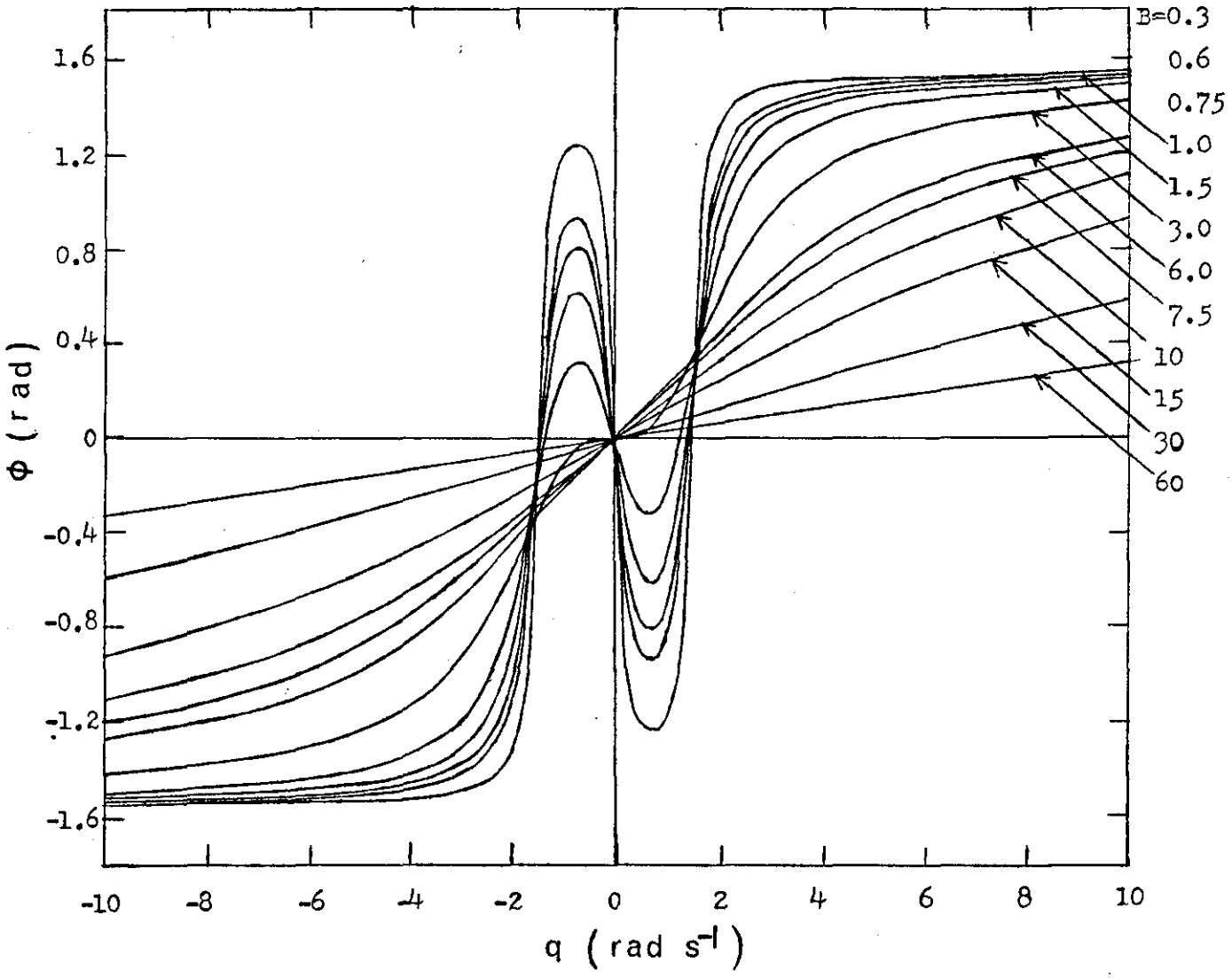

Figure 3.11 Phase as a function of detuning for different values of B and $2\Omega = 3.0$ rad s^{-1}.

$$q_{max} = \pm\tfrac{1}{2}\sqrt{4\ell(B^2 + \ell^2)^{\frac{1}{2}} - B^2}$$

the two values of q giving maximum velocity get closer as B is increased or as ℓ is reduced until only one peak is seen at $q = 0$. For very high values of B the value of β approaches nearly twice the value for the maximum normalised velocity for a singlet. Similarly for lower values of B the peaks of the combination agree with those of the components, i.e. the individual peaks behave more and more independently as singlets with maximum value of β approaching unity. In between these two extremes lies the doublet region.

A similar explanation holds good for the phase response curves of Figure 3.11. For very high values of B the phase response is nearly linear. The linear portion gets reduced to the region in the immediate vicinity of resonance, which is a characteristic of singlet resonance, as the value of B decreases until the doublet region is approached where the phase response exhibits the peculiar shape. For very low values of B the response curve tends to become independent singlet responses.

From the computed data the values of $\beta_{max} - \beta_{min}$ were calculated and plotted against log Q for different values of 2ℓ as shown in Figure 3.12 which gives a better idea as to where doublets appear in the system. The different curves are parallel to one another and exhibit linearity over a wide range. They become closer together towards higher separation where the singlet nature begins to appear. Obviously the present method is meant for the non-linear region where the value of $\beta_{max} - \beta_{min}$ is approximately less than 0.1.

Thus, the doublet response curves clearly exhibit three definite regions viz. the combined singlet region towards the lower Q values, the doublet region and the independent singlet region towards higher Q values. The range of each region is effectively decided by the values of 2ℓ and Q for a given value of ω_m. This behaviour is equally evident in Figure 3.13 which is a plot of β_{max} vs. log Q for different values of 2ℓ. Towards higher Q values the value of β_{max} tends to become unity as for

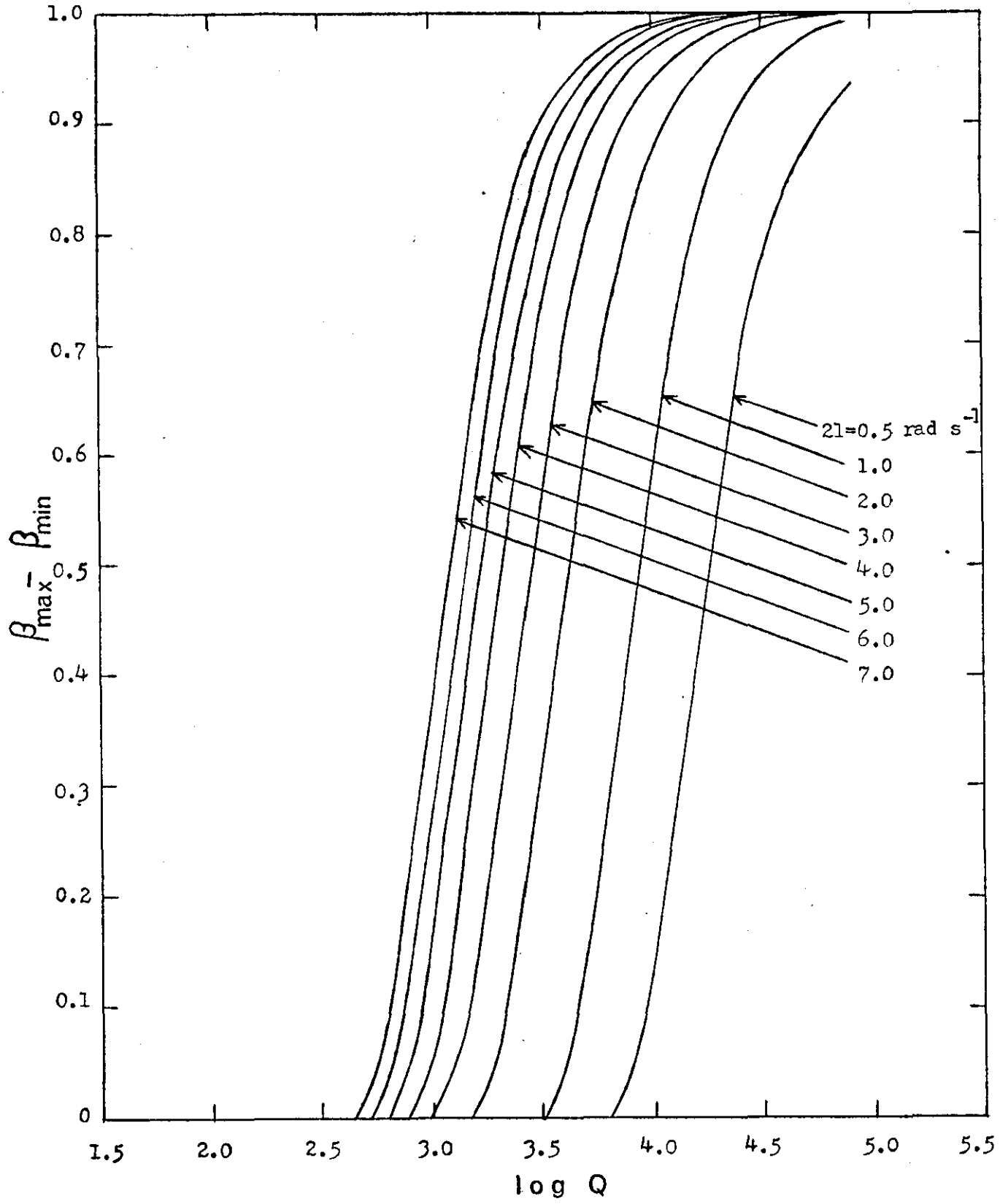

Figure 3.12 $\beta_{max} - \beta_{min}$ as a function of log Q for different values of 2l.

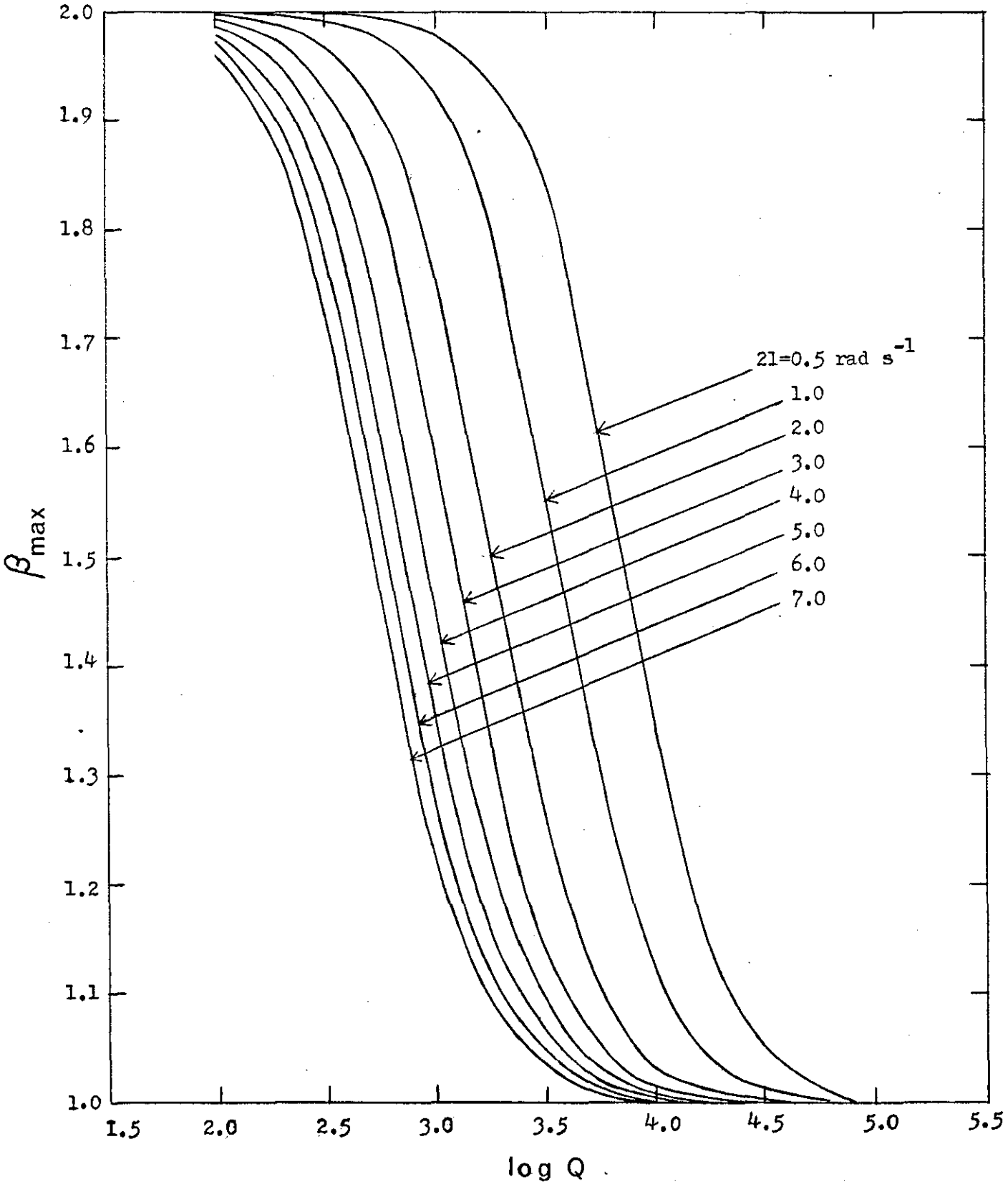

Figure 3.13 β_{max} as a function of log Q for different values of 2l.

singlet response and for lower values of Q, β_{max} approaches twice the maximum value for normalised velocity for a singlet - combined singlet response. From the graph the values of Q corresponding to both ends of the linear portion of each characteristic were determined and plotted against 2ℓ as shown in Figure 3.14 which clearly exhibits the three different regions.

3.9 EFFECT OF OFF-RESONANT VIBRATION

As in the case of singlet resonance the background signals play an important role in distorting the doublet response curves. In a tentative graphical analysis the velocity and phase response curves of a particular doublet were selected to find the effect of adding/subtracting a constant background contribution either with the inphase or quadrature component. In particular, the four special cases were considered as in singlet resonance, and the results are shown graphically in Figures 3.15 and 3.16. The effect of background contribution is more or less similar to that observed in singlet resonance. The situation becomes complicated when different damping levels are associated with the two components of the doublet.

3.10 CONCLUSIONS

It is seen from Table 3.3 that the values of B and 2ℓ obtained by the three methods, viz. new, direct and beating-decay, are in good agreement although the precision of the new method is a little worse than those of the other two. The new method can be used to measure B and 2ℓ whenever two peaks are seen in the response curves, i.e. $2\ell/B > 0.5$. The beating-decay method can be used when $2\ell/B > 1.0$, and is to be preferred on grounds of precision and convenience. The direct method is tedious and offers no practical advantage and hence its use is not recommended. The phase method, which is an alternative to the reverberation method, is susceptible to analytical and experimental errors and its use is also not recommended.

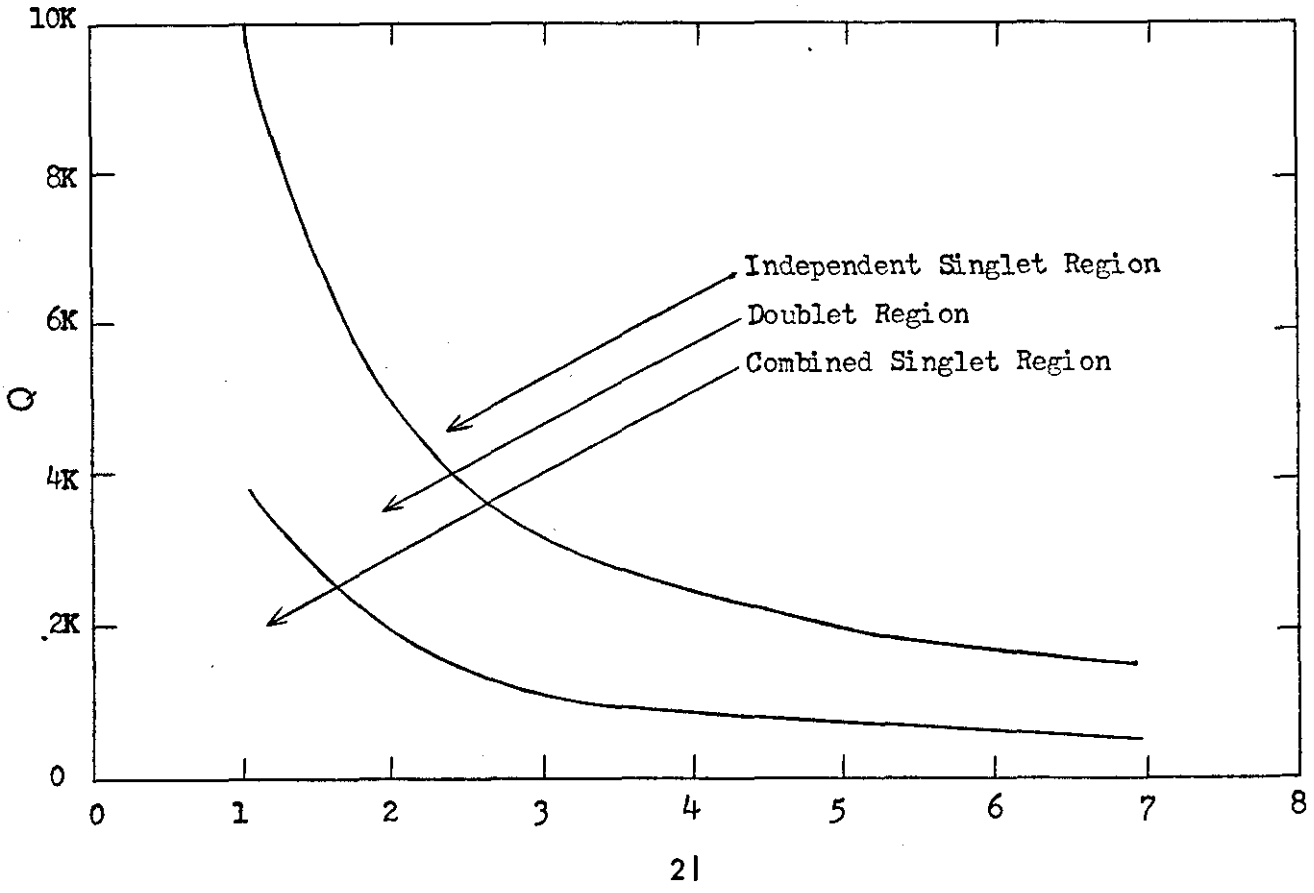

Figure 3.14 Off-doublet regions.

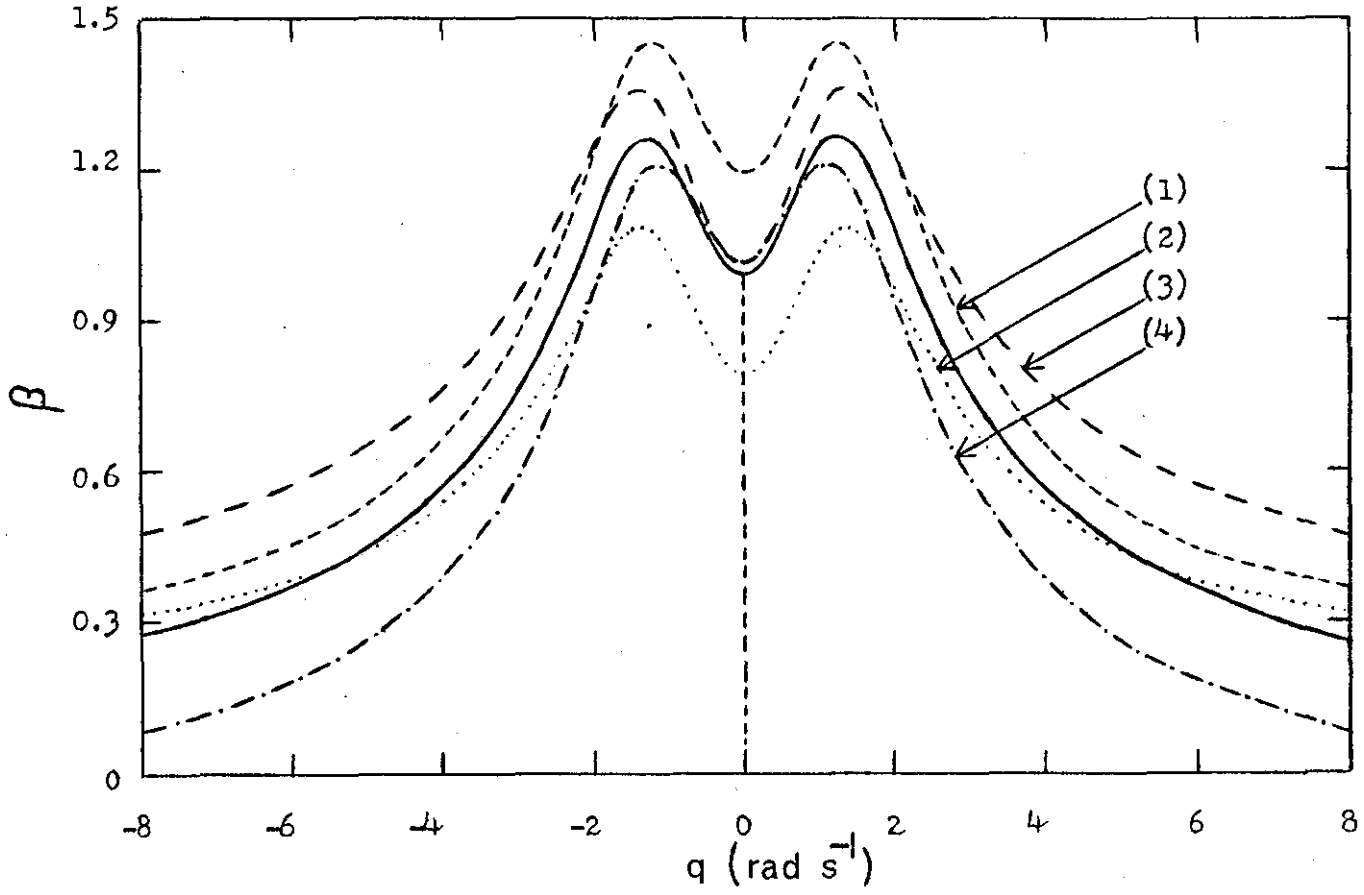

Figure 3.15 Effect of background contribution on normalised velocity response of a close high-Q doublet (solid line: original response curve).

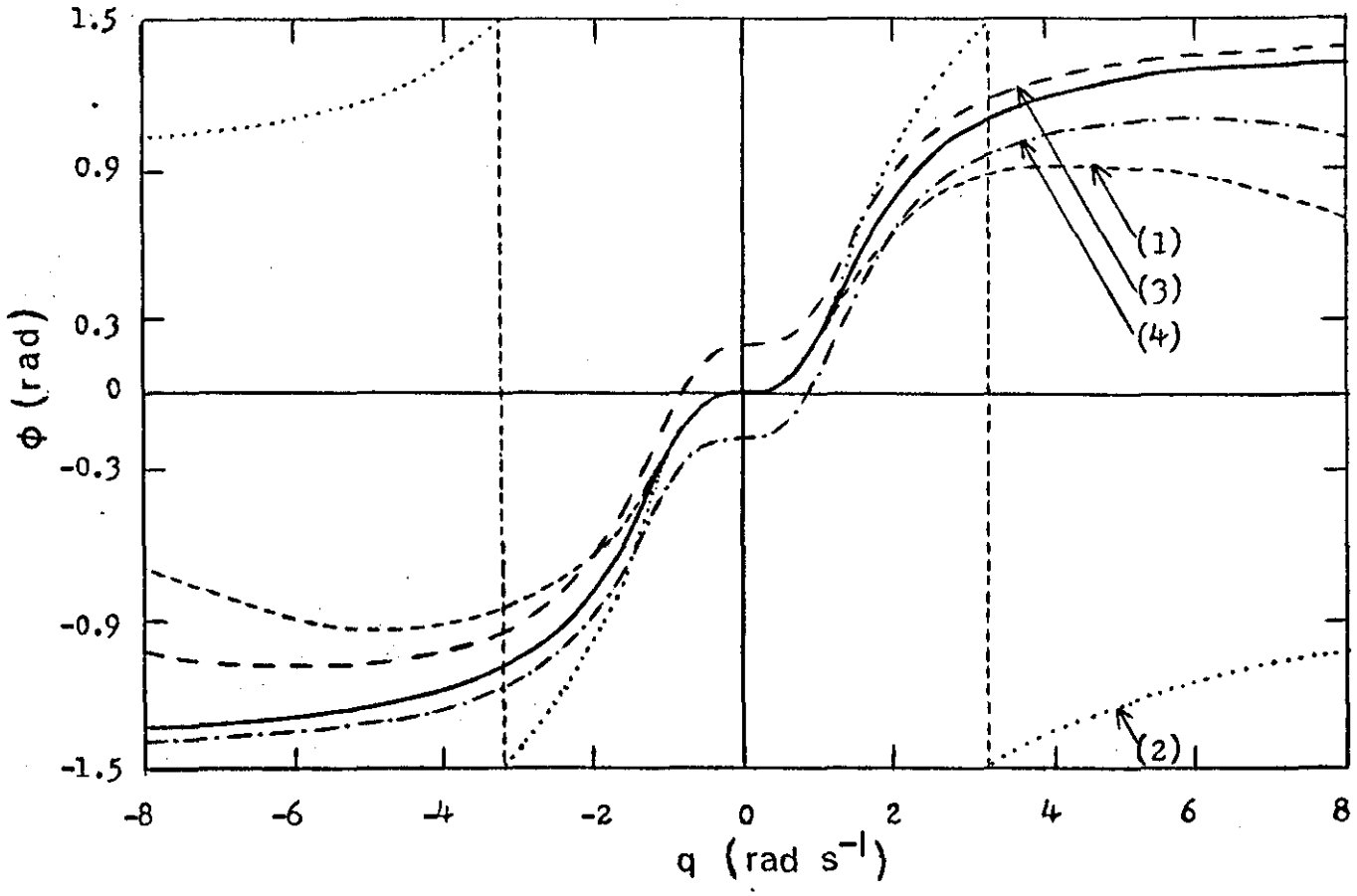

Figure 3.16 Effect of background contribution on phase response of a close high-Q doublet (solid line: original response curve).

Whenever background signals affect the doublet responses none of the above methods can be used with confidence. For very low levels of background contribution the error involved may not be large enough to be detected over other instrument and measuring errors. As the level of background vibration increases the new method fails completely, as also do the phase and reverberation methods. However, the direct method can be used to get approximate values for 2ℓ and B as follows. Under the influence of a constant background signal the asymmetrical apparent singlets will have peak responses slightly away from true resonances and one can obtain the values of ω_o and B from these distorted response curves using least-squares curve-fitting techniques as explained in the next chapter.

CHAPTER IV

SINGLET RESONANCE -

AN OPTIMISATION TECHNIQUE

4.1 INTRODUCTION

In vibration theory it is common to identify the resonant radian frequency ω_o as that corresponding to the maximum velocity response and to define the half-width B as the radian frequency interval between two points on the response curve where the velocity is $1/\sqrt{2}$ times its value at resonance, which are called the half-power points. Phase is defined with respect to the driving force and is zero at resonance and $\pm\pi/4$ at the half-power points. The "sharpness" of the peak is measured by $Q = \omega_o/B$ and for a high-Q system the response curve is effectively symmetrical about ω_o and a plot of $\tan\phi$ vs. P is effectively linear.

When one comes to measure ω_o and B for a mode of a practical high-Q system e.g., a bell, cone or ring, one finds that there is always a background signal present which varies with frequency in a smooth but irregular manner. This arises partly as an intrinsic background, being the vector sum of the "tails" of the response curves of the numerous modes, but mainly from stray electrical pick-up. A high impedance capacity transducer can never be screened perfectly from the strong electro-magnetic fields of the driving magnetic transducer or loudspeaker, and there is also a small contribution from any active filter used in the measuring system. Over the narrow frequency range of a high-Q peak - say 1Hz at 4000Hz - this background may safely be taken as constant in amplitude and phase.

As the driving frequency is swept through a strong high-Q singlet resonance the signal rises some 50dB above the background. The peak is symmetrical, the $\tan\phi$ plot linear, and both ω_o and B can be measured without difficulty.

A very weak resonance will show as a small peak of 5dB or so above the background from which it can be distinguished only as an increase or

decrease which is rapid compared with the slow "drift" of the back ground. With such a resonance one may be able to identify a nodal pattern, but measurement of B is impossible.

Between these two extremes lies the majority of the modes which are of interest. Their response curves are usually slightly asymmetrical because they are the sum of the true response curve and the background. The tanϕ plot is usually far from linear; this provides a test of whether or not background is important. Because of the obvious failure to meet the symmetry requirement there is little temptation to measure B from the observed half-power points. A second effect of the background signal is more insidious: it may shift the resonance peak away from its true value in either direction by an amount much greater than the precision with which it can be measured.

A method is therefore required for obtaining ω_0 and B from the observed data when the background is substantial and its amplitude and phase unknown but constant over the range of frequency covered by the observed peak.

Various authors have dealt with the problem of background vibration affecting the singlet response curves. Though the K - P Method [5] is able to identify closely spaced natural frequencies in the presence of extraneous vibration, the difficulty of identifying the resonance frequency by maximum frequency spacing technique and of fitting an equivalent circle through the observed data points makes it unsuitable to apply to individual singlet responses: the problem is not of missing a resonant mode but rather getting misleading results for ω_0 and B. GLADWELL's [26] refined method is suitable for symmetrical response curves only and EWINS' [27] estimation method deals with peak amplitude response levels only.

Through it is very difficult to predict and assess the degree and nature of this background signal its presence can be deduced from the asymmetrical shape of the otherwise symmetrical response curves. Accordingly, the equations developed in Chapter II for calculating the normalised rms velocity and phase of a high-Q singlet have been modified to account

for the asymmetry due to background signals. From such an asymmetrical response curve one can obtain good estimates of ω_o and B, and some measure of the background signal by using optimisation curve-fitting techniques.

4.2 SINGLET + BACKGROUND

The velocity response of a singlet under harmonic excitation is reproduced from Chapter II as

$$v = \frac{A_o \ell^{j(\omega t - \phi)}}{\sqrt{B^2 + (\omega - \frac{\omega_o^2}{\omega})^2}}$$

where

$$\phi = \tan^{-1} \left(\frac{\omega^2 - \omega_o^2}{\omega B} \right)$$

represents the phase difference between v and the applied force.

Defining $P = \omega - \omega_o$, the "detuning" of radian frequency from resonance, and under high-Q approximation the above equations simplify to

$$v = \frac{A_o}{\sqrt{B^2 + 4P^2}} \qquad (4.1)$$

$$\tan\phi = \frac{2P}{B} \qquad (4.2)$$

so that the inphase and quadrature components of v are given respectively by

$$v_I = \frac{A_o B}{B^2 + 4P^2} \qquad (4.3)$$

and

$$v_Q = \frac{2A_0P}{B^2 + 4P^2} \qquad (4.3)$$

Let the resultant background signal be represented by

$$a = a_0 \ell^{j\theta} \qquad (4.4)$$

where a_0 and θ are respectively the velocity amplitude and phase of the background signal so that the inphase and quadrature components of a become

$$\left.\begin{aligned} a_I &= a_0\cos\theta = C_1 \\ a_Q &= a_0\sin\theta = C_2 \end{aligned}\right\} \qquad (4.5)$$

Adding the respective components of equations (4.3) and (4.5) one gets the combined inphase and quadrature components of v, the resultant rms velocity of the system with background, as

$$\left.\begin{aligned} v_I &= \frac{A_0B}{B^2 + 4P^2} + C_1 \\ v_Q &= \frac{2A_0P}{B^2 + 4P^2} + C_2 \end{aligned}\right\} \qquad (4.6)$$

$$\therefore \quad v^2 = \frac{A_0^2 + a_0^2B^2 + 2A_0BC_1 + 4P\,(Pa_0^2 + A_0C_2)}{B^2 + 4P^2} \qquad (4.7)$$

where $a_0^2 = C_1^2 + C_2^2$

Putting $\frac{d}{dP}(v^2) = 0$ one gets the value of P at which v^2 becomes maximum, say P^1, and taking the positive root (see section 4.3 for details)

gives

$$P^1 = \frac{-(A_o + 2BC_1) + \sqrt{(A_o + 2BC_1)^2 + 4B^2C_2^2}}{4C_2} \qquad (4.8)$$

Substituting for P the value of P^1 in equation (4.7) one gets the maximum value of v^2, say v_o^2. Now, defining a normalised rms velocity $\gamma = v/v_o$, one gets

$$\gamma^2 = \frac{\left[A_o^2 + a_o^2B^2 + 2A_oBC_1 + 4P(Pa_o^2 + A_oC_2) \right](B^2 + 4P^{12})}{\left[A_o^2 + a_o^2B^2 + 2A_oBC_1 + 4P^1 (P^1a_o^2 + A_oC_2)\right](B^2 + 4P^2)} \qquad (4.9)$$

In the absence of any background signal equation (4.9) reduces to

$$\alpha^2 = \frac{B^2}{B^2 + 4P^2}$$

in agreement with equation (2.8) of Chapter II.

Also from equation (4.6) one gets

$$\tan\psi = \frac{2A_oP + C_2 (B^2 + 4P^2)}{A_oB + C_1 (B^2 + 4P^2)} \qquad (4.10)$$

where ψ is the resultant phase of the system with background. This reduces to equation (4.2) in the absence of background, as required.

Equation (4.9) and (4.10) can be rewritten by defining a new variable $R = A_o/a_o$ and by substituting for C1 and C2. This is advantageous because in iterative problems the computer time varies as some function of the number of variables. Therefore one has

$$\gamma^2 = \frac{\left[R^2 + B^2 + 2RB\cos\theta + 4P(P + R\sin\theta)\right]\left[B^2 + 4P1^2\right]}{\left[R^2 + B^2 + 2RB\cos\theta + 4P1(P1 + R\sin\theta)\right]\left[B^2 + 4P^2\right]} \qquad (4.9.1)$$

and

$$\tan\psi = \frac{2RP + (B^2 + 4P^2)\sin\theta}{RB + (B^2 + 4P^2)\cos\theta} \qquad (4.10.1)$$

4.3 ASYMMETRICAL RESPONSE CURVES

In order to understand the effect of background signal on singlet responses, let us compute γ^2 and $\tan\psi$ as functions of P for known values ω_o, B, R and θ by using equations (4.9.1) and (4.10.1) respectively and compare the results with those obtained by using equations (2.7) and (2.8) respectively. The results are shown graphically in Figures 4.1 and 4.2 and clearly demonstrate the extent of damage introduced into the original velocity and phase responses (thick lines) by the presence of a background signal. None of the response curves could be used with confidence to determine ω_o and B by the ordinary methods and one could learn little about the values of R and θ from them. Also it is evident that the peak response frequency is shifted to one side or the other from resonance depending upon the values of R and θ.

The fact that the maximum value of γ is unity is a significant advantage from the experimental point of view: one can always normalise the measured output voltage - which is proportional to velocity - with respect to the observed maximum value without any difficulty. It is also to be noted that this maximum value of unity for γ is obtained if and only if the positive root is taken for P^1 in equation (4.8) for calculating v_o.

When dealing with practical vibrating systems, one often comes across asymmetrical response curves similar to those shown in Figures 4.1 and 4.2. It is obvious that one cannot rely much on the value of the half-width obtained from the frequency interval corresponding to half-power points or from the slope of the phase response. The results can be out

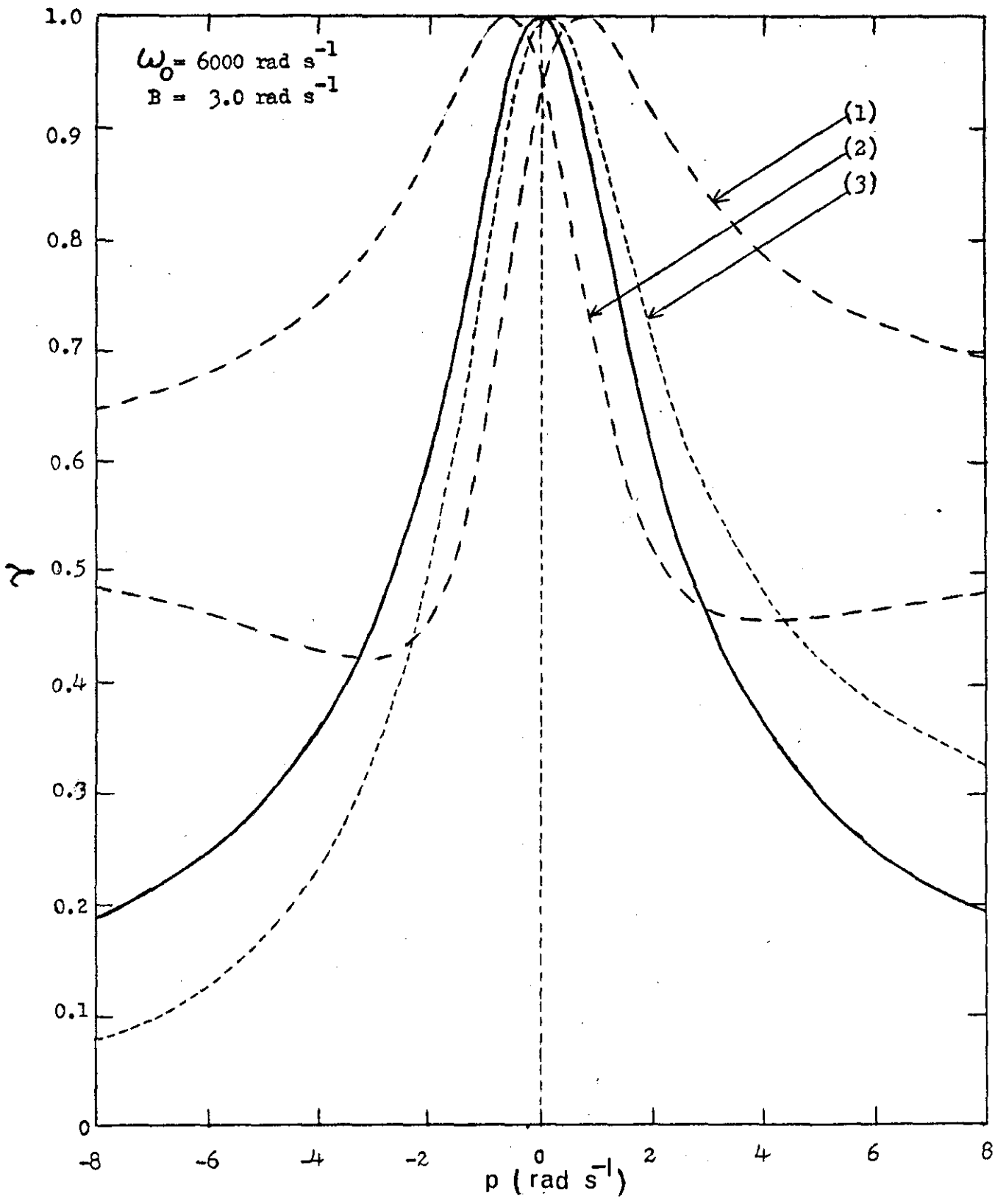

Figure 4.1 Normalised velocity response with background (solid line: original response curve with no background).

(1) R = 3.0 & θ = 1.309 rad.

(2) R = 3.0 & θ = 5.236 rad.

(3) R = 20.0 & θ = 1.309 rad.

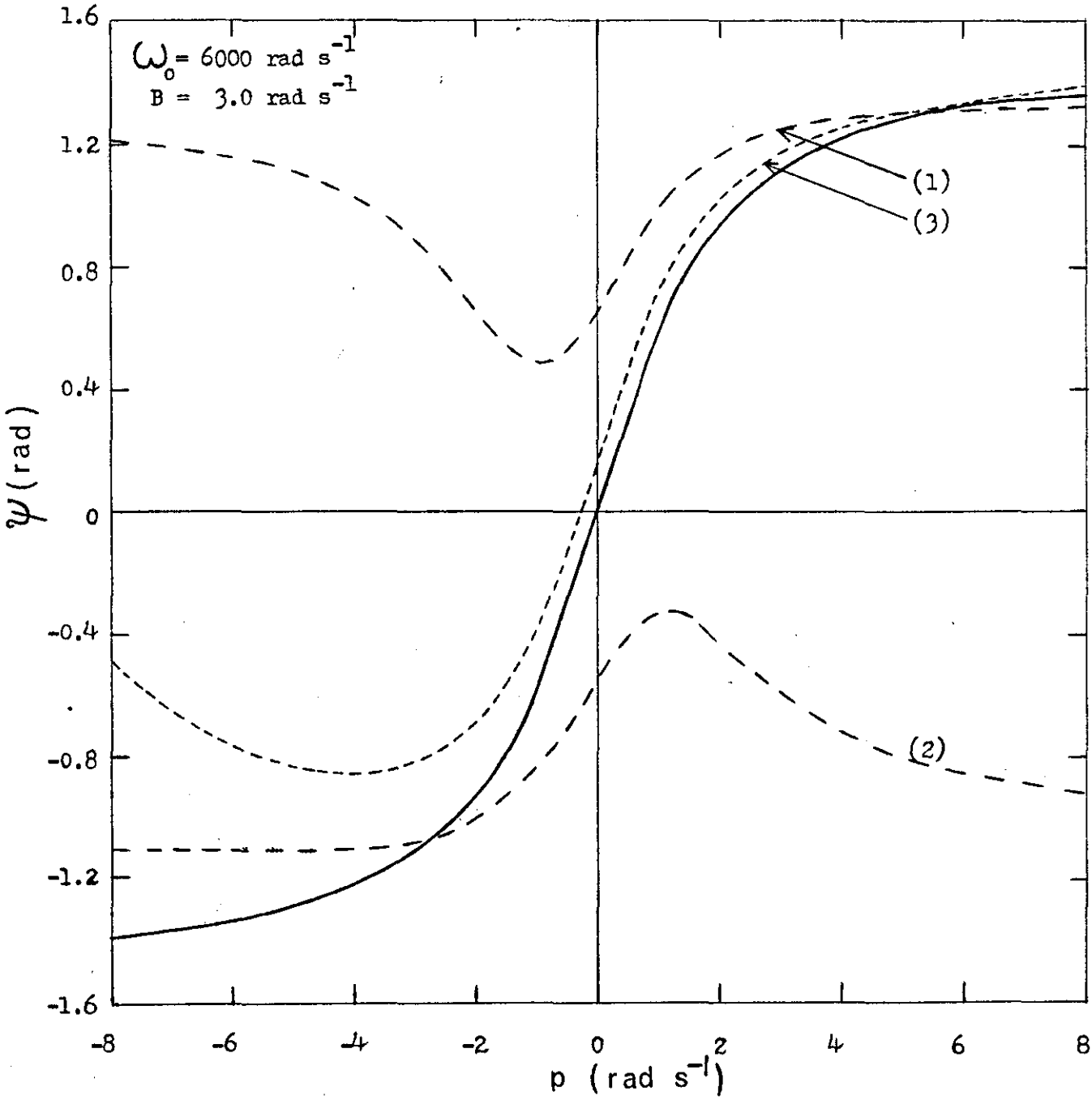

Figure 4.2. Phase response with background (solid line: original response with no background).

(1) R = 3.0 and θ = 1.309 rad.

(2) R = 3.0 and θ = 5.236 rad.

(3) R = 20.0 and θ = 1.309 rad.

by 50% or more from the true values. So if one has to make use of the asymmetrical response curves of a practical vibrating system to estimate ω_o and B, one should choose these four variables, viz. ω_o, B, R and θ, in such a way that the response curves calculated from equations (4.9.1) and (4.10.1) agree with the observed response curves to within some preset degree of accuracy using some optimisation technique.

4.4 THE METHOD OF LEAST-SQUARES

The theoretical and statistical background to the problem of least-squares technique can be had from any standard text-book on this subject. Accordingly, the following details are taken from WOLBERG [30].

Let the functional relationship between the true or mean values of the dependent variable γ, independent variable P and the unknown parameters X_ℓ be written as

$$\gamma_k = f(P_k, X_\ell) \qquad k = 1,2,3 \ldots\ldots, m \qquad \ell = 1,2,3 \ldots\ldots, n \qquad (4.11)$$

where m is the number of data points and n the number of unknown parameters.

As the functional form of the relationship remains the same for the observed, calculated and true variables, similar relations can be written for the observed and calculated variables as

$$\gamma^1_k = f(P^1_k, X^1_\ell) \qquad (4.11.1)$$

and

$$\gamma^{11}_k = f(P^{11}_k, X^{11}_\ell) \qquad (4.11.2)$$

respectively.

Now the difference between the observed and calculated variables is defined as the residual.

i.e.

$$R_k = \gamma^1{}_k - \gamma^{11}{}_k \qquad (4.12)$$

and the reciprocal of the square of the standard deviations σ_k of $\gamma^1{}_k$ is defined as the weight of the corresponding data point.

i.e.

$$W_k = \frac{1}{\sigma_k{}^2} \qquad (4.13)$$

The weighted sum of squares of the residuals is denoted by

$$S = \sum_{k=1}^{m} W_k R_k{}^2 \qquad (4.14)$$

and the method of least-squares is aimed at determining the value of X_ℓ which minimises S using the experimental data.

See Appendix II for further details.

4.5 TEST OF COMPUTER PROGRAMME

In order to test the optimisation programme the asymmetrical response curves of Figures 4.1 and 4.2 were used as input data to see whether the original values of ω_o, B, R and θ could be reobtained. Initial estimates of ω_o and B were obtained by using the ordinary methods. It is interesting to note that the values so obtained were out by more than 50% or so from the original values in the case of B and by 1.0 rad s^{-1} or so in the case of ω_o. No such estimates could be made for the values of R and θ.

See Appendix III for the computer programme.

The results of the test are shown in Tables 4.1 and 4.2. The results are quite promising in that the original values are obtained in all cases to a considerable degree of accuracy.

As is evident from Figure 4.2, the phase is never zero at the point when γ reaches its maximum value. This creates difficulty in using the phase response to obtain half-width from an experimental point of view. However, by making suitable changes in the formula for $\tan\psi$ one can overcome this difficulty.

Equation (4.8) corresponds to the value of P at which v becomes a maximum - say P^1. Substituting equation (4.8) into equation (4.10.1) one gets the value of $\tan\psi$ at P^1 as

$$\tan\psi_o = \frac{2RP^1 + (B^2 + 4P^{1^2}) \sin\theta}{RB + (B^2 + 4P^{1^2}) \cos\theta} \qquad (4.10.2)$$

so that $(\psi - \psi_o)$ gives the relative phase difference between any point on the phase response in Figure 4.2 and the point corresponding to the maximum value of v. Incorporating these modifications in the computer programme, the results shown in Table 4.3 were obtained corresponding to the results shown in Table 4.2.

4.6 EXPERIMENTAL TEST

The experimental set-up described in Chapter III was used for making measurements of singlet responses. As the system is axially symmetric most of the eigen-frequencies were degenerate doublets. However, by driving and detecting at a node/antinode of one component of the doublet one can obtain a singlet, the resonance frequency of which can be measured with considerable precision by using a leveller circuit [29] to measure the frequency of the decaying free oscillations. From the slope of the decay curves obtained on a logarithmic scale one can measure the reverberation time τ, whence B was obtained by using the relation $B = 2.2/\tau$.

TABLE 4.1

THEORETICAL ANALYSIS

NORMALISED VELOCITY RESPONSE

	ω_o (rad s^{-1})	B (rad s^{-1})	R	θ (rad)
Response Curve No.1				
Original Values	6000.00	3.000	3.000	1.309
Initial Estimates	6000.75	7.247	15.000	0.500
Final Least-Squares Estimates	6000.00	2.999	2.998	1.309
Response Curve No.2				
Original Values	6000.00	3.000	3.000	5.236
Initial Estimates	5999.40	5.000	10.000	2.000
Final Least-Squares Estimates	6000.00	3.000	3.001	5.236
Response Curve No.3				
Original Values	6000.00	3.000	20.000	1.309
Initial Estimates	6002.00	3.750	5.000	1.000
Final Least-Squares Estimates	6000.00	2.999	19.962	1.309

TABLE 4.2

THEORETICAL ANALYSIS - PHASE RESPONSE

	ω_o (rad s^{-1})	B (rad s^{-1})	R	θ (rad)
Response Curve No.1				
Original Values	6000.00	3.000	3.000	1.309
Initial Estimates	5998.00	3.332	6.000	0.900
Final Least-Squares Estimates	6000.00	3.001	3.000	1.309
Response Curve No.2				
Original Values	6000.00	3.000	3.000	5.236
Initial Estimates	5999.40	5.802	15.000	1.000
Final Least-Squares Estimates	6000.00	3.002	3.001	5.236
Response Curve No.3				
Original Values	6000.00	3.000	20.000	1.309
Initial Estimates	5998.00	3.749	7.000	0.500
Final Least-Squares Estimates	6000.00	3.000	20.001	1.309

TABLE 4.3

THEORETICAL ANALYSIS - RELATIVE PHASE RESPONSE

	ω_o (rad s^{-1})	B (rad s^{-1})	R	θ (rad)
Response Curve No.1				
Original Values	6000.00	3.000	3.000	1.309
Initial Estimates	6000.70	7.273	5.000	1.500
Final Least-Squares Estimates	6000.00	2.998	2.998	1.309
Response Curve No.2				
Original Values	6000.00	3.000	3.000	5.236
Initial Estimates	5999.40	5.802	15.000	1.000
Final Least-Squares Estimates	6000.00	3.006	3.002	5.236
Response Curve No.3				
Original Values	6000.00	3.000	20.000	1.309
Initial Estimates	6000.20	3.099	15.000	1.000
Final Least-Squares Estimates	6000.00	3.001	19.996	1.309

The frequency and the voltage output were measured at a number of points in the vicinity of resonance including the resonant frequency. With reference to the maximum output voltage at resonance one can normalise the response of other points and plot the normalised velocity response to obtain an initial estimate of ω_0 and B.

The phase of the system was also measured with respect to the phase of the driver. By noting the phase at the resonant frequency one can obtain the relative phase differences at a number of points in the vicinity of resonance and plot the relative phase response of the system when an initial estimate of B can be obtained by using the relation $B = 2/\frac{d\Psi}{dP}$ where $\frac{d\Psi}{dP}$ is the slope of the response curve at the resonant frequency.

Pure singlets can also be obtained in the case of circular rings vibrating in the torsional and extensional (radial) modes corresponding to n = 0 [3]. The experimental set-up remains the same except that the ring is suspended on a sharp blade held vertically.

The results of the experiment are given in Table 4.4. Although there is no direct way of checking the correctness of the values of the four parameters viz. ω_0, B, R and θ, obtained from least-squares estimates, one might expect to get the same values for these parameters from the velocity and phase responses as they were taken under the same conditions. As is evident from the table there is good agreement between the values of ω_0, B and θ obtained from the two responses, but the values of R varied substantially. One probable reason for this disagreement is the possibility of different solutions existing for R for the same values of ω_0, B and θ. Another reason may be the inadequacy of the assumption of constant background in the immediate vicinity of resonance. However, by viewing from another angle it can be argued that, of the four parameters, only ω_0 and B are of importance from a practical point of view.

Another interesting point worth mentioning is that for values of θ lying in the first two quadrants i.e.< Π rad, the observed values of ω_0 are always greater than the true values thereby showing the apparent shift in the resonance frequency in the presence of a background signal.

TABLE 4.4

EXPERIMENTAL RESULTS

Mode No.		$\omega_o(H_z)$	$B(H_z)$ (from half-width)	R	θ (rad)	$B(H_z)$ (from decay)
1.	Initial Estimates	3220.819	0.500	20.000	1.400	0.537
	Final Least-Squares Estimates from:					
	1. Nor. Vel. Response	3220.791	0.562	280.997	1.569	
	2. Rel. Phase Response	3220.781	0.557	356.559	1.559	
2.	Initial Estimates	3708.195	0.600	20.000	1.000	0.625
	Final Least-Squares Estimates from:					
	1. Nor. Vel. Response	3708.134	0.636	255.165	1.556	
	2. Rel. Phase Response	3708.112	0.636	69.656	1.573	
3.	Initial Estimates	4225.953	0.800	20.000	1.500	0.690
	Final Least-Squares Estimates from:					
	1. Nor. Vel. Response	4225.928	0.732	260.680	1.565	
	2. Rel. Phase Response	4225.902	0.715	24.005	1.559	
4.	Initial Estimates	4778.160	0.800	20.000	1.000	0.777
	Final Least-Squares Estimates from:					
	1. Nor. Vel. Response	4778.151	0.804	97.401	1.598	
	2. Rel. Phase Response	4778.143	0.808	228.600	1.701	
5.	Initial Estimates	5361.902	0.900	20.000	1.000	0.863
	Final Least-Squares Estimates from:					
	1. Nor. Vel. Response	5361.903	0.886	24.199	1.574	
	2. Rel. Phase Response	5361.897	0.896	269.462	1.496	

4.7 CONCLUSIONS

This simple method helps one to analyse the asymmetrical response curves of practical vibrating systems where the nature and level of background signals can not be predicted or assessed accurately. For low levels of background signals where the response curves are nearly symmetrical one may not find much advantage in using this new method over the other conventional methods. Yet one gets an additional way of checking the observed results by using this technique. However, in the worse case when one can no longer employ the ordinary methods to measure ω_o and B, one finds the definite advantage of using this new method to analyse the asymmetrical response curves with confidence. Moreover the values of ω_o and B obtained from least-squares estimates no longer critically depend upon measurements in the immediate vicinity of ω_o and half-power points as the accuracy of the new method depends equally on all the observed data points.

CHAPTER V

NORMAL MODES OF CIRCULAR RINGS

5.1 SIGNIFICANCE

Vibration studies of circular rings are of considerable importance as ring-like elements form a common unit in many engineering structures like rotating electrical machines [33], gear trains, stiffened cylindrical shells of launching vehicles, turbomachines, rockets etc. A fair knowledge of the various modes of ring vibration is essential in the design of noise-less electrical motors [34] and other rotating electrical machines, in the study of gear noise [35], in the evaluation of the performance of flywheel energy storage systems containing thick rings as the primary storage element [36], in the finite element analysis of axially symmetrical vibrating systems like bells and cones and in the problem of vibration control of aircraft and other space vehicles. Also ring elements find application in certain musical instruments like campaniform bell, solo instrument etc. [37]. Rings can be used as simple tone generators because once tuned they will retain their pitches indefinitely. The vibrations of rings and annular plates can be technically applied in their use as resonators. Hence the study of the natural frequencies of vibration of circular rings of rectangular cross-section in the audio-frequency range is of great technical interest as the most fundamental item of all.

5.2 DIFFERENT TYPES OF RING VIBRATION

The vibration of circular rings falls into three main classes viz. flexural, torsional and extensional [38].

5.2.1 Flexural Vibration

The flexural vibrations are lateral or transverse vibrations which are characterised by periodic bending and straightening of the elements of the centre line where each element moves to and fro at right angles to the normal configuration of the centre

line. The restoring force in this type of vibration is the resistance offered to bending and the elastic constants involved are E, ρ and σ, where E is Young's modulus, ρ is the density and σ is Poisson's ratio of the material. The flexural modes are most important and dominate the lower frequency region of the vibration spectrum.

The flexural vibrations fall into two types viz. one involving vibrations in the plane of the ring called "radials" and the other involving both displacements at right angles to the plane of the ring and twist called "axials".

5.2.2 Torsional Vibration

The torsional vibrations depend on the resistance offered to twisting and the elastic constants involved are G, ρ and σ, where G is the rigidity modulus of the material. Here the centre line of the ring remains undeformed and all the (circular) cross-sections rotate during vibration through an angle. Also each transverse cross-section remains in its own plane. However, with rectangular cross-sections the twist is accompanied by a warping of the layers of matter originally composing the normal sections.

5.2.3 Extensional Vibration

The extensional vibrations are pure radial vibrations which are similar to longitudinal vibrations of bars. Here the centre line of the ring forms a circle of periodically varying radius and all the cross-sections move radially without rotation. The restoring force in this case is the resistance offered by the rod to extension or compression.

5.3.4 General Remarks

Thus the normal modes of vibration of circular rings fall into four main types viz. RADIAL, AXIAL, TORSIONAL and EXTENSIONAL. However, some authors prefer to call the flexural vibrations as in-plane (radials) and out-of-plane (axials) vibrations. Also the radials are sometimes referred to as inextensional vibrations in order to differentiate them from extensionals which are also radial vibrations in the plane of the

ring. In practice these different modes of vibrations are found to be cross-coupled. However, as one component of motion predominates over other components they can be broadly classified as above.

Another important feature of ring vibration is that the eigen-frequencies of the various ring modes occur in nearly degenerate pairs called doublets which are characteristics of axially symmetrical vibrating systems. The only exceptions to this are the torsional and extensional modes corresponding to n = 0 [3].

5.3 VARIOUS RING THEORIES

The free vibration of circular ringshas been investigated by various authors over many years. The original solution for the radial vibration of a thin uniform ring was given by HOPPE [39] in 1871 and that for the axial vibration was given by MICHELL [40] in 1890. Provided the ring is thin these two modes dominate the lower frequency region of the vibration spectrum and can be described with sufficient accuracy by the "classical" theory summarised by LOVE [38], in which shear deflections and rotatory inertia are neglected and inextensibility is assumed. The torsional vibration was first recognised by BASSET [41] and the frequency of torsional vibration was given by him. The non-torsional circumferential modes of vibration were first recognised by POCHHAMMER [42] in a solid circular cylindrical bar and HOPPE [39] was the first to derive the frequency equation for these extensional modes for a thin circular ring. The problem of vibration of circular rings has also been discussed by LAMB [43], RAYLEIGH [44], TIMOSHENKO [33] etc.

The frequency equations derived by the above authors for the main four types of vibration are based on assumptions similar to those involved in the case of Euler-Bernoulli beam theory and are applicable only to low nodal diameter modes of thin uniform rings. However, experimental investigations of KUHL [45], KAISER [37], LINCOLN and VOLTERRA [46] etc. have shown that even for thin rings substantial error can result especially for higher modes. As the ring becomes thick the deviations from classical theory become greater. Hence many authors have tried

to improve the classical formulae by taking into account the various factors which affect the vibration of curved bars in an effort to find approximate or exact solutions for thick ring vibrations.

FEDERHOFER [47] has obtained an exact solution containing sets of Bessel functions which make it difficult to use in practice. BUCKENS [48] has derived a correction factor for the radial vibration of thick rings to obtain the deviation from the classical theory by taking into account the shear and extension effects. PHILIPSON [49] has shown that the effect of extension is quite negligible. SEIDEL and ERDELYI [50] have developed a frequency determinant for getting the eigen-frequencies of radial vibration of thick circular rings based on beam theory by taking into account bending, shear and extensional energies together with rotational and translational kinetic energies. Using an energy approach together with the assumption of non-linear variation of normal strain through the cross-section and an average shear angle they obtained a cubic frequency equation which was further reduced to a quadratic expression when mid-surface extension was neglected. RAO and SUNDARA-RAJAN [51] have developed a quadratic frequency equation for the radial motion of thick rings including the effects of shear deformation and rotatory inertia together with the assumption of inextensibility and linear variation of normal strain through the cross-section. RAO [52] has also investigated the effects of transverse shear and rotatory inertia on the axial vibration of thick rings. The governing equations of motion are developed from Hamilton's principle and the resulting cubic equation when solved gives three frequencies with the lowest one corresponding to flexural mode and the other two higher frequencies corresponding to torsional and transverse thickness-shear modes.

ENDO and TANIGUCHI [53,54,55,56] in a series of four papers have discussed the problem of flexural vibration of thick rings of rectangular and arbitrary cross-sections and have derived certain approximate formulae by using different approaches. CHARNLEY and PERRIN [57] have derived the classical formulae for the radial and axial vibrations of thin uniform rings in a more general form which hold good for any shape of cross-section. WILLIAMS [58] has derived the equations of motion governing small elastic displacements of thin rings, including both

warping and rotatory inertia effects, from Hamilton's theorem and presented numerical results for the frequencies and mode shapes. HAINES et al. [59] have obtained an exact solution for the radial motion of thin rings of rectangular cross-section by solving the equations of two-dimensional linear elasticity and have presented numerical results as dispersion curves, viz. three dimensional plots of frequency vs. wave number, for the harmonic waves propagating around the circumference. The solutions corresponding to discrete points on the dispersion curves give natural frequencies of ring vibration. HAINES [60] has also discussed the comparative merits of the classical approximate theories with the help of the exact solution in order to establish the appropriate frequency ranges for each theory in comparison with his three-mode theory for thin rings in which flexure, shear and extension are coupled. KIRKHOPE [61] has derived a frequency equation for the radial vibration of thick rings which provides a correction factor by which classical frequency is modified to account for transverse shear and rotatory inertia effects using an energy approach. KIRKHOPE [62,63] has also derived dynamic stiffness matrices for the radial and axial vibration of thick circular rings using an energy approach including the effects of transverse shear, rotatory and torsional inertia, mid-surface extension and non-linear variation of normal strain through the cross-section. HAWKINGS [64] has presented a generalised analysis of the various inextensional vibrations of a circular ring using a perturbation analysis without restricting the cross-sectional shape but assuming it to be constant around the circumference.

5.4 NEED FOR EXPERIMENTAL INVESTIGATION

Majority of the new theories mentioned above have limited practical utility eventhough very attractive theoretically. This is because the governing differential equations, derived by taking into account the various factors like shear, extension, rotation etc. can be solved only with the help of a computer. For example the frequency determinant of references [50,53,55,56,59,60], the cubic equation of reference [52], the dynamic stiffness matrices of references [62,63], the numerical solution of the simultaneous equations of reference [64] etc. all

require extensive computation to get the end results. However, with complicated systems where ring elements form common units it is essential to have simpler formulae to calculate the natural frequencies of the various modes of ring vibration.

Moreover, the various ring theories are centred around the consideration of the ring being either thin or thick and in certain cases as medium [54]. As the classical theory is supposed to hold good for thin rings i.e. $h/a,\ t/a << 1$, the newer theories are claimed to hold well for thick rings i.e. $h/a,\ t/a = 1$, where a is the radius of the centre-line of the ring, and h and t are the height and thickness of the cross-section respectively. In the absence of substantial experimentation it is very difficult to determine the region of applicability of the classical formulae as well as the newer ones. In the past only a few authors have done experimental investigation of rings' vibration [35,45,46,53, 55,57] . In the majority of these measurements usually the first few modes of radial and axial vibrations were involved. Most of the new theories are compared with these limited experimental data available [50,51,52,61,62,63].

Thus in the literature one comes across the classical theory which is valid only for thin rings in which the effects of shear deformation and rotatory inertia are neglected and inextensibility is assumed, numerous new theories in which those effects are considered, and limited experimental data available for comparison. Whereas the classical theory has not been fully tested for the range of its applicability, it is necessary to have a systematic experimental investigation into ring vibration to see how far the thin ring formulae hold well and whether one can obtain an empirical correction to apply for the case of thick rings. Hence the aim of the present investigation is to provide substantial experimental data to establish a criterion for the conditions under which the thin ring formulae may be used without serious error and to formulate an empirical correction to apply in the case of a thick ring.

5.5 EXPERIMENTAL TECHNIQUES

Various authors have used different methods to measure the frequencies of freely vibrating circular rings. In reference [37] the rings were either supported horizontally at the nodes on vertical pins or suspended by a loop of cord. The frequencies were more or less identical with both types of mounting. Tones were generated by striking the ring on the circumference with a light wooden mallet and the audible frequencies were determined with a standard stroboconn. In reference [46] the toroids suspended at three points by soft elastic cords were excited by electro-magnetic coils and the induced vibrations were detected by a piezo-electric crystal bonded to the surface of the toroid. By proper positioning of the coils the cross-sections of the toroid were excited either along a line in the plane of the ring or at right angles to it. A decade counter was used to measure frequency and there was no appreciable change in frequency as the points of suspension varied. In reference [53] the ring was hung by a slender steel wire and the vibrations generated by hitting the ring were measured by a condenser microphone feeding an oscilloscope via a $^1/_3$ octave filter. The natural frequencies were determined by forming the Lissajous pattern with the help of a standard oscillator. In reference [57] a loudspeaker was used to excite the ring, the vibrations induced were detected by a capacity transducer and a timer-counter was used to measure the frequency. This method of driving and detection avoided any contact with the ring other than the single sprung support. In reference [64] the ring was suspended vertically on a nylon chord and the natural frequencies were measured by gently tapping the ring and spectrally analysing the transient response as detected by miniature accelerometers.

Thus in general there are three main ways of exciting the ring viz. mechanical, magnetic and acoustic excitations, and three different methods of detection viz. stroboscopic, piezo-electric and capacitive. Also, there are different ways of suspending or supporting the ring. However, the general requirement of zero-stress boundary condition is better realised in a sprung support, in the magnetic and acoustic excitation, and in stroboscopic and capacitive detection. As the spring supported ring takes some time to settle down, the same boundary condition can more or less be obtained by allowing the ring to hang

on a sharp blade held vertically. Similarly capacitive detection is preferred to stroboscopic method of detection owing to practical convenience and suitability. Also as acoustic excitation is not suitable especially for the higher frequency ranges, magnetic excitation is generally used to cover the whole frequency range uniformly. Moreover, this has the advantage as the most suitable way of excitation especially while measuring the nodal circles and diameters around the circumference of the ring.

5.6 PRESENT INVESTIGATION

Four circular rings of varying rectangular cross-sectional dimensions but of the same mean radius 'a',as shown in Figure 5.1,were used in this investigation. Also, the thickness t of ring C was equal to the height h of the flat ring A. The rings were made of mild-steel cut from cylindrical disks and were machined in a lathe to the final dimensions shown in Table 5.1.

A magnetic transducer was used to excite the ring hung on a blade held vertically and a capacity transducer was used to pick up the induced vibrations. The frequencies of vibrations were measured with the help of a timer-counter. Further details of the measuring set-up and the ways of detecting the four types of vibration are given in the next Chapter. After taking the initial set of measurements the heights of the rings B, C and D were reduced by small amounts of the order of 0.5 mm and the thickness of ring A was reduced by cutting 0.25 mm from both inside and outside, so that the mean radius of the ring remained the same in all cases. The dimensions of the cross-sections were measured in each case and the natural frequencies of vibration were again determined. The process continued until rings B, C and D became so thin of the order of 1.0 mm or so and the ring A attained a thickness equal to that of ring C. This provided a huge volume of data for the various types of ring vibration under varying dimensions of cross-sections.

Regarding the accuracy of the measurements it can be stated that the frequencies of vibration showed negligible differences due to changes in the mounting conditions of the ring, viz. on blade, drawing pins etc. However in cases where the frequencies were recorded with different mountings, the mean value was calculated in each case and the corresponding standard deviation was noted in order to calculate the coefficient of variation, viz. standard deviation expressed as a percentage with respect to the mean value. These coefficients of variation were more or less constant throughout the whole frequency region, with a mean value of 0.034 ± 0.018.

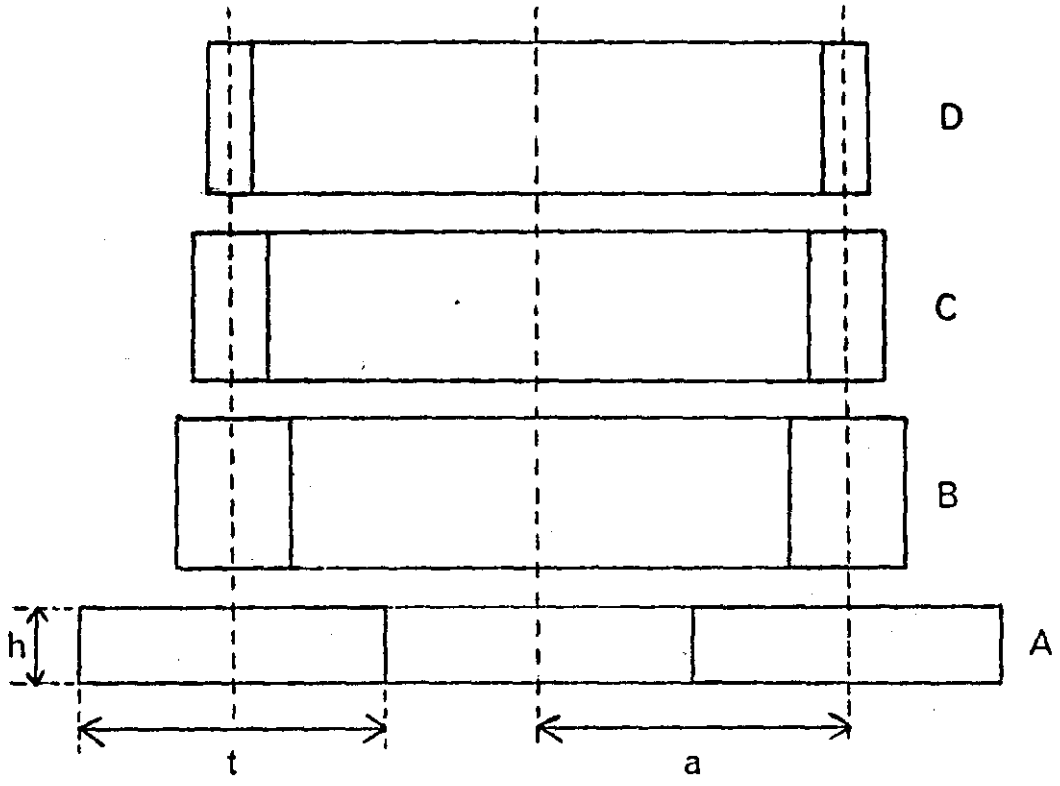

Figure 5.1 Nature of circular rings used for investigation.

TABLE 5.1

Initial dimensions of circular rings

Ring	Mean radius a (mm)	Height h (mm)	Thickness t (mm)	Mass M (kg)	Density ρ (kg m^{-3})
A	107.18 $\pm$0.03	5.93 $\pm$0.015	30.07 $\pm$0.015	0.934 $\pm$0.0001	7.777 x10^3
B	106.96	23.67	8.045	1.000	7.818
C	106.90	23.58	5.92	0.734	7.825
D	106.935	24.07	3.99	0.504	7.818

CHAPTER VI

EXPERIMENT AND RESULTS

6.1 INTRODUCTION

As has been mentioned earlier, the aim of the present investigation is to provide substantial experimental data to check the validity of the classical thin ring formulae and to formulate an empirical correction based on the experimental results to apply for the case of thick rings. This necessitated exciting the four types of vibration without difficulty and identifying the different modes from the overall vibration spectrum. To this end different methods of excitation and detection have to be used along with various types of mountings as the ring becomes thin. As the circular ring is an ideal example of an axially symmetrical vibrating system, most of the normal modes are degenerate doublets. During the course of the thinning operation, as the frequency change was many times greater than the splitting of the doublet components, the occurrence of these doublets did not create any serious problem as such. However, for small frequency changes only one component of the split doublet was considered throughout. Also, to ensure that the variations in room temperature did not affect the observed frequencies a constant room temperature of 20 $\pm$ 1^{o}C was maintained throughout.

6.2 EXPERIMENTAL SET-UP

The experimental set-up used for measuring the natural frequencies and the number of nodal diameters and circles of the different rings is shown in Figure 6.1. The set-up is essentially similar to the one used for doublet measurements as explained in Chapter III.

The ring is hung on a sharp blade held vertically and is excited by a megnetic transducer fed from an oscillator. The vibrations induced in the ring are detected by a capacity transducer feeding into a measuring amplifier and a slave filter which follows the oscillator. The out-put of the measuring amplifier is fed into a level recorder,

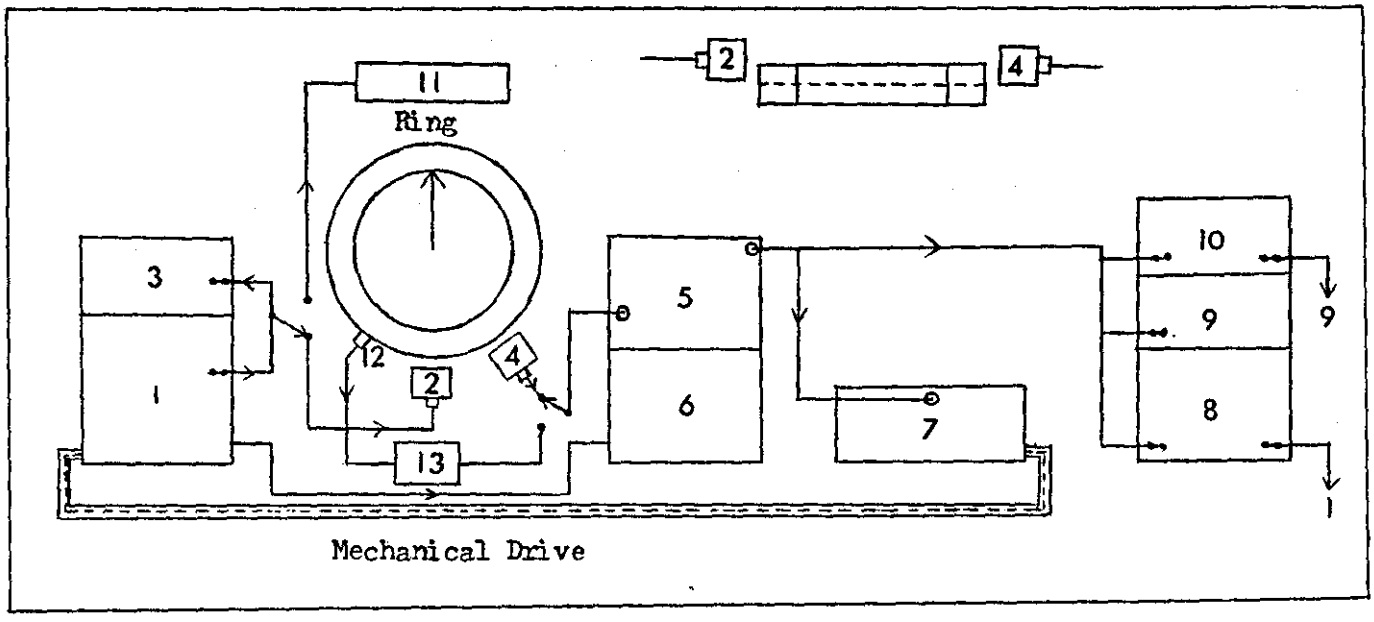

1. B & K Beat frequency oscillator Type 1022.
2. B & K Magnetic Transducer Type MM0002.
9,3. Advance Instruments Timer-counter Type TC9B/S.
4. B & K Capacitive Transducer Type MM0004.
5. B & K Measuring amplifier Type 2606.
6. B & K Heterodyne slave filter Type 2020.
7. B & K Level recorder Type 2305.
8. Solartron Oscilloscope.
10. Leveller of reference [29].
11. loudspeaker.
12. B & K Accelerometer Type 4344.
13. B & K Vibration pick-up pre-amplifier Type 2625.

Figure 6.1 Experimental set-up.

an oscilloscope, a counter and a leveller [29] if desired. The oscillator frequency can be adjusted either manually or driven mechanically by the level recorder. A miniature accelerometer is also used to detect the phase change on the ring's surface. The accelerometer can be connected to the measuring amplifier via a preamplifier.

Alternatively, the ring can be excited with the help of a loudspeaker placed about 30 cm distant and driven by the oscillator. Also the ring can be supported on three drawing pins held vertically and kept at the corners of an inscribed equilateral triangle.

6.3 EXCITATION/DETECTION OF DIFFERENT MODES

It may be recalled that the magnetic transducer, blade support, and the capacity pick-up are used so that there is minimum material contact between the ring surface and other measuring and supporting surfaces. Ideally the radial and extensional modes can be excited without any difficulty by keeping the driving transducer in the plane of the ring and the axial and torsional modes can be excited by keeping the transducer at right angles to this plane. For detection the capacity pick-up should also be in the same plane as the driving transducer. However, a number of trials have shown that all the four types of vibration can be excited simultaneously by keeping the magnetic transducer a bit off-centre, as shown in Figure 6.1, in the plane of the ring. The capacity transducer can now remain in the same plane facing the ring surface also situated a bit off-centre. This type of excitation is not really suitable especially for flat and very thick rings due to the heavy mass that has to be moved during vibration. This difficulty can be overcome by supporting the ring on three drawing pins kept at the corners of an inscribed equilateral triangle. The driver and detector should remain in the same plane, the radial and extensional modes are measured by keeping the transducers in the plane of the ring, and the torsional and axial modes by keeping them at right angles to this plane as before. These two different ways of excitation produce negligible differences in the measured frequencies provided the supporting pins are confined to their exact positions.

As the rings became thin, one method of excitation/detection was not enough to measure all modes of vibration, so also different mountings had to be used. For example, blade support, magnetic excitation and capacitive detection were enough to measure the radial and extensional modes of thin rings. For axial modes of thin rings loudspeaker excitation and capacity detection were found to be suited for the lower frequency modes. The torsional modes and higher axial modes of thin rings were better excited/detected on pin supports. The positioning of the ring is very critical when measuring the fundamental axial mode ($n = 2$), and the torsional and extensional modes corresponding to $n = 0$. When measurement was found to be difficult, especially towards higher frequency modes, the miniature accelerometer stuck to the ring's surface with plasticine was used for initial detection in many cases.

6.4 IDENTIFICATION OF THE DIFFERENT MODES

Keeping the magnetic transducer and the capacity pick-up in their respective off-centre positions in the plane of the ring, the oscillator is swept through the whole audio range and the resonant frequencies are marked on the chart of the level recorder with the help of the counter. In this preliminary run most of the normal modes can be marked on the vibration spectrum. Then the individual resonances are tuned one by one and their accurate frequencies are read on the counter to an accuracy of $\pm$ 0.1 Hz. A higher precision can be obtained by using the leveller circuit [29] to measure the frequency of the decaying oscillations, if desired. The genuine resonant frequencies of ring vibration are identified by observing the decay response on the level recorder or oscilloscope. A spurious resonance is identified by its fast decay compared with the slow decay of the ring mode, e.g. due to a support resonating.

Next, the different modes of vibration are identified. Without disturbing the set-up the resonant frequency is tuned in as usual. If now the capacity transducer is moved to and fro in a direction perpendicular to the plane of the ring, as shown in Figure 6.2, a radial mode is identified if the trace on the oscilloscope remained unaltered with respect to the fixed trace of the reference voltage. A change in

(a) Radial/Extensional Modes

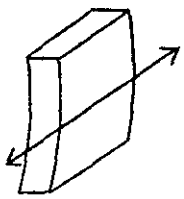

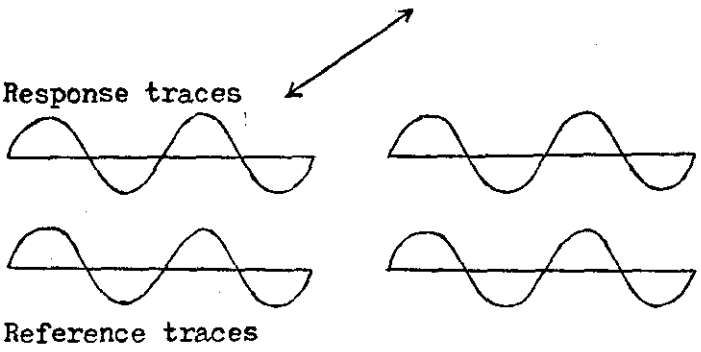

(b) Axial Modes

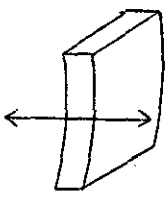

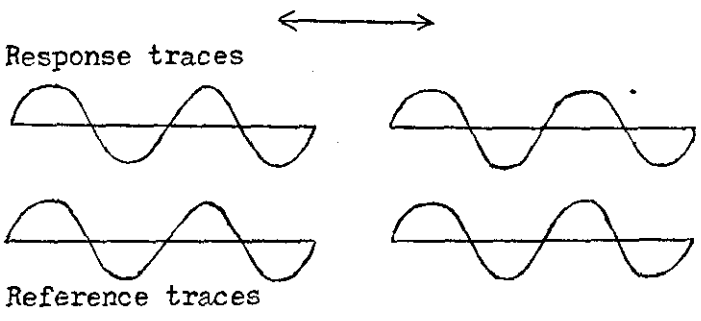

(c) Torsional Modes

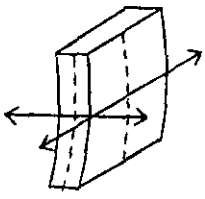

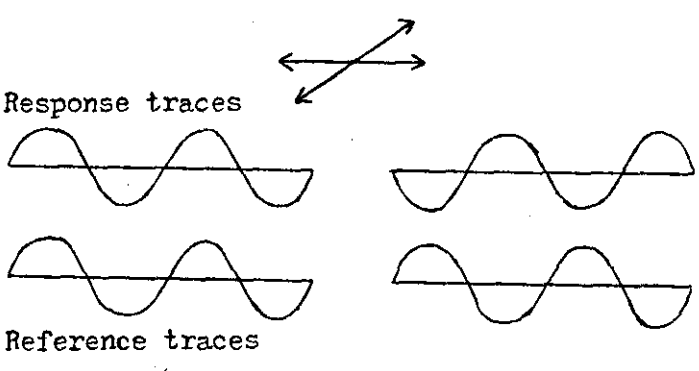

Figure 6.2 Identification of the various modes of vibration of circular rings.

position by Π radians indicates the presence of a torsional mode. The radial modes are further characterised by having greater vibration response in the plane of the ring compared with the out-of-plane response.

The radial modes are differentiated from the extensional modes by the absence of breathing (n = 0) and swinging (n = 1) modes [1]. Moreover the extensional modes generally occur towards the high frequency region of the vibration spectrum and hence there is no further difficulty in identifying extensional modes with n = 2 and higher.

To identify an axial mode the detector is moved along a line in the plane of the ring on one side, as shown in Figure 6.2. If there is no phase change the particular mode under observation is an axial one, as otherwise, it is a torsional mode. The axial mode is also characterised by having greater vibration response in the out-of-plane direction compared with the in-plane response. Further the torsional mode is characterised by the presence of nodal lines on both sides of the cross-section as shown in Figure 6.2.

Alternatively the radial and axial modes can be identified with the help of two detector transducers as shown in Figure 6.3. Holding the two transducers in the plane of the ring if the outputs of the two, as seen on an oscilloscope, are in anti-phase that mode is a radial one as otherwise the two outputs will be in phase for the axial mode. Similarly if the two transducers are held in the out-of-plane direction the two outputs will be in anti-phase for the axial mode and in phase for the radial mode. In general, the outputs of the axial mode in the first case and those of the radial mode in the second case will be very weak.

Next one has to measure the number of nodes for each observed mode. After tuning in the particular frequency the accelerometer is moved around the circumference of the ring. The presence of a node is characterised by the sudden change of phase by Π radians corresponding to a change in position of the trace on the oscilloscope with respect to the reference trace. It has to be remembered that the nodal points are never points of zero vibration. For example, in the case of radial

(a) Radial Modes (b) Axial Modes

Figure 6.3. Detection of flexural modes using two transducers.

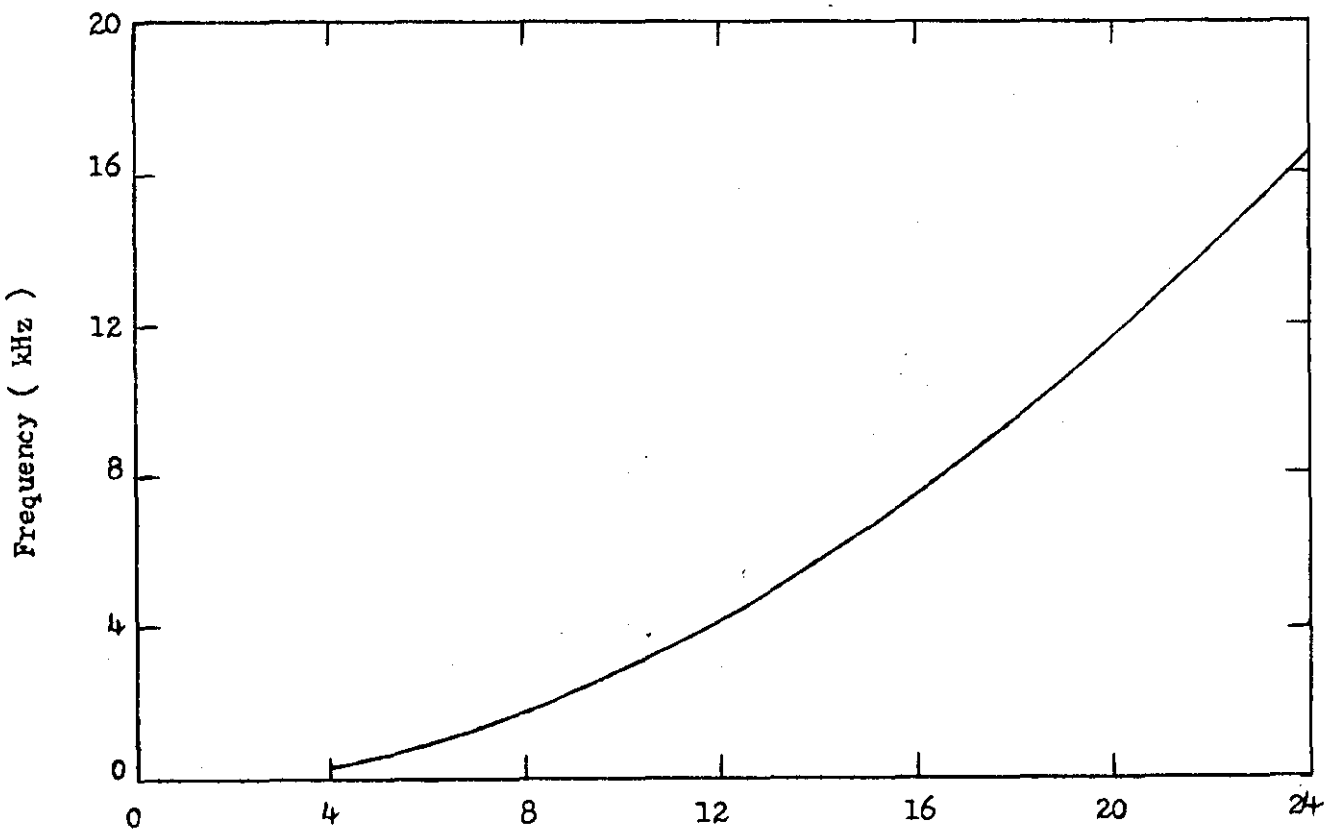

Figure 6.4. Plot of frequency vs. number of nodes of vibration of circular rings.

vibration the nodal points correspond to places of vanishing radial motion but the tangential motion there is a maximum.

Thus one can identify the four different types of vibration and the frequencies and number of nodes for each particular mode. Now, if one plots the frequencies of one type of vibration, say, radials against the number of nodes one gets a smooth curve as shown in Figure 6.4. This is advantegeous in the sense that any missing frequency can be easily identified by reading off the frequency corresponding to the number of nodes. This is also helpful in checking the correctness of the observed frequencies, as the various points should lie on a smooth curve. It occurs sometimes as two or three frequencies belonging to different types of vibration lie close to one another thereby making direct identification difficult, although the frequencies may be measured accurately. They can now be categorised from the curve.

6.5 COURSE OF THE EXPERIMENT

After completing one set of measurements on the four rings, the heights of rings B, C and D are reduced by 0.5 mm while the thickness of ring A is reduced by 0.25 mm from both inside and outside so that the mean radius remains the same in all cases. As before, the dimensions and mass of the ring are measured. The frequencies of the four different types of vibration and the number of nodes of each mode are measured as described in the previous sections. Whereas the frequencies of the radial and extensional modes did not change much for rings B, C and D, the frequencies of the axial and torsional modes varied considerably. However, for ring A the frequencies of the axial and extensional modes vary slowly and the frequencies of the radial and torsional modes vary considerably.

The procedure is repeated and the rings become thinner as the experiment proceeds. It may not be necessary to record the vibration spectrum after every thinning operation because by that time one clearly knows where to search for the next frequency. Sometimes the methods of excitation and detection have to be changed in order to ensure that all frequencies are identified and measured. The situation becomes complicated

when the ring becomes thin, and for very thin rings, the number of axial modes increases rapidly and the problem of identification becomes increasingly difficult. The number of radial, torsional and extensional modes, more or less, remain the same throughout the whole thinning operation. Also the measurement of the ring's dimensions becomes prone to errors as it becomes thinner. Hence the values of heights and thicknesses in many cases, as one can see later, have to be determined from the knowledge of the respective masses. The observations were continued until rings B, C and D became very thin - of the order of 1.0 mm or so - and ring A attained a thickness equal to that of ring C.

6.6 RESULTS

The investigation provided a large volume of frequency data for the different modes of vibration under varying conditions of cross-sectional dimensions. The results are shown graphically in Figures 6.5, 6.6, 6.7 and 6.8, where the frequencies of each type of vibration are plotted against thickness/height of the ring for each value of n. The exact values of the frequencies and the details of the dimensional parameters can be seen in Appendix IV.

Referring to the response curves certain interesting aspects of ring vibration can be seen. For radial modes the frequencies of vibration are practically independent of the variation in height of the cylinder as is evident from the response curves, for rings B, C and D, which are more or less parallel to the base. For ring A, where the frequencies are plotted against thickness, the frequencies of the radial mode vary linearly. The axial vibration also shows insensitivity to variation in thickness to a certain extent as seen in Figure 6.6(a) where the response curves are parallel to the base. In cases where the height of the cylinder is varied (rings B, C and D), the response curves change in a linear fashion up to a certain height and thereafter exhibit non-linearity. This height also depends upon the size of the cross-section.

The torsional response curves also exhibit a linear response upto a certain height of the cylinder and show non-linearity afterwards. For

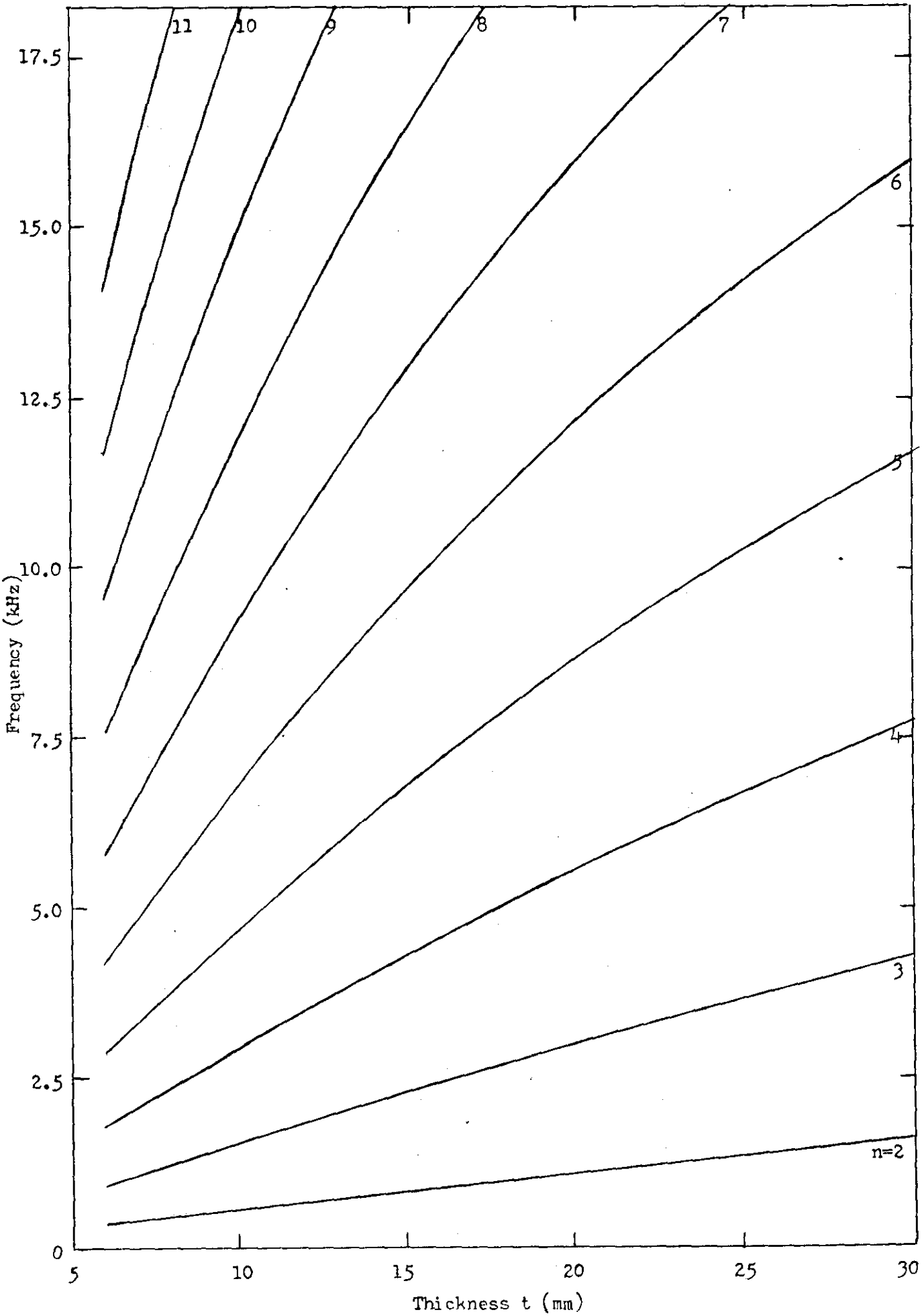

Figure 6.5 Natural frequencies of vibration of circular rings of rectangular cross-section. (a) Radial modes: Ring A.

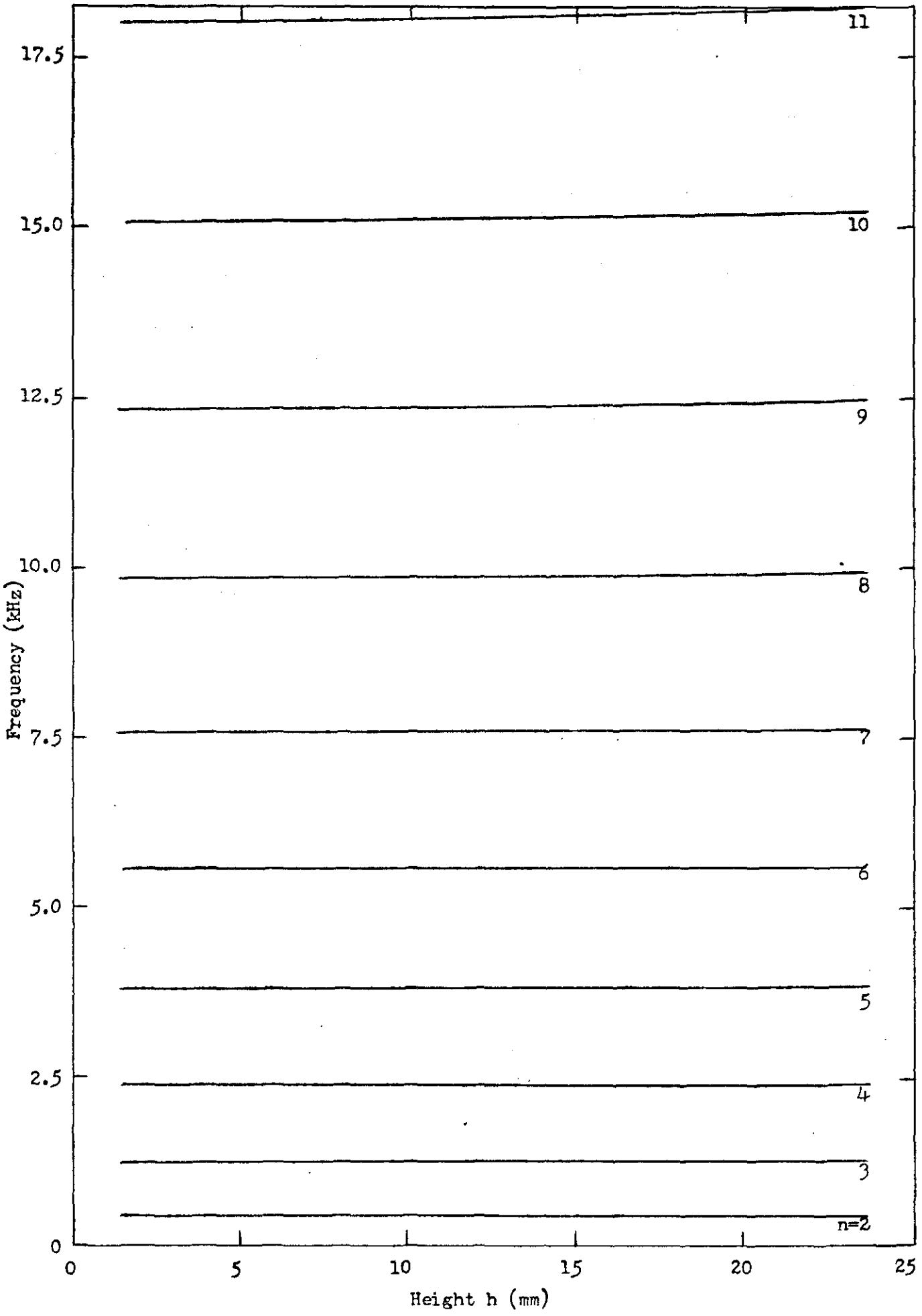

Figure 6.5 Natural frequencies of vibration of circular rings of rectangular cross-section. (b) Radial modes: Ring B.

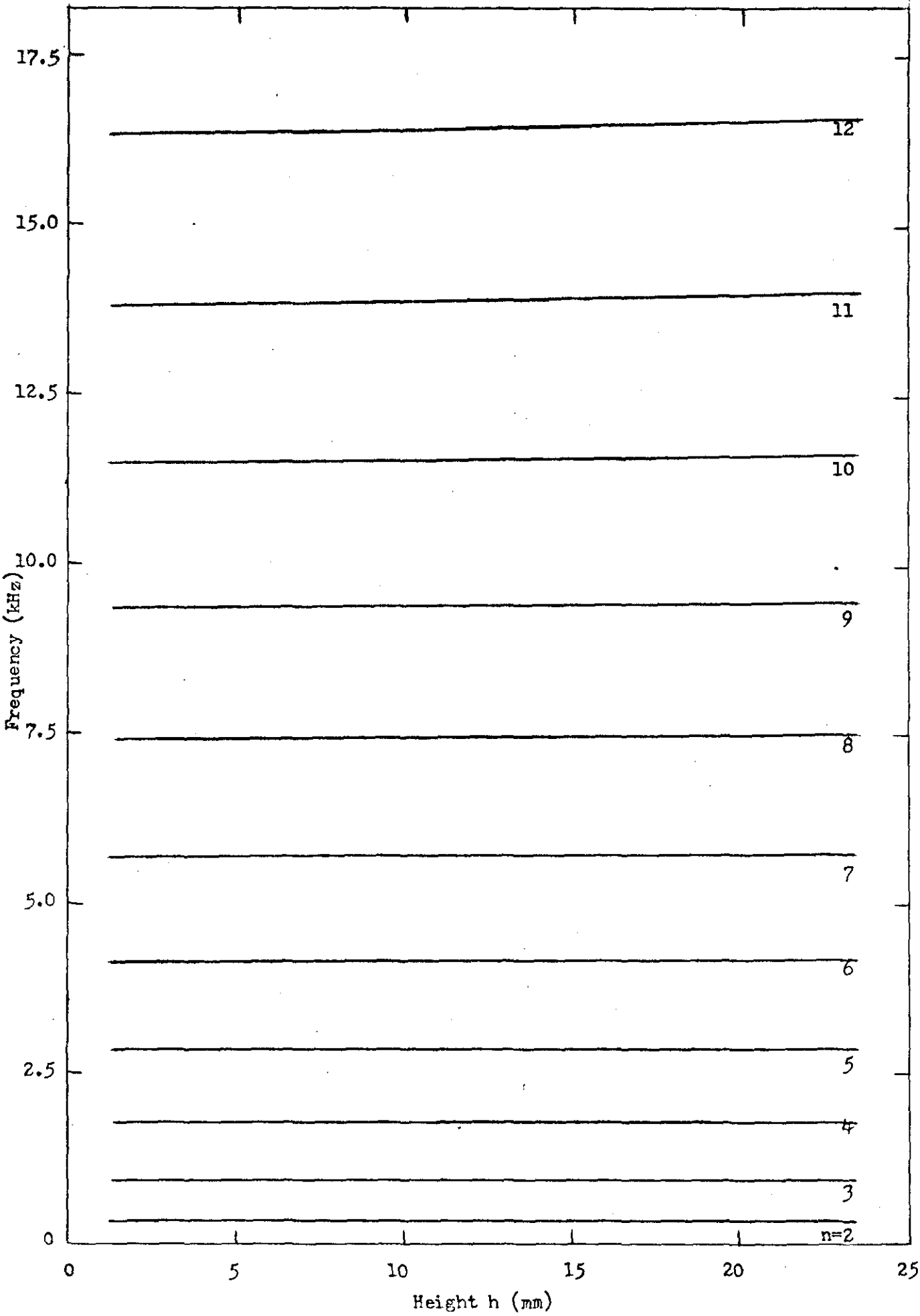

Figure 6.5 Natural frequencies of vibration of circular rings of rectangular cross-section. (c) Radial modes: Ring C.

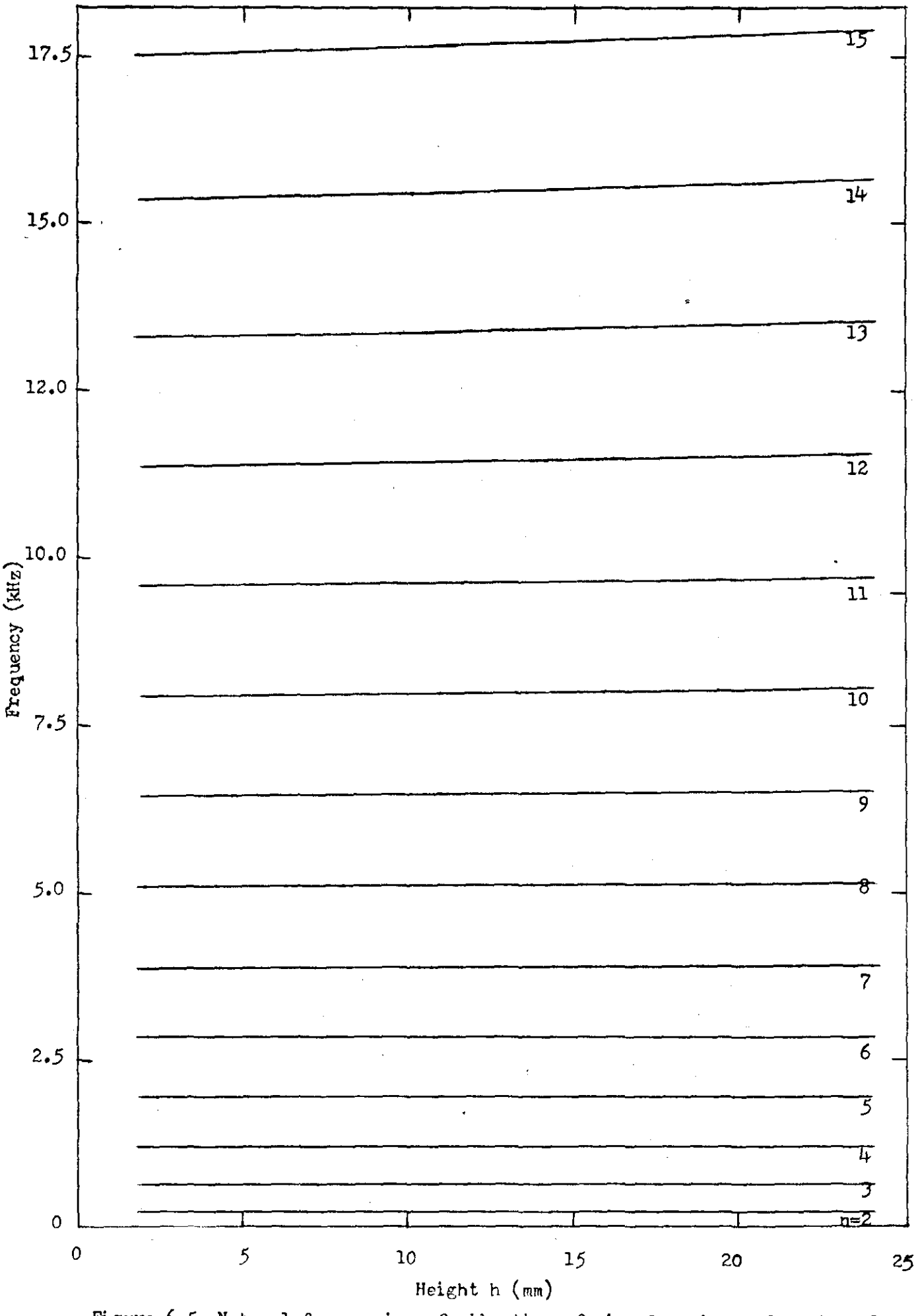

Figure 6.5 Natural frequencies of vibration of circular rings of rectangular cross-section. (d) Radial modes: Ring D.

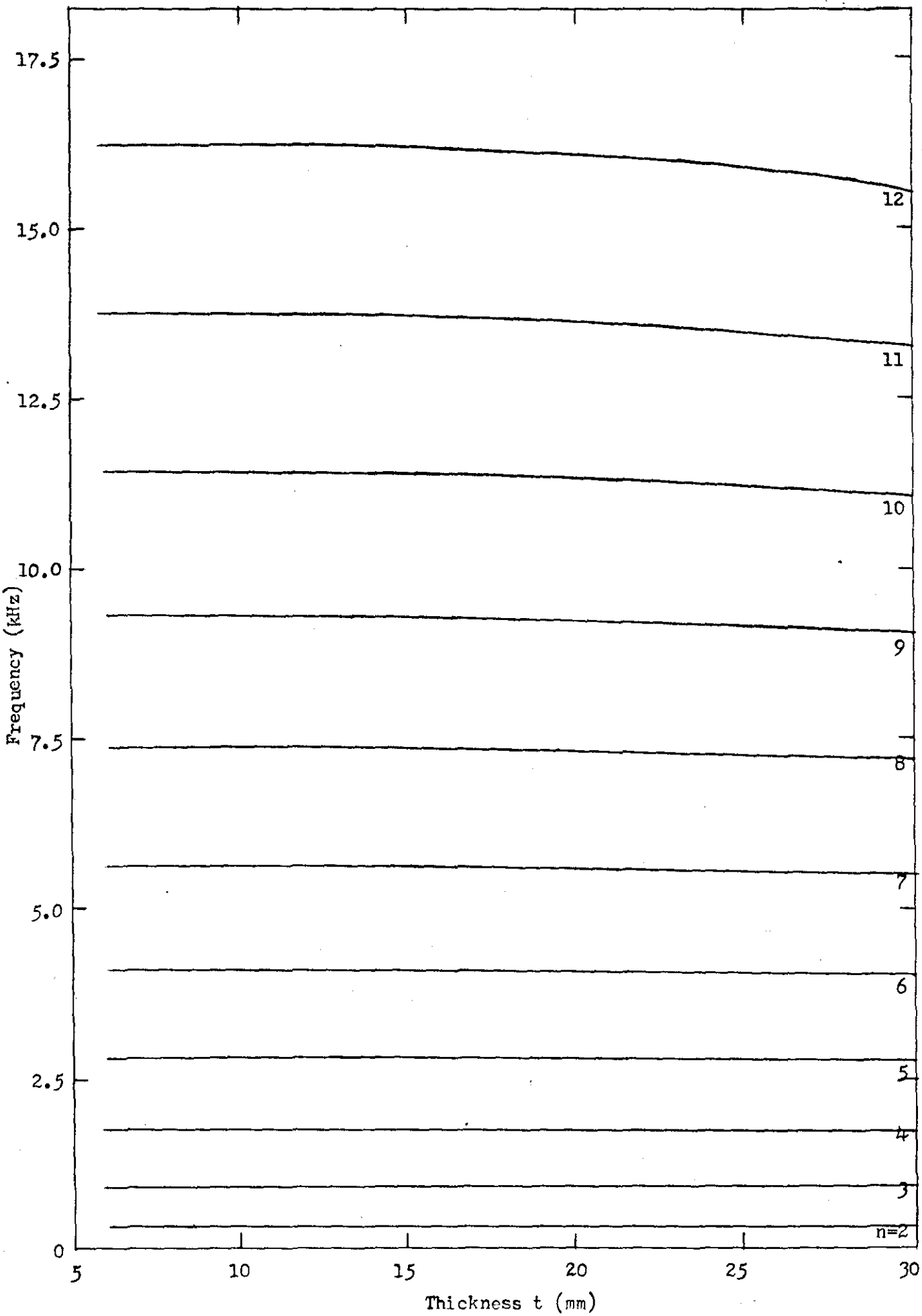

Figure 6.6 Natural frequencies of vibration of circular rings of rectangular cross-section. (a) Axial modes: Ring A.

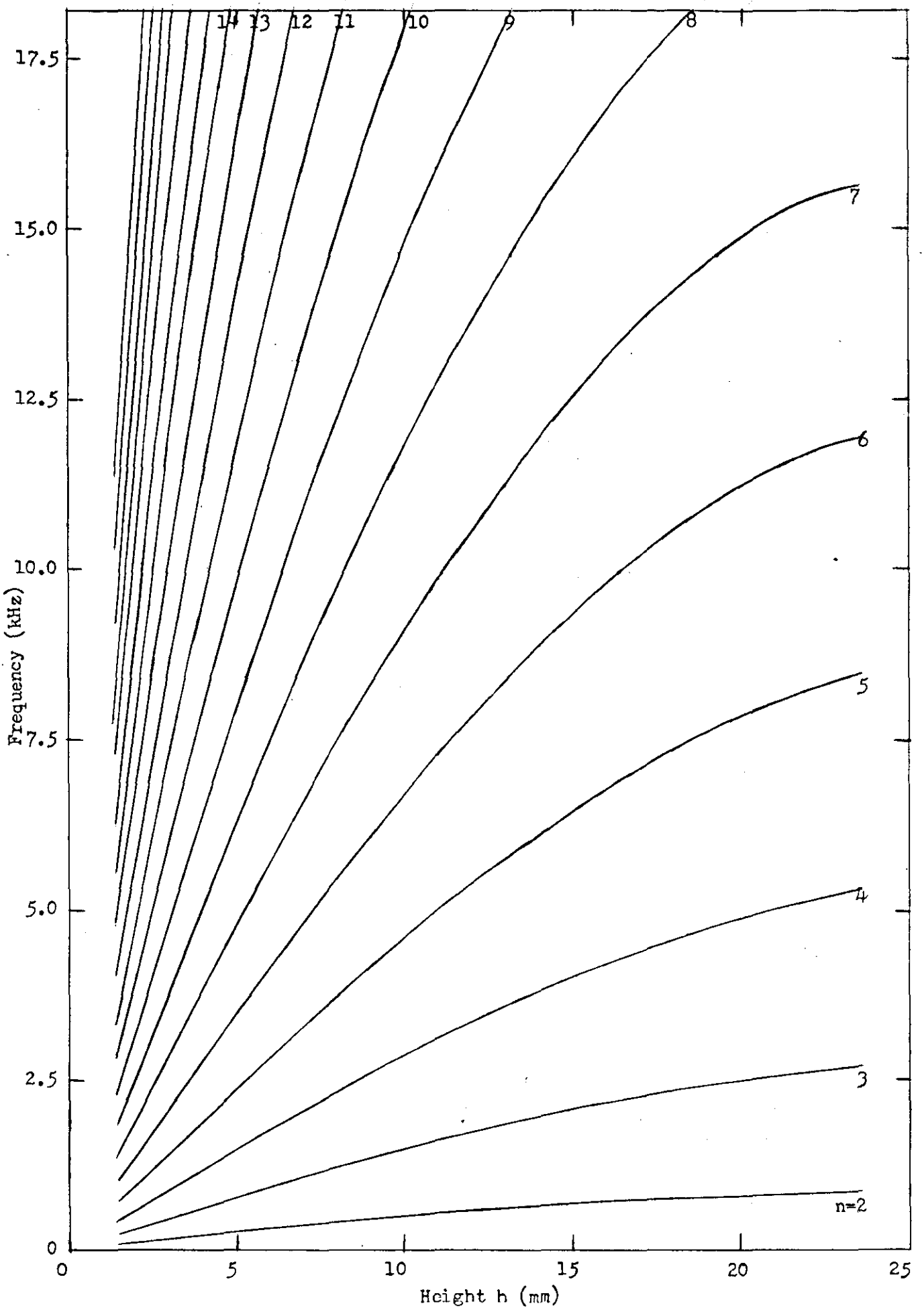

Figure 6.6 Natural frequencies of vibration of circular rings of rectangular cross-section. (b) Axial modes: Ring B.

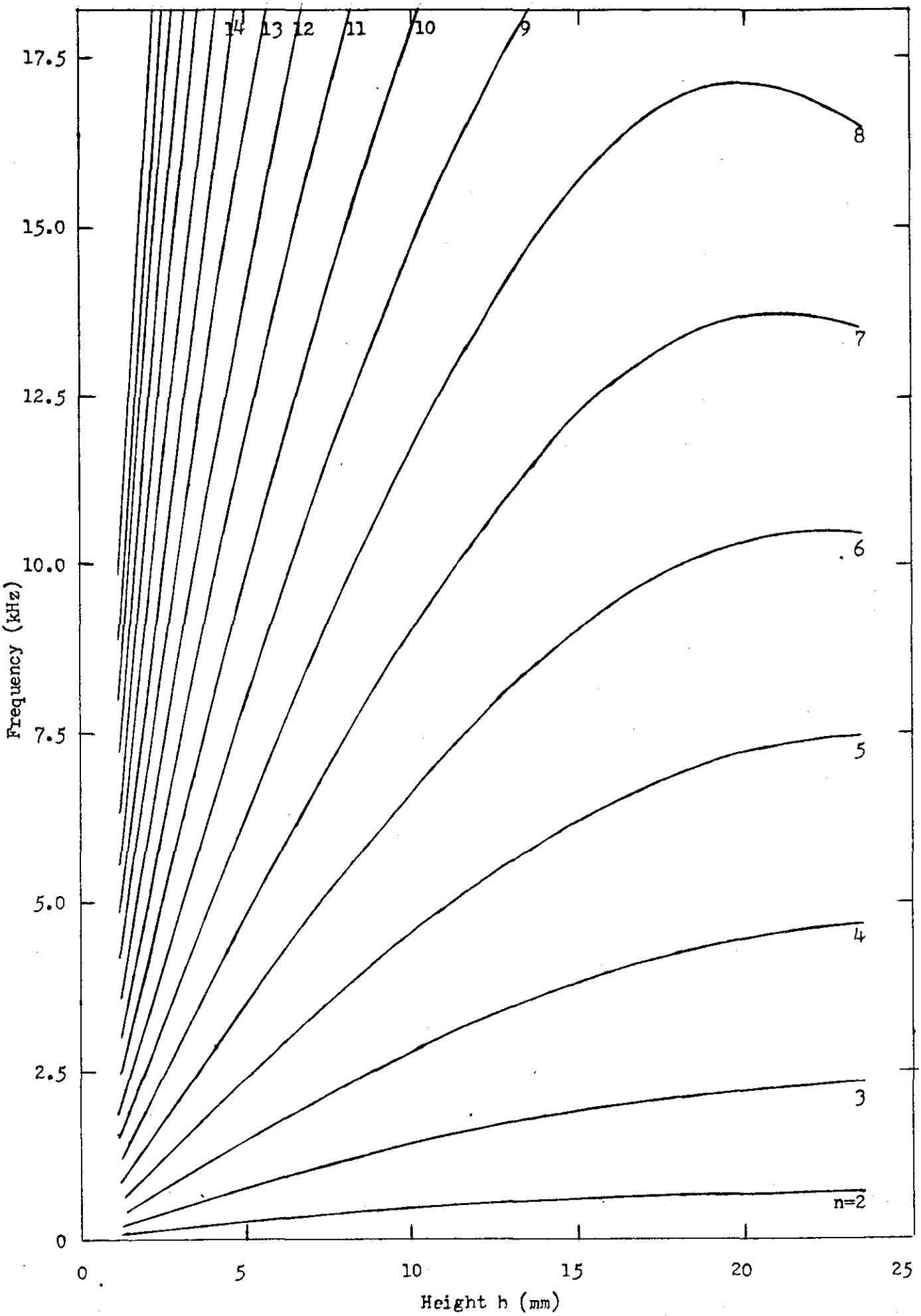

Figure 6.6 Natural frequencies of vibration of circular rings of rectangular cross-section. (c) Axial modes: Ring C.

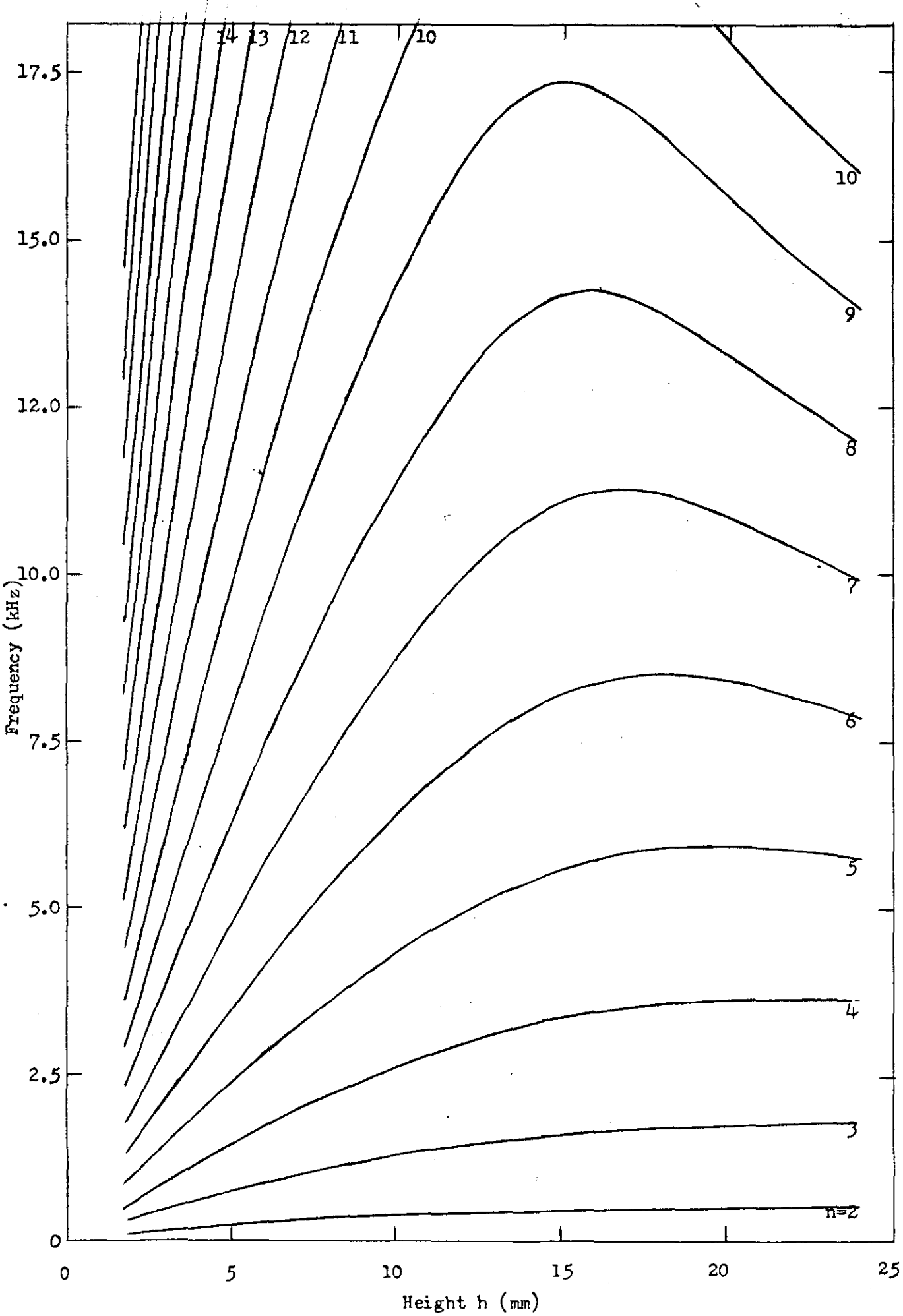

Figure 6.6 Natural frequencies of vibration of circular rings of rectangular cross-section. (d) Axial modes: Ring D.

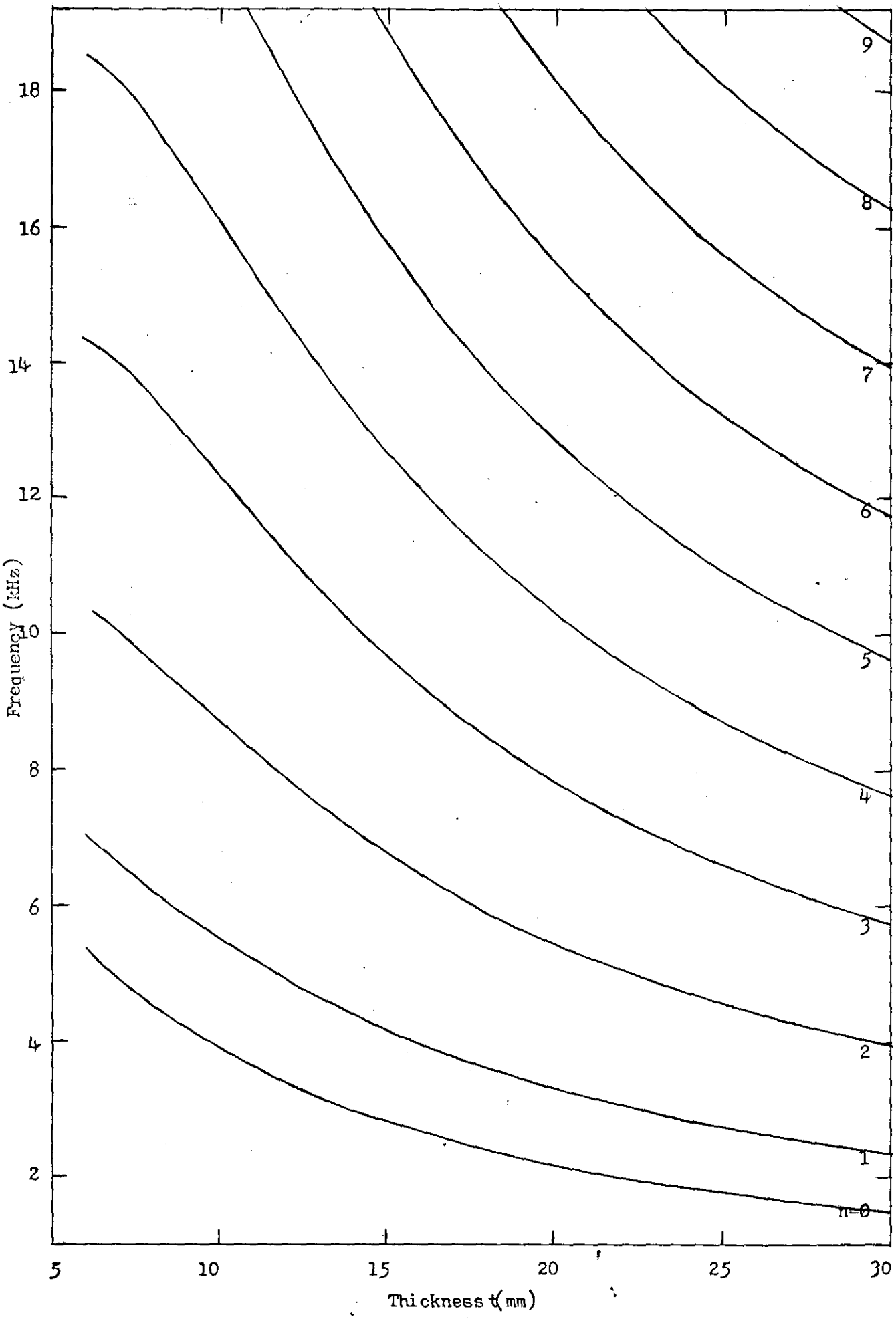

Figure 6.7 Natural frequencies of vibration of circular rings of rectangular cross-section. (a) Torsional modes: Ring A.

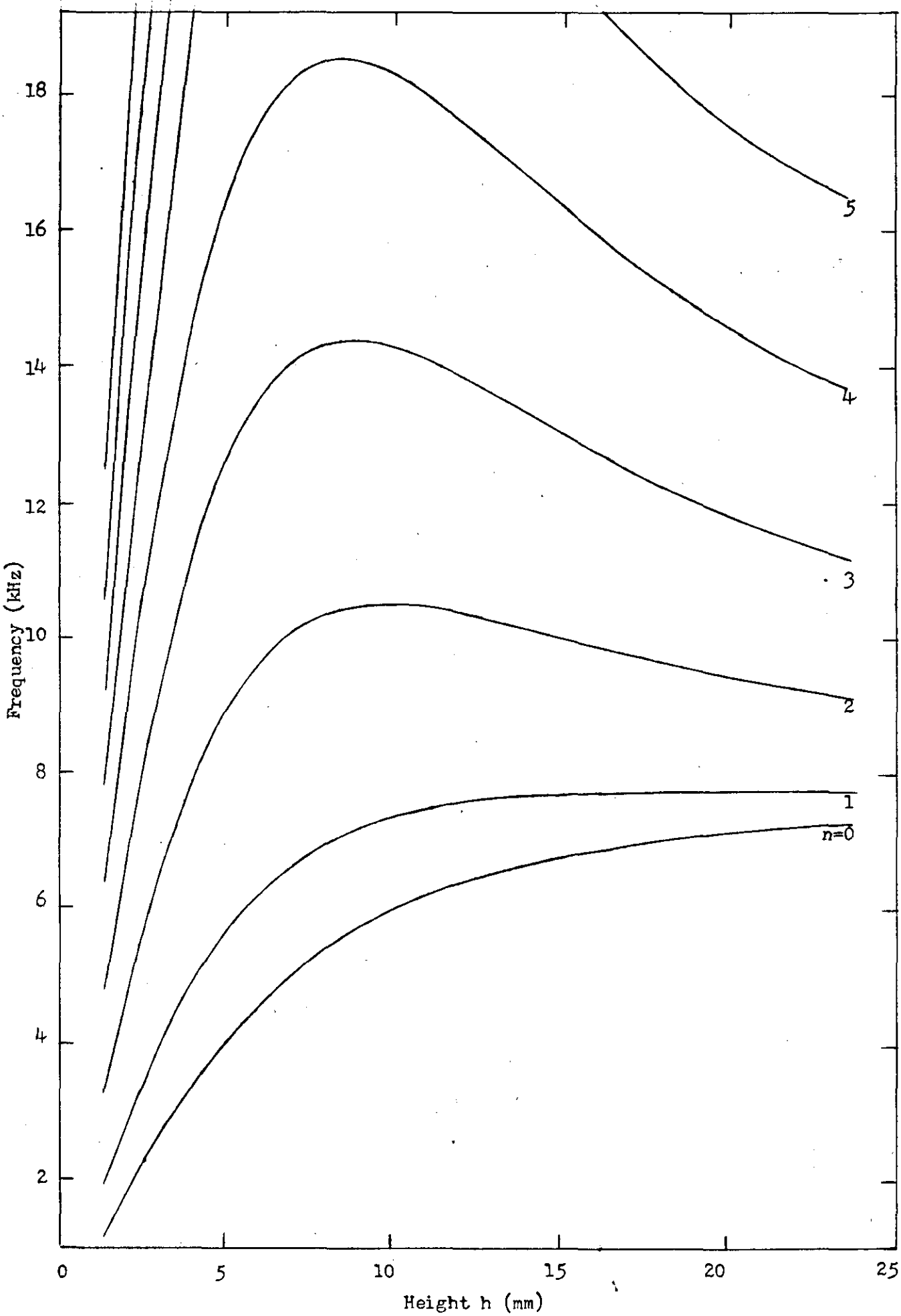

Figure 6.7 Natural frequencies of vibration of circular rings of rectangular cross-section. (b) Torsional modes: Ring B.

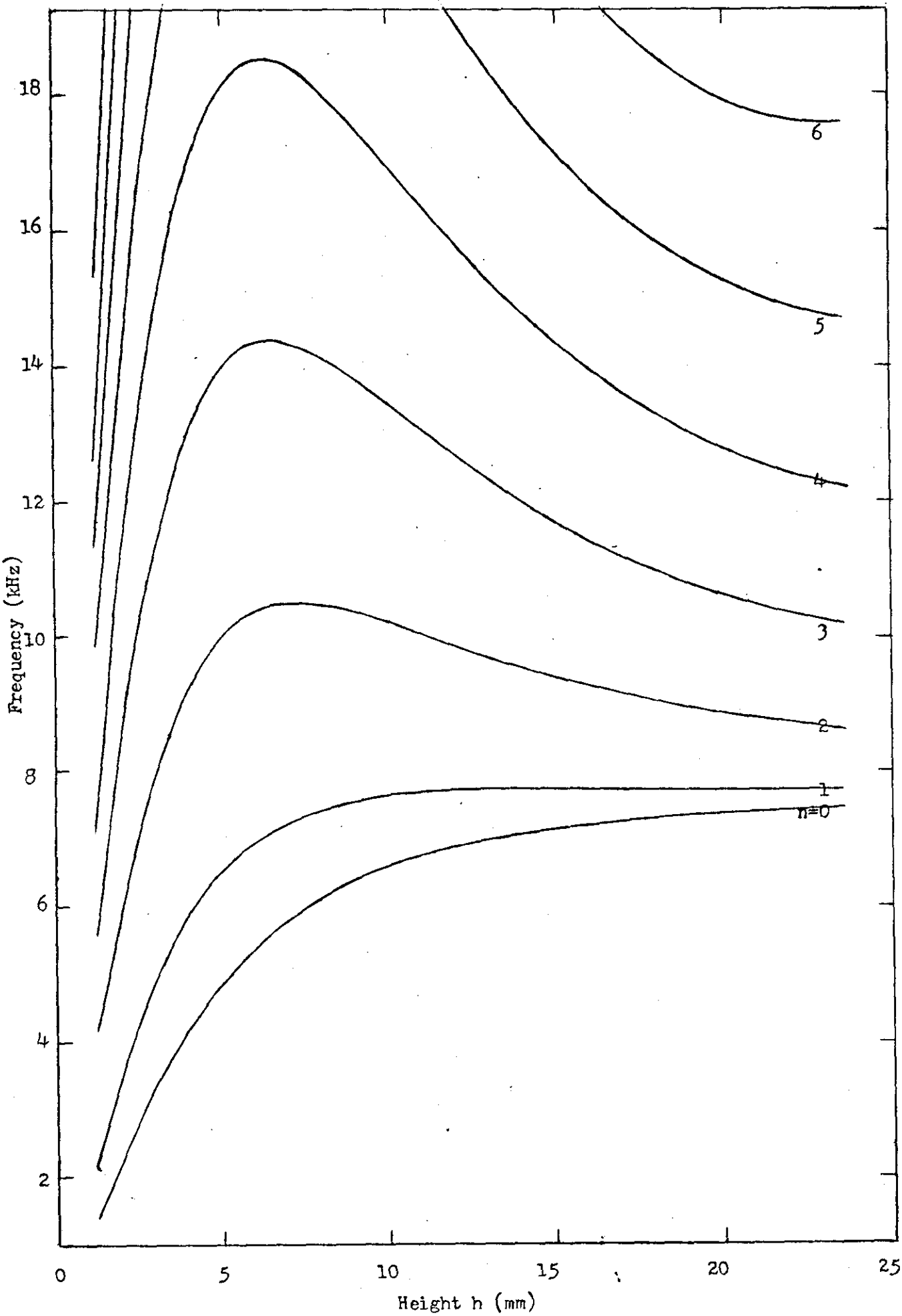

Figure 6.7 Natural frequencies of vibration of circular rings of rectangular cross-section. (c) Torsional modes: Ring C.

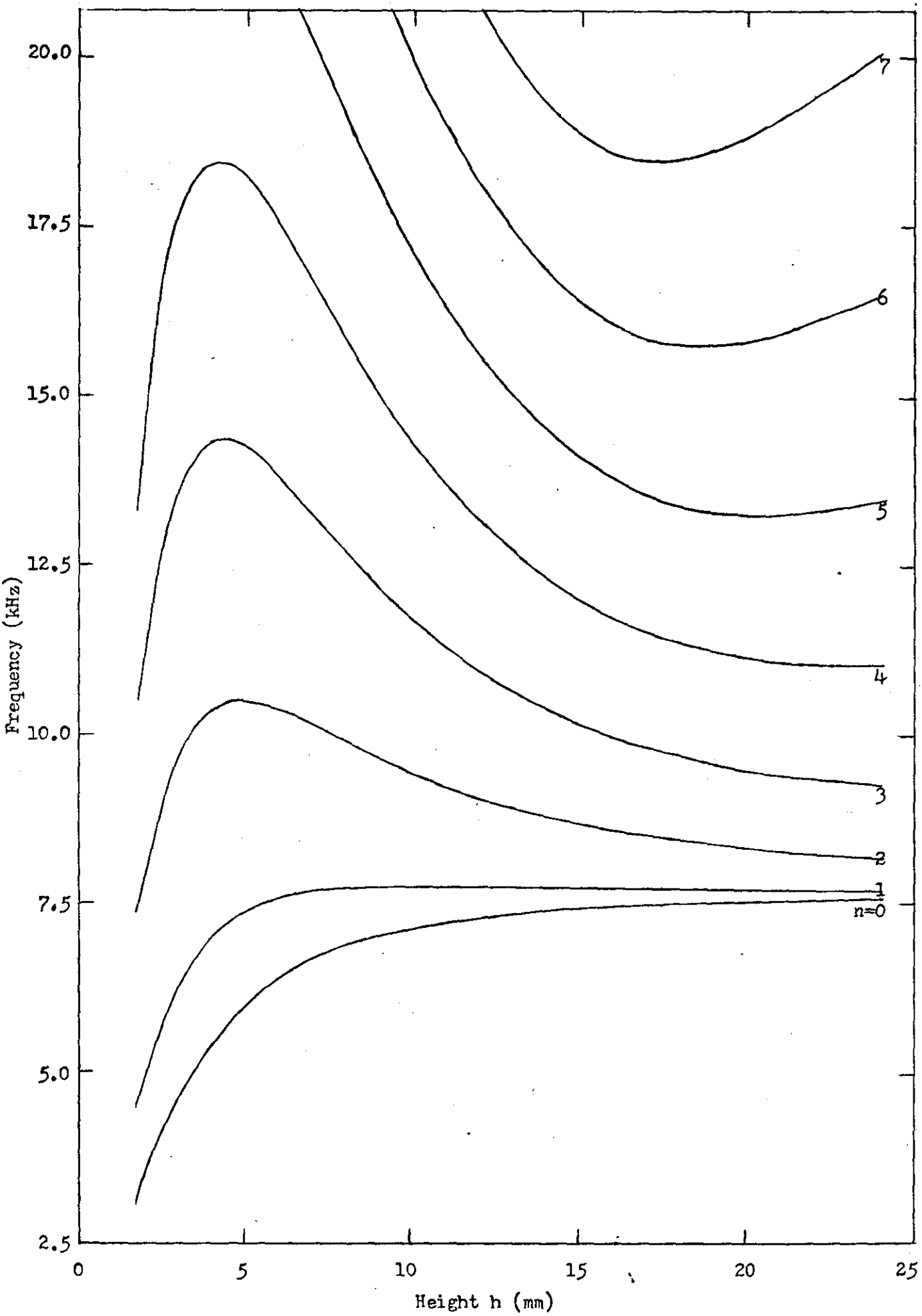

Figure 6.7 Natural frequencies of vibration of circular rings of rectangular cross-section. (d) Torsional modes: Ring D.

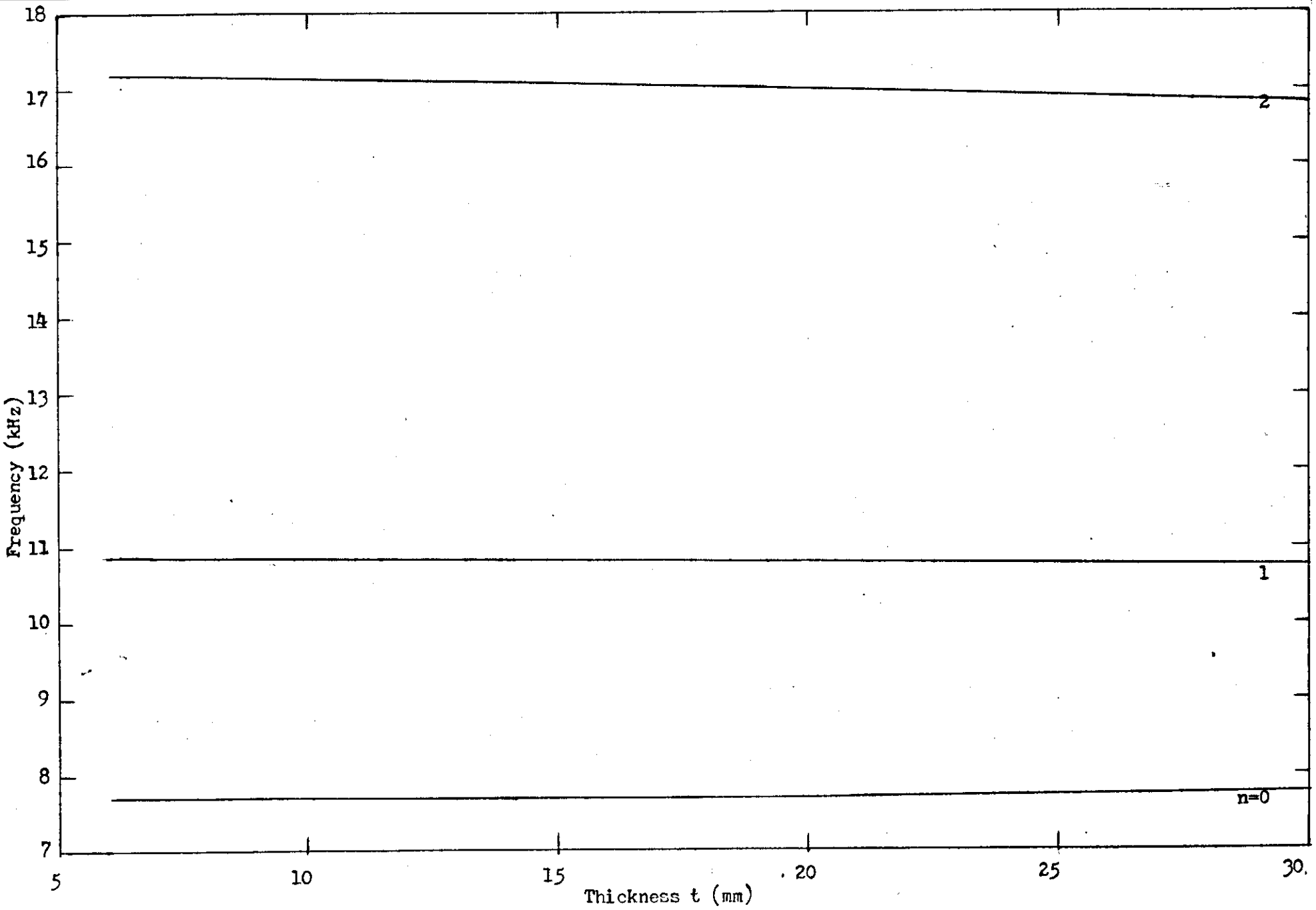

Figure 6.8 Natural frequencies of vibration of circular rings of rectangular cross-section.

(a) Extensional modes: Ring A.

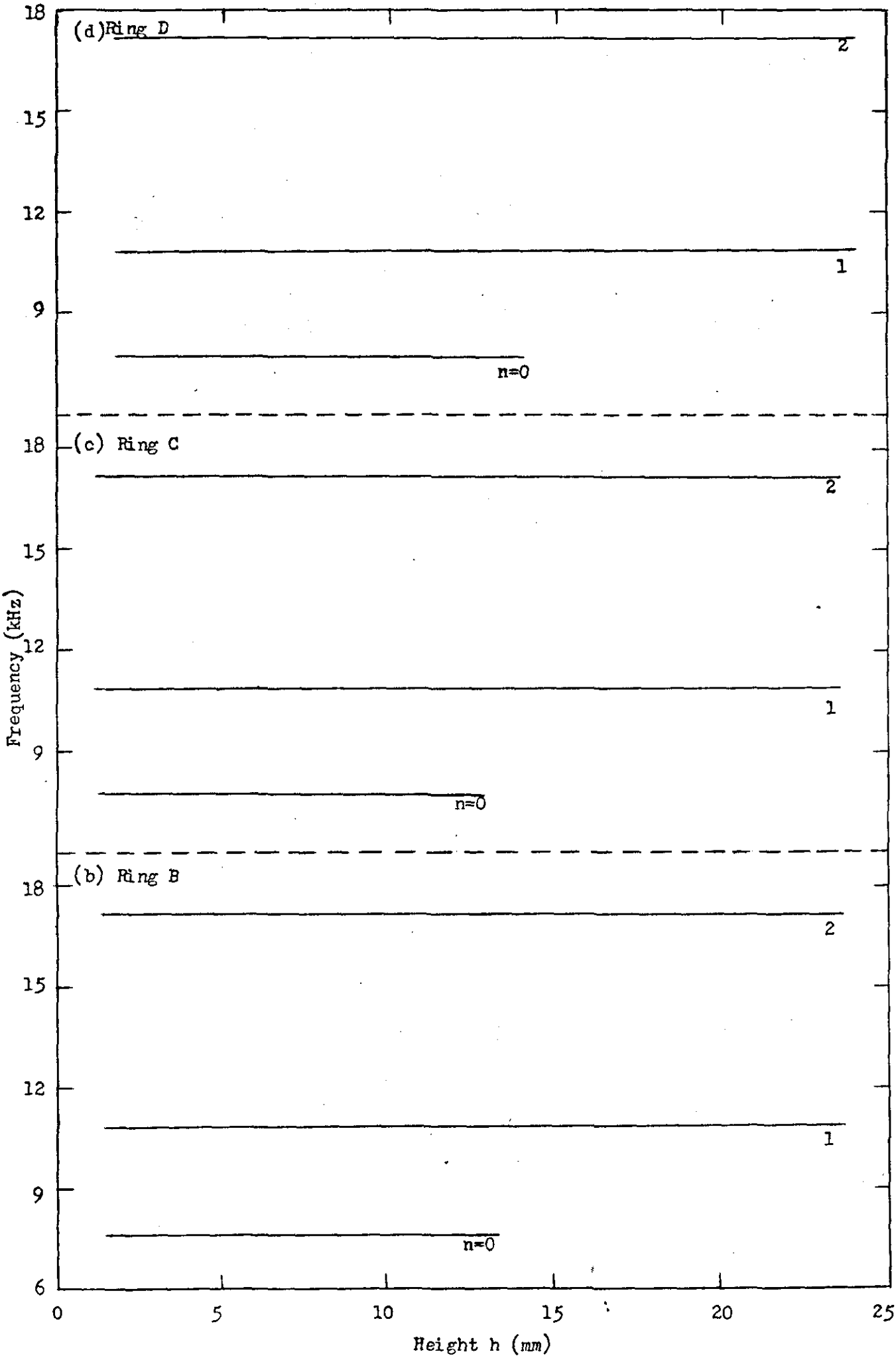

Figure 6.8 Natural frequencies of vibration of circular rings of rectangular cross-section. Extensional modes.

ring A where the thickness is varied a similar behaviour is observed. Like radials the extensional response curves are also parallel to the base and hence show very little variation in frequency with change of height/thickness.

Another interesting feature is the occurrence of increased number of axial modes as the rings become very thin. This shows the relative importance of flexural vibration towards the low frequency region of the vibration spectrum.

The fact that the torsional frequency response curves of Figure 6.7 exhibit peaks as the cross-section varies from rectangular through square can be explained with the help of St. Venant's theory of torsion of prismatic bars of non-circular cross-section. As torsion in these bars involves a distortion of the cross-section there is a non-uniform distribution of the shearing stress over the cross-section. The maximum stress occurs on the boundary at the points which are the nearest to the centroid of the cross-section. According to St. Venant, for a given cross-sectional area the torsional rigidity increases if the polar moment of inertia of the cross-section decreases[66]. It can be shown that for the same cross-sectional area a square cross-section has the minimum polar moment of inertia compared with that of a rectangular cross-section. As the frequency of vibration is proportional to the square root of torque/moment of inertia, the maximum frequency occurs at a square cross-section.

The axial response curves of Figure 6.6 also exhibit a similar behaviour as the height of the cylinder varies, i.e. the frequency of vibration attains a maximum value at a certain height. This can be explained by the theory of flexural vibration of thin cylindrical shells[67]. A cylindrical shell is capable of vibrating in a variety of ways depending upon the particular straining actions involved. It may be recalled that the axial modes consist of displacements at right angles to the plane of the ring plus a twist. Hence the major deformations are due to bending and stretching of the cross-section. However, when the height of the cylinder becomes of the order of half the axial wavelength the relative importance of the various deformations changes. By defining

an axial wavelength factor λ, viz. the ratio of the mean circumference to the axial wavelength, it can be shown that for a given cylinder and for the same number of axial half-waves, λ is inversely proportional to the height of the cylinder. It had been shown that for smaller values of λ (<0.5) the axial modes are mainly due to axial motion and for higher values of λ the axial and radial components become almost equal and the motion approximates to that of inextional radial vibration[67]. Also the strain energy due to stretching decreases rapidly towards higher values of n.

Moreover, in the region where the axial motion predominates the effect of torsion tends to shift the maxima towards the square cross-section expecially towards higher values of n.

CHAPTER VII

THEORETICAL

7.1 INTRODUCTION

In this Chapter the classical formulae for the different modes of ring vibration are discussed along with the improved versions and other new formulae. Only those modified versions are considered which have their end results in a directly applicable form. These modified new formulae are viewed in terms of the classical formulae aiming at developing some empirical correction e.g. a polynomial fit, to account for the dependence of the ring's frequencies on cross-sectional parameters with the help of the experimental results already presented in the previous chapter.

7.2 THE CLASSICAL FORMULAE

The classical theory of thin ring vibration is well known for the case of circular cross-sections. Consider a circular ring of constant cross-section which has an axis of symmetry situated in the plane of the ring. Also the cross-sectional dimensions viz. height h and thickness t, of the ring are considered to be small in comparison with the radius a of the centre line. Let u, v, w represent the displacement of an element of the centre line, as shown in Figure 7.1, whose polar co-ordinates are a and θ. Let A be the cross-sectional area and β the angle of twist of the cross-section about the neutral circle. When the element deforms the action of one part of the element on one side of the cross-section upon the other part is expressed by means of the reactions, estimated per unit area of the cross-section, which are statically equivalent to a force acting at the centroid and a couple. The classical theory, which is a generalisation of the Bernoulli-Euler beam theory, assumes that the stress couples are related to the curvature and twist of the element. The resulting equations of motion are well known and can be seen in references [38,43,57].

The classical formulae for thin ring vibration are derived under assumptions by which shear deflection and rotatory inertia of the element

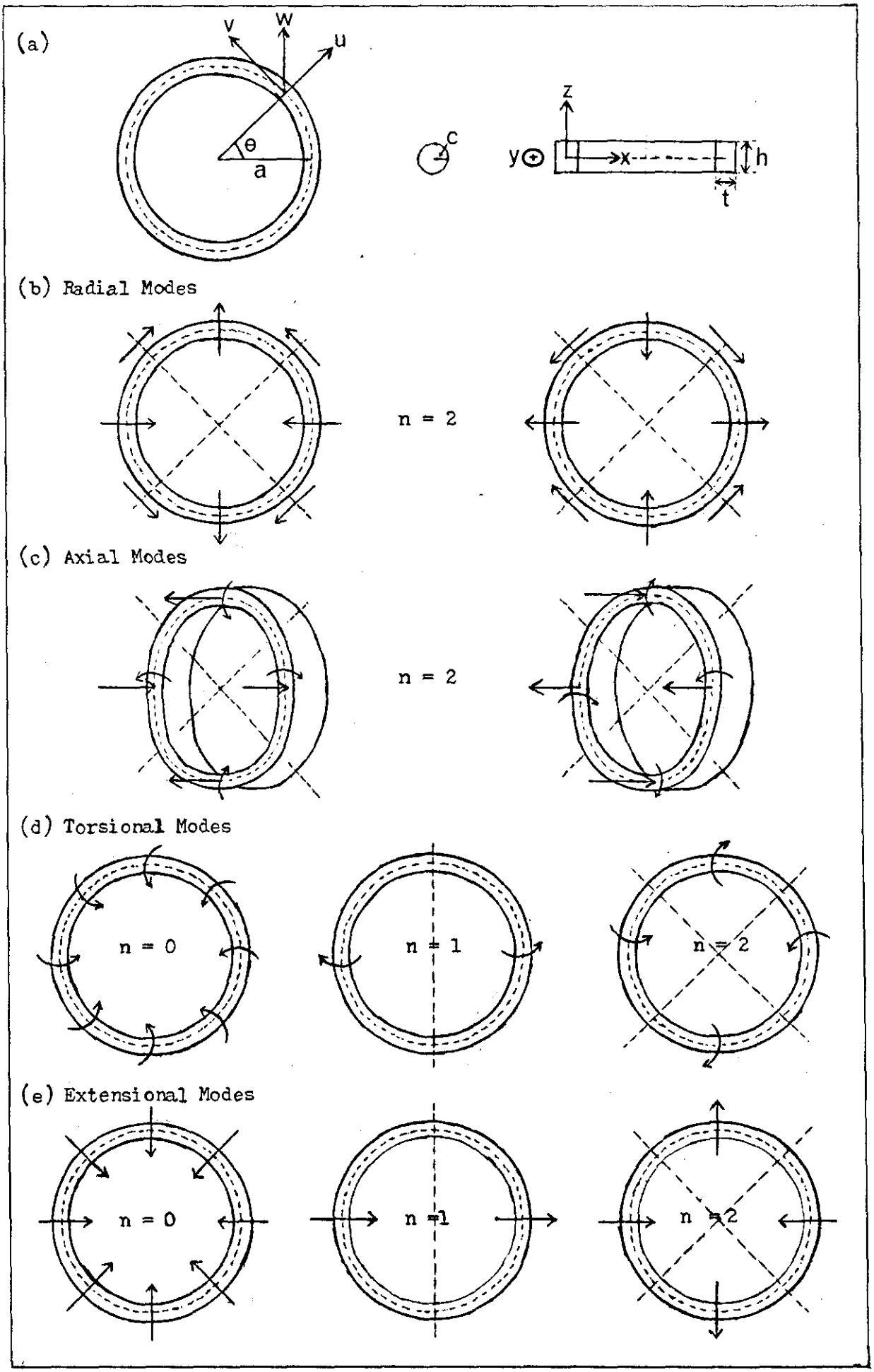

Figure 7.1 Normal modes of vibration of circular rings.

are neglected and inextensibility of the centre-line is assumed. For a circular ring with symmetrical cross-section these assumptions lead to the uncoupling of the radial and axial vibrations. Also other effects like warping vanish for circular cross-section.

7.2.1 The Radial Modes

The radial modes arise when w and β vanish and the motion is specified by displacement u or v: in this case one has flexural vibrations in the plane of the ring. The frequency of radial vibration is given by [38]

$$f_R^2 = \frac{E k_z^2 n^2(n^2 - 1)^2}{4\pi^2 \rho a^4 (n^2 + 1)} \qquad (7.1)$$

where E is Young's modulus of the material, ρ its density, k_z area radius of gyration of the cross-section parallel to z-axis and n is an integer. Here the extension is negligible and the energy is mainly due to bending. The frequencies are comparable with those of transverse vibrations of a bar. There are 2n nodes or places of vanishing radial motion as shown in Figure 7.1, but these are not points of rest: tangential vibration being a maximum at these points. In the case with n = 1 the circle is merely displaced without deformation and hence the period will be infinite. The most important case is that of n = 2 where the ring oscillates between two slightly elliptical forms. This mode is referred to as "hum" in bell terminology [1].

7.2.2 The Axial Modes

The axial modes arise when u = v = 0 and the motion is decided by w and β and one has a combined bending torsion mode involving both displacement at right angles to the plane of the ring and twist. The frequency of axial vibration is given by [38]:

$$f_A^2 = \frac{Ek_x^2}{4\Pi^2\rho a^4} \frac{n^2 (n^2 - 1)^2}{n^2 + 1 + \sigma} \qquad (7.2)$$

where k_x is the area radius of gyration of the rings cross-section parallel to the x-axis and σ the Poisson's ratio. It is to be noted that even in the lowest mode corresponding to n = 2 the frequency differs very little from the frequency for radial vibration given by equation (7.1).

7.2.3 The Torsional Modes

The torsional modes arise when u and v vanish and the motion is specified by w or β. Also w is supposed to be small in comparison with a β. The frequency of torsional vibration is given by [38]

$$f_T^2 = \frac{G}{4\Pi^2\rho_a^2} (1 + n^2 + \sigma) \qquad (7.3)$$

where G is the rigidity modulus of the material of the ring. When n = 0 the equation of motion can be satisfied by putting w = 0 and taking β to be independent of θ. The vibration of this mode is characterised by the fact that each (circular) cross-section of the ring is turned in its own plane through the same small angle β about the neutral circle while the circle itself is not displaced.

7.2.4 The Extensional Modes

The extensional modes arise when w and β vanish and inextensibility condition $u + \frac{\partial v}{\partial \theta} = 0$ does not hold good. The frequency of these pure radial vibrations is given by [38]

$$f_E^2 = \frac{E}{4\Pi^2\rho_a^2} (1 + n^2) \qquad (7.4)$$

This type of vibration is analogous to the longitudinal vibration of a straight bar, the potential energy being mainly due to extension. When $n = 0$, v vanishes and u is independent of θ. Here the centre-line of the ring forms a circle of periodically varying radius and all the cross-sections of the ring move radially without rotation. The modes with $n = 0$ for the torsionals and extensionals are referred to as "breathing" modes in bell terminology [1]. Also modes with $n = 1$ are referred to as "swinging" modes.

The classical formulae are derived for thin rings of circular cross-section where $k_x^2 = k_z^2 = c^2/4$, so that $k_y^2 = c^2/2$ and c is the radius of the cross-section. However they have been used for rectangular cross-sections also (approximately) in which case $k_x^2 = h^2/12$, $k_z^2 = t^2/12$ so that $k_y^2 = k_x^2 + k_z^2$.

7.3 IMPROVED RING FORMULAE

In this section only those modified ring formulae are discussed which are in a directly applicable form. This is because the main aim of the discussion is to obtain a trend of the deviation of the classical formulae when various effects are considered.

7.3.1 CHARNLEY-PERRIN Formulae

In reference [57] the classical formulae for the radial and axial modes have been derived in a more general form which is valid for any shape of uniform cross-section. The modified formula for the axial vibration is

$$f_A^2 = \frac{Ek_y^2}{8\pi^2\rho a^4} \frac{n^2(n^2 - 1)^2}{(1 + \sigma + \frac{1}{2}n^2k_y^2/k_x^2)} \qquad (7.5)$$

The formula for the radial mode is the same as equation (7.1). However, if the cross-section of the ring is such that it is invariant under rotations through $\pi/2$ radians about the y-direction, then $k_y^2 = 2k_x^2$ and the above equation reduces to the classical formula.

7.3.2 BUCKENS' Formula

BUCKENS [48] has derived a frequency equation for the radial vibration of thick rings by taking into account the effects of transverse shear in order to compute the deviation from the classical formula as

$$f_R^2 = f_o^2 \left[1 + C \left(\frac{t}{2a}\right)^2 + \ldots\ldots\right] \qquad (7.6)$$

where f_o is the classical formula for the radial mode as given by equation (7.1),

$$C = 0.6 - \frac{(n^2 - 1)(n^2 - 2)}{3(n^2 + 1)} - \frac{sn^2}{3}$$

is the correction factor ,

$$s = \frac{kE}{G} = 2k\,(1 + \sigma)$$

and k is the coefficient of proportionality between the average shearing stress on a cross-section and the shear strain measured at the neutral layer, whose value depends upon the shape of the cross-section. Assuming the value of σ = 0.29 and k = 1.5 for rectangular cross-section one gets the value of s = 3.87 whence one can determine the value of the corrective term for different values of n as shown below.

n	2	3	4	5	 10
C	-4.96	-12.877	-24.158	-38.727	-160.420

As the last term $sn^2/3 = 1.29n^2$ plays a predominant role in deciding the value of C, the effect of shear has larger effect on the natural frequency than other effects like rotatory inertia. Also the effect of shear becomes more and more predominant for higher modes of vibration.

7.3.3 RAO et al. Formula

RAO and SUNDARARAJAN [51] have developed the equations of motion for the radial vibration of a thick circular ring including the effects of shear and rotatory inertia and assuming inextensibility of the central line. They have obtained a frequency equation in the form of a quadratic in $A\rho a^4\omega^2/EI_z$ with two frequencies associated with the mode the smaller one corresponding to the flexural mode and the higher the thickness shear mode. On considering the effect of rotatory inertia alone the frequency equation simplifies to

$$f_R^2 = \frac{EI_z}{4\pi^2\rho A a^4} \left\{ \frac{n^6 - 2n^4 + n^2}{n^4\left(\frac{I_z}{Aa^2}\right) - n^2\left(2\frac{I_z}{Aa^2} - 1\right) + \left(\frac{I_z}{Aa^2} + 1\right)} \right\}$$

and rewriting in terms of the classical formula one has

$$f_R^2 = f_o^2 \left[1 + \frac{(t/2a)^2 (n^2 - 1)^2}{3 (1 + n^2)} \right]^{-1} \qquad (7.7)$$

They have shown that for a thin ring the effect of shear deformation predominates over the rotatory inertia in causing deviation from classical formula. This tendency is more pronounced at higher modes. For a thick ring the effect of rotatory inertia is also considerable. The above relation is calimed to hold good for values of t/a = 1.0.

7.3.4 KIRKHOPE's Formula

KIRKHOPE [61] has derived a simple frequency equation for the radial vibration of thick circular rings by taking into account the effects of transverse shear and rotatory inertia and demonstrated to be accurate even though rotatory inertia is neglected [63]. The simplified relation is

$$f_R^2 = f_o^2 (1 + n^2\gamma)^{-1} \qquad (7.8)$$

where $\gamma = (\frac{Iz}{Aa^2})\ (\frac{E}{KG})$ is the dimensionless shear factor, Iz is area moment of inertia of the cross-section about the z-axis and K is the shear correction coefficient which accounts the variation in shear strain across the cross-section whose value is 5/6 for rectangular cross-section. The above equation is claimed to give accurate frequencies within 10% upto a value of t/a = 1.0.

7.4 SCOPE FOR EMPIRICAL CORRECTION

It is evident from the above discussion of the modified ring formulae that the improved frequency relations can be written in terms of the classical formula multiplied by a certain polynomial, e.g.

$$f \text{ improved} = f \text{ classical } (A_0 + A_1x + A_2x^2 + A_3x^3 + ...)$$

where the coefficients A_0, A_1, A_2 etc. represent the combined effects of the dimensional parameters, quantum number n, variation of shearing strain across the cross-section, rotatory inertia etc. This is of practical advantage as one can use the experimental data of the previous chapter to find these coefficients by fitting the data points to a mathematical model involving the classical formula and the polynomial with the help of least-squares technique.

As the response curves for the different modes of vibration are not of the same nature one type of polynomial fitting may not be enough to deal with the different cases. For example, the polynomial fit for the radial and extensional modes of vibration may be of the same type whereas the fitting for the axial and torsional modes can be of another similar type. The results of these exercises are given in the next and final Chapter.

CHAPTER VIII

ANALYSIS

8.1 INTRODUCTION

In this Chapter the experimental results of the present investigation are analysed aiming at establishing a criterion for the conditions under which thin ring formulae may be used without serious error and formulating an empirical correction for the case of thick rings. The former involves comparing the experimental results with the classical formulae [38] and their generalised versions [57]. The latter involves using a computer programme for fitting polynomials of varying degrees to the experimental responses of ring vibration using least-squares technique. This has helped to establish an empirical relation for the frequency dependence on the ratio height/thickness of the cross-section. Finally, with the help of certain empirical correction graphs it is shown that one can always calculate the frequencies of vibration of thick circular rings of rectangular cross-section with the help of the classical formulae within reasonable accuracy limits.

Also, the improved thick ring formulae (7.6, 7.7, 7.8) are compared with the experimental results to check their range of applicability.

8.2 COMPARISON WITH VARIOUS RING THEORIES

As the present investigation provided ring's frequency data with varying dimensions of cross-section it is possible to compare the various ring formulae under different thickness conditions.

8.2.1 Comparison With Radial Modes

Using equation (7.1) the frequencies of radial modes are calculated for two extreme thickness conditions, viz. for a very thick ring and for a very thin ring, and the results are shown in Tables 8.1 and 8.2 for rings A and C respectively, along with the experimental results. Also,

TABLE 8.1

Natural frequencies of vibration of radial modes: Ring A

Mean radius a = 107.18 mm

Height h = 5.93 mm

	n	Measured frequency (Hz)	Calculated frequency from formula due to							
			LOVE		BUCKENS		RAO		KIRKHOPE	
			(Hz)	%	(Hz)	%	(Hz)	%	(Hz)	%
Thickness t = 30.07	2	1607.6	1632.5	1.5	1552.5	-3.4	1622.7	0.9	1570.5	-2.3
	3	4313.3	4617.4	7.0	4031.0	-6.5	4525.0	4.9	4243.4	-1.6
	4	7760.6	8853.5	14.1	6746.4	-13.1	8490.5	9.4	7693.7	-0.9
	5	11694.3	14317.9	22.4	8862.8	-24.2	13372.9	14.4	11654.8	-0.3
	6	15958.5	21004.1	31.6	9304.8	-41.7	19029.7	19.2	15963.1	0.0
	7	20436.6	28909.5	41.5	6822.6	-66.6	25324.7	23.9	20467.9	0.2
Thickness t = 5.99mm	2	333.7	325.2	-2.6	324.6	-2.7	325.2	-2.6	324.6	-2.7
	3	940.7	919.8	-2.2	915.2	-2.7	918.9	-2.3	916.1	-2.6
	4	1795.9	1763.6	-1.8	1747.8	-2.7	1760.1	-2.0	1753.0	-2.4
	5	2890.9	2852.2	-1.3	2809.4	-2.8	2843.6	-1.6	2823.6	-2.3
	6	4213.6	4184.1	-0.7	4092.0	-2.9	4167.3	-1.1	4125.5	-2.1
	7	5764.1	5758.8	-0.1	5586.1	-3.1	5724.3	-0.7	5649.4	-2.0
	8	7544.5	7576.2	0.4	7273.2	-3.6	7515.6	-0.4	7386.8	-2.1
	9	9523.2	9636.2	1.2	9144.7	-4.0	9539.8	0.2	9337.5	-2.0
	10	11688.0	11938.6	2.1	11186.5	-4.3	11795.4	0.9	11484.9	-1.7
	11	14046.1	14483.5	3.1	13382.7	-4.7	14266.2	1.6	13831.7	-1.5
	12	16580.2	17270.8	4.2	15699.2	-5.3	16959.9	2.3	16355.5	-1.4
	13	19284.8	20300.5	5.3	18148.6	-5.9	19874.2	3.1	19041.9	-1.3

$E = 2.0 \times 10^{11}$ N/m^2, $\rho = 7.815 \times 10^3$ kg/m^3, $\sigma = 0.29$

TABLE 8.2

Natural frequencies of vibration of radial modes: Ring C

Radius a =106.90 mm

Thickness t =5.92 mm

	n	Measured frequency (Hz)	Calculated frequency from formula due to							
			LOVE		BUCKENS		RAO		KIRKHØPE	
			(Hz)	%	(Hz)	%	(Hz)	%	(Hz)	%
Height h = 23.10 mm	2	329.4	323.1	-1.9	322.4	-2.1	323.1	-1.9	322.4	-2.1
	3	929.8	913.8	-1.7	909.2	-2.2	912.9	-1.8	910.2	-2.1
	4	1778.2	1752.2	-1.5	1736.4	-2.4	1748.7	-1.7	1741.6	-2.1
	5	2866.0	2833.6	-1.1	2791.1	-2.6	2825.1	-1.4	2805.3	-2.1
	6	4185.7	4156.8	-0.7	4065.4	-2.9	4140.2	-1.1	4098.6	-2.1
	7	5733.2	5721.4	-0.2	5549.7	-3.2	5687.0	-0.8	5612.7	-2.1
	8	7498.3	7527.0	0.4	7233.4	-3.5	7466.8	-0.4	7346.3	-2.0
	9	9475.8	9573.5	1.0	9094.8	-4.0	9477.8	0.0	9276.8	-2.1
	10	11652.0	11861.0	1.8	11125.6	-4.5	11718.7	0.6	11422.1	-2.0
	11	14017.8	14389.3	2.7	13310.1	-5.0	14173.5	1.1	13741.8	-2.0
	12	16567.0	17158.5	3.6	15631.4	-5.6	16849.7	1.7	16249.1	-1.9
	13	19282.7	20168.5	4.6	18071.0	-6.3	19745.0	2.4	18938.3	-1.8
Height h = 1.19 mm	2	327.3		-1.3		-1.5		-1.3		-1.5
	3	922.7		-1.0		-1.5		-1.1		-1.4
	4	1765.8		-0.8		-1.7		-1.0		-1.4
	5	2838.8		-0.2		-1.7		-0.5		-1.2
	6	4143.0		0.3		-1.9		0.1		-1.1
	7	5666.4	*	1.0	*	-2.1	*	0.4	*	-1.0
	8	7404.2		1.7		-2.3		0.8		-0.8
	9	9340.9		2.5		-2.6		1.5		-0.7
	10	11488.1		3.2		-3.2		2.0		-0.6
	11	13800.2		4.3		-3.6		2.7		-0.4
	12	16304.7		5.2		-4.1		3.3		-0.3
	13	18962.5		6.4		-4.7		4.1		-0.1

* No change in frequency w.r.t variation in h

$E = 2.0 \times 10^{11}$ N/m^2, $\rho = 7.815 \times 10^3$ kg/m^3, $\sigma = 0.29$

the frequencies calculated from equations (7.6, 7.7, 7.8) are shown for comparison.

It may be recalled that for ring A the frequencies of vibration were recorded with varying thickness of the cross-section while the height of the cross-section remained the same, whereas for ring C the thickness of the ring remained the same while the height varied. In other words, in the beginning, ring A could be taken as a flat ring and ring C as a short cylinder.

As is evident from Table 8.1, the classical formula is inadequate to obtain the frequencies of vibration of thick rings. Out of the three other theories KIRKHOPE's formula [61] is found to be better than other two for getting frequencies of thick flat rings. As the thickness decreases the accuracy of the classical formula is improved especially for the first few modes, so also that of RAO's [51].

Referring to Table 8.2, it is seen that the classical formula is found to hold well for the first few modes of the short cylindrical ring and the accuracy of RAO's formula [51] is slightly better than that of KIRKHOPE's. Again, for very thin rings the classical formula is better for the first few modes and KIRKHOPE's formula is better for higher modes. BUCKENS' formula [48] has insufficient accuracy for the cases considered above.

8.2.2 Comparison With Axial Modes

The experimental results for the axial modes were compared with the classical formula [38] and its generalised version [57] for the above two rings under consideration and the results are shown in Table 8.3.

As is evident from the table the classical formula is inadequate for thick rings, especially cylindrical ones. However, as the dimensions of the cross-section decrease its accuracy improves considerably. The accuracy of the generalised version is similar to that of the classical formula for thick rings and is slightly improved for very thin rings.

TABLE 8.3

Natural frequencies of vibration of axial modes

n	Ring A	Thickness t = 30.07 mm				Ring A	Thickness t = 5.99 mm			
	Measured frequency (Hz)	Calculated frequency				Measured frequency (Hz)	Calculated frequency			
		LOVE		CHARNLEY			LOVE		CHARNLEY	
		(Hz)	%	(Hz)	%		(Hz)	%	(Hz)	%
2	329.2	313.0	-4.9	355.7	8.0	312.0		0.3	313.4	0.4
3	912.0	897.7	-1.6	954.7	4.7	900.2		-0.3	898.2	-0.2
4	1730.8	1731.3	0.0	1794.3	3.7	1736.9		-0.3	1731.9	-0.3
5	2774.7	2808.0	1.2	2874.0	3.6	2809.7		-0.1	2808.7	0.0
6	4035.4	4126.0	2.2	4193.7	3.9	4107.2		0.5	4126.7	0.5
7	5505.2	5684.7	3.3	5753.4	4.5	5634.0	*	0.9	5685.4	0.9
8	7174.5	7483.7	4.3	7553.0	5.3	7368.3		1.6	7484.4	1.6
9	9032.3	9522.8	5.4	9592.6	6.2	9307.6		2.3	9523.6	2.3
10	11056.6	11802.1	6.7	11872.2	7.4	11440.2		3.2	11802.8	3.2
11	13249.8	14321.4	8.1	14391.8	8.6	13760.5		4.1	14322.2	4.1
12	15504.2	17080.7	10.2	17151.3	10.6	16257.9		5.1	17081.5	5.1
13	18098.2	20080.1	11.0	20150.8	11.3	18953.0		6.0	20080.3	6.0
	Ring C	Height h = 23.58 mm				Ring C	Height h = 1.19 mm			
2	711.0	1251.1	76	1135.0	60	75.9	63.1	-16.8	71.7	-5.5
3	2338.0	3588.2	53	3405.0	46	198.7	181.1	-8.9	192.6	-3.1
4	4683.0	6920.3	48	6703.4	43	371.8	349.2	-6.1	361.9	-2.7
5	7466.0	11224.2	50	10989.0	47	594.7	566.4	-4.8	579.7	-2.5
6	10460.0	16492.7	58	16246.8	55	867.1	832.3	-4.0	845.9	-2.4
7	13490.0	22723.1	68	22470.4	67	1188.3	1146.8	-3.5	1160.6	-2.3
8	16471.0	29914.1	82	29656.9	80	1560.3	1509.7	-3.2	1523.6	-2.4
9						1980.2	1921.0	-3.0	1935.0	-2.3
10						2449.2	2380.8	-2.8	2394.9	-2.2
11						2968.3	2889.0	-2.7	2903.2	-2.2
12						3536.3	3445.6	-2.6	3459.8	-2.2
13						4152.1	4050.7	-2.4	4064.9	-2.1
14						4818.9	4704.2	-2.4	4718.4	-2.1

* No change in frequency w.r.t variation in t.

$E = 2.0 \times 10^{11}$ N/m^2 , $\rho = 7.815$ kg/m^3 , $\sigma = 0.29$

Ring A: a = 107.18 mm, h = 5.93 mm

Ring C: a = 106.90 mm, t = 5.92 mm

8.2.3 Comparison With Torsional Modes

The frequencies of vibration for the torsional modes were calculated by using equation (7.3) and were compared with the experimental results for rings A and C as before. The results are shown in Table 8.4.

It is evident from the results that the classical formula for the torsional modes does not hold good either for thick rings (flat or cylindrical) or for very thin ones. However, when the dimensions of the cross-section approach to each other the difference between the experimental and theoretical results reduces considerably. This behaviour is well illustrated in Figure 8.1 where the difference between the normalised frequency ratios (normalised on n = 0) for the theoretical and experimental results are plotted against n for the same value of h or t for rings A and C. It is interesting to note that this difference becomes zero for a certain height or thickness of the cross-section for the particular ring under observation where the classical theory agrees well with the experimental results. This height or thickness obtained for the various rings used in the present investigation are given in Table 8.5. It is obvious that the classical theory is well observed for a ring of square cross-section.

8.2.4 Comparison With Extensional Modes

The frequencies of extensional vibration obtained by using the classical formula, viz. equation (7.4), are shown in Table 8.6 along with the corresponding experimental results for the two rings used for comparison.

As is evident from the table the classical formula for the extensional modes is reasonably accurate for a wide range of cross-sectional parameters.

8.2.5 General Precuations

During the course of the thinning operation it is always advantageous to note the mass M of the ring along with other dimensions as the

TABLE 8.4

Natural frequencies of vibration of the torsional modes

n	Calculated frequency (LOVE) (Hz)	Measured frequencies of Ring A for Thickness			
		Thickness t=30.07mm (Hz)	%	t=5.99 mm (Hz)	%
0	5311.8	1491.3	256	5373.8	-1.2
1	7077.3	2349.0	201	7021.4	0.8
2	10756.6	3946.3	172	10366.6	3.8
3	15002.2	5732.4	162	14325.4	4.7
4	19446.6	7625.6	155	18500.7	5.1
5	23979.6	9612.3	149		
6	28559.0	11703.7	144		
7	33165.6	13905.6	138		
8	37789.4	16248.9	133		
9	42424.9	18689.4	127		
	Ring C	Height h=23.58 mm		Height h =1.19 mm	
0	5325.7	7470.0	-29	1422.2	274
1	7095.8	7727.0	-8	2183.1	225
2	10784.8	8624.0	25	4151.1	160
3	15041.5	10173.0	48	5527.0	172
4	19497.6	12226.0	59	7107.9	174
5	24042.4	14688.0	64	9726.0	147
6	28633.8	17580.0	63	11350.0	152
7	33252.5			12595.4	164

Ring A

a=107.18 mm

h= 5.93 mm

$E = 2.0 \times 10^{11}$ N/m^2

$\rho = 7.815 \times 10^{3}$ kg/m^3

$\sigma = 0.29$

Ring C

a=106.9 mm

t= 5.92mm

TABLE 8.5

Ring	Height or Thickness of the ring h or t (mm)	Height or Thickness at which cross-over takes place (mm)
A	5.93	6
B	8.04	7.5
C	5.92	5.5
D	3.99	3.5

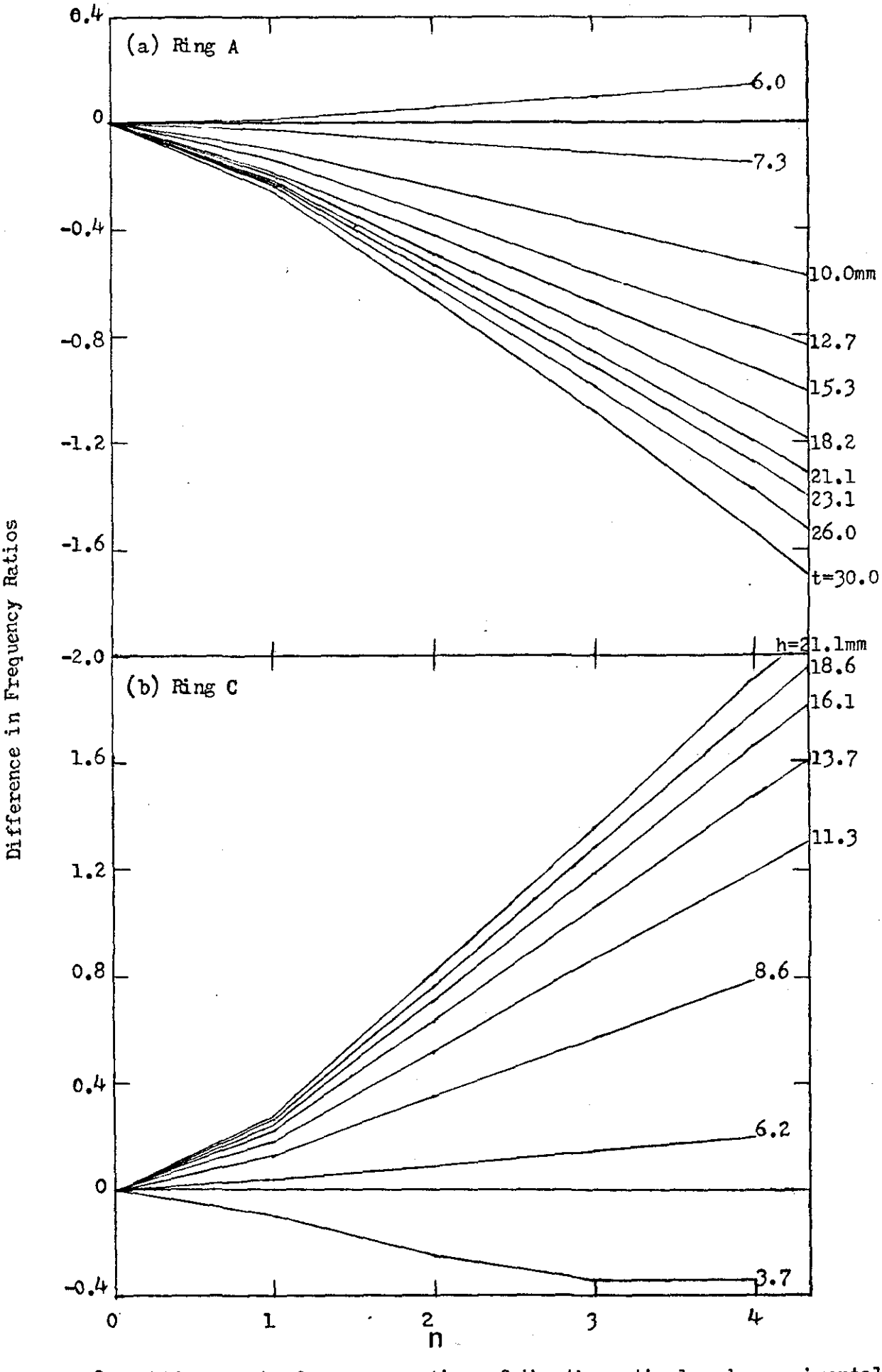

Figure 8.1 Difference in frequency ratios of the theoretical and experimental results as a function of n for various values of t,h for the torsional modes.

TABLE 8.6

Natural frequencies of vibration of the extensional modes

n	Calculated frequency (LOVE) (Hz)	Observed frequencies for Ring A: Thickness t=30.07mm (Hz)	%	Thickness t= 5.99mm (Hz)	%
0	7512.0	7734.0	-2.9	7693.0	-2.4
1	10623.6	10732.5	-1.0	10874.0	-2.3
2	16797.4	16799.4	0.0	17186.4	-2.3
		Ring C: Height h=23.58mm (Hz)	%	Height h=1.19mm (Hz)	%
0	7531.7			7748.0	-2.8
1	10651.4	10873.5	-2.0	10868.0	-2.0
2	16841.4	17189.0	-2.0	17209.0	-2.1

Ring A

Radius a = 107.18 mm

Height h = 5.93 mm

Ring C

Radius a = 106.90 mm

Thickness t = 5.92 mm

$E = 2.0 \times 10^{11}$ N/m^2 , $\rho = 7.815 \times 10^3$ kg/m^3

measurement of height or thickness becomes prone to errors especially towards the thin region. Hence it is necessary to calculate the ratio h/M or t/M and to obtain the mean value whence the acceptable limits of measurement can be known from a knowledge of the standard deviation of the various measurements. Then, those observed values which lie outside these limits can be noted and the new values of h or t can be calculated by using the relation $\Pi(a_1^2 - a_{11}^2)\, h\rho = M$, where a_{11} and a_1 are the inside and outside radii of the ring respectively.

8.3 ESTABLISHING A CRITERION FOR THIN RINGS

The results of the preceding section show many interesting aspects of ring vibration. As is evident from Table 8.1 the classical thin ring formula holds well for the radial modes provided the thickness of cross-section is small. As the variation in height of the cross-section does not affect the frequency of vibration appreciably, the thickness of cross-section is very critical in deciding the accuracy of the classical formula.

As for the axial modes the classical formula and its generalised version hold reasonably well for flat rings provided the thickness of cross-section is small. Also, the accuracy of these formulae improves considerably as the height of the cross-section decreases.

In order to appreciate the accuracy of the generalised formula for the axial modes as the height of the cross-section varied the graph shown in Figure 8.2, was drawn where the absolute ratios of the theoretical to experimental results are plotted against h or t for different values of n, i.e.

$$T = \frac{n = n_T}{n = 2_T} \qquad E = \frac{n = n_E}{n = 2_E}$$

$$\therefore \left(\frac{n = n_T}{n = n_E}\right)_{abs.} = \left(\frac{T}{E}\right)\left(\frac{n = 2_T}{n = 2_E}\right)$$

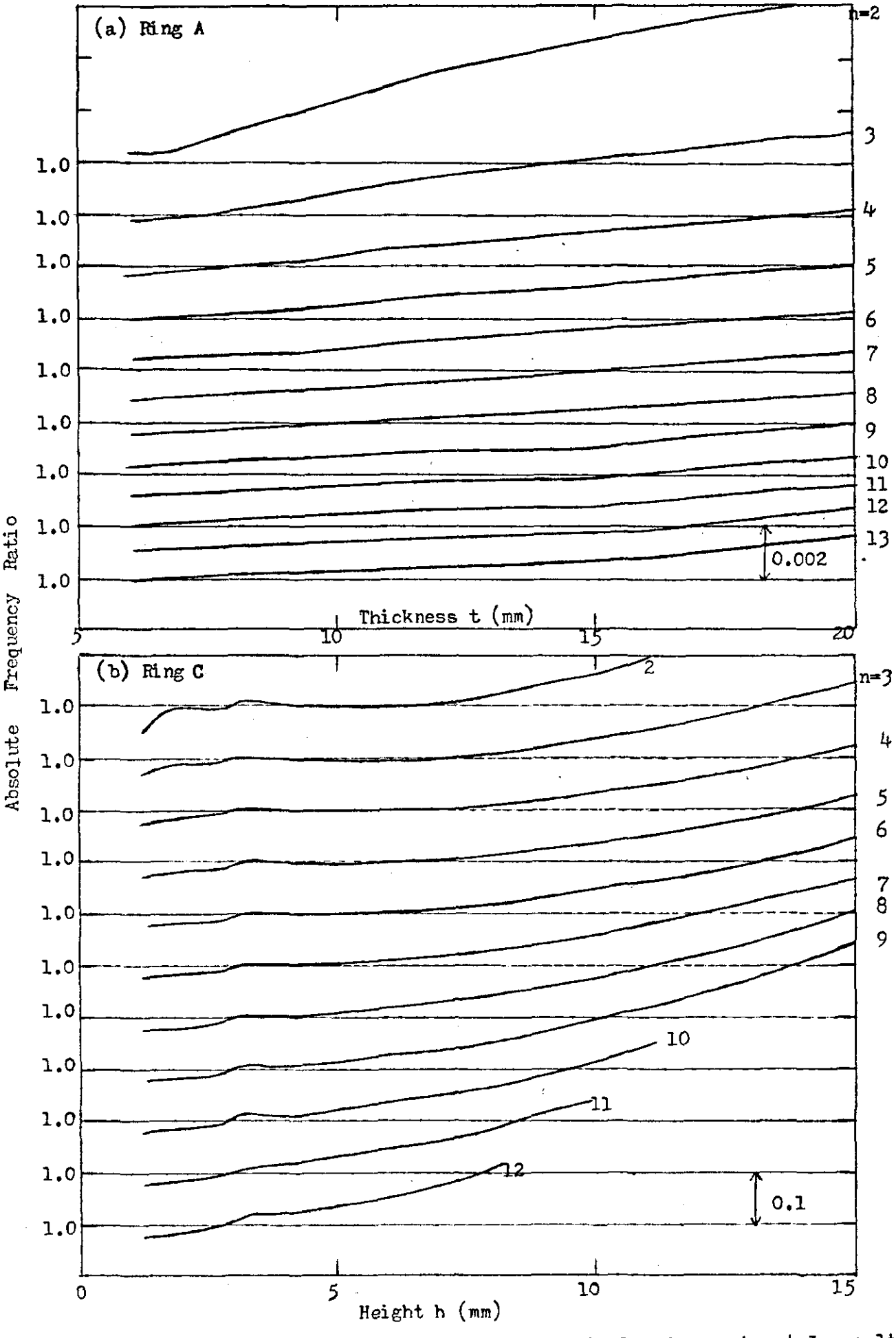

Figure 8.2 Absolute frequency ratio of the theoretical and experimental results as a function of t,h for different values of n for the axial modes.

It is interesting to note that this ratio becomes unity when the height of the cross-section becomes equal to the value of its thickness, or in other words when the cross-section becomes square. As the height of the cross-section is reduced further the value of this ratio does not change much from unity.

Similar behaviour is also observed for the radial modes of ring A where the absolute ratios of the theoretical to experimental values approach unity in and around square cross-section.

Similarly, for the torsional modes the difference between the frequency ratios for the experimental and theoretical (classical) results becomes zero for a square cross-section.

In view of the above mentioned facts it can be argued that the classical formulae for thin ring vibrations work well for circular rings of square - or nearly - square-rectangular cross-sections. Thus, the classical formula for the radial modes can be safely used for thin rings upto the square cross-section. Beyond this it is the increase of thickness rather the increase of height which causes deviation from theoretical results. Similarly, for the axial modes the generalised version of the classical formula, viz. equation (7.5), is suitable for circular rings with square cross-section and below towards the thin region. Hence a thin ring can be defined as one whose cross-section is square. However, as the present investigation is confined to values of h/a, t/a $\simeq$ 0.25, further work is needed to establish this definition for higher values of h/a, t/a.

8.4 EMPIRICAL CORRECTION FOR THICK RING VIBRATION

In this section the details of a computer analysis of the experimental results are given. As the classical thin ring formulae do not hold good for thick rings, it is necessary to have them corrected for thick rings. Since the present investigation relies more on the experimental results the obvious choice is to correct the classical theory to account for the experimental results. It may be recalled that the radial modes show greater sensitivity for variation in thickness of the cross-section

compared with its height variation. However, there is a slight but systematic variation in frequency with changes in height of the cross-section. Similarly, the axial modes show increased sensitivity for variation in height compared with thickness variation. The torsional frequencies vary with height as well as thickness of the cross-section. Hence, the present analysis is aimed at developing certain frequency correction factors to account for the variation in the cross-sectional parameters using polynomial curve-fitting technique.

8.4.1 Polynomial Fitting to Experimental Responses

The polynomial curve fitting technique is widely used to obtain the equation of a smooth curve which passes through a given set of data points. The process involved is essentially a least-squares technique where a polynomial of certain degree is fitted to a given experimental response curve. In the simplest case the problem reduces to fitting a straight-line in the form

$$Y_k = A_o + A_1 x_k \qquad k = 1,2 \ldots\ldots\ldots m \qquad (8.1)$$

to a given experimental response, say y_k against x_k, where k is an integer and m is the number of data points. The coefficients A_o and A_1 are determined using least-squares criterion (Appendix II) which requires that

$$S = \Sigma(Y_k - y_k)^2$$

be a minimum, where Y_k is evaluated from equation (8.1).

Further details can be seen in Appendix V.

8.5 FREQUENCY CORRECTION FOR RADIAL MODES

The empirical correction obtained for the radial and extensional modes in the present analysis is of similar nature.

8.5.1 Radial Modes

In the first place the variation in frequency for the radial modes with the height h of the cross-section is used to obtain an empirical relation for the dependence of frequency on h. As the classical formula and the improved versions do not involve h, it is essential to work out this dependence. Hence, the response curves of Figure 6.5 are used for the analysis.

Using a computer programme (Appendix VI) polynomials of varying degrees are fitted to m data points which are the observed frequencies at varying heights of the cross-section. As a result one obtains a set of $n' + 1$ coefficients for each polynomial fitted where n' is the degree of the polynomial. The process is repeated for the different response curves corresponding to different values of n, the quantum number, for rings B, C, and D. Out of the four different degrees of polynomials fitted, the straight-line fit ($n' = 1$) was found to be the most suitable one for the radial modes, from a practical point of view, where the first coefficient A_0 nearly represented a value comparable with the frequency given by the classical formula. The values of A_0 obtained in the four cases, corresponding to $n' = 1, 2, 3, 4$, were within $\pm 0.5\%$ with respect to the maximum value. Moreover, the other coefficients, viz. A_1, A_2 etc., showed a linear variation only for the polynomial fit corresponding to $n' = 1$. Hence, the straight-line fit was accepted for the present analysis.

Further, as the values of the coefficient A_1, obtained for the straight-line fit, were comparable for the different rings used in the investigation, their average value was taken for a particular value of n, as shown in Table 8.7. The coefficients so obtained were found to have a mean coefficient of variation of about 14%.

Next, the difference between the frequency of vibration obtained by using the classical formula (equation 7.1) and the coefficient A_0 was noted for each ring to calculate the percentage differences between the experimental (A_0) and theoretical values with respect to the experimental value. These, when plotted against the corresponding value of t/a produced Figure 8.3.

TABLE 8.7

Frequency correction coefficients (A_1) of the straight-line fit:Radial modes

n	2	3	4	5	6	7	8	9	10	11
Mean value of A_1	0.08	0.27	0.54	1.02	1.71	2.67	3.73	5.16	7.04	9.08
Standard deviation	0.01	0.06	0.06	0.17	0.25	0.34	0.46	0.62	0.69	1.03
Coefficient of variation %	16.2	21.0	11.6	16.7	14.8	12.6	12.3	12.1	9.8	11.33

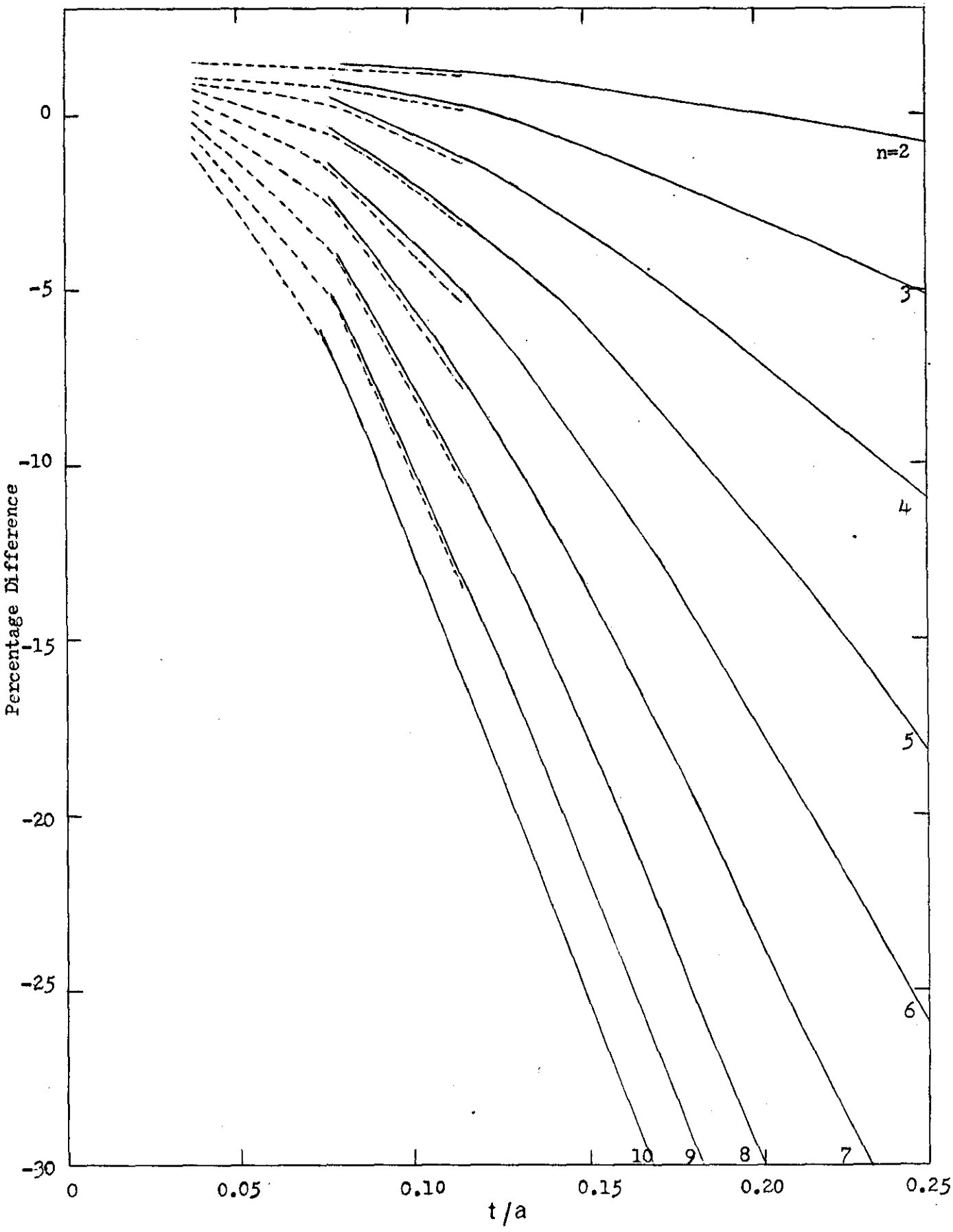

Figure 8.3 Percentage difference as a function of t/a for different values of n for the radial modes (solid line: the extended region).

In the second phase of the analysis the frequency data of ring A were used to obtain the percentage difference under varying values of t/a and hence to extend the range of the correction graphs shown in Figure 8.3 - solid lines are used to denote the extended region. As the corresponding curves merge to each other towards higher values of t/a, this approximate procedure can be accepted to account for the dependence of frequency on thickness of the cross-section.

Using the frequency correction coefficient A_1 of Table 8.7 and the correction graphs of Figure 8.3 one can correct the classical formula as follows. By reading off the value of A_1 for a particular value of n the frequency correction due to the height h of the cross-section can be obtained as $A_1 h$, where h has to be noted in mm. For the same value of n one can obtain the percentage difference from Figure 8.3 provided the value of t/a is known. Hence the final corrected frequency can be obtained as

$$f_{corrected} = f_o \pm \text{Percentage Difference} + A_1 h,$$

where f_o is the frequency obtained from classical formula.

In order to check the accuracy of this correction procedure two test rings - one thick and another flat - of known dimensions and frequencies were used for comparison. The frequencies obtained by using the classical formula and after applying the correction are shown in Table 8.8 along with the measured values. As is evident from the table the corrected frequencies agree well with the measured frequencies for both rings although the accuracy for the flat ring reduces towards higher modes.

8.5.2 Extensional Modes

As the straight-line fit was suitable for the radial modes the same procedure was followed for the extensional modes also. In the first phase of the analysis the response curves of Figure 6.8 for rings B, C, and D were used to obtain the value of the coefficient A_1 which

TABLE 8.8

Experimental verification of the empirical correction method

(Radial modes)

n	Ring 1 Radius a=103.97mm Height h=24.22mm Thickness t=12.01 mm Frequencies of vibration				Ring 2 Radius a=113.855 Height h =5.62mm Thickness t=28.45mm Frequencies of vibration			
	Classical (Hz)	Measured (Hz)	Corrected (Hz)	%	Classical (Hz)	Measured (Hz)	Corrected (Hz)	%
2	692.9	702.6	702.9	0.04	1368.8	1361.0	1358.2	-0.20
3	1959.8	1967.4	1966.6	-0.04	3871.4	3683.0	3671.6	-0.31
4	3757.8	3721.0	3720.1	-0.02	7423.1	6684.0	6609.6	-1.11
5	6077.2	5918.0	5910.5	-0.13	12004.7	10166.0	9825.6	-3.40
6	8915.1	8507.0	8492.9	-0.17	17610.7	14030.0	13076.7	-6.79
7	12270.5	11452.0	11396.5	-0.48	24238.9	18107.0	16206.6	-10.50
8	16142.9	14704.0	14554.4	-1.02				
9	20532.1	18224.0	17957.1	-1.46				
10	25437.9							

$E = 2.0 \times 10^{11}\ N/m^2$, $\rho = 7.815 \times 10^3\ kg/m^3$, $\sigma = 0.29$

gave the dependence of frequency on the height h (mm) of the cross-section. As before, the mean value of the coefficients obtained for the various rings was taken. Moreover, the value of the coefficient A_0 obtained in these cases were comparable with the frequency given by the classical formula. Hence, the percentage difference was calculated as before. Also, as the values of the percentage difference were comparable for various rings for a particular value of n, the average value was taken.

In the second phase of the analysis the response curves for ring A, from Figure 6.8, were used to work out the dependence of frequency on thickness t (mm) of the cross-section. The first coefficient A_0 nearly represented the frequency given by the classical formula as before, and the values of the percentage difference were of the same order as in the previous phase. Hence, the average of both the values were taken for the final correction. The values of these coefficients and the percentage difference are shown in Table 8.9.

Following the procedure adopted for the radial modes the corrected frequency for the extensional modes can be obtained as

$$f_{corrected} = f_0 + 2.38\% + A_1 h + A_1' t$$

where f_0 is the frequency given by the classical formula and A_1 and A_1' are the frequency correction coefficients to account for h and t of the cross-section respectively. The corrected frequencies for the two rings, used for the earlier comparison, are given in Table 8.10 along with the measured and classical frequencies. As is evident from the table there is good agreement between measured and corrected frequencies.

8.6 ANALYSIS OF THE AXIAL AND TORSIONAL MODES

Although the polynomial fitting technique works well for the axial and torsional modes for higher degrees, the values of the coefficients obtained, viz. A_0, A_1, A_2, ... , cannot be interpreted as easily as for the radial modes. Hence the results of the analysis

TABLE 8.9

Frequency correction coefficients for the extensional modes

n	Percentage difference for variation in			Coefficient A_1 to account for	
	Height h	Thickness t	Mean	Height h	Thickness t
0	2.54	2.20	2.37	-2.0	1.26
1	1.94	2.65	2.30	+0.2	-6.10
2	2.04	2.93	2.48	-0.75	-16.00
Mean of mean values			2.38		

TABLE 8.10

Experimental comparison of the empirical correction method

(Extensional modes)

n	Ring 1 Radius a=103.97 mm Height h =19.38mm thickness t=12.01mm				Ring 2 Radius a =113.855mm Height h = 5.62 mm Thickness t = 28.01 mm			
	Frequencies of vibration				Frequencies of vibration			
	Classical (Hz)	Measured (Hz)	Corrected (Hz)	%	Classical (Hz)	Measured (Hz)	Corrected (Hz)	%
0	7744.0	7920.1	7904.7	-0.19	7071.6	7288.4	7264.0	-0.33
1	10951.6	11157.3	11142.9	-0.13	10000.8	10145.1	10069.1	-0.75
2	17316.0	17611.0	17521.4	-0.51	15812.6	15928.0	15736.6	-1.20

$E = 2.0 \times 10^{11}\ N/m^2$, $\rho = 7.815 \times 10^3\ kg/m^3$, $\sigma = 0.29$

are inconclusive and not examined in detail.

8.7 CONCLUSIONS

The present analysis has helped to establish a criterion for using the classical thin ring formulae without serious error and to formulate an empirical correction for the radial modes of vibration of thick rings. As the experimental data were confined to values of h/a, t/a ≈ 0.25, further work is needed to establish the present conclusions for higher values h/a, t/a.

REFERENCES

1. R. PERRIN and T. CHARNLEY 1973 Journal of Sound and Vibration 31, 411-418. Group theory and the bell.

2. T. CHARNLEY and R. PERRIN 1978 Journal of Sound and Vibration 58, 517-525. Studies with an eccentric bell.

3. R. PERRIN 1971 Acustica 25, 69-72. Selection rules for the splitting of the degenerate pairs of natural frequencies of thin circular rings.

4. J.W. PENDERED 1965 Journal of Mechanical Engineering Science 7, 372-379. Theoretical investigation into the effects of close natural frequencies in resonance testing.

5. C.C. KENNEDY and C.D.P. PANCU 1947 Journal of the Aeronautical Sciences 14, 603-625. Use of vectors in vibration measurement and analysis.

6. A. CRAGGS and M.R. NORTH 1966 MIRA Report 6, 4-20. A study of the frequency response curves of a system with close natural frequencies by means of an analogue computer.

7. R.W. TRAILL-NASH, G. LONG and C.M. BAILEY 1967 Journal of Mechanical Engineering Science 9, 402-413. Experimental determination of the complete dynamical properties of a two-degree-of-freedom model having nearly coincident natural frequencies.

8. A.M. REAY and R. SHEPHERD 1971 Journal of Sound and Vibration 17, 149-155. The separation of two combined normal modes.

9. W.L. HALLAUER, Jr., T.A. WEISSHAAR and A.G. SHOSTAK 1978 Journal of Sound and Vibration 61, 245-254. A simple method for designing structural models with closely spaced modes of vibration.

10. B.J. LAZAN 1968 Damping of Materials and Members in Structural Mechanics. Oxford: Pergamon Press.

11. C. ZENER 1937 Physical Review 52, 230-235. Internal friction in solids 1. Theory of internal friction in reeds.

12. D.R. BLAND 1960 The Theory of Linear Viscoelasticity. Oxford: Pergamon Press.

13. C.W. BERT 1973 Journal of Sound and Vibration 29, 129-153. Material Damping: An introductory review of mathematical models, measures and experimental techniques.

14. W.B. GRAHAM 1973 UTIAS Review No.36. Material damping and its role in linear dynamic equations.

15. A.L. KIMBALL and D.E. LOVELL 1927 Physical Review Series 2, 30, 948-959. Internal friction in solids.

16. R.L. WEGEL and H. WALTHER 1935 Physics 6, 141-157. Internal friction in solids for small cyclic strains.

17. H.J. CUNNINGHAM 1971 Journal of Sound and Vibration 14, 142-144. In defence of modern damping theory in flutter analysis.

18. R.E.D. BISHOP 1955 Journal of the Royal Aeronautical Society 59, 738-742. The treatment of damping forces in vibration theory.

19. T.J. REID 1956 Journal of the Royal Aeronautical Society 60, 283. Free vibration and hysteretic damping.

20. L.J. GRIFFITHS, D.J. PARRY and R.P. WORTHINGTON 1979 Institute of Physics Conference Ser. No. 47; Chapter I, 62-70. A comparison of optical and strain gauge techniques in the determination of the dynamic mechanical behaviour of carbon-fibre composite using a split Hopkinson pressure bar.

21. W.A. ZDANIEWSKI, G.E. RINDONE and D.E. DAY 1979 Journal of material science 14, 763-775. The internal friction of glasses (Review).

22. R.E.D. BISHOP and G.M.L. GLADWELL 1963 Philosophical Transactions of the Royal Society Ser. A 255, 241-280. An investigation into the theory of resonance testing.

23. J.W. PENDERED and R.E.D. BISHOP 1963 Journal of Mechanical Engineering Science 5, 345-367. A critical introduction to some industrial resonance testing techniques.

24. C.V. STAHLE and W.R. FORLIFER 1958 Proceedings of AIA-AFOSR Flight Flutter Testing Symposium. Ground vibration testing of complex structures.

25. T. CHARNLEY, V. MOHANAN and R. PERRIN 1980 Journal of Sound and Vibration 68, 609-619. Measurement of the separation and half-width of the components of close doublets in high-Q systems.

26. G.M.L. GLADWELL 1962 Journal of the Royal Aeronautical Society 66, 124-125. A refined estimate for the damping coefficient.

27. D.J. EWINS 1975 Journal of Sound and Vibration 43, 595-605. Estimation of resonant peak amplitudes.

28. W. SOEDEL and M. DHAR 1978 Journal of Sound and Vibration 58, 27-38. Difficulties in finding modes experimentally when several contribute to a resonance.

29. T. CHARNLEY and R. PERRIN 1971 Acustica 25, 240-246. Characteristic frequencies of a symmetrically loaded ring.

30. J.R. WOLBERG 1967 Prediction Analysis. Princeton, New Jersey: D. Van Nostrand Company, Inc.

31. NAGFLIB 1975 1310/428: Mk5: Nov. E04 FAF Minimising or maximising a function.

32. G. PECKHAM 1970 The Computer Journal 13, 418-420. A new method for minimising a sum of squares without calculating gradients.

33. S. TIMOSHENKO 1955 Vibration Problems in Engineering. New York: D. Van Nostrand Company, Inc. Third edition.

34. E. ERDELYI and G. HORVAY 1957 Journal of Applied Mechanics 24, 39-57. Vibration modes of stators of induction motors.

35. R.E. PETERSON 1930 Transactions of the American Society of Mechanical Engineers 52, APM-52-1. An experimental investigation of ring vibration in connection with the study of gear-noise.

36. C.W. BERT and T.L.C. CHEN 1978 Journal of Sound and Vibration 61, 517-530. On vibration of a thick flexible ring rotating at high speed.

37. E.R. KAISER 1953 The Journal of the Acoustical Society of America 25, 617-623. Acoustical vibrations of rings.

38. A.E.H. LOVE 1944 A Treatise on the Mathematical Theory of Elasticity. New York: Dover Publications. Fourth edition.

39. R. HOPPE 1871 Crelle Journal of Mathematics 73, 158-170. The bending vibrations of a circular ring.

40. J.H. MICHELL 1890 Messenger of Mathematics 19, 68-82. The small deformation of curves and surfaces with application to the vibrations of a helix and a circular ring.

41. A.B. BASSET 1891-1892 Proceedings of London Mathematical Society 23, 105-127. On the theory of elastic wires.

42. L. POCHHAMMER 1876 Z. Reine Angew. Math. (Crelle) 81, 324-336. Über die Fortpflanzungsgeschwindigkeiten Kleiner Schwingungen in einem unbegrenzten isotropen Kreiscylinder.

43. HORACE LAMB 1925 The Dynamical Theory of Sound. New York: Dover Publications, Inc. Second edition.

44. LORD RAYLEIGH 1894 The Theory of Sound (two volumes). New York: Dover Publications. Second edition, 1945 reissue. 1,304.

45. W. KUHL 1942 Akustische Zeitschrift 7, 125-152. Measurements to the theories of resonant vibrations of circular rings of arbitrary wall thickness.

46. J.W. LINCOLN and E. VOLTERRA 1967 Experimental Mechanics 7, 211-217. Experimental and theoretical determination of frequencies of elastic toroids.

47. K. FEDERHOFER 1935 S-B Akad. Wiss. Wien 144, series IIA, 561-575. Two-dimensional theory of vibrations of a circular ring of rectangular cross-section.

48. F. BUCKENS 1950 The Journal of the Acoustical Society of America 22, 437-443. Influence of the relative radial thickness of a ring on its natural frequencies.

49. L.L. PHILIPSON 1956 Journal of Applied Mechanics 23, 364-366. On the role of extension in the flexural vibrations of rings.

50. B.S. SEIDEL and E.A. ERDELYI 1964 Transactions of the ASME, Journal of Engineering for Industry 86, 240-244. On the vibration of a thick ring in its own plane.

51. S.S. RAO and V. SUNDARARAJAN 1969 Transactions of the ASME, Journal of Applied Mechanics 91, 620-625. In-plane flexural vibrations of circular rings.

52. S.S. RAO 1971 Journal of Sound and Vibration 16, 551-566. Effects of transverse shear and rotatory inertia on the coupled twist-bending vibrations of circular rings.

53. MITSURU ENDO and OSAMU TANIGUCHI 1969 Bulletin of the JSME 12, 747-755. Flexural vibrations of a ring of rectangular cross-section.

54. OSAMU TANIGUCHI and MITSURU ENDO 1971 Bulletin of the JSME 14, 348-354. An approximate formula for the flexural vibration of a ring of rectangular cross-section.

55. MITSURU ENDO and OSAMU TANIGUCHI 1971 Bulletin of the JSME 14, 761-771. Flexural vibrations of a ring.

56. MITSURU ENDO 1972 Bulletin of the JSME 15, 446-454. Flexural vibrations of a ring with arbitrary cross-section.

57. T. CHARNLEY and R. PERRIN 1973 Acustica 28, 139-146. Perturbation studies with a thin circular ring.

58. H.E. WILLIAMS 1973 Journal of Sound and Vibration 26, 465-488. On the equations of motion of thin rings.

59. D.W. HAINES, N. CHANG and C.H. HUANG 1974 Journal of the Acoustical Society of America 55, 1138-1143. Wave propagation in elastic rings and helical coils of small pitch.

60. D.W. HAINES 1974 International Journal of Solids and Structures 10, 1405-1416. Approximate theories for wave propagation and vibrations in elastic rings and helical coils of small pitch.

61. J. KIRKHOPE 1976 Journal of the Acoustical Society of America 59, 86-88. Simple frequency expression for the in-plane vibration of thick circular rings.

62. J. KIRKHOPE 1976 Journal of the Engineering Mechanics Division 102, 239-247. Out-of-plane vibration of thick circular ring.

63. J. KIRKHOPE 1977 Journal of Sound and Vibration 50, 219-227. In-plane vibration of a thick circular ring.

64. D.L. HAWKINGS 1977 Journal of Sound and Vibration 54, 67-74. A generalised analysis of the vibration of circular rings.

65. SHAN. S. KUO 1972 Computer Applications of Numerical Methods. Reading, Massachusetts: Addison-Wesley Publishing Company.

66. S. TIMOSHENKO 1934 Theory of Elasticity. New York: McGraw-Hill Book Company, Inc. First edition.

67. R.N. ARNOLD and G.B. WARBURTON 1949 Proceedings of Royal Society, Series A 197, 238-256. Flexural vibrations of the walls of thin cylindrical shells having freely supported ends.

APPENDIX I COMPUTER PROGRAMME FOR DOUBLET RESPONSE

```
LOUGHBOROUGH UNIVERSITY COMPUTER CENTRE GEORGE 2L MK4C STREAM B      RUN ON
        JOB VMDQMCAL,PH,VH3624                                  6/05/78 AT 17,39
        CARDLIST
        LUFORTRAN
        VOLUME 5000
        JOBCORE 50K
        RUN ,,1000
        ****
  5990.      6010.          201
  6000.      6003.
   100.       200.       400.       600.       800.
  1000.      2000.      4000.      6000.      8000.
 10000.     20000.     40000.     60000.     80000.

FORTRAN COMPILATION BY WXFAT IK 6B    DATE  26/05/78  TIME  17/40/01


0001                    LIST
0002                    SEND TO (LP,SEMICOMPUSER,AXXX)
0003                    DUMP ON (LP,PROGRAM USER)
0004                    WORK (LP,WORKFILEUSER)
0005                    RUN
0006                    LIBRARY(EP,SUBGROUPGRAF)
0007                    PROGRAM (PLOT)
0008                    COMPACT
0009                    INPUT 1 = CRD
0010                    OUTPUT 2 = LPU
0011                    COMPRESS INTEGER AND LOGICAL
0012                    TRACE 2
0013                    END




0014                    MASTER DOUBLET
0015                    DIMENSION ALPHA(500),TANFI(500),FI(500)
0016                    DIMENSION ALPHA1(500),TANFI1(500),COSFI1(500),SINFI1(5
0017                    DIMENSION ALPHA2(500),TANFI2(500),COSFI2(500),SINFI2(5
0018                    COMMON W(500)                                          00)
0019                    DIMENSION D(3,5)                                       00)
0020                    CALL UTPOP
0021                    READ(1,30)START,STOP,IMAX
0022                 30 FORMAT(2F10.2,I10)
0023                    WRITE(2,35)START,STOP,IMAX
0024                 35 FORMAT(1H1,2F10.2,I10)
0025               C  INITIAL AND FINAL VALUES OF OMEGA AND NO. OF POINTS
0026                    STEP=(STOP-START)/(IMAX-1)
0027                    DO 40 I=1,IMAX
0028                    W(I)=START+(I-1)*STEP
0029                 40 CONTINUE
0030                    READ(1,50)WO1,WO2
0031               C TWO  RESONANCE  FREQUENCIES  OF  DOUBLET
0032                    WRITE(2,50)WO1,WO2
0033                 50 FORMAT(1H ,2F10.2)
0034                    READ(1,45)D
0035                 45 FORMAT(5F10.2)
```

Contd.

```
0036                    DO 80 N=1,5
0037                    DO 90 M=1,3
0038                    Q=D(M,N)
0039                    CALL RES (WO1,Q,ALPHA1,TANFI1,COSFI1,SINFI1,IMAX)
0040                    CALL RES (WO2,Q,ALPHA2,TANFI2,COSFI2,SINFI2,IMAX)
0041                    DO 60 I=1,IMAX
0042                    A=ALPHA1(I)*COSFI1(I)+ALPHA2(I)*COSFI2(I)
0043                    B=ALPHA1(I)*SINFI1(I)+ALPHA2(I)*SINFI2(I)
0044                    ALPHA(I)=SQRT((A*A)+(B*B))
0045                    TANFI(I)=B/A



0046                    FI(I)=ATAN(TANFI(I))
0047                60  CONTINUE
0048                    WRITE(2,65)Q
0049                65  FORMAT(1H1,E15.6)
0050                    CALL UTP4A (5990.0,6010.0,0.0,2.2,8.0,6.0,12HFREQUENCY
0051                   12,12HAMPLITUDE    ,2)                                  ^HZ,
0052                    CALL UTP4B (W,ALPHA,200,0)
0053                    CALL UTP4A (5990.0,6010.0,-1.8,+1.8,8.0,6.0,12HFREQUE
0054                   12,12HPHASE RAD    ,2)
0055                    CALL UTP4B (W,FI,200,0)                              Y^HZ,
0056                90  CONTINUE
0057                80  CONTINUE
0058                    CALL UTPCL
0059                    STOP
0060                    END

END OF SEGMENT, LENGTH    313, NAME  DOUBLET


0061                    SUBROUTINE RES (WO,Q,ALPHA,TANFI,COSFI,SINFI,IMAX)
0062                    DIMENSION ALPHA(500),TANFI(500),COSFI(500),SINFI(500)
0063                    COMMON W(500)
0064                    B=WO/Q
0065                    DO 80 I=1,IMAX
0066                    P=W(I)-WO
0067                    R=SQRT((B*B)+4.0*P*P)
0068                    ALPHA(I)=B/R
0069                    TANFI(I)=2.0*P/B
0070                    COSFI(I)=B/R
0071                    SINFI(I)=2.0*P/R
0072                80  CONTINUE
0073                    RETURN
0074                    END

END OF SEGMENT, LENGTH    130, NAME  RES


0075                    FINISH

END OF COMPILATION -  NO ERRORS
```

APPENDIX II

THE METHOD OF LEAST-SQUARES

In quantitative experiments the analysis of the observed results is often made by fitting them to a suitable mathematical model using the method of least-squares which is an analytical technique of extracting information from experimental responses. The problem involves the formulation of an objective function representing the relationship between the dependent and independent variables including the unknown parameters. From initial guessed values of the unknown parameters the least-squares method provides good estimates of these parameters after adjusting the computed responses so that the experimental and computed responses agree to within some preset degree of accuracy. The values of the parameters so obtained are distributed normally about the true values with the least possible standard deviation. The method is based on the assumption that the observed values of the variables are distributed about the true or mean values and are not affected by whether these variables are random or deterministic. Often the method is used for the final analysis of the experimental data, the preliminary analysis of which can be carried out with the help of the well known graphical method.

The problem of finding the good estimates of the unknown parameters reduces to the solution of m non-linear equations in n variables which minimises S. This was effected by using a subroutine [31] from NAG Library Functions which employs a method due to PECKHAM [32]. The procedure is essentially Gauss-Newton in that the residuals R_k are approximated at the point X_1 in a linear form $R_k = h + J X_1$, where h is a constant vector and J is the Jacobian matrix $J_{kl} = \partial R_k / \partial X_1$ calculated at X_1. From an initial estimate of the minimum point a new set of at least m + 1 points is generated and the corresponding residuals are calculated. The coefficients of linear approximation viz. J and h, are now obtained in terms of R_k and X_1 by minimising S at the point X_1, the weights being chosen giving more emphasis to the function values near the minimum. By successive approximation the points of a current set of X_1 having the largest sum of squares are

replaced by a new set until S has attained the minimum value satisfying some pre-set degree of accuracy. The corresponding values of X_1 now gives the good estimates of the unknown parameters.

APPENDIX III COMPUTER PROGRAMME FOR SINGLET RESONANCE-OPTIMISATION

```
      SLIST VMR_SOFTAMP
C       PROGRAM FOR L_S CURVE FITTING USING NAGF E04FAF
C       M = NO. OF DATA POINTS
C       N = NO. OF UNKNOWN PARAMETERS
C       OMEGA = FREQUENCY
C       ALPHA = AMPLITUDE(CAL.)
C       ALPHAM = AMPLITUDE(MEAS.)
C       X = UNKNOWN PARAMETERS VIZ. WO, B, R, TA
        DOUBLE PRECISION X,R1,F,FTOL,XTOL,
       1STEPMX,W,RR,X02AAF,E04FAF
        DIMENSION OMEGA(50),ALPHA(50),ALPHAM(50),X(10),R1(50),
       1STEPMX(10),W(700)
        INTEGER M,N,IW,IPRINT,MAXCAL,IFAIL,I,J
        COMMON OMEGA,ALPHA,ALPHAM
        EXTERNAL RESID,MONIT
C       WRITE(1,910)
        READ(5,*)M,N
C       WRITE(1,920)
        READ(5,*)(OMEGA(I),I=1,M)
C       WRITE(1,930)
        READ(5,*)(ALPHAM(I),I=1,M)
C       WRITE(1,940)
        READ(5,*)(X(I),I=1,N)
C       WRITE(1,950)
        READ(5,*)(STEPMX(I),I=1,N)
C       WRITE(1,960)
        READ(5,*)IPRINT
        READ(5,*)FTOL
        READ(5,*)XTOL
        IW=N+3+N/3
        IW=N*(4+M)+2*M+IW*(M+2+2*N)+N*(N+1)/2
        IFAIL=0
        MAXCAL=400
        CALL E04FAF(M,N,X,R1,F,FTOL,XTOL,STEPMX,W,IW,RESID,MONIT,
       1IPRINT,MAXCAL,IFAIL)
        WRITE(1,110)F,FTOL
        WRITE(1,120)(X(I),I=1,N)
        WRITE(1,130)IFAIL
        WRITE(1,140)(OMEGA(I),ALPHAM(I),ALPHA(I),R1(I),I=1,M)
110     FORMAT(' FINAL SUM OF SQUARES IS',E20.12,'FINAL
       1FTOL WAS',E20.12)
120     FORMAT('FINAL LEAST SQUARES ESTIMATES OF X ARE',4E20.12)
130     FORMAT(9H IFAIL = ,I2)
140     FORMAT(4E15.6)
C10     FORMAT('PL INPUT VALUES OF M,N')
C20     FORMAT('PL INPUT VALUES OF OMEGA(M)')
C30     FORMAT('PL INPUT VALUES OF ALPHAM(M)')
C40     FORMAT('PL INPUT VALUES OF X(N)')
C50     FORMAT('PL INPUT VALUES OF STEPMX(N)')
C60     FORMAT('PL INPUT ALUES OF IPRINT')
        CALL EXIT
        END
```

Contd.

```
      SUBROUTINE RESID(M,N,X,R1)
C     CALCULATES RESIDUALS AT XS
      INTEGER M,N,I
      DOUBLE PRECISION X,R1
      DIMENSION OMEGA(50),ALPHA(50),ALPHAM(50),R1(50),X(10)
      COMMON OMEGA,ALPHA,ALPHAM
      WO=X(1)
      B=X(2)
      R=X(3)
      TA=X(4)
      CALL RES(WO,B,M,ALPHA,R,TA)
      DO 10 I=1,M
      R1(I)=DBLE(ALPHAM(I)-ALPHA(I))
10    CONTINUE
      RETURN
      END
      SUBROUTINE RES(WO,B,M,ALPHA,R,TA)
      DIMENSION OMEGA(50),ALPHA(50)
      COMMON OMEGA
      DO 20 I=1,M
      P=OMEGA(I)-WO
      X1=R+2.0*B*COS(TA)
      X2=2.0*B*SIN(TA)
      X3=R*R+B*B+2.0*R*B*COS(TA)
      P1=(-X1+SQRT(X1*X1+X2*X2))/(4.0*SIN(TA))
      X4=4.0*P*(P+R*SIN(TA))
      X5=B*B+4.0*P1*P1
      X6=4.0*P1*(P1+R*SIN(TA))
      X7=B*B+4.0*P*P
      ALPHA(I)=SQRT(((X3+X4)*X5)/((X3+X6)*X7))
20    CONTINUE
      RETURN
      END
      SUBROUTINE MONIT(M,N,X,F,ITERC,SING,LIM)
C     PRINTS OUT VALUES OF EERY IPRINT ITERATIONS
      LOGICAL SING,LIM
      DOUBLE PRECISION X,F
      DIMENSION X(10)
      WRITE(1,510)ITERC,F
      WRITE(1,520)(X(I),I=1,N)
      IF (SING) WRITE(1,540)
      IF (LIM) WRITE(1,530)
510   FORMAT('AFTER',I4,'ITERATION','THE SUM OF SQUARES IS',E20.12)
520   FORMAT('AT THE POINT',4E20.12)
530   FORMAT(8H LIMITED/)
540   FORMAT(9H SINGULAR/)
      RETURN
      END
```

APPENDIX IV

NATURAL FREQUENCIES OF VIBRATION , HEIGHT / THICKNESS OF CROSS-SECTION AND MASS OF CIRCULAR RINGS USED IN THE PRESENT INVESTIGATION

RING A

RADIAL(INEXTENSIONAL)

NO	T (MM)	FREQUENCIES IN HZ AT N= 2	3	4	5	6	7	8	9
1	30.07	1607.6	4313.3	7760.6	11694.3	15958.5	20436.6		
2	29.10	1558.4	4193.0	7566.2	11435.6	15646.2	20080.5		
3	27.97	1499.7	4049.3	7326.4	11119.9	15261.0	19639.3		
4	27.00	1450.0	3940.0	7145.0	10860.0	14930.0	19250.0		
5	26.02	1400.8	3802.8	6926.5	10568.1	14580.9	18854.4		
6	25.02	1351.7	3680.1	6719.2	10285.0	14228.7	18445.3		
7	24.02	1300.3	3548.2	6489.2	9980.7	13848.0	17997.8		
8	23.10	1251.7	3423.2	6285.0	9686.2	13476.2	17559.1		
9	22.13	1202.5	3296.5	6066.7	9381.6	13088.6	17099.5		
10	21.13	1147.7	3155.0	5827.8	9036.5	12647.9	16570.5	20730.2	
11	20.14	1095.6	3019.5	5594.3	8699.7	12211.7	16045.2	20126.3	
12	19.23	1048.0	2894.0	5375.4	8382.4	11799.0	15543.9	19546.0	
13	18.25	996.2	2757.3	5136.8	8032.3	11341.0	14983.2	18891.5	
14	17.25	943.1	2615.0	4885.0	7665.0	10851.4	14379.6	18183.8	
15	16.28	890.0	2474.6	4632.8	7292.3	10353.7	13761.7	17453.5	
16	15.29	836.9	2330.8	4376.0	6925.6	9835.2	13115.1	16682.2	20489.1
17	14.45	794.1	2212.9	4159.6	6573.4	9400.2	12566.0	16023.5	19726.3
18	13.58	746.5	2084.5	3929.3	6210.4	8917.1	11953.3	15282.0	18862.6
19	12.70	699.4	1955.0	3692.9	5857.2	8421.2	11318.3	14509.8	17956.8
20	11.86	653.4	1830.3	3460.0	5507.1	7933.0	10686.3	13734.8	17041.1
21	10.93	600.0	1688.1	3200.0	5100.7	7382.8	9953.7	12828.9	15964.1
22	9.99	550.2	1545.5	2935.7	4689.6	6788.6	9198.9	11887.2	14833.0
23	9.13	504.4	1419.9	2699.1	4320.4	6232.1	8510.9	11024.1	13790.7
24	8.22	454.4	1273.7	2434.3	3903.8	5665.1	7728.9	10034.2	12583.7
25	7.32	406.4	1145.0	2184.6	3508.9	5100.4	6971.1	9110.0	11409.4
26	6.39	353.5	1002.1	1911.6	3074.4	4477.5	6111.9	8006.8	10083.6
27	5.99	333.7	940.7	1795.9	2890.9	4213.6	5764.1	7544.5	9523.2

10	11	12	13
20572.1			
19326.0			
18010.5			
16786.0	19987.4		
15360.3	18342.0		
13963.6	16717.4	19656.8	
12372.6	14852.9	17514.3	20345.5
11688.0	14046.1	16580.2	19284.8

RING B

RADIAL(INEXTENSIONAL)

NO	H (MM)	FREQUENCIES IN HZ AT N=							
		2	3	4	5	6	7	8	9
1	23.67	446.0	1257.4	2397.4	3849.0	5601.0	7632.0	9924.0	12466.0
2	23.15	446.1	1257.2	2397.1	3848.5	5600.1	7631.0	9924.0	12465.0
3	22.66	446.1	1257.0	2396.3	3848.6	5598.6	7630.0	9920.3	12463.1
4	22.16	446.3	1256.7	2395.9	3847.3	5597.7	7628.0	9919.0	12458.8
5	21.70	446.2	1256.3	2395.6	3845.9	5593.9	7627.0	9913.4	12453.1
6	21.21	446.0	1256.0	2395.1	3844.6	5591.9	7623.0	9910.4	12445.5
7	20.71	446.0	1256.0	2394.8	3844.3	5591.1	7619.2	9907.8	12443.0
8	20.21	445.7	1256.1	2395.0	3844.3	5590.6	7619.3	9906.8	12441.7
9	19.73	445.8	1255.8	2394.4	3843.1	5588.8	7615.2	9903.3	12435.6
10	19.23	445.8	1255.8	2394.2	3843.0	5588.9	7613.4	9900.0	12431.7
11	18.74	445.9	1255.4	2394.2	3842.8	5588.0	7610.7	9897.0	12428.6
12	18.25	445.9	1255.8	2394.1	3842.7	5587.3	7610.9	9896.1	12427.0
13	17.74	445.7	1255.4	2393.9	3842.0	5586.0	7607.1	9890.2	12419.8
14	17.24	445.9	1255.6	2393.8	3841.6	5585.3	7605.2	9891.8	12419.7
15	16.76	445.9	1255.6	2393.4	3841.4	5584.6	7607.3	9890.2	12417.2
16	16.27	445.8	1255.5	2393.3	3840.7	5583.5	7605.5	9888.2	12414.0
17	15.77	445.8	1255.3	2393.1	3839.9	5582.3	7603.6	9887.0	12411.0
18	15.27	445.8	1254.9	2392.0	3838.4	5580.0	7599.2	9881.2	12404.1
19	14.78	445.8	1254.6	2392.0	3838.3	5579.7	7598.5	9877.6	12401.6
20	14.27	445.6	1254.6	2392.0	3837.8	5579.8	7597.4	9875.9	12397.0
21	13.77	445.6	1254.5	2391.5	3837.1	5577.8	7595.5	9876.2	12393.3
22	13.30	445.6	1254.4	2390.8	3836.1	5575.9	7593.0	9869.2	12391.6
23	12.79	445.7	1254.0	2390.2	3835.3	5574.7	7591.2	9870.3	12389.3
24	12.32	445.5	1253.7	2389.9	3834.3	5573.3	7590.0	9864.8	12382.9
25	11.79	445.3	1253.4	2389.8	3833.5	5572.1	7586.9	9861.5	12380.0
26	11.21	445.2	1253.2	2389.5	3833.7	5572.1	7586.6	9861.6	12379.3
27	10.79	445.2	1253.0	2389.6	3833.4	5571.7	7586.8	9860.7	12377.7
28	10.30	445.1	1252.8	2388.6	3831.9	5569.3	7582.0	9855.1	12371.2
29	9.79	445.1	1252.6	2388.0	3831.0	5568.2	7580.7	9852.3	12366.3
30	9.33	445.2	1252.7	2388.2	3831.3	5568.4	7582.1	9853.9	12368.2
31	8.84	445.2	1252.9	2388.5	3831.8	5568.1	7582.3	9854.2	12367.0
32	8.40	444.9	1252.3	2387.7	3830.4	5567.1	7579.1	9851.3	12365.5
33	7.91	444.8	1252.2	2387.3	3829.9	5566.3	7578.2	9849.7	12362.5
34	7.38	445.1	1252.4	2387.4	3830.2	5566.6	7578.5	9850.0	12362.5
35	6.87	444.8	1252.6	2387.5	3830.4	5567.1	7578.6	9850.6	12362.4
36	6.36	445.0	1252.3	2387.7	3830.2	5566.4	7578.7	9850.7	12361.3
37	5.93	445.0	1251.8	2387.5	3829.4	5565.3	7576.8	9848.0	12359.8
38	5.43	444.7	1251.2	2387.4	3829.0	5565.5	7576.0	9847.0	12358.5
39	4.91	444.6	1251.1	2387.4	3828.8	5565.0	7576.0	9846.0	12358.0
40	4.43	445.0	1251.2	2387.4	3828.6	5565.0	7576.0	9846.0	12357.5
41	3.92	445.2	1251.1	2387.4	3828.5	5565.0	7575.0	9846.0	12356.0
42	3.44	445.2	1251.0	2387.4	3828.5	5565.1	7575.5	9846.5	12356.3
43	2.88	445.3	1251.0	2387.4	3828.4	5565.0	7575.6	9846.5	12357.4
44	2.38	444.8	1250.7	2387.4	3828.3	5565.6	7575.9	9847.9	12358.8
45	1.86	444.8	1250.6	2387.3	3828.2	5565.9	7576.4	9851.7	12360.9
46	1.38	444.7	1250.3	2387.2	3828.3	5565.5	7575.0	9848.2	12360.0

Contd.

RING B

RADIAL(INEXTENSIONAL)

NO	H (MM)	FREQUENCIES IN HZ AT N= 10	11	12
1	23.67	15236.0	18215.0	
2	23.15	15235.0	18214.0	
3	22.66	15231.6	18208.0	
4	22.16	15224.6	18200.0	
5	21.70	15216.6	18191.6	
6	21.21	15204.8	18196.0	
7	20.71	15197.0	18184.0	
8	20.21	15202.0	18176.0	
9	19.73	15198.0	18163.3	
10	19.23	15191.8	18158.0	
11	18.74	15183.0	18152.1	
12	18.25	15183.0	18145.0	
13	17.74	15173.0	18138.6	
14	17.24	15170.7	18136.3	
15	16.76	15169.1	18135.2	
16	16.27	15166.0	18135.0	
17	15.77	15161.8	18130.0	
18	15.27	15154.9	18120.0	
19	14.78	15150.9	18110.0	
20	14.27	15145.6	18097.8	
21	13.77	15138.9	18096.0	21237.0
22	13.30	15134.3	18096.0	21228.4
23	12.79	15132.9	18086.6	21224.0
24	12.32	15123.6	18075.6	21211.7
25	11.79	15119.2	18066.8	21204.5
26	11.21	15119.0	18065.5	21203.8
27	10.79	15119.2	18065.4	21198.7
28	10.30	15110.2	18054.2	21189.0
29	9.79	15103.6	18045.0	21185.1
30	9.33	15104.6	18048.3	21179.9
31	8.84	15103.8	18048.8	21180.0
32	8.40	15099.3	18044.4	21170.0
33	7.91	15097.5	18038.0	21168.8
34	7.38	15096.0	18040.0	21168.5
35	6.87	15095.1	18040.2	21168.5
36	6.36	15094.8	18037.2	21166.0
37	5.93	15091.7	18035.3	21161.6
38	5.43	15088.0	18035.0	21159.0
39	4.91	15086.4	18035.0	21158.0
40	4.43	15088.0	18035.0	21157.0
41	3.92	15089.0	18035.0	21156.0
42	3.44	15090.7	18034.5	21158.0
43	2.88	15090.0	18036.0	21156.0
44	2.38	15091.1	18037.0	21160.9
45	1.86	15088.9	18039.0	21154.6
46	1.38	15079.2	18030.0	21147.2

OK,

RING C

RADIAL(INEXTENSIONAL)

NO	H (MM)	FREQUENCIES IN HZ AT N=							
		2	3	4	5	6	7	8	9
1	23.58	329.5	930.0	1779.0	2867.0	4188.0	5736.0	7499.0	9481.0
2	23.10	329.4	929.8	1778.2	2866.0	4185.7	5733.2	7498.3	9475.8
3	22.59	329.4	929.6	1778.3	2865.8	4185.6	5733.4	7498.3	9472.6
4	22.07	329.5	929.8	1778.1	2865.3	4184.7	5731.3	7495.1	9470.5
5	21.58	329.3	929.1	1777.4	2864.0	4182.9	5728.0	7490.1	9463.1
6	21.08	329.2	929.0	1776.7	2862.4	4180.4	5725.4	7485.7	9456.3
7	20.58	329.2	929.1	1776.7	2862.1	4180.1	5723.5	7484.3	9454.0
8	20.07	329.2	929.0	1776.8	2862.8	4180.1	5724.6	7483.7	9452.6
9	19.59	329.2	928.7	1776.4	2861.8	4178.6	5722.2	7480.4	9449.7
10	19.10	329.1	928.5	1776.1	2860.9	4177.0	5719.2	7477.5	9447.9
11	18.60	328.9	928.4	1775.3	2859.8	4175.6	5717.3	7473.7	9441.8
12	18.11	329.0	928.2	1774.6	2858.6	4173.5	5713.9	7470.0	9436.4
13	17.65	328.9	928.3	1774.4	2857.8	4172.5	5712.3	7466.9	9431.4
14	17.13	328.7	928.4	1774.9	2858.7	4173.2	5713.8	7467.8	9432.8
15	16.63	328.7	928.3	1775.1	2859.0	4173.1	5712.9	7467.8	9431.3
16	16.11	328.8	928.1	1774.3	2857.3	4170.9	5709.3	7462.4	9424.9
17	15.65	328.9	928.0	1774.5	2857.8	4171.4	5709.7	7462.5	9424.3
18	15.16	328.8	927.7	1773.8	2856.5	4169.2	5706.7	7458.6	9419.3
19	14.69	328.8	928.0	1773.8	2856.4	4169.2	5706.3	7457.8	9417.5
20	14.21	328.7	927.4	1773.3	2855.0	4167.9	5704.2	7454.6	9415.1
21	13.72	328.7	926.9	1772.0	2853.6	4165.1	5700.2	7449.7	9406.2
22	13.22	328.6	927.0	1771.9	2853.8	4164.5	5699.5	7448.6	9403.9
23	12.70	328.4	927.0	1772.2	2853.4	4164.3	5699.2	7447.3	9402.2
24	12.21	328.4	926.8	1772.0	2852.7	4163.3	5696.8	7444.6	9398.4
25	11.68	328.5	926.9	1771.1	2851.7	4161.6	5694.5	7440.8	9393.7
26	11.26	328.6	926.1	1771.3	2851.4	4161.0	5693.8	7439.1	9391.1
27	10.70	328.6	926.1	1770.7	2850.6	4159.6	5691.6	7438.0	9389.2
28	10.18	328.6	926.3	1770.5	2850.4	4159.3	5690.8	7435.9	9386.5
29	9.67	328.4	925.8	1769.6	2849.1	4157.0	5688.2	7431.8	9384.2
30	9.17	328.3	925.4	1769.3	2848.3	4156.1	5687.1	7430.0	9378.0
31	8.63	328.3	925.6	1769.6	2848.7	4156.7	5687.7	7430.4	9377.5
32	8.16	328.4	925.3	1769.1	2848.3	4155.8	5686.2	7429.0	9374.3
33	7.66	328.2	925.2	1768.8	2847.8	4154.8	5684.6	7426.7	9374.1
34	7.13	328.2	925.2	1768.5	2847.0	4154.0	5684.0	7425.5	9372.0
35	6.61	328.0	925.0	1768.3	2846.7	4153.5	5683.1	7424.5	9371.2
36	6.15	328.0	924.7	1768.4	2846.8	4153.0	5683.1	7424.4	9369.6
37	5.66	327.7	924.4	1768.0	2846.2	4151.2	5680.1	7421.2	9367.3
38	5.17	327.7	924.1	1767.3	2844.4	4149.5	5678.1	7418.0	9362.8
39	4.66	327.7	924.1	1767.3	2844.4	4149.1	5678.3	7418.8	9363.0
40	4.15	327.6	923.4	1766.2	2842.7	4146.6	5674.7	7414.2	9357.1
41	3.67	327.8	923.2	1766.5	2843.0	4146.5	5675.0	7414.0	9366.1
42	3.17	327.6	923.1	1766.6	2843.0	4146.5	5675.1	7414.3	9360.4
43	2.63	327.3	922.8	1765.8	2841.6	4144.1	5672.3	7412.0	9354.1
44	2.15	327.6	922.6	1765.5	2840.9	4143.0	5670.9	7408.4	9349.3
45	1.69	327.4	922.9	1765.7	2841.7	4143.1	5672.3	7411.8	9351.6
46	1.19	327.3	922.7	1765.8	2838.8	4143.0	5666.4	7404.2	9340.9

OK,

Contd.

RING C

RADIAL(INEXTENSIONAL)

NO	H (MM)	FREQUENCIES IN HZ AT N= 10	11	12	13
1	23.58	11655.0	14020.0	16574.0	19288.0
2	23.10	11652.0	14017.8	16567.0	19282.7
3	22.59	11650.5	14015.0	16561.0	19283.1
4	22.07	11645.9	14006.0	16558.8	19291.3
5	21.58	11637.4	14000.6	16544.7	19281.3
6	21.08	11630.3	13992.8	16544.0	19271.8
7	20.58	11626.4	13988.0	16544.0	19270.0
8	20.07	11624.2	13985.5	16525.0	19250.8
9	19.59	11620.5	13978.0	16518.0	19231.0
10	19.10	11613.7	13971.0	16506.0	19219.7
11	18.60	11609.0	13963.3	16496.0	19208.0
12	18.11	11601.5	13954.2	16491.5	19195.0
13	17.65	11596.2	13947.0	16486.0	19184.2
14	17.13	11595.7	13948.0	16481.3	19187.0
15	16.63	11593.6	13944.7	16473.0	19176.7
16	16.11	11586.1	13935.8	16465.2	19168.0
17	15.65	11584.9	13933.3	16464.4	19160.8
18	15.16	11578.5	13924.1	16450.8	19151.0
19	14.69	11575.3	13922.3	16445.1	19141.6
20	14.21	11569.6	13913.2	16441.2	19131.0
21	13.72	11560.2	13908.0	16422.5	19111.7
22	13.22	11558.6	13901.0	16418.4	19109.5
23	12.70	11555.5	13895.5	16412.8	19100.5
24	12.21	11552.6	13888.6	16405.8	19091.4
25	11.68	11554.6	13881.2	16398.0	19079.2
26	11.26	11554.1	13877.0	16392.0	19074.0
27	10.70	11537.3	13871.9	16384.5	19064.1
28	10.18	11532.9	13865.7	16378.8	19057.5
29	9.67	11526.3	13858.0	16370.0	19044.4
30	9.17	11522.7	13853.9	16359.4	19037.4
31	8.63	11525.8	13853.5	16359.3	19032.0
32	8.16	11520.5	13849.5	16358.8	19029.2
33	7.66	11517.6	13845.3	16354.0	19023.0
34	7.13	11515.0	13842.0	16348.0	19018.0
35	6.61	11512.1	13839.1	16343.7	19014.6
36	6.15	11514.4	13839.3	16343.8	19008.0
37	5.66	11507.7	13833.3	16336.7	19005.0
38	5.17	11501.6	13826.8	16328.6	18998.5
39	4.66	11503.9	13826.8	16331.3	18998.0
40	4.15	11495.9	13818.8	16320.6	18996.5
41	3.67	11497.0	13819.0	16321.0	18992.0
42	3.17	11496.6	13819.4	16320.9	18986.0
43	2.63	11492.3	13813.6	16314.3	18976.0
44	2.15	11488.8	13809.0	16309.4	18971.0
45	1.69	11491.0	13804.0	16306.0	18966.0
46	1.19	11488.1	13800.2	16304.7	18962.5

OK,

RING D

RADIAL(INEXTENSIONAL)

NO	H (MM)	FREQUENCIES IN HZ AT N=							
		2	3	4	5	6	7	8	9
1	24.07	222.0	627.0	1201.5	1942.0	2846.0	3910.5	5136.0	6518.0
2	23.55	221.8	627.1	1201.5	1941.9	2845.3	3910.1	5133.9	6515.6
3	23.05	222.0	627.4	1201.7	1942.2	2845.4	3910.1	5133.8	6515.4
4	22.54	222.1	627.0	1201.5	1941.5	2845.3	3908.5	5131.4	6510.0
5	22.05	221.9	627.1	1200.8	1940.8	2842.9	3906.3	5128.5	6508.5
6	21.56	221.9	626.5	1200.4	1939.6	2841.6	3904.2	5125.7	6505.4
7	21.07	221.6	626.5	1200.4	1939.6	2841.2	3903.9	5124.9	6501.7
8	20.52	221.8	626.4	1200.2	1939.3	2840.8	3903.1	5123.4	6499.4
9	20.04	221.6	626.5	1200.1	1939.2	2840.4	3902.4	5122.6	6497.6
10	19.58	221.6	626.5	1200.2	1938.8	2840.0	3901.2	5120.7	6497.0
11	19.12	221.8	626.4	1199.3	1937.7	2837.9	3898.2	5116.8	6490.6
12	18.63	221.6	625.8	1198.8	1937.1	2837.1	3897.1	5115.3	6488.6
13	18.11	221.6	625.9	1199.0	1937.0	2836.8	3896.2	5114.1	6486.0
14	17.61	221.8	626.4	1199.3	1937.5	2837.2	3897.0	5114.4	6485.5
15	17.10	221.7	626.2	1199.3	1937.3	2836.8	3896.3	5113.2	6483.6
16	16.60	221.8	626.6	1199.0	1936.8	2836.0	3895.4	5111.9	6482.4
17	16.10	221.7	626.2	1199.0	1936.9	2836.2	3895.1	5111.4	6484.1
18	15.58	221.6	625.7	1198.5	1935.8	2834.3	3892.0	5107.6	6475.7
19	15.07	221.4	625.5	1198.5	1935.9	2834.4	3891.7	5106.7	6474.2
20	14.60	221.4	625.6	1198.1	1934.6	2832.2	3888.8	5103.2	6469.9
21	14.12	221.2	625.0	1196.9	1934.1	2830.0	3885.7	5098.9	6464.1
22	13.63	221.0	625.2	1197.0	1933.6	2830.9	3886.3	5099.4	6464.4
23	13.13	221.2	625.1	1196.9	1933.3	2830.4	3885.2	5097.7	6463.3
24	12.62	221.1	624.9	1196.5	1932.6	2828.8	3883.7	5095.6	6458.9
25	12.14	221.0	624.7	1195.5	1931.2	2827.0	3880.5	5091.6	6453.5
26	11.66	221.2	624.8	1196.1	1931.7	2827.0	3880.7	5091.4	6453.5
27	11.19	221.1	624.8	1195.8	1930.8	2825.8	3879.6	5089.5	6450.4
28	10.68	221.3	624.6	1195.3	1930.4	2825.5	3878.3	5087.6	6448.2
29	10.17	221.0	624.4	1195.4	1930.6	2825.5	3878.4	5088.0	6448.0
30	9.66	221.0	624.2	1195.0	1929.7	2824.1	3876.5	5085.2	6444.9
31	9.15	221.1	624.5	1195.3	1930.6	2824.7	3877.1	5085.4	6444.8
32	8.67	221.1	624.1	1194.6	1929.1	2823.2	3875.5	5083.1	6441.9
33	8.18	221.1	623.6	1193.9	1928.0	2821.1	3871.9	5078.9	6436.0
34	7.67	221.3	624.7	1194.0	1928.5	2822.0	3873.0	5080.0	6443.6
35	7.17	221.0	624.1	1194.2	1929.1	2822.6	3873.9	5081.3	6438.8
36	6.71	221.3	624.0	1194.5	1929.4	2821.0	3874.2	5081.6	6438.8
37	6.21	221.2	623.3	1193.7	1928.2	2819.2	3869.0	5074.8	6431.5
38	5.72	221.1	623.7	1193.4	1927.6	2820.2	3870.2	5076.3	6432.9
39	5.22	221.2	623.6	1193.5	1928.3	2821.0	3871.1	5077.7	6434.7
40	4.72	221.3	623.9	1193.2	1928.1	2820.5	3870.0	5076.2	6432.6
41	4.24	221.4	623.7	1193.4	1927.8	2821.0	3870.5	5077.0	6434.5
42	3.70	221.3	623.0	1192.5	1926.5	2819.1	3868.0	5073.8	6429.1
43	3.23	221.4	622.7	1191.3	1926.0	2817.8	3865.9	5071.4	6426.7
44	2.74	221.2	623.3	1190.5	1925.0	2816.1	3863.1	5069.1	6422.5
45	2.25	221.2	622.1	1190.3	1924.8	2815.6	3863.0	5068.7	6422.7
46	1.78	221.2	621.5	1191.2	1925.2	2816.1	3863.3	5069.5	6424.1

OK.

Contd.

RING D

RADIAL(INEXTENSIONAL)

NO	H (MM)	FREQUENCIES IN HZ AT N=						
		10	11	12	13	14	15	16
1	24.07	8054.0	9738.0	11570.0	13540.0	15661.0	17908.0	20306.0
2	23.55	8052.8	9737.0	11564.2	13538.0	15656.0	17898.0	20294.0
3	23.05	8051.0	9738.0	11562.2	13534.0	15650.0	17888.1	20284.8
4	22.54	8044.0	9730.0	11557.4	13528.0	15642.0	17877.0	20270.0
5	22.05	8040.0	9723.5	11549.3	13518.5	15633.0	17866.2	20257.4
6	21.56	8035.2	9717.2	11543.0	13512.0	15624.0	17856.4	20249.9
7	21.07	8033.3	9716.5	11539.6	13507.0	15614.7	17849.4	20242.0
8	20.52	8031.2	9710.9	11534.5	13502.0	15605.0	17842.1	20233.0
9	20.04	8027.3	9709.3	11531.8	13496.0	15601.3	17836.0	20224.0
10	19.58	8024.2	9700.5	11526.1	13491.4	15590.0	17828.8	20212.0
11	19.12	8019.3	9693.7	11515.6	13481.5	15580.2	17811.0	20207.0
12	18.63	8015.2	9690.6	11510.7	13474.0	15572.0	17805.8	20193.0
13	18.11	8012.4	9687.0	11508.0	13467.0	15565.0	17800.0	20174.0
14	17.61	8011.2	9685.7	11504.5	13465.0	15560.0	17795.6	20162.0
15	17.10	8009.7	9683.2	11502.4	13464.5	15556.5	17785.0	20146.6
16	16.60	8006.8	9678.3	11495.6	13455.0	15548.4	17776.2	20136.0
17	16.10	8003.9	9673.0	11493.8	13444.0	15540.0	17770.5	20124.0
18	15.58	7997.2	9667.4	11482.2	13436.4	15528.6	17752.3	20110.0
19	15.07	7996.3	9667.2	11477.1	13432.0	15520.0	17743.7	20096.0
20	14.60	7990.1	9654.5	11469.3	13421.7	15509.2	17730.0	20078.0
21	14.12	7982.0	9644.5	11464.0	13412.0	15498.0	17716.0	20063.0
22	13.63	7982.3	9642.0	11456.6	13405.0	15487.1	17703.2	20049.3
23	13.13	7979.4	9640.3	11451.5	13398.0	15479.0	17692.0	20035.0
24	12.62	7975.1	9635.6	11443.6	13389.7	15466.0	17682.3	20023.1
25	12.14	7967.1	9626.6	11432.3	13375.8	15452.2	17663.8	20000.6
26	11.66	7966.7	9625.3	11426.6	13373.0	15450.4	17656.5	19990.0
27	11.19	7963.6	9620.8	11423.2	13363.3	15440.2	17647.3	19979.7
28	10.68	7960.7	9615.5	11417.6	13357.0	15434.0	17635.3	19965.4
29	10.17	7959.4	9615.9	11415.7	13354.6	15426.0	17631.1	19962.4
30	9.66	7954.7	9609.8	11408.4	13346.0	15416.2	17617.9	19945.6
31	9.15	7954.8	9608.6	11407.5	13343.2	15412.0	17606.0	19937.8
32	8.67	7949.3	9603.8	11400.0	13333.3	15402.2	17600.0	19922.7
33	8.18	7943.6	9595.8	11389.9	13322.1	15396.0	17592.0	19912.0
34	7.67	7952.0	9596.0	11386.0	13322.0	15390.0	17586.0	19906.0
35	7.17	7945.5	9598.0	11382.0	13322.4	15384.0	17579.0	19900.3
36	6.71	7945.3	9598.9	11380.0	13311.0	15384.3	17577.0	19892.0
37	6.21	7936.0	9586.1	11377.3	13304.6	15378.0	17564.0	19884.0
38	5.72	7936.2	9587.5	11378.2	13306.2	15373.0	17555.5	19878.0
39	5.22	7938.8	9590.2	11382.1	13309.5	15369.3	17552.0	19875.7
40	4.72	7936.5	9585.3	11376.9	13304.5	15360.2	17545.0	19867.8
41	4.24	7937.9	9586.5	11372.0	13305.1	15364.1	17540.0	19862.6
42	3.70	7931.2	9578.7	11370.2	13296.2	15352.0	17535.0	19855.8
43	3.23	7928.2	9575.7	11367.0	13291.7	15344.5	17528.0	19850.0
44	2.74	7923.6	9568.9	11359.6	13284.4	15340.5	17523.6	19842.0
45	2.25	7922.8	9565.2	11358.2	13281.5	15334.7	17514.9	19838.0
46	1.78	7922.5	9574.7	11357.7	13284.4	15330.0	17510.0	19834.7

OK.

RING A

EXTENSIONAL(RADIAL)

NO	T (MM)	FREQUENCIES IN HZ FOR N=				
		0	1	1	2	2
1	30.07	7734.0	10732.5	10740.5	16799.4	16804.8
2	29.10	7730.7	10732.7	10742.4	16820.0	16825.5
3	27.97	7719.7	10737.7	10744.5	16843.6	16849.0
4	27.00	7715.0	10742.0	10751.0	16864.0	16871.0
5	26.02	7712.5	10752.1	10757.7	16884.3	16889.8
6	25.02	7717.5	10758.6	10766.5	16904.0	16909.4
7	24.02	7709.1	10765.3	10773.4	16925.3	16930.0
8	23.10	7707.2	10772.0	10778.3	16941.8	16947.3
9	22.13	7707.4	10782.5	10788.8	16960.8	16966.2
10	21.13	7697.3	10786.0	10793.0	16979.7	16985.2
11	20.14	7700.0	10791.7	10799.5	16996.8	17002.2
12	19.23	7699.2	10797.8	10803.6	17010.0	17016.0
13	18.25	7693.1	10803.1	10807.9	17023.6	17029.0
14	17.25	7690.5	10808.4	10814.6	17040.4	17045.8
15	16.28	7696.1	10814.7	10823.5	17057.6	17063.1
16	15.29	7697.5	10823.3	10833.3	17077.3	17082.6
17	14.45	7699.7	10829.2	10836.1	17088.6	17094.2
18	13.58	7692.8	10832.6	10840.7	17098.2	17103.6
19	12.70	7697.9	10837.8	10846.2	17111.4	17118.2
20	11.86	7697.1	10843.4	10847.5	17120.4	17125.3
21	10.93	7696.1	10847.6	10851.7	17130.1	17135.7
22	9.99	7693.1	10847.4	10862.2	17141.1	17145.2
23	9.13	7698.7	10852.3	10864.6	17150.0	17153.5
24	8.22	7697.8	10860.0	10866.0	17158.4	17164.0
25	7.32	7695.0	10866.7	10876.8	17174.1	17182.4
26	6.39	7698.7	10872.0	10884.0	17183.5	17188.5
27	5.99	7693.0	10874.0	10886.6	17186.4	17191.8

OK.

RING B

EXTENSIONAL(RADIAL)

NO	H (MM)	FREQUENCIES IN HZ FOR N= 0	1	2
1	23.67		10877.0	17168.0
2	23.15		10866.0	17168.5
3	22.66		10868.8	17167.1
4	22.16		10864.4	17171.3
5	21.70		10865.6	17169.5
6	21.21		10864.7	17168.5
7	20.71		10872.0	17171.0
8	20.21		10865.1	17169.7
9	19.73		10865.0	17169.8
10	19.23		10865.6	17172.8
11	18.74		10864.0	17171.4
12	18.25		10864.4	17174.3
13	17.74		10867.1	17172.0
14	17.24		10868.8	17173.2
15	16.76		10871.7	17174.4
16	16.27		10862.1	17174.5
17	15.77		10868.3	17174.7
18	15.27		10862.4	17174.8
19	14.78		10862.9	17176.5
20	14.27		10864.5	17174.4
21	13.77	7628.0	10871.4	17175.2
22	13.30	7635.7	10867.6	17174.5
23	12.79	7630.0	10872.0	17179.1
24	12.32	7630.0	10862.2	17174.0
25	11.79	7621.0	10867.7	17173.8
26	11.21	7633.5	10863.4	17178.8
27	10.79	7633.0	10868.8	17178.0
28	10.30	7633.0	10862.0	17180.3
29	9.79	7637.5	10858.4	17171.9
30	9.33	7625.7	10859.0	17177.2
31	8.84	7633.0	10866.3	17176.0
32	8.40	7623.5	10871.4	17179.0
33	7.91	7647.0	10861.2	17178.0
34	7.38	7632.9	10860.4	17181.5
35	6.87	7629.2	10860.9	17179.2
36	6.36	7633.4	10862.7	17176.8
37	5.93	7649.6	10860.8	17181.8
38	5.43	7646.4	10861.6	17178.2
39	4.91	7623.8	10860.8	17178.8
40	4.43	7651.1	10860.2	17186.4
41	3.92	7641.0	10863.8	17186.1
42	3.44	7649.4	10871.7	17186.8
43	2.88	7645.1	10870.3	17187.3
44	2.38	7648.9	10863.8	17186.6
45	1.86	7647.3	10866.0	17184.0
46	1.38	7642.5	10857.8	17181.7

OK.

RING C

EXTENSIONAL(RADIAL)

NO	H (MM)	FREQUENCIES IN HZ FOR N= 0	1	2
1	23.58		10873.5	17189.0
2	23.10		10872.5	17190.0
3	22.59		10871.0	17190.2
4	22.07		10875.5	17191.2
5	21.58		10874.4	17192.5
6	21.08		10874.4	17194.3
7	20.58		10875.4	17190.7
8	20.07		10875.2	17194.5
9	19.59		10874.0	17196.0
10	19.10		10875.1	17197.4
11	18.60		10874.5	17197.0
12	18.11		10878.0	17198.1
13	17.65		10869.7	17193.0
14	17.13		10878.6	17193.0
15	16.63		10868.5	17191.6
16	16.11		10873.9	17197.5
17	15.65		10874.9	17201.3
18	15.16		10872.9	17198.8
19	14.69		10876.6	17195.3
20	14.21		10876.8	17199.7
21	13.72	7712.8	10871.0	17196.0
22	13.22	7715.1	10873.0	17198.0
23	12.70	7717.5	10876.4	17194.8
24	12.21	7704.0	10867.0	17196.0
25	11.68	7711.8	10875.0	17197.0
26	11.26	7698.2	10871.7	17198.6
27	10.70	7676.6	10877.9	17204.8
28	10.18	7671.0	10871.9	17200.0
29	9.67	7731.5	10865.3	17196.7
30	9.17	7733.8	10876.8	17198.5
31	8.63	7742.3	10871.5	17197.2
32	8.16	7733.6	10873.8	17202.2
33	7.66	7743.5	10877.6	17203.0
34	7.13	7764.9	10870.8	17203.0
35	6.61	7727.0	10873.4	17201.3
36	6.15	7730.0	10868.8	17202.3
37	5.66	7746.0	10872.0	17200.0
38	5.17	7756.4	10872.0	17207.5
39	4.66	7762.6	10872.0	17207.0
40	4.15	7779.0	10871.1	17207.5
41	3.67	7771.0	10871.0	17208.4
42	3.17	7778.7	10870.0	17208.0
43	2.63	7770.0	10869.3	17211.4
44	2.15	7766.2	10864.2	17210.0
45	1.69	7742.5	10872.9	17211.0
46	1.19	7748.1	10868.0	17209.7

OK,

RING 0

EXTENSIONAL(RADIAL)

NO	H (MM)	FREQUENCIES IN HZ FOR N= 0	1	2
1	24.07		10873.0	17187.0
2	23.55		10873.4	17186.3
3	23.05		10872.2	17189.0
4	22.54		10867.8	17189.5
5	22.05		10873.4	17188.0
6	21.56		10868.6	17188.6
7	21.07		10878.0	17185.7
8	20.52		10880.5	17188.1
9	20.04		10879.1	17192.5
10	19.58		10860.4	17196.1
11	19.12		10870.0	17192.0
12	18.63		10879.8	17192.0
13	18.11		10871.8	17192.5
14	17.61		10868.8	17193.0
15	17.10		10876.4	17193.1
16	16.60		10860.0	17190.3
17	16.10		10880.8	17193.5
18	15.58		10879.7	17198.1
19	15.07		10877.4	17197.8
20	14.60		10869.6	17197.0
21	14.12	7710.9	10867.5	17196.6
22	13.63	7712.5	10851.8	17201.3
23	13.13	7714.1	10851.8	17198.7
24	12.62	7715.7	10856.1	17199.0
25	12.14	7722.6	10850.7	17196.0
26	11.66	7718.7	10875.0	17200.6
27	11.19	7724.2	10850.0	17200.7
28	10.68	7723.2	10850.7	17199.5
29	10.17	7720.0	10847.5	17198.7
30	9.66	7723.1	10848.2	17205.1
31	9.15	7731.6	10850.0	17192.0
32	8.67	7718.5	10851.0	17198.0
33	8.18	7738.5	10852.3	17197.5
34	7.67	7734.0	10859.9	17187.4
35	7.17	7733.0	10847.7	17207.3
36	6.71	7731.6	10862.6	17207.6
37	6.21	7746.7	10859.0	17195.9
38	5.72	7742.8	10854.5	17192.4
39	5.22	7733.4	10851.7	17194.0
40	4.72	7744.8	10870.3	17197.1
41	4.24	7750.6	10873.7	17194.5
42	3.70	7747.2	10883.4	17194.5
43	3.23	7746.0	10880.0	17201.0
44	2.74	7744.9	10874.2	17208.8
45	2.25	7750.0	10860.0	17206.2
46	1.78	7748.1	10847.8	17206.1

OK,

RING A

AXIAL

NO	T (MM)	FREQUENCIES IN HZ AT N=							
		2	3	4	5	6	7	8	9
1	30.07	329.2	912.0	1730.8	2774.7	4035.4	5505.2	7174.5	9032.3
2	29.10	329.4	913.0	1732.7	2778.5	4042.0	5516.0	7190.6	9052.9
3	27.97	329.6	914.2	1734.8	2782.7	4049.1	5528.4	7209.9	9081.4
4	27.00	329.7	915.0	1736.8	2787.0	4055.5	5539.0	7225.0	9106.0
5	26.02	329.8	916.2	1739.3	2790.5	4064.4	5550.9	7243.7	9125.0
6	25.02	330.3	917.1	1741.2	2794.5	4069.7	5558.8	7253.8	9147.3
7	24.02	330.3	917.8	1743.2	2798.4	4076.4	5569.7	7269.8	9164.9
8	23.10	330.4	918.7	1744.7	2801.0	4080.6	5575.6	7280.3	9182.2
9	22.13	330.7	919.1	1746.4	2804.6	4086.6	5584.7	7290.5	9197.5
10	21.13	330.4	919.7	1747.7	2807.2	4091.0	5589.0	7301.7	9207.3
11	20.14	330.3	920.2	1749.3	2810.3	4095.0	5596.2	7309.3	9226.1
12	19.23	330.2	920.6	1750.4	2812.1	4098.0	5603.2	7319.9	9237.3
13	18.25	330.1	921.2	1752.0	2814.9	4102.6	5606.0	7327.5	9243.0
14	17.25	330.0	921.4	1753.3	2816.3	4105.3	5609.5	7336.6	9254.6
15	16.28	329.8	921.6	1754.8	2819.3	4109.3	5616.9	7342.2	9266.0
16	15.29	330.0	921.9	1755.8	2821.6	4113.0	5624.0	7350.9	9275.5
17	14.45	329.7	922.1	1756.5	2823.5	4116.0	5628.1	7355.3	9285.4
18	13.58	329.0	922.0	1756.8	2825.3	4119.8	5632.1	7361.4	9292.0
19	12.70	328.8	921.5	1757.0	2826.5	4122.0	5636.0	7365.5	9295.0
20	11.86	327.7	920.7	1756.6	2826.0	4122.8	5638.6	7367.4	9297.6
21	10.93	326.6	919.4	1755.4	2825.5	4122.5	5639.0	7367.5	9300.9
22	9.99	325.2	918.0	1754.2	2824.8	4122.7	5640.6	7369.8	9303.4
23	9.13	324.0	916.1	1752.6	2823.9	4121.6	5640.5	7370.6	9305.8
24	8.22	321.6	913.4	1750.0	2821.7	4120.9	5640.3	7371.5	9307.5
25	7.32	318.7	909.3	1745.7	2817.8	4117.5	5637.8	7369.6	9306.1
26	6.39	314.5	903.5	1740.0	2812.3	4109.9	5635.8	7370.0	9307.5
27	5.99	312.0	900.2	1736.9	2809.7	4107.2	5634.0	7368.3	9307.6

OK,

Contd.

RING A

AXIAL

NO	T (MM)	FREQUENCIES IN HZ FOR N=				
		10	11	12	13	14
1	30.07	11056.6	13249.8	15504.2	18098.2	20708.7
2	29.10	11090.0	13296.0	15615.0	18196.0	20828.7
3	27.97	11126.0	13350.5	15700.0	18273.2	20908.4
4	27.00	11160.0	13390.0	15780.0	18340.0	21094.9
5	26.02	11190.2	13430.5	15832.4	18400.0	21166.0
6	25.02	11220.6	13463.3	15881.0	18465.3	21236.1
7	24.02	11250.7	13505.0	15929.2	18520.0	21300.1
8	23.10	11273.8	13535.1	15967.8	18566.2	
9	22.13	11295.0	13570.0	16009.0	18633.4	
10	21.13	11303.0	13593.5	16038.4	18678.7	
11	20.14	11331.7	13619.1	16071.9	18720.8	
12	19.23	11343.4	13634.6	16091.7	18746.0	
13	18.25	11359.6	13649.9	16122.3	18771.3	
14	17.25	11374.0	13668.7	16136.1	18813.0	
15	16.28	11384.8	13685.8	16167.3	18832.0	
16	15.29	11398.0	13695.0	16190.0	18860.0	
17	14.45	11408.2	13712.0	16210.0	18880.0	
18	13.58	11416.0	13727.0	16218.0	18893.1	
19	12.70	11422.9	13730.2	16221.6	18909.0	
20	11.86	11424.5	13736.9	16225.8	18910.0	
21	10.93	11425.7	13738.2	16226.5	18920.0	
22	9.99	11430.9	13745.1	16243.9	18926.7	
23	9.13	11432.4	13750.0	16240.0	18939.2	
24	8.22	11435.2	13750.2	16242.2	18940.0	
25	7.32	11436.5	13753.2	16243.6	18937.7	
26	6.39	11439.4	13758.2	16250.0	18943.0	
27	5.99	11440.2	13760.5	16257.9	18953.0	

OK,

RING B

AXIAL

NO	H (MM)	FREQUENCIES IN HZ AT N=							
		2	3	4	5	6	7	8	9
1	23.67	864.0	2714.0	5328.0	8468.0	11962.0	15646.0	19423.0	
2	23.15	852.4	2688.3	5279.1	8407.0	11894.0	15600.0	19414.0	
3	22.66	844.8	2660.4	5227.9	8334.0	11815.3	15534.3	19379.5	
4	22.16	837.4	2631.9	5172.7	8256.3	11737.3	15450.6	19320.3	
5	21.70	829.4	2602.3	5117.1	8176.0	11631.4	15352.8	19241.6	
6	21.21	821.5	2574.0	5055.3	8086.3	11520.4	15221.0	19134.6	
7	20.71	812.0	2540.3	4992.2	7991.7	11401.0	15108.1	19010.2	
8	20.21	802.7	2506.1	4923.0	7880.0	11269.8	14954.0	18851.1	
9	19.73	793.5	2470.8	4854.4	7783.7	11134.4	14782.4	18681.3	
10	19.23	788.0	2435.3	4783.0	7665.6	10981.7	14621.3	18484.7	
11	18.74	773.4	2393.6	4702.4	7552.4	10824.0	14395.0	18285.0	
12	18.25	762.3	2358.8	4623.7	7422.2	10655.4	14215.2	18031.0	
13	17.74	750.7	2314.4	4534.4	7286.0	10468.1	13967.2	17760.0	
14	17.24	739.4	2275.8	4453.3	7153.7	10290.0	13768.0	17500.0	
15	16.76	728.2	2231.5	4366.6	7024.4	10104.8	13522.1	17168.0	21151.0
16	16.27	714.9	2182.5	4272.6	6875.2	9902.4	13265.0	16915.8	20790.0
17	15.77	707.2	2137.7	4179.0	6721.5	9695.0	12991.0	16573.0	20438.5
18	15.27	688.1	2086.6	4077.2	6558.3	9464.0	12716.0	16248.0	20036.0
19	14.78	674.0	2040.9	3977.5	6398.7	9245.0	12426.0	15916.0	19637.0
20	14.27	658.9	1993.1	3868.9	6227.6	9007.0	12120.0	15527.0	19201.0
21	13.77	643.3	1937.4	3763.8	6055.8	8749.0	11815.0	15143.0	18820.0
22	13.30	628.4	1883.6	3656.7	5883.7	8526.0	11502.0	14755.0	18306.0
23	12.79	610.6	1820.6	3537.8	5699.5	8239.7	11130.0	14340.0	17798.0
24	12.32	594.2	1767.2	3422.5	5506.0	7991.0	10797.0	13922.0	17287.0
25	11.79	576.9	1704.8	3306.3	5327.3	7723.6	10410.0	13475.0	16728.0
26	11.21	557.6	1642.1	3181.3	5090.0	7400.0	10000.0	12950.5	16140.0
27	10.79	539.2	1583.1	3063.3	4936.4	7167.4	9723.0	12568.3	15682.5
28	10.30	519.8	1519.7	2936.9	4732.9	6876.5	9324.6	12087.7	15096.2
29	9.79	499.1	1453.7	2806.0	4522.2	6575.4	8937.3	11588.7	14470.2
30	9.33	479.6	1385.6	2686.0	4329.0	6297.8	8568.7	11116.7	13899.0
31	8.84	459.4	1328.7	2559.3	4125.4	6005.4	8177.6	10623.5	13306.0
32	8.40	440.1	1252.4	2440.6	3934.0	5729.3	7808.0	10152.5	12713.8
33	7.91	417.9	1199.5	2306.0	3717.1	5416.4	7389.2	9618.6	12060.0
34	7.38	395.1	1130.4	2170.8	3499.3	5102.1	6965.8	9076.0	11418.9
35	6.87	370.0	1054.8	2023.3	3261.0	4752.2	6501.0	8480.0	10681.2
36	6.36	345.2	980.7	1878.9	3028.3	4419.6	6044.7	7892.5	9954.6
37	5.93	323.2	915.2	1750.5	2822.7	4121.3	5640.4	7371.3	9306.5
38	5.43	298.4	841.8	1609.4	2593.8	3789.1	5189.2	6787.4	8578.1
39	4.91	273.0	766.2	1464.0	2359.6	3448.1	4724.5	6185.7	7824.8
40	4.43	247.5	693.4	1323.2	2131.5	3115.8	4264.4	5597.0	7086.9
41	3.92	221.2	616.7	1176.4	1895.2	2771.0	3800.9	4983.2	6314.5
42	3.44	194.0	539.1	1026.0	1652.5	2416.0	3250.0	4400.0	5550.0
43	2.88	167.1	460.7	875.8	1409.4	2061.1	2829.1	3713.0	4711.6
44	2.38	140.0	383.7	727.2	1169.5	1709.5	2346.8	3080.8	3911.1
45	1.86	111.6	302.1	570.5	916.2	1338.4	1837.4	2388.1	3063.3
46	1.38	85.8	228.1	427.6	686.0	1001.1	1373.2	1802.5	2289.1

OK,

Contd.

RING B

AXIAL

NO	H (MM)	FREQUENCIES IN HZ FOR N = 10	11	12	13	14	15	16	17
24	12.32	20889.0							
25	11.79	20323.0							
26	11.21	19655.0							
27	10.79	19036.0							
28	10.30	18342.5							
29	9.79	17617.3	20973.7						
30	9.33	16989.8	20186.1						
31	8.84	16258.0	19367.0						
32	8.40	15604.0	18600.0						
33	7.91	14668.6	17668.1	20787.9					
34	7.38	13957.2	16700.0	19693.0					
35	6.87	13082.5	15750.0	18525.0					
36	6.36	12138.0	14772.8	17337.7	20116.0				
37	5.93	11434.0	13750.0	16328.9	18899.4				
38	5.43	10538.0	12689.2	15077.4	17593.1	20187.1			
39	4.91	9632.1	11592.6	13758.0	16115.4	18524.9	21127.0		
40	4.43	8736.3	10543.1	12499.3	14629.1	16932.0	19337.8		
41	3.92	7783.5	9412.0	11174.4	12996.2	15226.2	17248.7	19567.7	
42	3.44	6900.0	8350.0	9850.0	11459.3	13700.0	15166.2	17259.0	19367.0
43	2.88	5823.4	7047.1	8380.9	9812.2	11371.9	13027.8	14990.0	16831.7
44	2.38	4837.0	5856.2	6970.0	8177.8	9475.0	10865.0	12343.5	13983.7
45	1.86	3790.0	4591.2	5468.2	6418.8	7444.0	8543.4	9713.5	10958.7
46	1.38	2831.9	3285.2	4090.8	4762.2	5572.6	6281.0	7281.9	8219.5

OK.

RING C

AXIAL

NO	H (MM)	FREQUENCIES IN HZ FOR N=							
		2	3	4	5	6	7	8	9
1	23.58	711.0	2338.0	4683.0	7466.0	10460.0	13490.0	16471.0	0.0
2	23.10	707.2	2326.2	4661.9	7449.7	10479.3	13565.8	16588.0	0.0
3	22.59	702.8	2311.4	4636.1	7440.7	10492.6	13627.5	16733.4	19782.5
4	22.07	698.4	2293.6	4607.1	7406.9	10486.8	13674.2	16847.7	19963.7
5	21.58	693.4	2273.0	4573.7	7371.0	10471.5	13701.9	16942.8	20128.4
6	21.08	688.7	2253.3	4538.8	7329.4	10452.8	13721.6	17025.3	20288.2
7	20.58	683.2	2238.6	4499.6	7279.3	10405.3	13710.6	17079.0	20417.1
8	20.07	677.7	2215.3	4457.3	7227.8	10352.3	13689.2	17113.2	20529.6
9	19.59	671.6	2190.0	4411.4	7164.1	10286.1	13643.6	17120.0	20607.7
10	19.10	665.6	2168.2	4364.4	7090.1	10208.0	13577.9	17090.2	20647.0
11	18.60	659.0	2138.3	4308.3	7008.5	10112.1	13488.7	17031.0	20656.0
12	18.11	652.2	2110.2	4251.4	6925.6	10003.1	13372.6	16938.8	20613.0
13	17.65	645.0	2080.4	4192.0	6832.6	9915.0	13240.0	16812.8	20507.0
14	17.13	638.0	2052.4	4128.8	6728.4	9755.0	13092.0	16669.0	20393.0
15	16.63	629.7	2024.0	4060.4	6624.8	9604.8	12914.7	16468.7	20206.8
16	16.11	620.6	1983.0	3983.8	6496.0	9450.0	12704.0	16233.3	19971.6
17	15.65	612.6	1951.2	3913.6	6381.7	9300.0	12514.5	16019.0	19731.0
18	15.16	603.5	1914.0	3832.9	6250.6	9096.7	12282.5	15747.0	19434.4
19	14.69	593.2	1882.5	3754.4	6120.9	8897.8	12051.0	15475.8	19123.2
20	14.21	583.7	1839.4	3673.0	5989.5	8702.0	11802.0	15172.0	18787.0
21	13.72	573.4	1804.7	3580.3	5834.0	8507.3	11520.0	14844.0	18375.0
22	13.22	561.7	1752.1	3484.4	5683.7	8283.0	11198.0	14450.0	17941.0
23	12.70	548.8	1703.2	3380.9	5505.3	8042.0	10885.0	14067.0	17518.0
24	12.21	536.4	1662.1	3281.7	5344.6	7798.0	10565.0	13688.0	17021.0
25	11.68	522.1	1603.6	3170.2	5162.5	7531.9	10237.9	13242.0	16489.0
26	11.26	508.8	1554.5	3080.8	5020.0	7284.7	9909.0	12870.0	16059.0
27	10.70	494.3	1499.8	2951.7	4801.7	6999.9	9528.0	12364.0	15453.0
28	10.18	477.6	1451.3	2831.8	4603.6	6709.8	9160.4	11878.0	14862.0
29	9.67	461.0	1384.6	2712.2	4406.1	6436.7	8775.2	11440.2	14293.0
30	9.17	443.8	1324.3	2588.3	4202.3	6126.0	8378.4	10896.1	13692.0
31	8.63	425.6	1262.4	2461.8	3993.9	5800.0	7950.0	10336.9	13008.4
32	8.16	407.6	1201.9	2338.5	3791.9	5542.8	7573.0	9864.4	12391.0
33	7.66	388.0	1137.5	2208.4	3578.5	5232.0	7154.1	9327.0	11735.7
34	7.13	367.4	1070.6	2070.0	3359.5	4911.1	6719.1	8769.4	11046.7
35	6.61	345.3	1000.1	1932.6	3127.6	4574.6	6262.3	8180.2	10316.4
36	6.15	323.8	933.8	1800.4	2912.0	4259.8	5834.9	7628.3	9627.3
37	5.66	302.5	866.8	1668.1	2703.2	3945.3	5406.6	7074.0	8938.5
38	5.17	279.2	795.4	1528.0	2468.7	3611.6	4951.3	6483.5	8201.2
39	4.66	255.1	722.7	1385.8	2237.9	3273.7	4490.5	5883.8	7448.3
40	4.15	230.2	646.9	1237.3	1996.7	2921.5	4008.8	5255.5	6659.2
41	3.67	205.3	575.2	1098.9	1772.0	2593.0	3559.1	4668.4	5918.4
42	3.17	178.7	497.0	947.5	1526.5	2233.2	3066.0	4023.8	5104.0
43	2.63	152.9	422.0	802.0	1291.1	1888.6	2594.8	3350.0	4225.0
44	2.15	126.8	347.4	569.3	1058.8	1547.9	2125.3	2792.2	3540.0
45	1.69	102.5	276.5	521.7	837.6	1222.9	1678.9	2246.2	2799.0
46	1.19	75.9	198.7	371.8	594.7	867.1	1188.3	1560.3	1980.2

OK.

RING C

AXIAL

NO	H (MM)	FREQUENCIES IN HZ FOR N=							
		10	11	12	13	14	15	16	17
23	12.70	21134.0							
24	12.21	20610.0							
25	11.68	19994.0							
26	11.26	19427.0							
27	10.70	18785.0							
28	10.18	18134.6							
29	9.67	17396.6	20695.3						
30	9.17	16688.2	19877.0						
31	8.63	15936.6	18991.2						
32	8.16	15175.0	18144.6	21289.8					
33	7.66	14337.7	17260.8	20235.8					
34	7.13	13538.0	16239.8	19139.0					
35	6.61	12655.3	15150.0	17927.5	20867.0				
36	6.15	11801.3	14257.5	16832.1	19553.1				
37	5.66	10986.1	13200.0	15550.0	18222.7				
38	5.17	10076.7	12130.6	14388.4	16865.6	19406.3			
39	4.66	9161.9	11050.0	13098.1	15487.1	17700.0	20148.8		
40	4.15	8214.5	9918.6	11779.6	14012.3	16007.7	18295.2		
41	3.67	7307.3	8830.0	10462.0	12545.7	14230.5	16231.2	18408.9	20241.0
42	3.17	6306.0	7629.5	9068.1	10624.6	12392.9	14088.2	16059.3	17988.7
43	2.63	5280.0	6400.0	7600.0	8900.0	10449.3	11970.1	13591.4	15250.0
44	2.15	4382.1	5308.0	6329.0	7414.4	8594.1	9857.0	11203.1	12580.0
45	1.69	3462.6	4195.4	4944.2	5864.8	6803.1	7807.7	8880.2	10018.4
46	1.19	2449.2	2968.3	3536.3	4152.1	4818.9	5532.9	6296.6	

OK.

RING 0

AXIAL

NO	H (MM)	FREQUENCIES IN HZ FOR N=							
		2	3	4	5	6	7	8	9
1	24.07	530.0	1812.0	3650.0	5750.0	7867.0	9930.0	11952.0	13970.0
2	23.55	530.0	1801.6	3657.3	5784.8	7945.2	10052.0	12114.6	14159.6
3	23.05	530.0	1798.9	3662.8	5816.9	8018.7	10169.7	12268.9	14352.9
4	22.54	528.0	1800.8	3667.0	5845.2	8092.7	10293.6	12436.1	14555.3
5	22.05	527.5	1790.3	3668.1	5872.6	8164.2	10417.7	12608.0	14766.7
6	21.56	525.5	1787.7	3667.5	5897.9	8232.9	10538.3	12778.9	14980.1
7	21.07	525.0	1783.0	3664.2	5916.1	8294.7	10652.3	12945.3	15189.4
8	20.52	522.0	1770.2	3655.0	5927.4	8353.5	10776.2	13124.8	15426.5
9	20.04	520.0	1768.4	3646.3	5936.2	8403.7	10865.5	13295.7	15647.8
10	19.58	516.0	1765.3	3635.0	5935.1	8436.4	10974.1	13449.3	15859.0
11	19.12	513.0	1743.8	3620.5	5932.9	8471.0	11062.0	13604.0	16080.0
12	18.63	508.0	1733.2	3602.3	5917.4	8492.1	11142.0	13757.8	16297.0
13	18.11	505.0	1721.7	3579.3	5899.6	8492.0	11204.6	13900.3	16517.4
14	17.61	502.0	1710.6	3552.2	5868.5	8488.8	11249.4	14023.2	16727.3
15	17.10	497.0	1700.4	3522.1	5836.2	8471.7	11275.8	14118.7	16912.1
16	16.60	491.0	1673.5	3487.1	5790.4	8423.8	11278.7	14195.5	17083.4
17	16.10	487.0	1661.2	3449.5	5732.1	8371.5	11259.4	14243.0	17199.4
18	15.58	482.0	1635.4	3404.2	5662.9	8296.0	11200.5	14238.8	17315.4
19	15.07	477.6	1613.4	3356.8	5588.0	8204.5	11118.0	14197.0	17355.0
20	14.60	473.3	1591.8	3307.0	5508.7	8114.0	11013.0	14115.0	17338.0
21	14.12	467.6	1567.5	3251.4	5422.2	7995.0	10860.0	13986.8	17242.3
22	13.63	462.3	1541.7	3192.3	5318.3	7851.7	10704.2	13807.4	17094.1
23	13.13	455.7	1513.5	3126.9	5213.0	7681.0	10500.0	13589.6	16875.8
24	12.62	448.6	1483.0	3055.6	5085.2	7519.8	10283.5	13324.8	16575.0
25	12.14	441.3	1450.6	2982.5	4964.7	7335.7	10021.0	13050.0	16265.0
26	11.66	434.4	1435.4	2911.6	4843.5	7135.1	9805.0	12675.0	15928.4
27	11.19	425.7	1384.7	2833.2	4700.2	6945.9	9521.7	12387.0	15545.0
28	10.68	417.3	1363.5	2741.0	4546.0	6716.4	9234.0	11993.0	15030.0
29	10.17	406.9	1304.8	2647.2	4383.9	6474.5	8875.3	11552.8	14531.0
30	9.66	396.3	1262.7	2550.0	4215.8	6207.1	8544.3	11098.8	13996.5
31	9.15	385.0	1215.8	2447.7	4039.4	5945.4	8184.5	10685.6	13444.1
32	8.67	373.6	1169.2	2353.9	3861.8	5696.0	7822.4	10235.3	12837.7
33	8.18	360.4	1119.3	2234.6	3675.3	5417.3	7441.9	9709.3	12225.8
34	7.67	346.4	1067.9	2122.5	3485.7	5138.3	7055.1	9228.1	11628.8
35	7.17	331.3	1012.1	2003.8	3283.2	4834.1	6642.1	8691.7	10972.3
36	6.71	316.6	958.0	1889.4	3090.3	4547.6	6248.8	8153.2	10316.8
37	6.21	300.0	900.0	1767.7	2885.7	4245.0	5833.5	7642.4	9663.2
38	5.72	282.1	838.5	1640.5	2674.7	3931.1	5402.8	7081.8	8960.3
39	5.22	263.4	775.6	1511.6	2471.9	3614.4	4968.1	6514.6	8248.8
40	4.72	243.6	709.9	1377.7	2239.2	3289.9	4519.3	5928.2	7512.0
41	4.24	222.0	643.7	1246.8	2020.3	2964.8	4075.5	5349.3	6782.1
42	3.70	198.6	570.0	1080.0	1780.7	2611.8	3591.0	4714.6	5980.9
43	3.23	176.4	502.5	966.6	1563.7	2292.8	3151.9	4139.2	5254.1
44	2.74	152.0	429.7	780.0	1330.9	1951.0	2681.7	3520.6	4473.6
45	2.25	126.7	355.3	622.5	1096.7	1606.9	2208.5	2902.4	3686.2
46	1.78	102.0	283.6	540.9	872.3	1277.1	1755.0	2306.6	2929.9

OK.

Contd.

RING D

AXIAL

NO	H (MM)	FREQUENCIES IN HZ FOR N= 10	11	12	13	14	15	16
1	24.07	16015.0	18113.0	20279.0				
2	23.55	16233.3	18352.3	20535.0				
3	23.05	16454.0	18595.3	20798.1				
4	22.54	16682.4	18850.5	21073.9				
5	22.05	16928.3	19123.7					
6	21.56	17178.0	19402.6					
7	21.07	17428.6	19678.0					
8	20.52	17706.0	19995.0					
9	20.04	17976.0	20303.2					
10	19.58	18231.0	20599.0					
11	19.12	18505.0	20913.0					
12	18.63	18788.8	21252.0					
13	18.11	19071.1						
14	17.61	19359.0						
15	17.10	19632.0						
16	16.60	19898.5						
17	16.10	20119.0						
18	15.58	20351.2						
19	15.07	20510.0						
20	14.60	20587.0						
21	14.12	20578.1						
22	13.63	20493.0						
23	13.13	20314.6						
24	12.62	20047.0						
25	12.14	19716.0						
26	11.66	19339.0						
27	11.19	18905.0						
28	10.68	18365.8						
29	10.17	17751.0	21112.6					
30	9.66	17162.0	20395.0					
31	9.15	16454.0	19628.1					
32	8.67	15775.0	18852.7					
33	8.18	15102.0	18019.4	21109.9				
34	7.67	14333.8	17127.2	20135.8				
35	7.17	13500.0	16150.0	19046.0				
36	6.71	12720.0	15300.0	18026.0	20927.0			
37	6.21	11874.1	14270.0	16952.3	19749.8			
38	5.72	10927.6	13263.4	15708.1	18371.7	21064.1		
39	5.22	10092.0	12173.0	14512.6	16979.2	19532.5		
40	4.72	9263.8	11176.7	13252.0	15592.7	17900.7	20342.8	
41	4.24	8369.5	10108.0	12013.5	14074.4	16278.4	18511.6	20927.1
42	3.70	7386.7	8928.9	10605.2	12413.1	14371.3	16459.5	18715.9
43	3.23	6492.8	7854.2	9337.7	10938.8	12655.6	14528.7	16449.1
44	2.74	5531.1	6696.0	7966.2	9339.5	10816.7	12394.5	14107.5
45	2.25	4560.6	5524.1	6585.1	7716.4	8942.9	10255.7	11654.2
46	1.78	3626.4	4395.2	5234.9	6145.3	7127.3	8178.9	9300.9

OK.

RING A

TORSIONAL

NO	T (MM)	FREQUENCIES IN HZ FOR N= 0	1	2	3	4	5	6	7
1	30.07	1491.3	2349.0	3946.3	5732.4	7625.6	9612.3	11703.7	13905.6
2	29.10	1540.4	2417.8	4055.3	5880.6	7808.8	9850.6	11962.2	14195.2
3	27.97	1596.8	2497.3	4180.8	6058.0	8039.6	10108.2	12270.8	14531.8
4	27.00	1650.0	2550.0	4300.0	6215.0	8250.0	10370.0	12575.0	14860.0
5	26.02	1709.0	2653.5	4429.7	6406.1	8477.3	10639.8	12879.5	15215.1
6	25.02	1767.0	2740.0	4565.7	6590.3	8722.1	10927.0	13219.0	15593.5
7	24.02	1837.9	2836.0	4713.6	6802.1	8991.5	11250.6	13596.2	16016.8
8	23.10	1907.5	2934.6	4865.2	7013.0	9265.2	11583.0	13977.6	16449.4
9	22.13	1984.1	3038.5	5033.5	7250.2	9563.2	11948.7	14401.4	16928.7
10	21.13	2073.3	3166.8	5226.6	7520.7	9911.5	12368.2	14891.8	17475.5
11	20.14	2166.8	3292.1	5427.6	7795.5	10269.4	12804.0	15399.2	18032.4
12	19.23	2259.2	3422.3	5613.8	8077.1	10621.7	13229.4	15899.7	18631.5
13	18.25	2366.7	3566.0	5852.3	8380.2	11033.0	13728.4	16482.8	19289.2
14	17.25	2490.2	3737.0	6112.7	8758.3	11493.6	14294.9	17146.3	20049.5
15	16.28	2625.0	3917.7	6385.4	9140.0	11989.2	14897.2	17855.1	
16	15.29	2778.2	4115.0	6686.2	9550.7	12520.1	15551.0	18626.9	
17	14.45	2907.8	4287.6	6958.4	9917.0	12984.3	16117.0	19286.8	
18	13.58	3065.4	4494.0	7260.2	10385.5	13538.1	16789.6	20079.2	
19	12.70	3241.9	4718.6	7589.0	10794.0	14116.1	17496.4	20912.3	
20	11.86	3424.3	4939.0	7919.2	11243.6	14698.4	18207.2		
21	10.93	3654.7	5219.4	8315.1	11784.6	15389.4	19052.0		
22	9.99	3915.4	5526.7	8727.7	12338.5	16096.4	19911.8		
23	9.13	4172.4	5794.7	9096.9	12827.0	16713.1	20646.8		
24	8.22	4480.7	6124.9	9510.0	13387.6	17391.2			
25	7.32	4812.3	6500.0	9905.4	13839.2	17973.3			
26	6.39	5202.1	6874.2	10248.2	14220.2	18391.0			
27	5.99	5373.8	7021.4	10366.6	14325.4	18500.7			

8	9
16248.9	18689.4
16542.1	19013.3
16912.8	19404.8
17280.0	19780.0
17648.3	20204.7
18065.8	20636.2
18535.2	21136.4
19003.0	
19529.3	
20144.8	
20782.8	

RING B

TORSIONAL

NO	H (MM)	FREQUENCIES IN HZ FOR N= 0	1	2	3	4	5	6	7	8
1	23.67	7281.0	7744.0	9118.0	11186.0	13677.0	16464.0			
2	23.15	7263.2	7748.2	9161.0	11262.0	13786.0	16582.0			
3	22.66	7245.3	7748.2	9200.6	11341.9	13886.8	16702.0	19715.2		
4	22.16	7228.2	7750.3	9246.2	11430.9	14005.6	16841.7	19880.0		
5	21.70	7209.2	7750.5	9287.2	11504.2	14116.4	16976.2	20008.0		
6	21.21	7188.3	7753.2	9332.0	11596.3	14242.1	17121.5	20180.2		
7	20.71	7168.2	7752.4	9372.0	11684.7	14372.0	17287.7	20356.8		
8	20.21	7143.6	7749.6	9427.7	11805.0	14516.0	17463.4	20557.0		
9	19.73	7119.2	7747.1	9474.4	11878.6	14650.8	17638.0	20763.3		
10	19.23	7091.8	7750.2	9520.1	11981.7	14802.2	17823.3	20985.0		
11	18.74	7063.6	7749.4	9570.0	12090.0	14961.0	18032.3			
12	18.25	7033.5	7742.3	9628.3	12204.0	15138.0	18241.0			
13	17.74	6999.5	7738.4	9694.2	12328.7	15305.6	18475.7			
14	17.24	6965.0	7734.2	9748.6	12438.0	15476.0	18682.8			
15	16.76	6929.6	7722.7	9796.0	12558.6	15653.0	18918.1			
16	16.27	6888.8	7714.8	9850.0	12686.0	15837.0	19164.8			
17	15.77	6845.7	7712.0	9920.0	12823.4	16040.0	19407.0			
18	15.27	6797.4	7702.9	9970.3	12960.0	16249.2	19690.0			
19	14.78	6747.3	7689.6	10030.0	13092.5	16446.0	19959.8			
20	14.27	6691.6	7667.8	10114.6	13230.2	16657.3	20213.0			
21	13.77	6631.6	7656.3	10178.6	13372.0	16866.8	20500.0			
22	13.30	6568.9	7642.7	10233.0	13504.9	17070.0	20762.0			
23	12.79	6495.8	7619.8	10297.2	13669.8	17295.1	21080.1			
24	12.32	6419.6	7600.0	10347.8	13800.0	17488.1				
25	11.79	6337.2	7555.1	10397.8	13918.4	17691.1				
26	11.21	6244.4	7501.2	10442.8	14050.0	17892.4				
27	10.79	6148.9	7451.1	10475.8	14136.6	18061.0				
28	10.30	6039.2	7386.1	10499.4	14253.1	18217.5				
29	9.79	5916.6	7312.8	10498.9	14320.0	18343.4				
30	9.33	5797.3	7237.6	10491.3	14360.0	18438.2				
31	8.84	5650.0	7147.1	10461.3	14362.9	18493.7				
32	8.40	5525.9	7073.1	10423.4	14350.0	18524.0				
33	7.91	5354.1	6913.1	10338.7	14305.7	18481.5				
34	7.38	5174.6	6764.1	10212.4	14184.1	18357.0				
35	6.87	4955.2	6578.3	10046.6	14000.0	18167.8				
36	6.36	4720.7	6357.8	9813.7	13747.1	17850.1				
37	5.93	4501.6	6130.0	9568.8	13444.0	17477.2				
38	5.43	4240.7	5861.2	9243.3	13034.1	16974.1				
39	4.91	3950.4	5590.0	8830.0	12479.6	16290.2	20148.3			
40	4.43	3644.1	5232.2	8338.0	11828.6	15444.1	19115.4			
41	3.92	3302.3	4818.3	7754.9	11030.4	14433.0	17864.1			
42	3.44	2950.2	4342.6	7059.6	10076.3	13191.2	16352.4			
43	2.88	2508.2	3811.1	6253.2	8954.2	11730.9	14564.2	17405.6	20270.9	20048.2
44	2.38	2082.2	3237.5	5351.4	7719.0	10180.5	12598.4	15054.4	17547.8	16300.3
45	1.86	1600.0	2443.1	4322.6	6249.3	8216.7	10212.7	12275.0	14267.5	12487.3
46	1.38	1170.3	1924.6	3288.4	4803.9	6381.0	7810.3	9213.2	10600.0	

RING C

TORSIONAL

NO	H (MM)	FREQUENCIES IN HZ FOR N= 0	1	2	3	4	5	6	7
1	23.58	7470.0	7727.0	8624.0	10173.0	12226.0	14688.0	17580.0	
2	23.10	7450.0	7730.0	8659.6	10215.0	12276.0	14733.0	17560.0	
3	22.59	7435.0	7732.5	8686.6	10274.4	12345.3	14783.8	17585.6	20740.0
4	22.07	7429.0	7735.5	8714.0	10334.4	12421.0	14855.6	17610.6	20730.3
5	21.58	7416.1	7738.2	8756.8	10385.7	12487.4	14929.0	17659.6	20726.8
6	21.08	7403.5	7741.0	8785.5	10452.8	12572.4	15006.0	17724.2	20720.0
7	20.58	7390.1	7743.8	8828.1	10535.1	12661.6	15102.3	17802.5	20715.0
8	20.07	7376.5	7746.0	8868.0	10604.8	12765.4	15210.6	17905.0	20833.0
9	19.59	7360.8	7748.2	8908.5	10681.7	12865.5	15328.4	18021.1	20937.1
10	19.10	7345.0	7750.3	8942.1	10757.0	12976.3	15459.6	18145.1	21056.0
11	18.60	7327.0	7753.0	8987.5	10856.4	13135.0	15615.0	18312.0	
12	18.11	7309.5	7755.3	9038.9	10951.0	13246.4	15784.8	18506.0	
13	17.65	7286.3	7757.8	9075.7	11043.0	13378.7	15948.3	18683.6	
14	17.13	7267.3	7760.0	9130.8	11144.6	13533.3	16140.0	18902.0	
15	16.63	7242.0	7761.0	9198.9	11264.1	13707.6	16345.0	19145.0	
16	16.11	7218.7	7761.2	9258.8	11385.6	13872.5	16578.4	19409.8	
17	15.65	7191.6	7760.0	9308.5	11519.0	14052.7	16806.1	19687.0	
18	15.16	7158.6	7757.6	9369.5	11644.0	14254.4	17063.5	19998.0	
19	14.69	7127.5	7755.1	9444.8	11791.0	14445.6	17312.5	20317.0	
20	14.21	7092.5	7750.2	9512.3	11912.0	14656.8	17586.0	20633.0	
21	13.72	7052.0	7745.2	9584.7	12068.5	14887.8	17885.0	20998.0	
22	13.22	7008.9	7739.5	9664.2	12232.4	15134.4	18214.4		
23	12.70	6960.4	7732.5	9748.8	12416.4	15409.2	18566.1		
24	12.21	6906.5	7723.4	9827.6	12616.0	15664.8	18913.6		
25	11.68	6844.7	7713.0	9915.0	12777.8	15954.8	19295.6		
26	11.26	6786.0	7703.0	9980.0	12950.0	16200.0	19640.0		
27	10.70	6712.9	7688.0	10089.7	13158.0	16529.5	20055.7		
28	10.18	6629.4	7667.6	10175.3	13351.5	16829.1	20452.8		
29	9.67	6539.8	7632.4	10252.0	13530.0	17116.2	20790.8		
30	9.17	6433.9	7598.9	10329.8	13733.2	17417.0	21237.3		
31	8.63	6317.8	7518.2	10399.8	13912.4	17690.0			
32	8.16	6192.6	7460.0	10450.8	14069.5	17951.8			
33	7.66	6047.1	7415.0	10485.7	14216.5	18174.5			
34	7.13	5863.5	7260.0	10486.4	14295.7	18400.0			
35	6.61	5673.0	7142.0	10472.5	14366.1	18487.6			
36	6.15	5478.4	6993.5	10403.6	14342.9	18506.0			
37	5.66	5254.1	6825.0	10286.1	14262.3	18442.0			
38	5.17	4952.1	6625.0	10095.3	14077.0	18235.4			
39	4.66	4682.5	6368.4	9803.9	13736.1	17841.6			
40	4.15	4328.6	6015.7	9368.2	13246.6	17225.1	21289.4		
41	3.67	3962.4	5607.5	8869.2	12309.0	16331.8	20100.0		
42	3.17	3525.0	5104.5	8176.3	11618.4	15184.7	18700.0		
43	2.63	3014.6	4428.3	7334.5	10456.0	13650.0	16959.7	20265.2	
44	2.15	2492.3	3825.0	6298.4	9069.2	11893.0	14833.5	17628.3	20528.0
45	1.69	1958.6	3090.9	5197.4	7493.5	9868.0	12258.5	14643.4	17066.0
46	1.19	1422.2	2183.1	4151.1	5527.0	7107.9	9726.0	11350.0	12595.4

K.

RING D

TORSIONAL

NO	H (MM)	FREQUENCIES IN HZ FOR N=							
		0	1	2	3	4	5	6	7
1	24.07	7586.0	7688.0	8183.0	9272.0	11051.0	13467.0	16505.0	20050.0
2	23.55	7579.7	7691.0	8197.2	9293.5	11043.7	13420.2	16400.0	19900.0
3	23.05	7575.9	7694.4	8210.0	9320.3	11044.4	13377.6	16301.8	19737.5
4	22.54	7570.6	7697.4	8226.1	9340.1	11046.3	13343.8	16197.8	19581.1
5	22.05	7564.8	7698.3	8249.2	9365.0	11054.3	13308.2	16117.5	19422.6
6	21.56	7559.4	7702.6	8271.9	9378.9	11068.3	13281.3	16018.7	19273.4
7	21.07	7554.1	7705.0	8287.4	9408.2	11085.8	13261.3	15948.1	19131.6
8	20.52	7546.3	7707.0	8310.0	9442.8	11112.4	13249.6	15873.2	18980.0
9	20.04	7542.3	7710.8	8330.6	9493.5	11145.3	13257.3	15825.5	18861.7
10	19.58	7533.6	7712.5	8354.5	9519.8	11185.0	13270.0	15795.8	18760.0
11	19.12	7528.4	7714.5	8389.2	9573.9	11231.6	13292.8	15765.0	18657.0
12	18.63	7517.3	7717.7	8412.4	9626.0	11285.6	13332.7	15760.0	18583.1
13	18.11	7507.9	7720.0	8450.0	9687.5	11348.6	13382.4	15774.5	18517.7
14	17.61	7497.6	7722.4	8473.8	9755.1	11420.4	13448.4	15794.0	18467.7
15	17.10	7487.4	7724.5	8514.9	9801.3	11503.7	13522.4	15848.0	18474.6
16	16.60	7473.8	7727.1	8543.3	9876.0	11600.4	13630.0	15933.3	18492.4
17	16.10	7462.5	7730.0	8588.4	9957.3	11708.5	13770.0	16041.3	18572.7
18	15.58	7446.3	7733.5	8623.2	10037.1	11837.6	13910.3	16184.3	18668.0
19	15.07	7428.4	7735.0	8690.3	10120.0	11971.7	14073.0	16354.0	18837.0
20	14.60	7413.0	7738.0	8733.0	10241.8	12116.6	14238.0	16550.6	19025.0
21	14.12	7392.3	7739.5	8791.5	10353.5	12275.0	14437.3	16772.5	19256.2
22	13.63	7374.3	7744.6	8850.1	10473.5	12450.4	14659.2	17036.0	19534.3
23	13.13	7351.0	7748.6	8915.0	10604.1	12649.6	14922.0	17324.4	19869.0
24	12.62	7324.6	7749.0	8978.7	10751.3	12864.7	15194.6	17666.0	20218.0
25	12.14	7292.1	7750.9	9053.4	10889.6	13094.4	15493.3	18031.5	20665.9
26	11.66	7268.5	7753.0	9121.3	11051.4	13319.6	15799.0	18381.4	21084.8
27	11.19	7233.3	7751.3	9206.5	11230.1	13591.1	16147.5	18834.3	
28	10.68	7190.7	7754.0	9288.8	11425.7	13884.7	16531.0	19303.0	
29	10.17	7144.6	7752.5	9400.2	11633.8	14198.8	16952.4	19820.7	
30	9.66	7098.4	7748.6	9498.9	11854.0	14533.4	17399.4	20377.4	
31	9.15	7033.5	7744.0	9608.9	12094.3	14906.7	17890.7		
32	8.67	6970.0	7737.0	9725.1	12389.4	15288.0	18398.7		
33	8.18	6906.0	7724.9	9860.0	12616.0	15696.5	18936.5		
34	7.67	6833.7	7707.4	9971.7	12876.0	16097.5	19470.2		
35	7.17	6700.0	7682.0	10112.2	13165.0	16550.1	20073.3		
36	6.71	6580.0	7644.0	10214.1	13420.0	16963.8	20623.2		
37	6.21	6440.0	7603.6	10323.1	13700.0	17394.2	21196.1		
38	5.72	6285.0	7537.1	10414.1	13975.4	17790.4			
39	5.22	6078.3	7440.0	10483.8	14171.1	18127.7			
40	4.72	5810.0	7281.6	10501.7	14321.0	18391.8			
41	4.24	5530.0	7093.0	10420.0	14348.0	18425.0			
42	3.70	5176.2	6810.5	10230.0	14220.3	18325.0			
43	3.23	4794.4	6450.0	9925.6	13850.0	17973.0			
44	2.74	4452.4	5988.5	9306.0	13229.1	17172.0	21160.0		
45	2.25	3838.2	5303.1	8400.0	12039.2	15740.0	19455.3		
46	1.78	3070.9	4511.7	7391.0	10474.0	13298.0	15346.5		

RING A

THICKNESS & MASS

NO	T (MM)	M (KG)
1	30.07	0.9339
2	29.10	0.9033
3	27.97	0.8688
4	27.00	0.8087
5	26.02	0.7788
6	25.02	0.7479
7	24.02	0.7187
8	23.10	0.6889
9	22.13	0.6739
10	21.13	0.6567
11	20.14	0.6259
12	19.23	0.5982
13	18.25	0.5676
14	17.25	0.5362
15	16.28	0.5053
16	15.29	0.4738
17	14.45	0.4486
18	13.58	0.4213
19	12.70	0.3938
20	11.86	0.3678
21	10.93	0.3383
22	9.99	0.3090
23	9.13	0.2833
24	8.22	0.2545
25	7.32	0.2273
26	6.39	0.1982
27	5.99	0.1858

OK.

RINGS B , C & D

HEIGHT & MASS

NO	B		C		D	
	H (MM)	M (KG)	H (MM)	M (KG)	H (MM)	M (KG)
1	23.67	1.0005	23.58	0.7837	24.07	0.5045
2	23.15	0.9788	23.10	0.7188	23.55	0.4938
3	22.66	0.9584	22.59	0.7028	23.05	0.4837
4	22.16	0.9370	22.07	0.6869	22.54	0.4731
5	21.70	0.9172	21.58	0.6713	22.05	0.4625
6	21.21	0.8963	21.08	0.6555	21.56	0.4520
7	20.71	0.8756	20.58	0.6401	21.07	0.4420
8	20.21	0.8542	20.07	0.6246	20.52	0.4305
9	19.73	0.8341	19.59	0.6093	20.04	0.4203
10	19.23	0.8131	19.10	0.5944	19.58	0.4107
11	18.74	0.7921	18.60	0.5786	19.12	0.4006
12	18.25	0.7709	18.11	0.5629	18.63	0.3902
13	17.74	0.7492	17.65	0.5481	18.11	0.3796
14	17.24	0.7290	17.13	0.5328	17.61	0.3690
15	16.76	0.7090	16.63	0.5175	17.10	0.3590
16	16.27	0.6878	16.11	0.5014	16.60	0.3482
17	15.77	0.6670	15.65	0.4868	16.10	0.3378
18	15.27	0.6453	15.16	0.4713	15.58	0.3267
19	14.78	0.6247	14.69	0.4567	15.07	0.3160
20	14.27	0.6031	14.21	0.4420	14.60	0.3061
21	13.77	0.5821	13.72	0.4265	14.12	0.2958
22	13.30	0.5617	13.22	0.4109	13.63	0.2854
23	12.79	0.5394	12.70	0.3942	13.13	0.2748
24	12.32	0.5184	12.21	0.3790	12.62	0.2642
25	11.79	0.4976	11.68	0.3626	12.14	0.2537
26	11.21	0.4756	11.26	0.3476	11.66	0.2443
27	10.79	0.4553	10.70	0.3317	11.19	0.2338
28	10.30	0.4340	10.18	0.3155	10.68	0.2233
29	9.79	0.4124	9.67	0.2997	10.17	0.2127
30	9.33	0.3928	9.17	0.2838	9.66	0.2021
31	8.84	0.3725	8.63	0.2678	9.15	0.1914
32	8.40	0.3535	8.16	0.2526	8.67	0.1810
33	7.91	0.3325	7.66	0.2370	8.18	0.1706
34	7.38	0.3117	7.13	0.2211	7.67	0.1603
35	6.87	0.2892	6.61	0.2048	7.17	0.1496
36	6.36	0.2674	6.15	0.1898	6.71	0.1397
37	5.93	0.2485	5.66	0.1750	6.21	0.1295
38	5.43	0.2276	5.17	0.1595	5.72	0.1191
39	4.91	0.2064	4.66	0.1440	5.22	0.1089
40	4.43	0.1859	4.15	0.1280	4.72	0.0985
41	3.92	0.1648	3.67	0.1133	4.24	0.0884
42	3.44	0.1433	3.17	0.0973	3.70	0.0775
43	2.88	0.1218	2.63	0.0819	3.23	0.0677
44	2.38	0.1008	2.15	0.0670	2.74	0.0574
45	1.86	0.0785	1.69	0.0527	2.25	0.0471
46	1.38	0.0585	1.19	0.0372	1.78	0.0374

OK,

APPENDIX V

FITTING A nTH DEGREE POLYNOMIAL TO m DATA POINTS

The following details regarding polynomial fitting are taken from KUO [65]. It may be remembered that the least-squares technique is aimed at finding a minimum value for

$$S = \sum_{k=1}^{m} (Y_k - y_k)^2 \qquad k = 1,2, \ldots\ldots, m$$

where Y_k is evaluated from the polynomial

$$Y_k = A_o + A_1 x_k + A_2 x_k^2 + \ldots\ldots\ldots + A_n x_k^n$$

and y_k are the observed values corresponding to x_k. To obtain a minimum value for S which is a function of n + 1 variables, viz. A_o, A_1, A_2 ... ., A_n, the following n + 1 first partial derivatives are set to zero.

$$\frac{\partial S}{\partial A_o} = \Sigma 2 \, (A_o + A_1 x_k + A_2 x_k^2 + \ldots\ldots\ldots + A_n x_k^n - y_k) = 0$$

$$\frac{\partial S}{\partial A_1} = \Sigma 2 x_k (A_o + A_1 x_k + A_2 x_k^2 + \ldots\ldots\ldots + A_n x_k^n - y_k) = 0$$

$$\vdots$$

$$\frac{\partial S}{\partial A_n} = \Sigma 2 x_k^n (A_o + A_1 x_k + A_2 x_k^2 + \ldots\ldots\ldots + A_n x_k^n - y_k) = 0$$

where the symbol Σ implies summation for k from 1 to m. We now obtain n + 1 simultaneous linear equations which, when expressed in the matrix notation, have the form

$$(P)\,(Q) = (R),$$

where

$$(P) = \begin{bmatrix} m & \Sigma x_k & \Sigma x_k^2 & \ldots\ldots\ldots & \Sigma x_k^n \\ \Sigma x_k & \Sigma x_k^2 & \Sigma x_k^3 & \ldots\ldots\ldots & \Sigma x_k^{n+1} \\ \vdots & & & & \\ \Sigma x_k^n & \Sigma x_k^{n+1} & \Sigma x_k^{n+2} & \ldots\ldots\ldots & \Sigma x_k^{2n} \end{bmatrix}$$ is a

symmetric matrix and

$$(Q) = \begin{bmatrix} A_o \\ A_1 \\ \vdots \\ A_n \end{bmatrix}$$ and $$(R) = \begin{bmatrix} \Sigma y_k \\ \Sigma x_k y_k \\ \vdots \\ \Sigma x_k^n y_k \end{bmatrix}$$ are

column matrices. In particular (Q) is referred to as the regression coefficient vector.

A computer programme formed on the above lines for polynomial fitting is given in Appendix VI.

APPENDIX VI COMPUTER PROGRAMME FOR POLYNOMIAL FITTING

```
    SLIST VMR_PLFITM
GO
C     POLYNOMIAL FIT TO N DATA POINTS BASED ON L_S CRITERION
C     M= DEGREE OF POLYNOMIAL
C     N= NO. OF DATA POINTS
C     M1= NO. OF EQUATIONS
C     N1= NO. OF UNKNOWNS
C     NUMP= NO. OF POLYNOMIALS TO BE FITTED
C     IDEGS= DEGREES OF THE POLYNOMIALS TO BE FITTED SAY 1,2,4,5 ETC.
C     PY= VALUES OF Y AS PER POLYNOMIAL FIT
C     RESID= Y-PY
C     DT= DATA TABLE
C     IR= NO. OF ROWS OF DT
C     IC= NO. OF COLS OF DT
C     NRC=NO. OF ROWS * NO. OF COLMS
      DOUBLE PRECISION A,B,C,QR,ALPHA,E,Y1,Z,R,X02AAF,XXXX,F04AMF
      DIMENSION X(50),Y(50),XX(50,50),SX(50),YY(50,50),SY(50)
      DIMENSION PY(50),RESID(50),IDEGS(50)
      DIMENSION A(50,50),B(50,50),C(50,50),QR(50,50),ALPHA(50),E(50),
     1Y1(50),Z(50),R(50)
      INTEGER IA,IB,IC,M1,N1,IR,IQR,IPIV(50),IFAIL,I,J
C     WRITE(1,910)
      READ(5,*)NUMP
C     WRITE(1,920)
      READ(5,*)(IDEGS(I),I=1,NUMP)
C     WRITE(1,930)
      READ(5,*)N
C     WRITE(1,940)
      READ(5,*)(X(I),I=1,N)
C     WRITE(1,950)
      READ(6,*)(Y(I),I=1,N)
      DO 120 ID=1,NUMP
      M=IDEGS(ID)
      M1=M+1
      M2=2*M
C     ARITHMETIC FOR GETTING COEFFT. MATRIX
      DO 20 I=1,N
      DO 10 J=1,M2
      XX(J,I)=X(I)**J
10    CONTINUE
20    CONTINUE
C     SUMMATION S(I)= XX(1,1)+XX(1,2)+- - - - +X(1,N)
      DO 40 J=1,M2
      S=0.
      DO 30 I=1,N
      S=S+XX(J,I)
      S=S
30    CONTINUE
      SX(J)=S
40    CONTINUE
C     TO GET THE COEFFT. MATRIX A
      SX(0)=N
      DO 60 J=1,M1
      DO 50 I=1,M1
      A(I,J)=DBLE(SX(I+J-2))
50    CONTINUE
60    CONTINUE
```

Contd.

```
C       TO GET RHS MATRIX C
        DO 80 I=1,N
        DO 70 J=1,M1
        YY(J,I)=Y(I)*(X(I)**(J-1))
70      CONTINUE
80      CONTINUE
C       SUMMATION SY(I)=YY(1,1)+YY(1,2)+-------+YY(1,N)
        DO 100 J=1,M1
        T=0.
        DO 90 I=1,N
        T=T+YY(J,I)
        T=T
90      CONTINUE
        SY(J)=T
100     CONTINUE
        DO 110 J=1,M1
        C(J,1)=DBLE(SY(J))
110     CONTINUE
C       A(M,N)*B(N,N) = C(M,N)
C       COEFFT. MATRIX * REGRESSION VECTOR = RHS C MATRIX
C       SUBROUTINE F04AMF IS CALLED IN TO SOLVE THE M+1 SIMULTANEOUS EQUNS
        N1=M+1
        IP=1
        IR=1
        IFAIL=1
        CALL F04AMF(A,50,B,50,C,50,M1,N1,IR,X02AAF(XXXX),QR,50,ALPHA,E,Y1,
       1Z,R,IPIV,IFAIL)
        DO 116 I=1,N
        P=0.
        DO 115 J=1,N1
        P=P+B(J,1)*(X(I)**(J-1))
115     CONTINUE
        PY(I)=P
        RESID(I)=Y(I)-PY(I)
116     CONTINUE
        WRITE(1,130)M
        WRITE(1,135)N
        WRITE(1,139)
        WRITE(1,140)(I,X(I),Y(I),PY(I),RESID(I),I=1,N)
        WRITE(1,150)IFAIL
        WRITE(1,160)((B(I,J),J=1,IP),I=1,N1)
120     CONTINUE
130     FORMAT(//,'DEGREE OF POLYNOMIAL =',I2)
135     FORMAT('NUMBER OF DATA POINTS =',I2)
139     FORMAT(//,2X,'NO',6X,'X',10X,'Y',9X,'PY',7X,'RESID',//)
140     FORMAT(X,I3,2X,F7.3,2X,F10.1,2X,F10.1,2X,F7.4)
150     FORMAT('IFAIL =',I2)
160     FORMAT(12HCOEFFICIENTS/(1H ,E15.8))
C10     FORMAT('PL. INPUT THE VALUE OF NUMP')
C20     FORMAT('PL. INPUT THE VALUES OF IDEGS')
C30     FORMAT('PL. INPUT THE VALUE OF N')
C40     FORMAT('PL. INPUT THE VALUES OF X')
C50     FORMAT('PL. INPUT THE VALUES OF Y')
        CALL EXIT
        END

OK,
```